VYSOKÉ UČENÍ TECHNICKÉ V BRNĚ
BRNO UNIVERSITY OF TECHNOLOGY

FAKULTA STROJNÍHO INŽENÝRSTVÍ
FACULTY OF MECHANICAL ENGINEERING

LETECKÝ ÚSTAV
INSTITUTE OF AEROSPACE ENGINEERING

NÁVRH VÝUKOVÉHO EXPERIMENTU PRO PŘEDMĚT AERODYNAMIKA I
CREATION OF EDUCATIONAL EXPERIMENT FOR AERODYNAMICS I COURSE

BAKALÁŘSKÁ PRÁCE
BACHELOR'S THESIS

AUTOR PRÁCE — **Daniel Fenech**
AUTHOR

VEDOUCÍ PRÁCE — **Ing. Robert Popela, Ph.D.**
SUPERVISOR

BRNO 2019

BRNO UNIVERSITY OF TECHNOLOGY
FACULTY OF MECHANICAL ENGINEERING

Specification Bachelor's Thesis

Department:	Institute of Aerospace Engineering
Student:	**Daniel Fenech**
Study programme:	Engineering
Study field:	Fundamentals of Mechanical Engineering
Leader:	**Ing. Robert Popela, Ph.D.**
Academic year:	2018/19

Pursuant to Act no. 111/1998 concerning universities and the BUT study and examination rules, you have been assigned the following topic by the institute director Bachelor's Thesis:

Creation of educational experiment for Aerodynamics I course

Concise characteristic of the task:

Practical experiments are important part of engineering study. For aerodynamics courses wind tunnel test is most appropriate for gaining practical experience. For introduction of such experiment there is necessary to prepare test set–up and methodology.

Goals Bachelor's Thesis:

Preparation of experimental measurement of aerodynamic characteristics of classical plane configuration in Institute os Aerospace Engineering wind tunnel. Preparation of methodology and practical test verification.

Recommended bibliography:

POPE, A., BARLOW, J., RAE, H., Low-Speed Wind Tunnel Testing, Wiley and sons, ISBN 0-47--55774-9.

Deadline for submission Bachelor's Thesis is given by the Schedule of the Academic year 2018/19

In Brno,

L. S.

doc. Ing. Jaroslav Juračka, Ph.D.	doc. Ing. Jaroslav Katolický, Ph.D.
Director of the Institute	FME dean

ABSTRACT

The goal of this thesis is to create a semester-long project for students of the course Aerodynamics I to follow in order to understand better, and gain first-hand experience, how one can determine aerodynamic characteristics through computations and by the use of wind-tunnel. The procedure highlights are how to obtain the geometries of a model using 3-D scanning and manipulating the scanned item to get the required geometries, using XFOIL to obtain 2-D aerodynamic characteristics of aerofoils, using Glauert III alongside basic computations to obtain aerodynamic coefficients distributions along a whole surface and solving for total forces acting on the model. Finally, wind tunnel test of the model is carried out for validation of the computational part.

KEYWORDS

Aerodynamics, Wind-Tunnel, Testing, 3D-Scan, Model Aircraft, P-47 Thunderbolt, XFOIL, GLAUERT III, Creo Parametric 3.0, Microsoft Excel, DEWESoft X.

ABSTRAKT

Cílem bakalářské práce je vytvořit semestrální projekt pro studenty kurzu Aerodynamika I, který dále využijí pro lepší porozumění a získání zkušeností, jak lze určit aerodynamické charakteristiky pomocí výpočtů a pomocí aerodynamického tunelu. Nejdůležitějšími kroky je získání geometrie modelu pomocí 3-D skenování a manipulace se skenovanou položkou tak, aby bylo dosaženo požadovaných geometrií, pomocí XFOIL získání 2-D aerodynamických charakteristik aerofoilů, pomocí Glauert III vedle základních výpočtů získání aerodynamických koeficientů rozložených podél celého povrchu a řešení pro celkové síly působící na model. Závěrem je provedena zkouška modelu aerodynamického tunelu pro ověření výpočetní části.

KLÍČOVÁ SLOVA

Aerodynamika, Aerodynamický tunel, Testování, 3D sken, Modelová letadla, P-47 Thunderbolt, XFOIL, GLAUERT III, Creo Parametric 3.0, Microsoft Excel, DEWESoft X.

Bibliographic Citation

FENECH, D. *Creating of educational experiment for Aerodynamics I course*. Brno: Brno University of Technology, Faculty of Mechanical Engineering, 2019. ***146p***. Thesis Supervisor Ing. Robert Popela, Ph.D.

AKNOWLEDGEMENTS

I would like to start off by thanking my thesis supervisor Ing. Robert Popela Ph.D. for his mentorship, Ing. Tomáš Hájek, Ing. Petr Dvořák and Ing. Jiří Matějů for their assistance and advice. The Institute of Aerospace Engineering for the model, wind-tunnel and work space provided and StrojLAB for the 3-D scanning facilities. Finally, I would like to thank my family, my girlfriend Kristýna Suchá and my close friends for their love, constant support and encouragement throughout my studies.

AFFIRMATION

I declare that this bachelor thesis is based on my own work, led by my Bachelor's thesis supervisor Ing. Robert Popela, Ph.D., and all utilized sources are properly listed in the bibliography. I proclaim that all presented information is accurate.

In Brno 23.05.2019

_____

Daniel Fenech

Contents

1 Introduction

An Aerodynamics course opens the doors for future engineers to a vast options of career paths, whether in aerospace, automotive and even renewable energy amongst others. The material provided during the course Aerodynamics 1 at the Brno University of Technology is quite vast and robust, and it prepares the students to take on aerodynamic-related challenges in both their education and their careers. It is a known fact that to excel in any engineering sector, practice and experience are key elements, along with the theoretical knowledge.

The goal of this project is to introduce an experimental project within the course Aerodynamics 1 that will help students get a better idea and understanding of the subject. Whilst experimental projects do exist within the course, such as a wind tunnel exercise on a NACA0012 aerofoil, 2D analysis of the same aerofoil using XFOIL and determination of 3D aerodynamical properties of an aircraft using a faculty-developed software Glauert III, there lacks the combination of the three together to create a more realistic project that represents day-to-day tasks faced in the aerodynamics sector. Therefore, this projects intents to help the students relate different topics covered throughout the course together for better understanding, and better visualise how each software, or similar ones, and the wind-tunnel itself, can be manipulated to derive results for testing and design.

The main procedure in the theoretical part of the project starts with a 3D-scanning of the model aircraft using the Atos III Triple Scan Industrial Optical 3D Digitizer provided by StrojLAB, followed by the use of GOM software to fix and edit the generated mesh. Creo Parametric 3.0 was used to solidify the mesh and manipulate the model to measure geometric and aerodynamic features such as aerofoil section, chord lengths and planform areas. XFOIL is used to generate aerodynamic properties and curves for the 2-D aerofoils used in the wing and horizontal tail unit (HTU), whereas GLAUERT III was used to generate and compute aerodynamic properties across the whole wing and HTU. Furthermore, in Excel sheets the data obtained by both was tabulated to generate aerodynamic curves and compute the required values such as Lift (L), Drag (D) and Pitching Moment (M) coefficients, and eventually forces at different boundary conditions. Finally, the individual forces were summed together to get the total forces acting on the model's aerodynamic centre (AC). The methodological computations will

serve as a guide for future students whilst working on their semesterly project, to help understand the logic behind the methodology itself.

During the practical part, the results generated theoretically will be used to calibrate a wind-tunnel balance to which the model will be fixed during the testing phase. The model will be mounted to the balance at the AC used for the summation of forces, and there the balance will measure the total forces and generate results which will be used both as a reference, and as well as for validation to which the lecturer and students can compare the values of their theoretical part.

2 Model

2.1 UMX P-47 BL BNF Basic with AS3X

The model aircraft used in this thesis is a UMX P-47 BL BNF Basic with AS3X, shown in Figure 1. It is a lightweight R/C aircraft made from foam.

Figure 1 UMX P-47 BL BNF Basic with AS3X model [1]

2.2 Overview

The Republic P-47D, also known as “Thunderbolt”, was a fighter and fighter-bomber used by the Allied forces during World War II. It was a single-seat, low-wing fighter developed for the U.S. Army Air Forces (USAAF) by Republic Aviation and it was the largest single-engine piston fighter to ever be produced at the time. Although not as agile as its British counterpart, the Supermarine Spitfire, it had the advantage of being able to carry a much heavier payload, enabling it to act as both a fighter and a bomber, thus giving it its reputation for versatility. The model is constructed from a lightweight foam and features a realistic outline and stand-out details to represent the livery of Major Howard D. "Deacon" Hively’s P-47D [2].

2.3 Scale

The E-flite® UMX™ P-47 BL model is a warbird designed outline the shape of the actual P-47, however when analysing the measurements for both, one will find that a scale does not seem to exist. Ratios of lengths and wing spans give different values. The Republic P-47 Thunderbolt had a length of 11.02 m, wing span of 12.44m and a wing area of 27.87 sq. m., whereas the E-flite® UMX™ P-47 BL is listed to having a length of 434mm, wing span of 482 mm and wing area of 4.45 sq. dm. Should a scale have been used, the ratio of lengths and wing spans should be the same. The ratios were computed by the actual value over the modelled value [1][2].

Table 1 Comparison between the model used and the actual P-47D Thunderbolt [1][2]

	LENGTH	**WING SPAN**	**WING AREA**	**WEIGHT**
P-47D THUNDERBOLT	11.02 m	12.44 m	27.87 sq.m.	6577 kg
E-FLITE® UMX™ P-47 BL	0.434 m	0.482 m	0.0445 sq.m.	0.095 kg
RATIO	25.39	25.81	-	-

This means that analysis of the model has to be done, and geometry details such as aerofoils and planforms cannot be measured from actual plans and scaled down.

2.4 Extra Information

Other information provided includes the usage of a 180BL brushless out runner motor, AS3X® (Artificial Stabilization – 3-aXis) Technology and removable landing gear. The brushless motor and landing gear can be manipulated for the project by testing the model within the wind-tunnel with them both activated or deactivated, to get a wider spectrum of results [1].

2.5 Limitation

Since the model is manufactured from lightweight foam, the rigidity is a main limitation for wind-tunnel testing. Therefore, throughout the theoretical computations four boundary conditions will be analysed to see which gives the best balance between forces acting on the model and good results. This is given importance as a low speed will be gentler on the model but the readings will be more limited. At low velocities low forces

are generated, therefore it increases the complexities of designing a wind-tunnel balance that can read such small differences. On the other hand, a high speed will give better results to design the balance, whilst the same forces acting on the model can exceed its mechanical properties' limitations and risk a catastrophic failure of the model. The boundary condition deemed to give the best results will be chosen to build and calibrate the wind-tunnel balance to carry out the wind-tunnel testing.

3 Model Geometry Acquisition

3.1 Geometry Reading Techniques

The first step prior to starting aerodynamic computations, is to obtain geometric properties of the model so that computations can be carried out successfully. To do so, two main approaches were evaluated. The first one was photographing the model, scaling on a Computer Aided Design (CAD) software and measuring the geometries. The second option was 3D scanning of the model, converting to a CAD solid and manipulating it to obtain the required geometry. Manual metrology would be close to impossible, and full of inaccuracies given the complex shape of the model.

The first method evaluated immediately proved inefficient; because the lens produces its own distortion, there is no guarantee that the picture is shot at precisely the right angle to capture, for instance a side, top or front view and the difficulty to level the model perfectly given its complex shape. It was nonetheless tried for comparison with the second method.

3.1.1 Photography Scaling

In Figure 2, a top shot of the model was imported on Autodesk Inventor 2018 and scaled to have a wingspan of 482 mm and length of 432 mm. The tiles were used for alignment, and even after editing the picture on Adobe Lightroom to counter the lens' distortion, immediately it can be seen that the tiles have a distortion in them, meaning the picture will be inaccurate [1].

The way of obtaining the geometries would be to create a sketch by tracing around the part needed, as shown in Figure 2 around the wing. The sketch could easily be manipulated, for example, sectioning at different parts to obtain different chord lengths in order to compute the mean aerodynamic chord (C_{MAC}) and obtaining wing Area. Whilst this was feasible, there is a limitation in trying to read sections from the sides, mainly to analyse the aerofoils used, as the picture is in 2D and thus, would be impossible to read geometric or aerodynamic twists for instance. With such disadvantages, this idea was scrapped and 3D scanning was put forward.

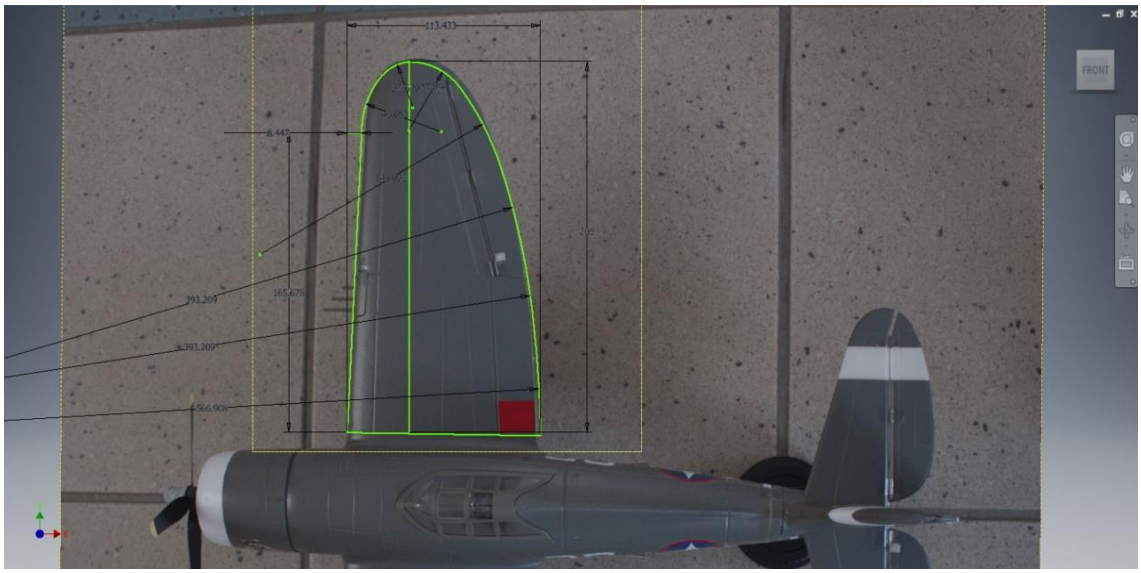

Figure 2 A screenshot of Autodesk Inventor showing a scaled picture of the model with a sketch tracing the wing prior to sectioning it

3.1.2 3-D Scanning

The 3D scanning was done using the Atos III Triple Scan Industrial Optical 3D Digitizer. The model was covered in marker stickers which acted as reference point for the scanner only on half of the body. To save time and resources it was decided that the model could be scanned halfway through and then mirrored through software, assuming that the geometry is symmetrical. Once placed on a turn table, the model was scanned using GOM software for three times, each time using a different angle to capture as much detail as possible. Some parts of the model had reflective paint on, and being concerned with the preservation of the model's integrity, could not be coated with paint. This resulted in some defects, mainly holes, in the resulting mesh.

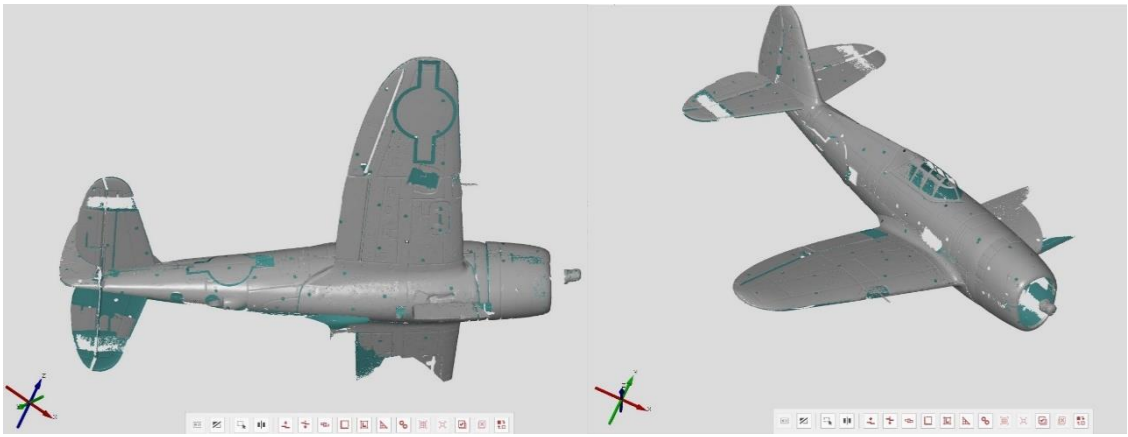

Figure 3 Screenshots of GOM Inspect showing the resulting 3D scan mesh prior to post processing

As shown in Figure 3, considering the left-hand side only, the worst parts in the scan were the HTU, and the leading edge (LE) of the wing. The holes on the fuselage where not much of a concern as they are on a relatively flat surface and could easily be closed.

Using GOM Inspect, the mesh was fixed by bridging and closing holes, and refining the mesh as much as possible. A plane was created slicing the model through the centre, and used to erase the right-hand side of the model, which was to be ignored with the intention of mirroring the left-hand side. The model was exported to a stereolithography file (.STL) and opened in Creo Parametric 3.0, where using the shrink-wrap function, it was turned into a solid part as portrayed in Figure 4. Once the solid was generated, a set of planes and co-ordinate system were created and the half model was mirrored to create a full one.

The main errors that resulted in the scan were the HTU having the elevators activated slightly, due to them being flimsy and not fastened. Also, reflective parts, like stickers, on the model resulted in holes in the scanned mesh and closing them was not 100% accurate.

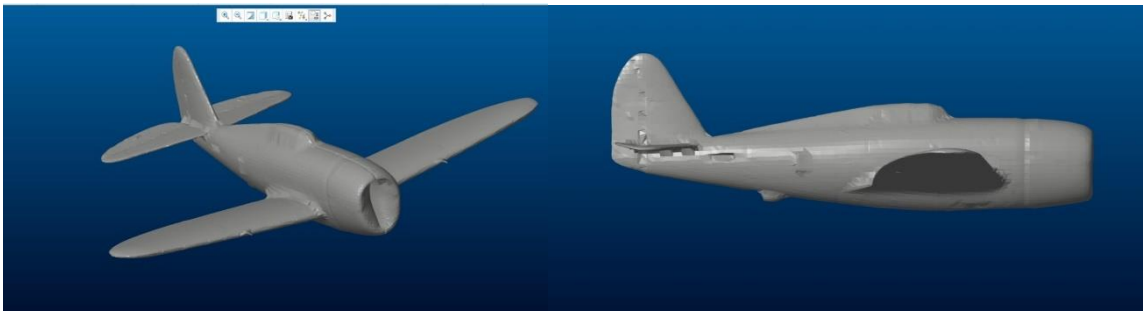

Figure 4 Screenshots of the resulting model on Creo Parametric 3.0

The 3D scan opened doors for a wide range of advantages in the way the model could be manipulated. Through the CAD solid, the wing could be sectioned to have the aerofoil at that position analysed, dimensions could be read off directly from the CAD solid, and in case a computational fluid dynamics (CFD) software would be used sometime in the future, the model could easily be exported into a STEP file to be used in the CFD software.

In conclusion, 3D scanning was the obvious way-to-go, its advantages by far outweighed the disadvantages brought about by some errors.

3.2 Planform Geometry

One main important detail for computations is the planform, both for the wings and the HTU. A planform is the shape or outline of an aircraft wing as projected upon a horizontal plane.

3.2.1 Planform Area

The planform area was the simpler geometry to obtain. Using a top view of the CAD solid, the wing's outline was projected on a horizontal plane. The projection at the root was extended tangentially to the centre of the fuselage, and finally filled to create a surface. The resulting surface's area was measured using the Measure function on the software.

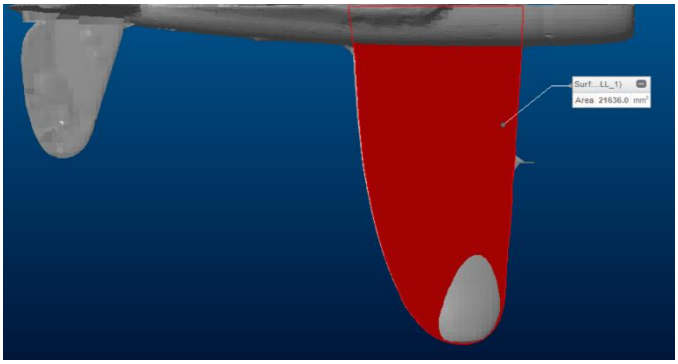

Figure 5 Projection around wing, filled and area enclosed measured.

The half-span area of the wing was found to be 21636 sq.mm. while the whole wing area was measured at 43272 sq.mm. The area given by the supplier is that of 44500 sq.mm, which is very close to the one measured using this method. When the manufacturing inaccuracies and scan imperfections are taken into consideration, the area was right on target [1].

The same procedure was repeated for the HTU, providing an area of 5453 sq.mm. The only difference here was that the HTU was simplified by extending the elevator tangentially to the centre of the fuselage so as to simplify computations by treating it as an elliptical wing.

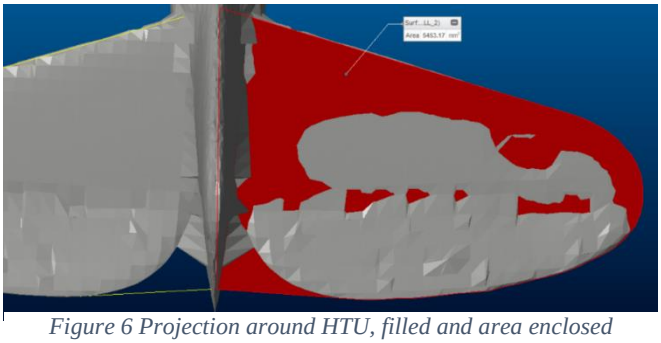

Figure 6 Projection around HTU, filled and area enclosed measured

3.2.2 Planform Sectioning

This was the most important step to be able to compute the C_{MAC}. Planform sectioning involves the segmentation of the wing, or HTU, along the span (y-axis) to obtain chord lengths at different displacements.

Using the same sketch generated in the step for planform area analysis, planform section was performed by first creating a reference line splitting the wing along the y-axis from the wing-tip to the root. The reference line splits the wing into two parts, LE side and the Trailing Edge (TE) side. The reference line, 239 mm long, was then split at intervals of 5 mm, resulting in 49 intersections. At each interval a perpendicular line was created, joining the reference line to the LE, with another line joining the reference line to the TE. For each point on the reference line, there were two lines, one joining to the LE and the other to the TE. Together they form the chord length at that point, tabulated as the definitive chord length which will be used for the mean aerodynamic centre (MAC) and C_{MAC} calculations.

Using the measure tool, each segment was measured and tabulated on Excel. The reference line intervals give displacement in the y-axis, whilst the segments at each interval were tabulated as chord displacement from the reference line; positive for the LE and negative for the TE. The LE and TE values were plotted against the reference line, producing a curve with a shape representing the planform of the wing accurately. Note that the reference line starts at 0 lying on the root chord, which lies on the centre of the fuselage, and increases towards the wing-tip.

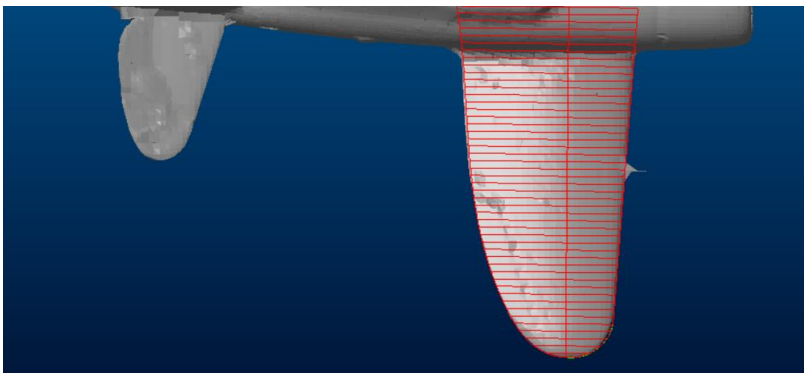

Figure 7 Sectioning of the wing planform

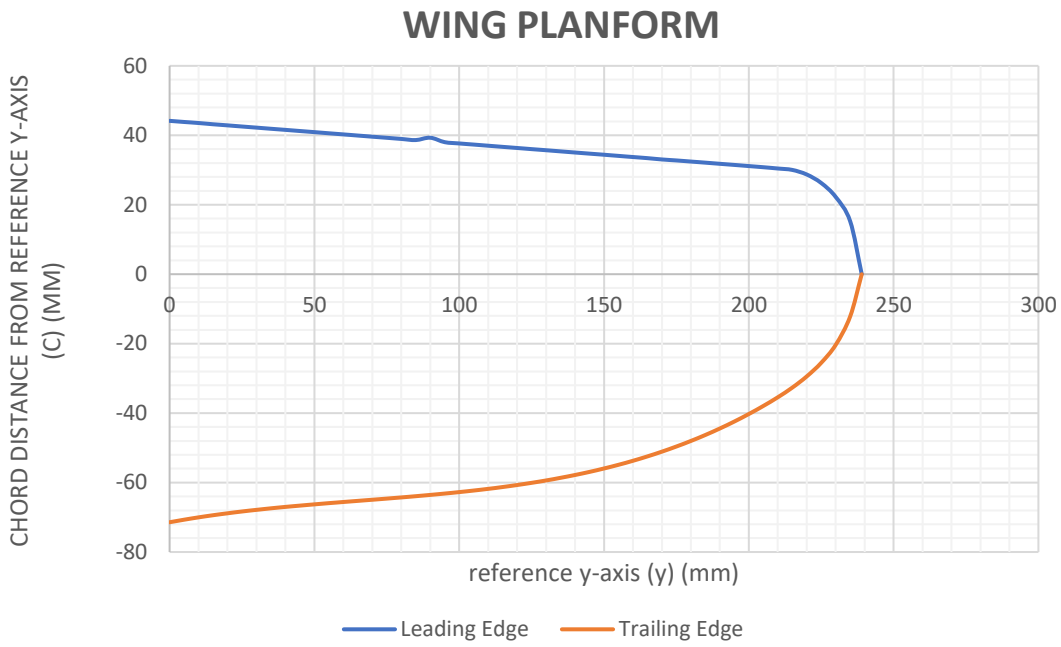

Figure 8 Plotting of the wing sectioning readings

The same exact procedure was applied for the HTU; however, the sectioning was done at different intervals given that it has a simpler shape. This helped to make the process more time efficient and to achieve simpler computations.

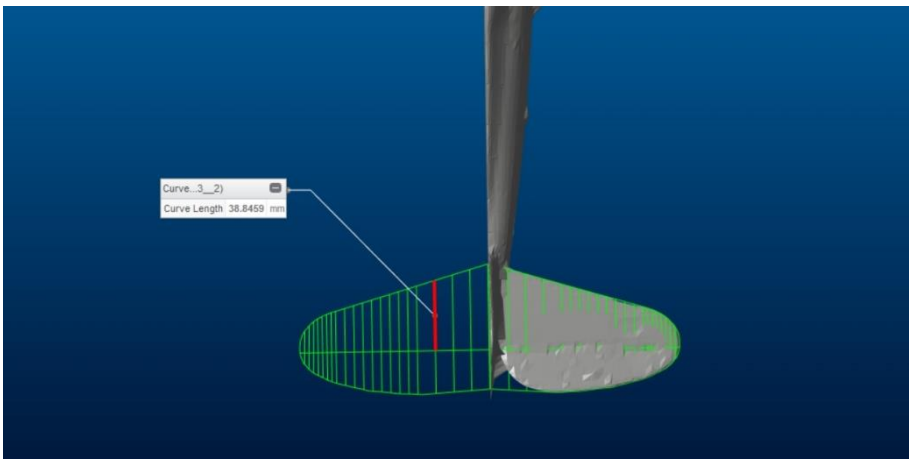

Figure 9 Measurement of a segment in the HTU

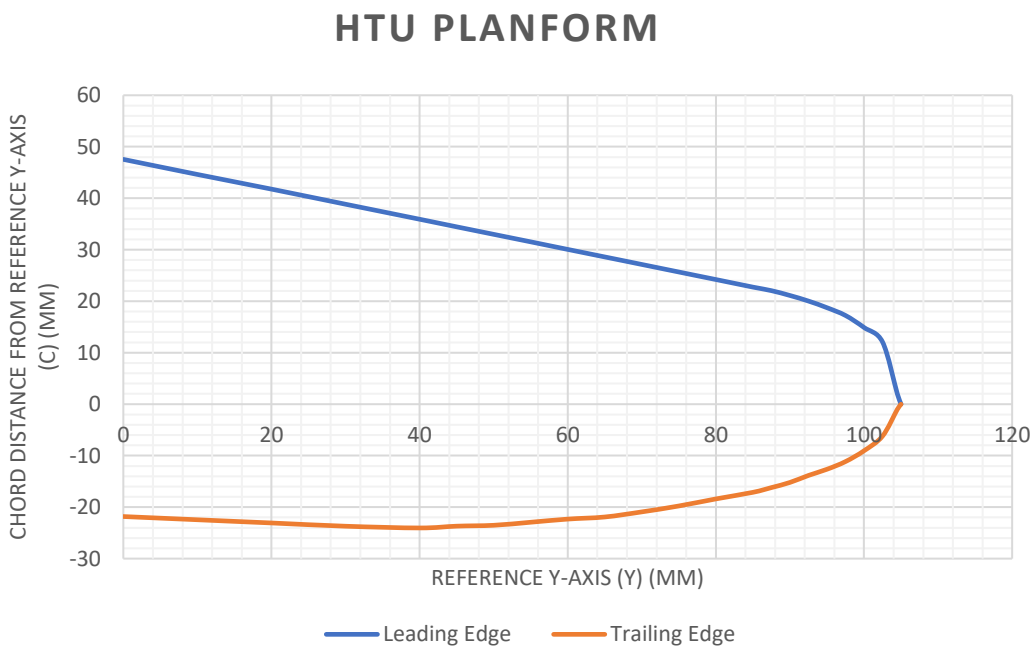

Figure 10 Plotting of the HTU sectioning readings

For both the wing and HTU it can be said that very satisfactory results were obtained as both curves represent almost identically the planform of the respective part.

3.2.3 Horizontal Tail Unit – Elevator Dimensions

The model is required to be tested in the wind tunnel with different angles of the elevator, as it is deemed necessary to study the case at which the highest lift is generated. This feature will be implemented in Glauert III and the geometry acquisition is similar to the acquisition of the planforms.

For Glauert III to depict and compute with the flaps, it requires inputs defining the root and tip location of the flap (elevator) along the wing's length, lift coefficients at root and tip of flap, and chord length in terms of percentage of the whole chord at that section.

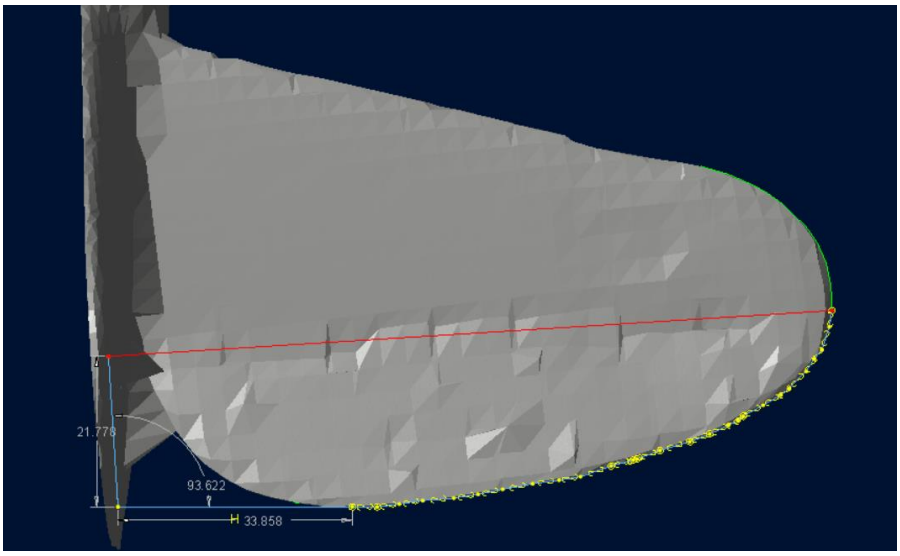

Figure 11 Planform view to measure elevator dimensions

The same planform of the HTU was modified such that it ends along the elevator's pivot edge, and from there measurements could easily be obtained. The percentage chord was considered to be the same along the whole span of the surface, and as at the root the chord of the elevator measures 21.7 mm and the root chord is 69.3 mm, this results in a chord percentage of 31%.

3.3 Other Geometries

3.3.1 Aerofoil Analysis

It must be noted that an assumption of no aerodynamic twist was made for both the wings and the HTU. To determine which aerofoil is used in the model, the method of visual comparison was used, as no other information was provided with regards to the model's aerodynamic properties.

A plane was created alongside the model, and dragged over the wing to section the wing at that instant. Since the 3D scan was not perfect, the wing did not have perfect aerofoils all along, and the location with the best aerofoil was found to be at y=140 mm. The aerofoil's outline at this section was projected to highlight it visually, and placed over several NACA aerofoils.

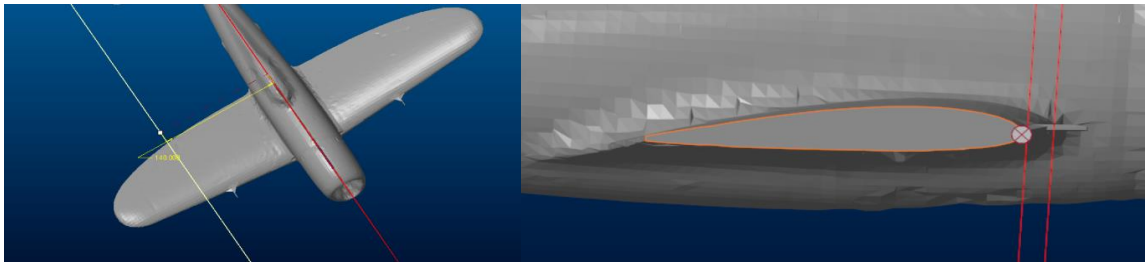

Figure 12 Sectioning the wing at y=140mm

The projection was then placed over a NACA aerofoil and resized in a scaled manner to fit in such a way that the leading and trailing edges respectively lied on top of each other the most aligned possible. As the aerofoil taken from the model had a trimmed TE, this had to be compensated for by placing the aerofoil over the NACA aerofoil in such a way that an imaginary TE would meet at the same place. Figure 13 shows the aerofoil chosen. The red line is the NACA aerofoil generated, NACA2313, and the background is the model's section cut at y=140 mm. Airfoiltools.com was used to generate the different NACA aerofoils.

The aerofoil NACA2313 appeared to fit best with the model's aerofoil, and it was chosen for the proceeding computations.

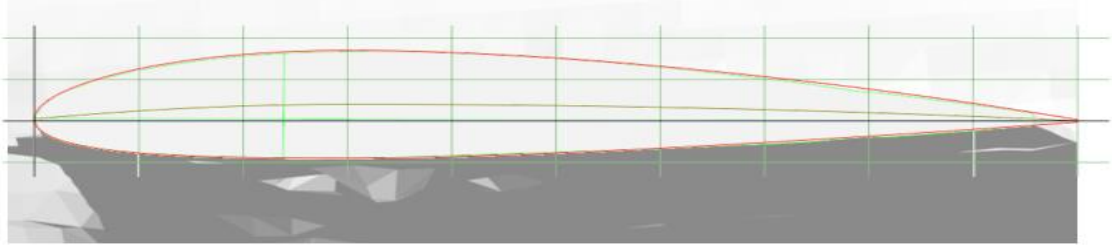

Figure 13 NACA2313 (red) placed on the wing section (background) for comparison.[3]

For the HTU, again, the same procedure was used. The elevator in the scan had a deflection, and to overcome this, a screenshot was used and edited to cut the elevator section and rotated to make a straight HTU.

It must be noted that since the HTU had a more deformed structure, the best aerofoil in the scan still was imperfect, and the selected aerofoil, NACA0005 was the best approximation that could be obtained.

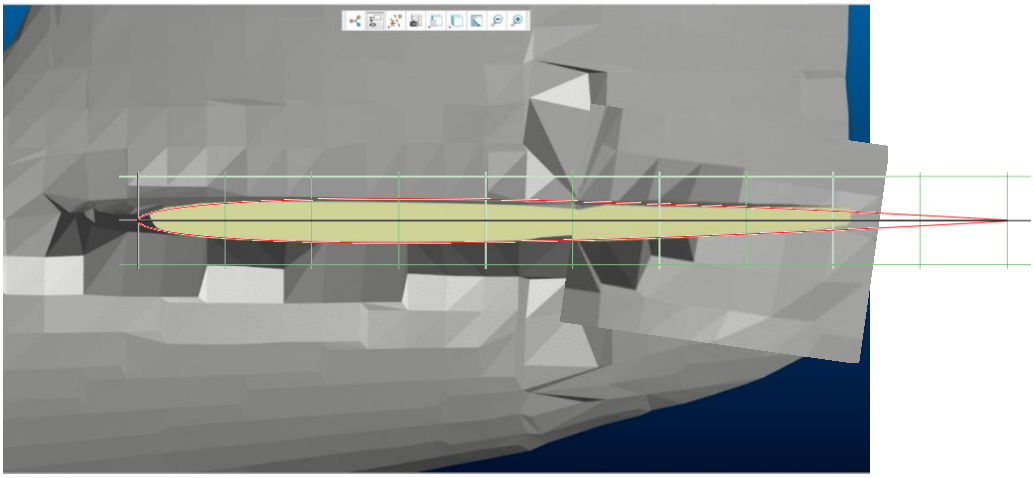

Figure 14 NACA0005 aerofoil(red) on HTU aerofoil section (Background) for comparison [3]

3.3.2 Dihedral Angle

One feature on the model's wing is a dihedral angle. If at a relatively large angle, this angle can affect the measurements read from the top view. Inspection of the dihedral angle resulted in it being small enough to be neglected. The dihedral angle is only 4° to the horizontal, as shown below, and it would leave an insignificant impact on the dimensions.

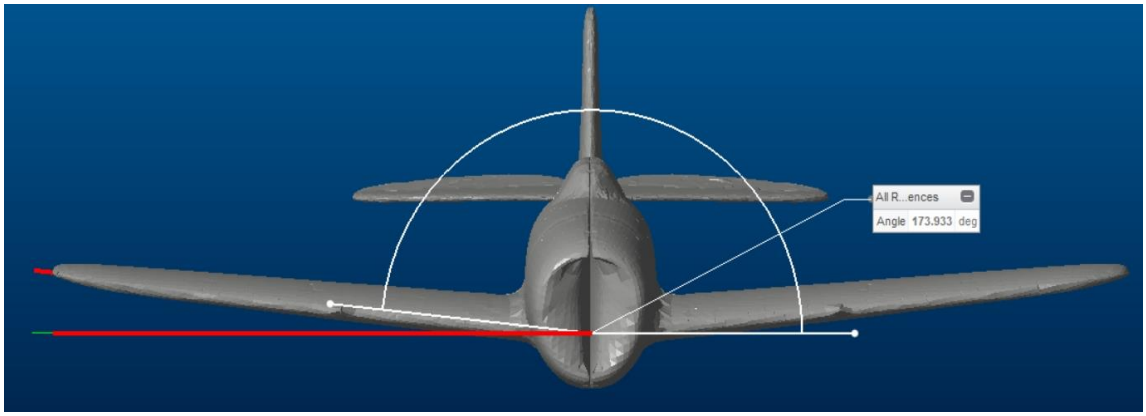

Figure 15 Analysing the dihedral angle

To prove this, consider the wing's actual length to be 'x', using trigonometry to evaluate horizontally (a) it would be:

$$\cos(4) = \frac{a}{x}$$

$$\mathrm{x} * \cos(4) = a$$

But as cos(4) = 0.9976, it could be said that x would be equivalent to a.

The HTU had no dihedral angle.

3.3.3 Wing Twist Analysis

Geometric twist along the wing can be present to enhance the aerodynamic properties of an aircraft. Since a wing twist will alter results, it is important to take it into consideration.

To check for wing-twist, sections of the wings were taken at the root, aerofoil selection (mid) location, and close to the tip. For each section, a chord line was drawn to join the LE to the TE, followed by a horizontal line parallel to the x-axis. The chord line would have a different angle for each aerofoil, given that there will be a wing-twist. The root aerofoil was not taken at the fuselage's centre, as in the 3-D model it would not be visible. The final aerofoil was taken at a distance slightly shorter than that of the wing-tip; due to the elliptical shape an aerofoil at the exact tip would be inexistent.

3.3.3.1 Root Air-Foil

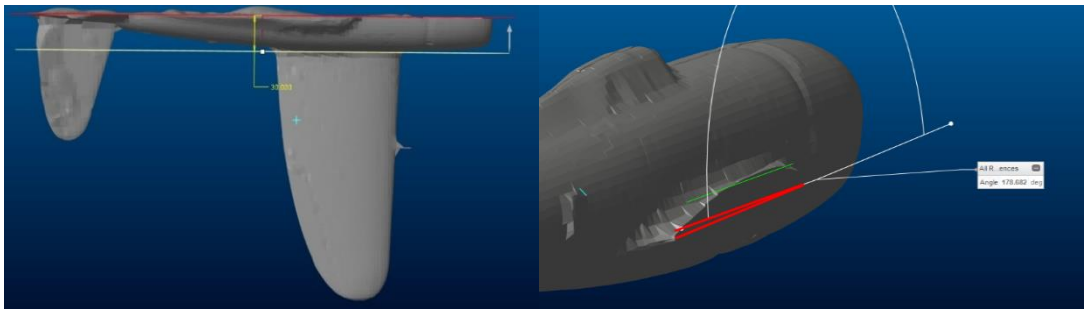

Figure 16 Wing Twist measurement at y=30 mm

3.3.3.2 Mid Air-Foil

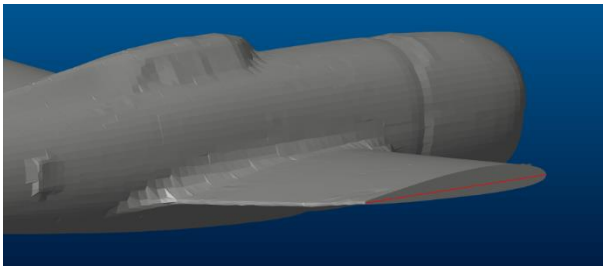

Figure 17 Wing Twist measurement at y=140 mm

3.3.3.3 Wing-Tip Air-Foil

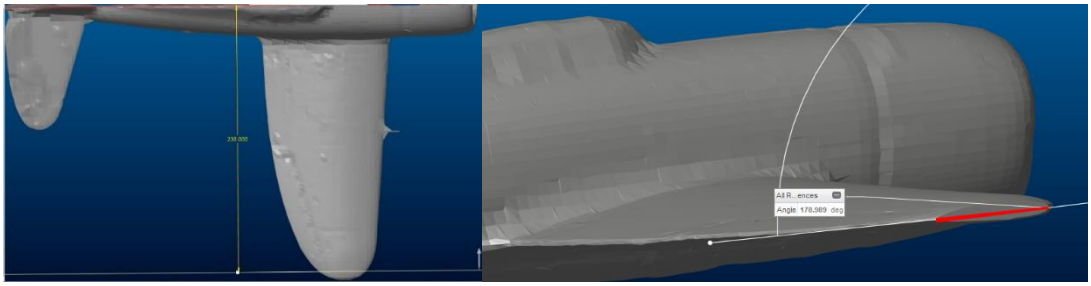

Figure 18 Wing Twist measurement at y=230 mm

At 30 mm from the fuselage centre, the angle to the horizontal was 178.68°, or 1.32°.

At 230mm from the fuselage centre, at close proximity to the wing tip, the angle to the horizontal was found to be that of 178.989°, or 1.011°. However, this is an opposite orientation, therefore it would be -1.011° and meaning that in 200 mm there is a twist of 2.3°.

The physical wing-root was extrapolated to the computational root, which lies on the centre of the fuselage. The section close to the wingtip was extrapolated to the actual wingtip, to a total distance of 239 mm. It was assumed that the twist is taking place uniformly along the wing.

The following calculations were carried out to determine the wing-twist:

$$200\ mm = 2.3°$$

This means there is an increment rate of:

$$\frac{2.3}{200} = \ 0.0115°/\text{mm}$$

At the root the angle is a sum of that measured at 30 mm from the computational wing root plus the product of the increment rate multiplied by the distance of 30 mm:

$$1.32 + (0.0115 * 30) = 1.665°$$

This is considered as a setting angle.

Similarly, at the wing tip, the angle is a subtraction of that measured at 9 mm from the wing-tip minus the product of the increment rate multiplied by the distance of 9 mm:

$$-1.011 - (0.0115 * 9) = -1.1145°$$

As a conclusion, including the setting angle, when the aircraft is flying a perfectly horizontal path, the angles are of 1.665° at the root and -1.1145° at the tip. The total twist is that of 2.77°.

$$Wing\ Twist = 2.77°$$

The difference in sign for computations between root and tip is because the angle is decreasing towards the tip. When the root is considered to have 0°, the wing-tip is to be considered to have -2.77°, therefore the increments are negative.

In Glauert III, the values are inputted such that the wing-root has 0° twist, as the setting angle for now is to be excluded.

3.3.4 Wing Setting Angle

The root of the wing was found to have 1.665° to the horizontal, which is the setting angle. For the computations of the separate wing, it will be considered as 0°, as the angle of the wing to the rest of the plane is irrelevant, however it must be taken into consideration when resolving for the lift the HTU's lift coefficient with respect to the position of the wing. As the HTU lies on the horizontal at 0°, when the wing is at a specific angle of attack (AoA, α), the HTU is experiencing the same AoA minus the setting angle.

For instance, if the computations result in a maximum wing lift coefficient at α=1.665°, at that AoA the HTU would be at 0°, therefore the corresponding lift generated by the HTU when the wing is generating maximum lift is at 0°. Then, the total lift coefficient of the model is the lift coefficient of the wing at 1.665°, plus the lift coefficient of the HTU at 0°.

3.3.5 Fuselage's Surface Area

The surface area of the fuselage is required for the computation of the skin friction drag, the only force required to be computed regarding the fuselage. In order to obtain the surface area, some modifications to the model had to be made.

First off, the model was split into half, for simplifications, and by creating planes and extruding with the option to remove material, the wing and HTU were removed. This left the model with only half of the fuselage.

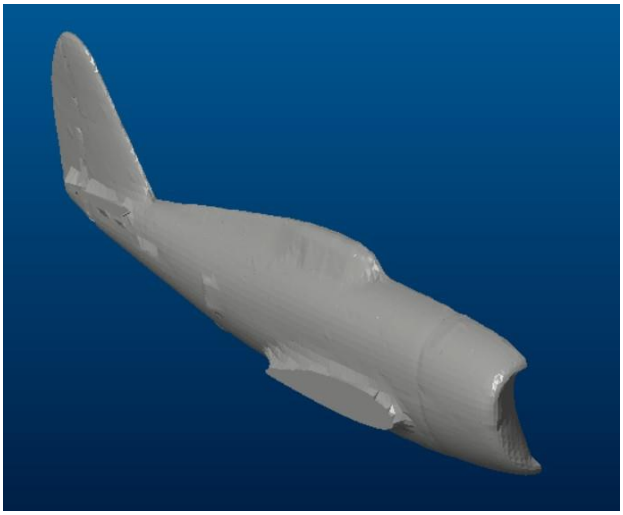

Figure 19 Modified solid model to show only half of the fuselage

Then, using the area measurement function on Creo, the surface area of the selected mesh was given automatically. The area is only an approximation, as the wing and HTU's trimming left holes in the mesh, and the nose was deformed when compared to the actual model. As Figure 20 shows, however, the area not measured across the wing's section is approximately compensated for by the excess mesh at the root.

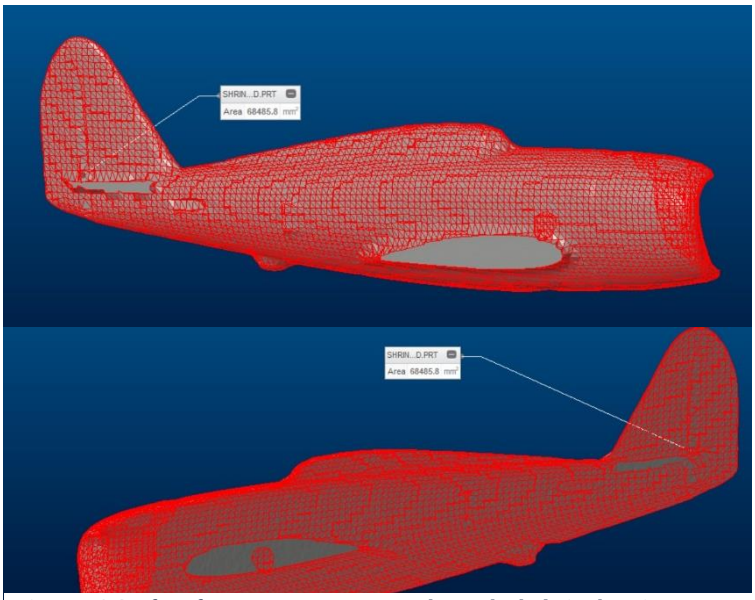

Figure 20 Surface for area measurement, shows the hole in the wing's cross section and the hole on the symmetric plane

The surface along the symmetric plane, which was not required, was not measured because there exists a created surface and not a mesh. The total area would simply be the resulting value multiplied by two.

$$A_{Fuselage} = Area \times 2$$

$$A_{Fuselage} = 136971.6mm^2 = 0.1369716\, m^2$$

4 Theoretical Computations

This section deals with the theoretical computations carried out in the methodological part of the project. The aim here is to serve as a guide to students of the course Aerodynamics I when working on the semesterly project. This is done by providing an estimate of the results that should be obtained practically for both the students and the lecturer, as well as by providing forces which will enable the design and calibration of the wind-tunnel balance for practical testing.

The wing and HTU follow the same path of computations; XFOIL and Glauert III software for data acquisition and analysis, and finally derivation of the Lift, Drag and Pitching Moment for each condition. The boundary conditions are computed after the C_{MAC} is located, so that the Reynolds numbers (RE) can be evaluated at that same chord. The fuselage will be considered to have a negligible lift, and only computations for the drag are carried out.

The computations' methodologies show the procedures and data required for the computations of one condition only for each aerodynamic component and varying set-ups, with the exception of some cases where it is necessary to differentiate between computing for maximum and for cruise lift coefficients. The data required for the rest of the computations is fixed in the respective appendices.

4.1 Mean Aerodynamic Chord (C_{MAC})

C_{MAC} defines the wing's AC, a point at which the lift acting on it can be represented by a continuous pressure distribution over the whole wing surface.

C_{MAC} is essential for the mounting in the wind-tunnel. By locating the C_{MAC}, the quarter chord point can be easily identified to find the wing's aerodynamic centre (MAC). The model can then be stiffened at a location close to the quarter chord point, at which point an insert can be implemented into the model for safe mounting in the wind-tunnel [4][5][6].

4.1.1 Wing

C_{MAC} was obtained using the following equation [4]:

$$C_{MAC} = \frac{2}{A}\int_0^{b/2} c(y)^2\, dy$$

Where:

A_{wing} = Wing Area

c(y) = chord length at current y position

b = Wing span.

In the computation, half of the wing was considered, therefore 2/A was implemented to half the area, and b/2 was implemented to half the span.

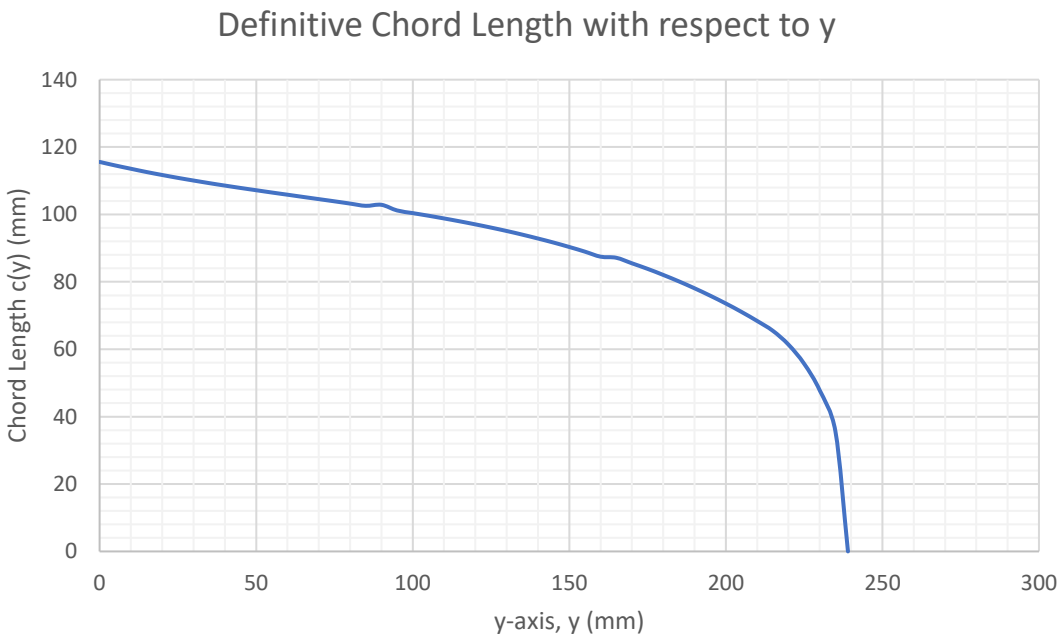

Figure 21 A graph of wing's Definitive Chord Length vs Y: Derived from the Geometry Acquisition section

The limit defined the whole integrating area under the graph of definitive chord length c(y) vs y; however, this integration procedure is carried out in steps, from one chord to another. Hence, when integrating the individual chords, the limit would be from current location of chord in y, to the location of the previous chord. As the wing was sectioned at 5 mm intervals in the y-axis, the limits would be from 5 mm to 0 mm for each chord length.

Solving the integral resulted in:

$$C_{MAC} = \frac{2}{A}(c(y)^2.y)|_0^5$$

Substituting the values in the solved integral equation gave:

$$C_{MAC} = \frac{2}{43272}[c(y)^2.y]|_0^5$$

This equation was applied for each section along the y-axis, at each instance substituting c(y) by the definitive chord length at that position and y by 5 then by 0 as upper and lower limits respectively, and tabulating both results. Note that the lower limit would always result in zero; hence the final result for each integration at the chords would equal the one as given by the upper limit. A summation of all integrals results in the C_{MAC}'s length, which in this case was 95.25 mm. To locate where it would lie on the wing, comparing the result to the planform sectioning tabulation showed that it can be approximated to lie at y=130 mm. The MAC acts at 25 % of the C_{MAC} from the Leading Edge (LE), therefore 23.21 mm from the LE. A virtual line joining perpendicularly the centreline of the fuselage to the AC of the MAC marks the mounting place of the model to be fixed in the wind tunnel [4][5].

25	120	36.35	-60.71	97.06
26	125	36.02	-60.08	96.1
27	130	35.7	-59.4	95.1
28	135	35.37	-58.64	94.01
29	140	35.04	-57.82	92.86

Figure 22 A part of the table of the planform sectioning showing where MAC fits best

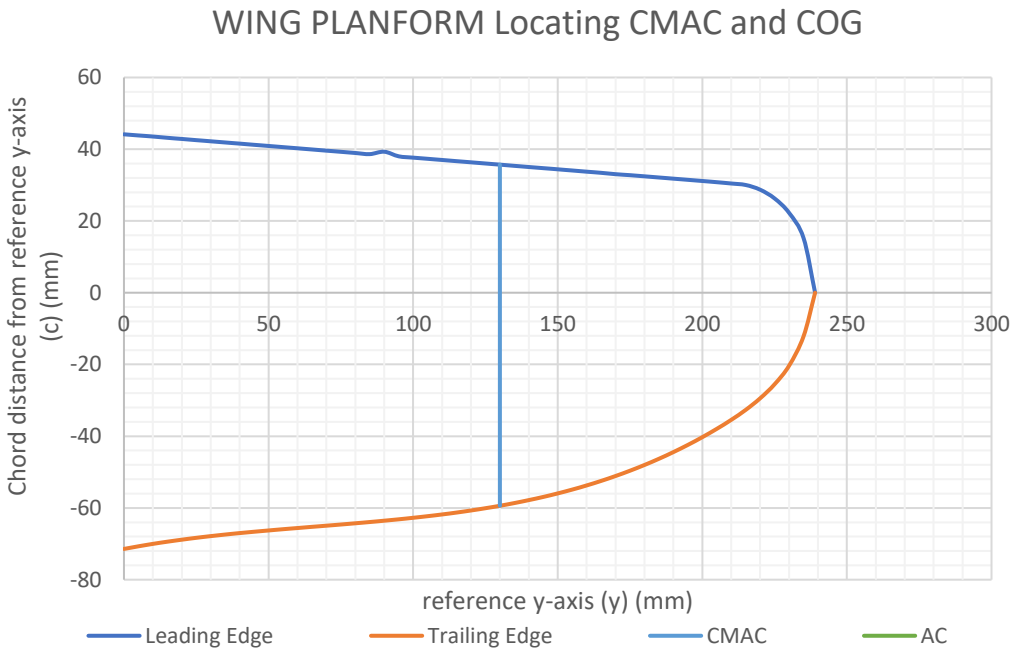

Figure 23 A graph depicting the planform of the wing, representing the MAC and AC

4.1.2 Horizontal Tail Unit

For the HTU, the same exact procedure was followed, with the only difference in the limits of integration. This was due to the fact that the sections were taken at different intervals. The first four sections were taken at 10 mm intervals, the following nine sections were taken at 5 mm intervals and the remaining seven sections were taken at 2.5 mm intervals. As a result, the limits were changed to be from 10 to 0 mm, 5 to 0 mm and 2.5 mm for their respective sections. This was done to obtain a planform as accurate as possible given that the HTU's planform converges at a much faster rate than in the wing.

The C_{MAC} for the HTU resulted in 53.6 mm. From the sections taken, this fits best at y=55 mm. The AC lies at 25% from the LE, therefore at 13.38 mm from the LE.

45	34.45	-23.69	58.14
50	32.99	-23.52	56.51
55	31.53	-22.93	54.46
60	30.06	-22.32	52.38
65	28.6	-21.91	50.51

Figure 24 A part of the table of the planform sectioning showing where MAC fits best

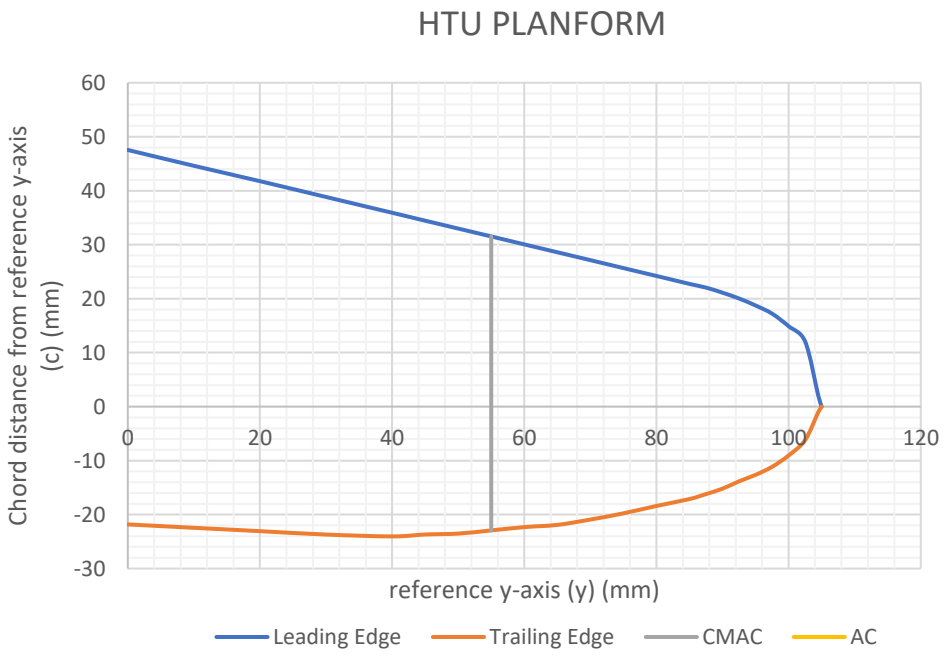

Figure 25 A graph depicting the planform of the horizontal tail unit, representing the MAC and AC

4.2 Boundary Conditions

The Reynolds numbers for the different conditions was calculated based on air's properties at 20°C. A fluids properties calculator was used to obtain the said properties, which would be the same for all conditions. Setting input values as air for fluid, 20°C for temperature and 5 for decimal placing, the results shown in Figure 26 were obtained [7]:

Results		
Density:	1.2047	(kg/m^3)
Dynamic Viscosity:	1.8205E-5	(kg/m.s)
Kinematic Viscosity:	1.5111E-5	(m^2/s)
Specific Heat: c_p	1.0061E+3	(J/kg.K)
Conductivity: k	0.025596	(W/m.K)
Prandtl number:	0.71559	
Thermal Diffusivity:	2.1117E-5	(m^2/s)
Thermal Expansion Coefficient:	3.4112E-3	(1/K)

Figure 26 Results table showing air's properties at 20°C [7]

The next step was to set the boundary conditions. It was decided to try four different velocities at which the model could be tested in the wind-tunnel, hence methodological computations would be carried out for each condition to determine which one would work best for the model in question.

The velocities chosen were 10 m/s, 20 m/s, 30 m/s and 45 m/s.

RE was determined for each velocity using the equation:

$$Re = \frac{\rho v l}{\mu} = \frac{v l}{\nu}$$

Where, l=characteristic length (chord length of aerofoil), ρ=density of fluid, μ=dynamic viscosity of fluid, ν=kinematic viscosity of fluid and v=velocity of fluid. On the right-hand side of the equation, everything is a constant for air at 20°C except for v, which is the factor affecting the different boundary conditions.

For chord length, l, the C_{MAC} of the wing, 0.095 m, was chosen assuming that the RE along the wing would not change significantly, and the change would result in negligible differences in results.

Table 2 shows the boundary conditions obtained.

Table 2 Boundary Conditions

VELOCITY	10 M/S	20 M/S	30 M/S	45 M/S
REYNOLDS NUMBER	*62868*	*125736*	*188604*	*282906*

Having obtained these results, the next step of generating aerodynamic data on XFOIL was possible.

4.3 2D Aerofoils - XFOIL

As defined by the User Guide, "XFOIL is an interactive program for the design and analysis of subsonic isolated aerofoils. It consists of a collection of menu-driven routines which perform various useful functions…" [8].

XFOIL was of high priority in this project, in the sense that it was used to generate tabulations of lift coefficients, moment coefficients, drag coefficients and their respective angles of attack for every boundary condition, and for each different aerofoil set-up (Wing and HTU). The values obtained through the use of XFOIL are used as inputs in Glauert III as well as used in computations with the results of Glauert III to determine the lift, drag and moment coefficients distributions over wing/HTU.

4.3.1 Wing

The first step before using XFOIL was to determine the aerofoil section, which was explained already in the Model Geometry Acquisition section. However, one geometric property which has so far been ignored was the TE thickness.

Using the measure function on Creo Parametric 3.0, at y=140 mm (the same section used to analyse the aerofoil), it was found that the wing's TE had a thickness of approximately 1.5 mm. The thickness was found to be approximately uniform along the whole wing.

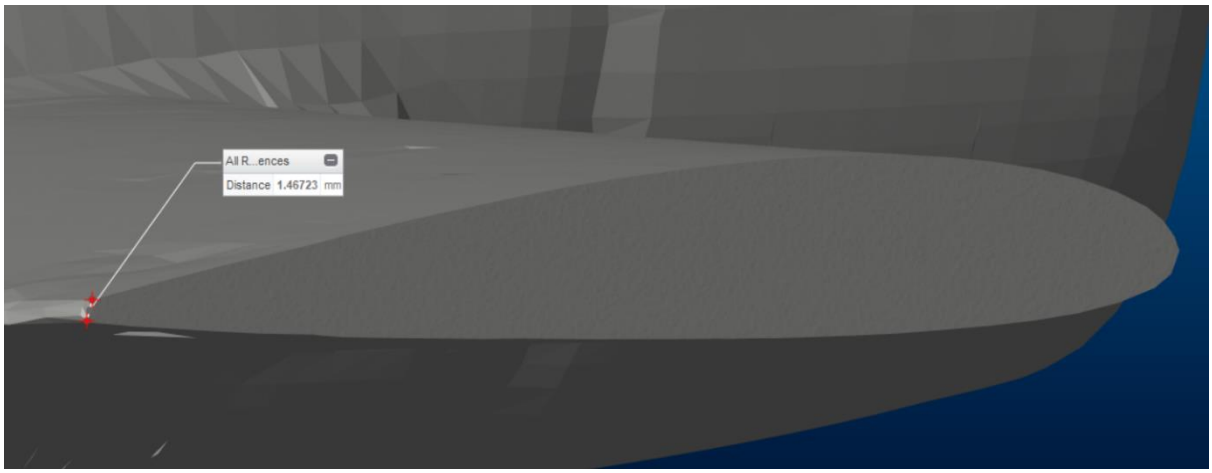

Figure 27 Measuring the Thickness of the Trailing Edge

A small modification of the aerofoil loaded in XFOIL was subsequently required. The aerofoil NACA2313, as loaded on XFOIL, has negligible thickness as the TE converges into a point. To solve this, a specific command GDES→TGAP was used. As XFOIL works in terms of percentage of the chord, in such a way that the chord of the aerofoil in question is considered as 1, then, other dimensions are taken as a fraction of a whole [8].

In this case, the TE thickness in XFOIL should be represented as follows:

$$Chord: 95.25\ mm = 1$$

$$Trailing\ Edge_{Thickness}: 1.5 = ?$$

$$\frac{Trailing\ Edge_{Thickness}}{C_{MAC}} = \frac{1.5}{95.25} \times 1 = 0.0157$$

XFOIL asked to enter the new gap, 0.0157, followed by blending distance which should be 1 given that the thickness modification lies only at the end of the aerofoil. The aerofoil was then re-scaled such that the distance from the LE to the new TE is set again to 1 automatically.

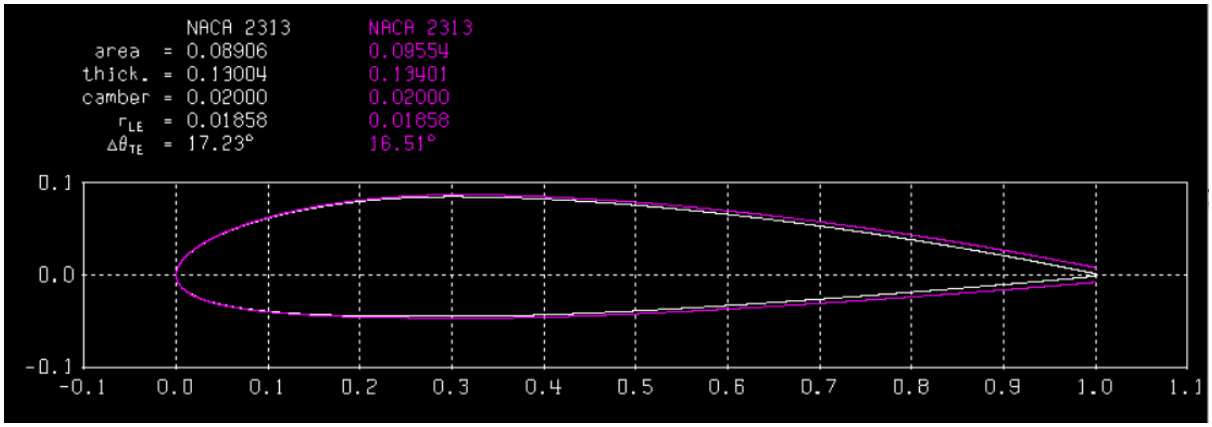

Figure 28 XFOIL screenshot showing the original NACA2313(white) and the newly modified aerofoil(purple)

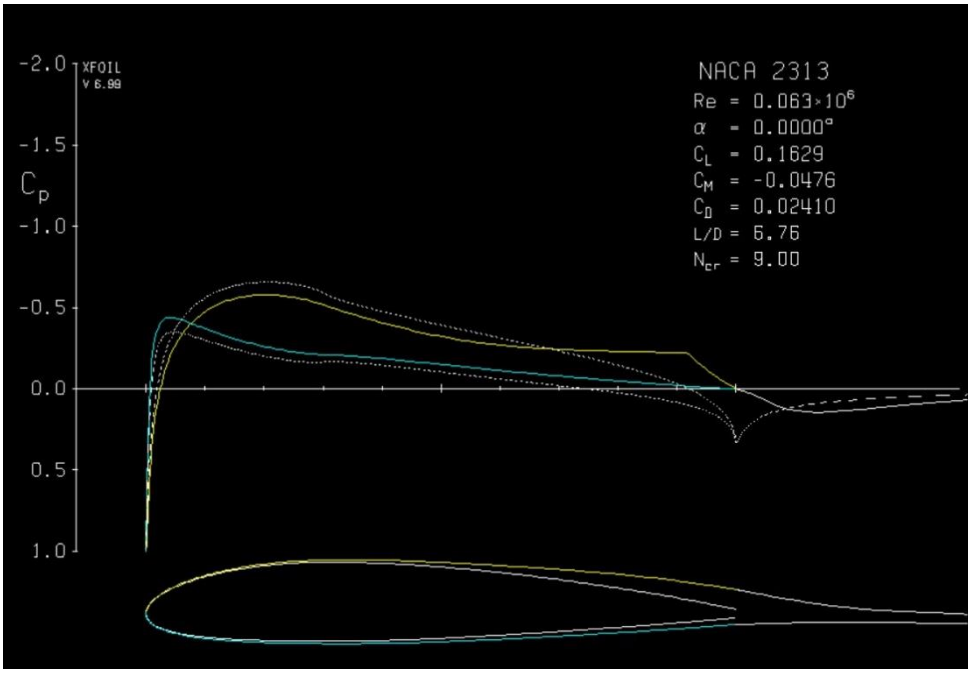

Figure 29 XFOIL screenshot of aerodynamic characteristics at Re=62868

As can be seen from Figure 28, should the modified aerofoil's TE be extended to converge to a point, it would still be a NACA2313 aerofoil, just on a bigger scale, as in our case.

It was important to save the buffer aerofoil to be used as the current aerofoil through the eXec command whilst still under the .Gdes sub-menu. XFOIL could be used to obtain the aerodynamic characteristics for each boundary condition. Under the OPER function, the RE was inputted, number of iterations was increased for more accurate readings, and the AoA was set to zero to compute aerofoil characteristics at a neutral position. XFOIL then printed the characteristics automatically as in Figure 29 [8].

CPWR function was used to store pressure coefficient distribution into a file, and then ASEQ command was used to compute a sequence of angles of attack and provide aerodynamic properties for each AoA [8].

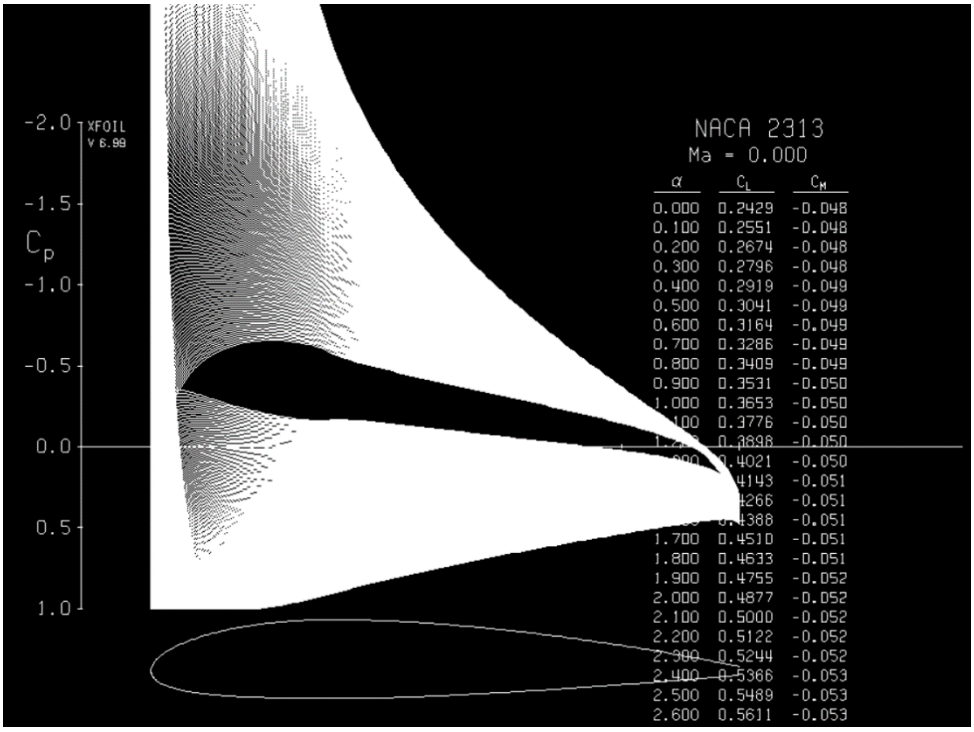

Figure 30 XFOIL screenshot showing a graph of Pressure Coefficient vs Chord changing with α. A tabulated list of computed parameters is also visible in the background.

The data generated was stored in a text file, which could then be loaded into Excel for analysing. Figure 31 shows a sample of the table generated on Excel for the first boundary condition:

XFOIL	Version	6.99					
Calculated	polar	for:	NACA	2313			
1	1	Reynolds	number	fixed	Mach	number	fixe
xtrf	=	1	(top)	1	(bottom)		
Mach	=	0	Re	=	0.063	e	

alpha	CL	CD	CDp	CM	Top_Xtr	Bot_Xtr
0	0.163	0.0241	0.0153	-0.048	0.9188	1
0.1	0.185	0.0241	0.0152	-0.05	0.9122	1
0.2	0.208	0.024	0.0151	-0.052	0.9059	1
0.3	0.231	0.0239	0.015	-0.054	0.8997	1
0.4	0.254	0.0238	0.0148	-0.057	0.8936	1
0.5	0.277	0.0236	0.0146	-0.059	0.8881	1
0.6	0.296	0.0235	0.0145	-0.06	0.8811	1
0.7	0.314	0.0234	0.0144	-0.061	0.874	1
0.8	0.331	0.0233	0.0142	-0.062	0.8668	1
0.9	0.348	0.0232	0.0141	-0.063	0.8595	1
1	0.364	0.0231	0.014	-0.064	0.8521	1
1.1	0.379	0.023	0.0139	-0.064	0.8447	1
1.2	0.393	0.0229	0.0138	-0.064	0.8371	1
1.3	0.407	0.0228	0.0137	-0.065	0.8296	1
1.4	0.42	0.0228	0.0136	-0.065	0.822	1
1.5	0.433	0.0227	0.0135	-0.065	0.8145	1
1.6	0.445	0.0226	0.0134	-0.065	0.8069	1
1.7	0.457	0.0226	0.0134	-0.064	0.7995	1
1.8	0.469	0.0226	0.0133	-0.064	0.7922	1
1.9	0.481	0.0225	0.0132	-0.064	0.785	1

Figure 31 Excel Screenshot of XFOIL data for Re=62868

Having generated this table, three aerodynamic curves could be plotted followed by three important parameters. Firstly, the graph of lift coefficient against AoA is generated, depicted in Figure 32, which is of utmost importance to obtain the maximum lift coefficient (C_{Lmax}), the gradient C_L- α and the value of C_L at zero α (α_0) [5].

The aerofoil maximum lift coefficient, C_{Lmax}, could be easily read as the peak of the curve, in this case C_{Lmax}=1.36.

Similarly, α_0 could be read at the intersection with the x-axis, giving a value of α_0=-0.7.

The gradient, however, required a small computation:

$$C_L\alpha = \frac{(C_{L2} - C_{L1})180}{(\alpha_2 - \alpha_1)\pi}$$

It was important to convert to radians by the 180/pi. Solving from C_{Lmax} to C_{L0} resulted in $C_L\alpha$=6.12.

All three values are required as inputs in Glauert III.

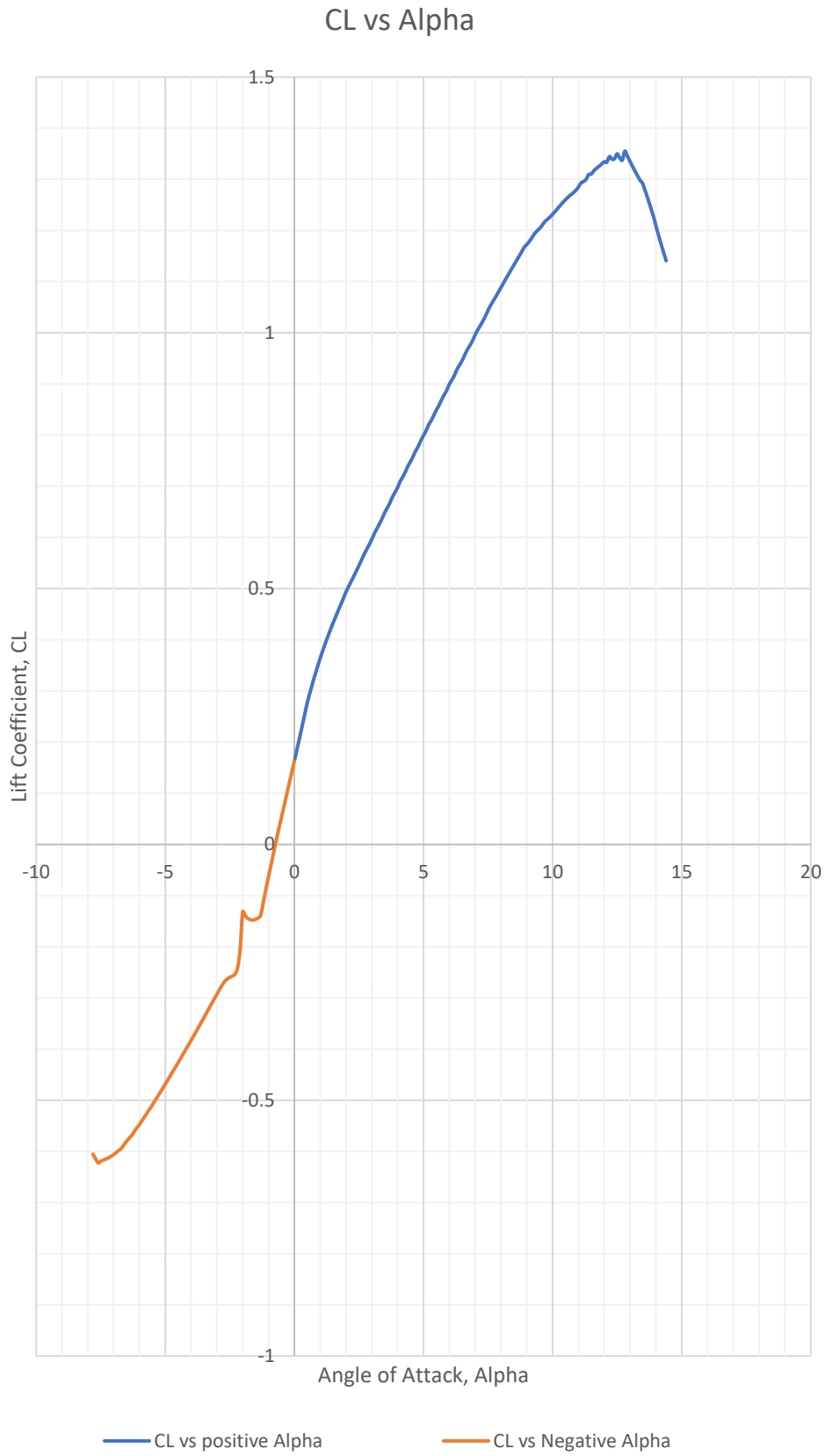

Figure 32 NACA2313's C_L vs Alpha graph at Re=62868

Two more graphs which were useful in the following computations were those of lift coefficient versus drag coefficient (C_L-C_D) as can be seen in Figure 33, and lift coefficient vs pitching moment coefficient (C_L-C_M) as shown in Figure 34.

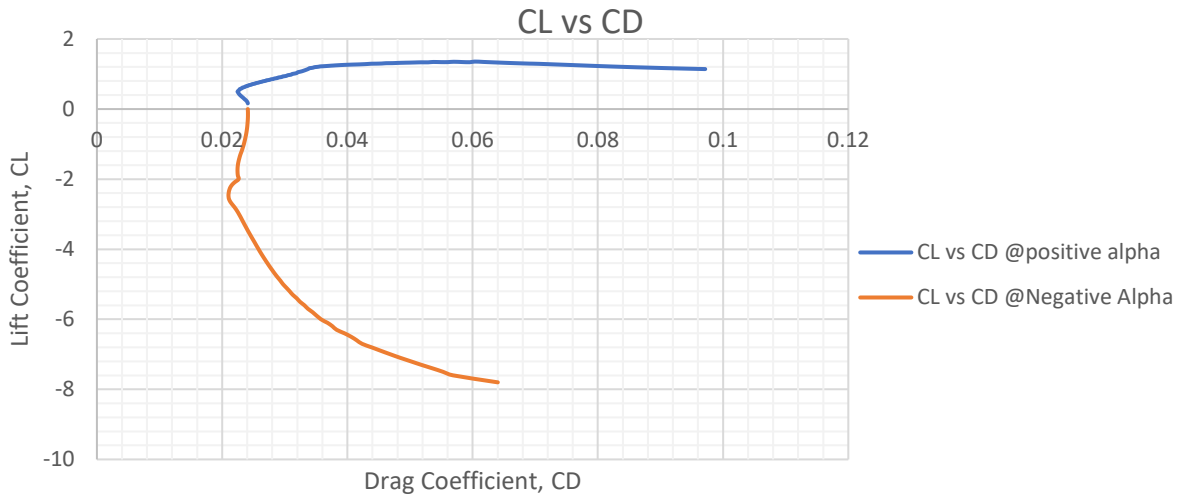

Figure 33 NACA2313's C_L vs C_D graph at Re=62868

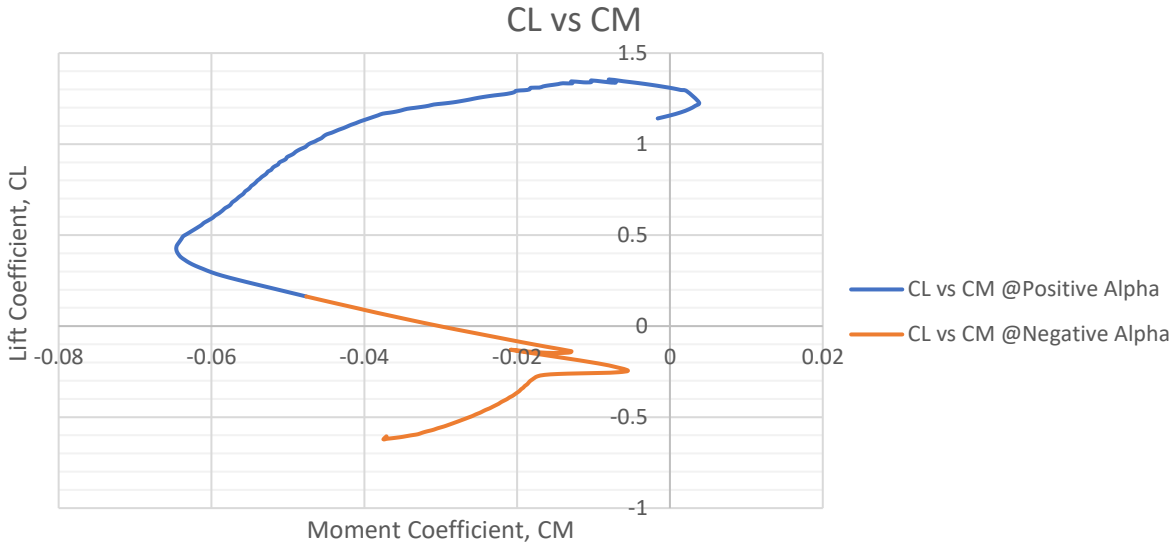

Figure 34 NACA2313's CL vs CM graph at Re=62868

This procedure was repeated for the other three boundary conditions, and the results in Table 3 were obtained:

Table 3 NACA2313's Aerodynamic Properties as derived through XFOIL

REYNOLDS	**62868**	**125736**	**188604**	**282906**
C_{LMAX}	1.36	1.33	1.40	1.39
A_0	-0.70	-1.60	-2.00	-2.10
C_{LA}	6.12	4.48	4.62	4.18

4.3.2 Horizontal Tail Unit – No Elevator

The same exact procedure as for the wings was carried out for the HTU, with the only difference of using the NACA0005 aerofoil instead. The TE was modified in the same manner, but with a different value of 0.026. Upon initial inspection, the HTU can be said to resemble a plate more than an aerofoil. XFOIL immediately proved this. Under the first boundary condition, results were given without a problem, however at higher Reynolds numbers, XFOIL failed to converge results, which might have been because of the very sharp LE and respectively thick TE.

This meant that no accurate values for aerodynamic properties generated by XFOIL could be obtained at the last three boundary conditions, as the resulting data was insufficient. Given that the HTU's aerofoil and planform areas were relatively smaller than the wing's, the lift, moment and drag generated by the wings and fuselage would reduce those generated by the HTU to negligible, therefore it was assumed that it is safe to use parameters for the HTU as obtained only at RE=62868 throughout the computations. The same lift curve was used to find the respective HTU's lift coefficient relative to the wing's AoA at all wing's conditions, whilst the drag and moment coefficients are taken as the same value for all conditions.

Figures 35, 36 and 37 show the aerodynamic curves for NACA0005 with at Re=62868 without an elevator deflection.

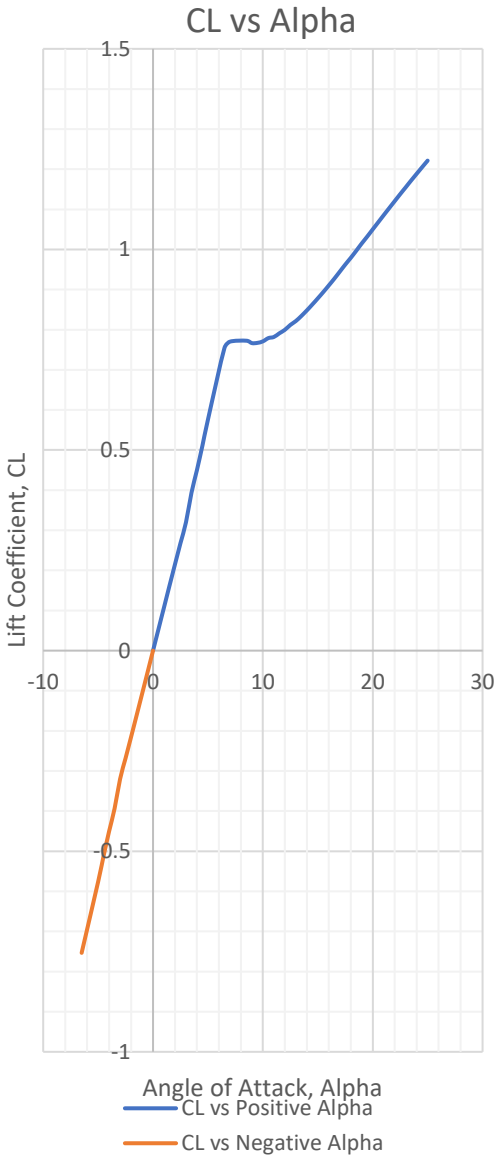

Figure 35 NACA0005's CL vs Alpha graph at Re=62868 [No Elevator Deflection]

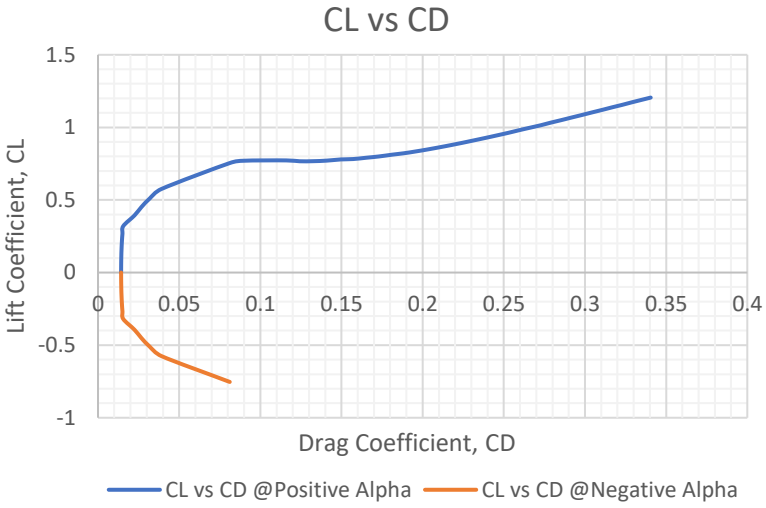

Figure 36 NACA0005's C_L vs C_D graph at Re=62868 [No Elevator Deflection]

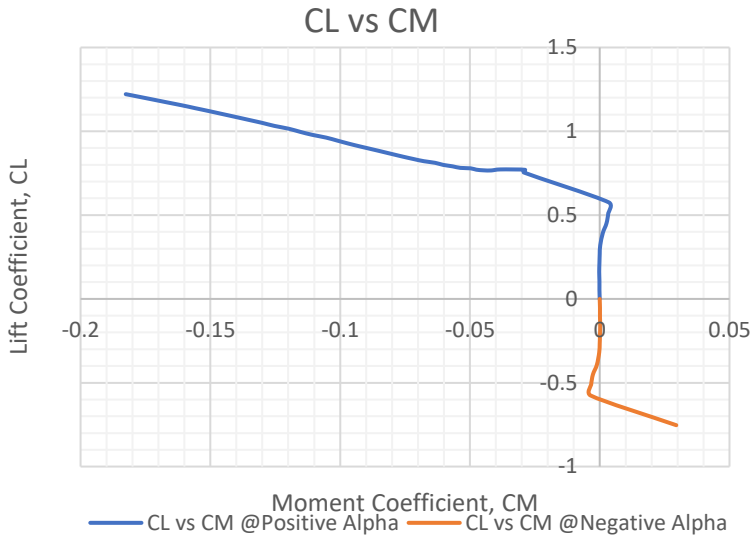

Figure 37 NACA0005's C_L vs C_M graph at Re=62868 [No Elevator Deflection]

4.3.3 Horizontal Tail Unit – Elevator 15°

In order to analyze the aerodynamic properties better, it was required to test the model at the condition when it would be generating maximum lift, that is with the elevator activated in a way that it would make the plane increase altitude when in flight. Whilst the overall procedure in computations was the same, some modifications were required in XFOIL and Glauert III. In XFOIL, under the .GDES sub-menu, after the TE has been modified, the command FLAP rrr was used to set and deflect a flap on the aerofoil loaded. XFOIL asked to enter flap hinge x location 69 % from the LE. The input in XFOIL should therefore be 0.69 [8].

The next information to input was flap hinge y location, which should be 0 given that 0 lies on the centre line of the aerofoil and there was an assumption that it is hinged at the middle. The final input was the deflection in°, which should be negative fifteen since the elevator was required to be deflected upwards. The resulting aerofoil is shown in Figure 38. The command eXec was given to save the aerofoil as the current one and the procedure as for the previous aerofoil could then be continued [8].

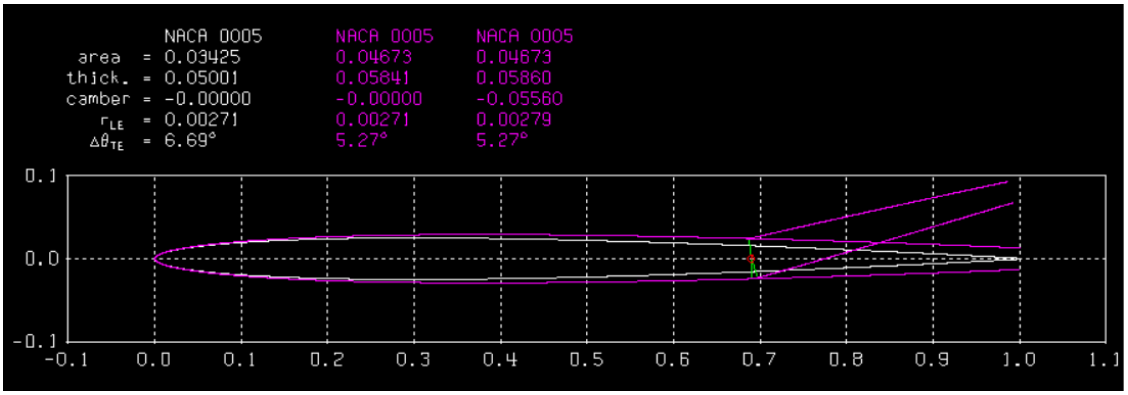

Figure 38 XFOIL modification of the trailing edge and elevator deflection

A deflection of 30° was also tested, however XFOIL was once more failing to converge.

Figures 39, 40 and 41 show the aerodynamic curves for NACA0005 with an elevator deflection of -15° at Re=62868.

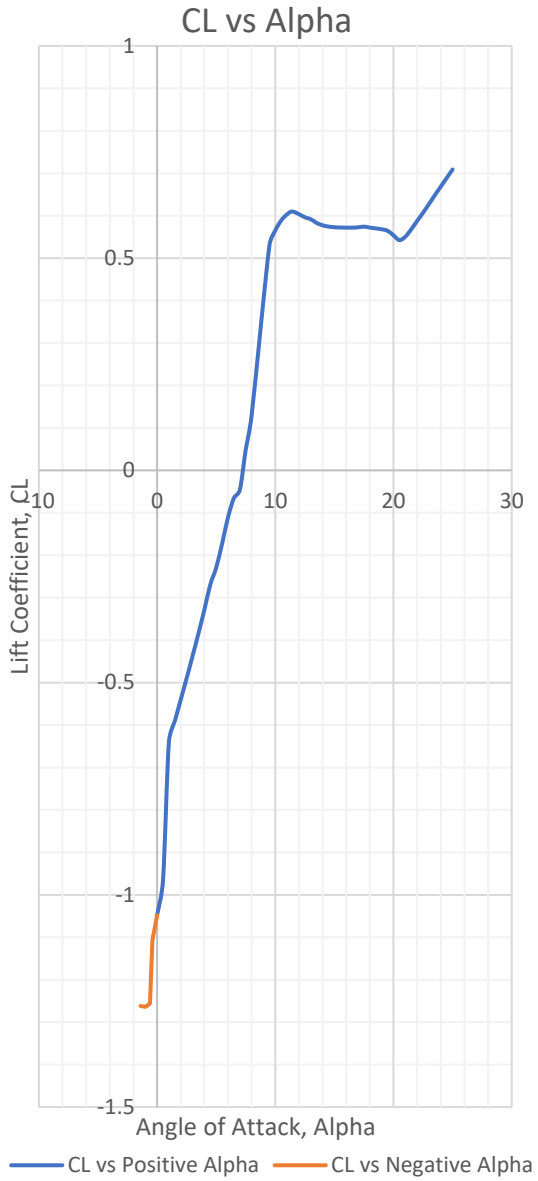

Figure 39 NACA0005's CL vs Alpha graph at Re=62868 [Elevator Deflection -15°]

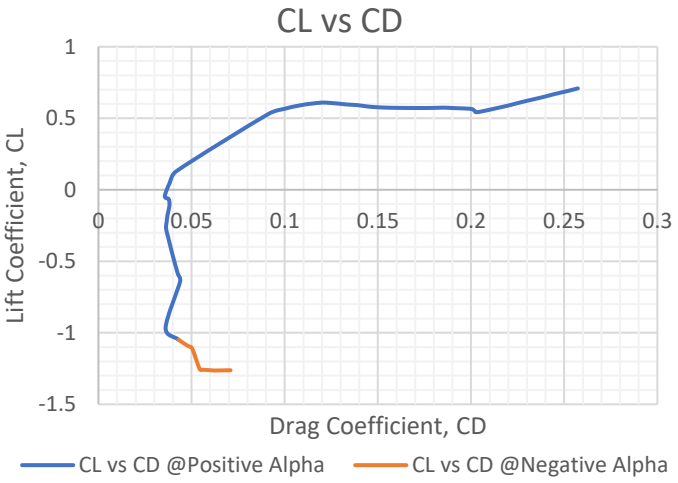

Figure 40 NACA0005's C_L vs C_D graph at Re=62868 [Elevator Deflection -15°]

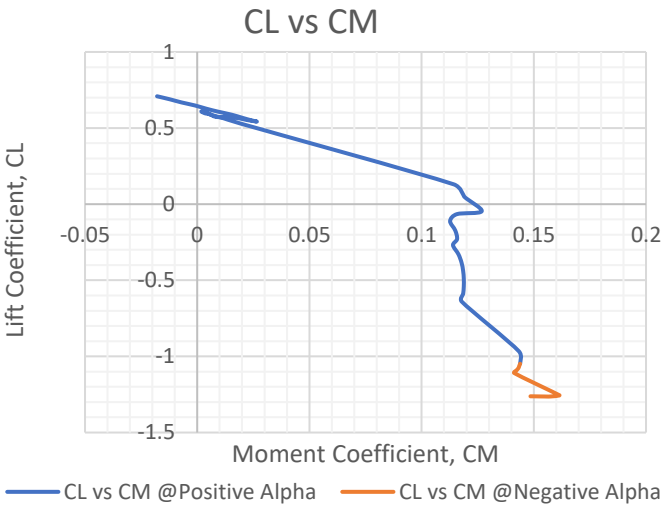

Figure 41 NACA0005's C_L vs C_M graph at Re=62868 [Elevator Deflection -15°]

Table 4 Horizontal Tail Unit's Aerodynamic Properties as derived through XFOIL, RE=62868

DEFLECTION	**0°**	**15°**	**30°**
C_{LMAX}	0.77	0.610	N/A
AOA_0	0	7.25	N/A
C_L-AOA	6.3	10.123	N/A

Table 4 shows the resulting properties for different set-ups of the HTU at RE=62868.

The resulting graphs for both the wing's and HTU's aerofoils at each boundary conditions can be found in Appendix A.

4.4 Finite Wings - Glauert III

Having obtained the graphs for C_L-α, C_L-C_M and C_L-C_D and derived the C_{Lmax}, α_0 and $C_L\alpha$ for each aerofoil, the next step in the computational part could be initiated. This brought about the use of Glauert III, a software developed within the Brno University of Technology itself. Glauert III is a tool for lift distribution calculation along the whole wing using the so called Glauert method. The program can be primarily used as a source of entry data for following wing structural calculations. The secondary use is the preliminary aerodynamic wing design [9].

This part aimed at generating the wing lift distribution, which helped in understanding the conditions for flow separation and through which the wing drag coefficient, C_{Dwing}, and wing moment coefficient, C_{Mwing}, were computed. It also involved the generation of the wing lift curve properties $C_{Lwingmax}$, α_{0Wing} c_{Lwing}-α which were used to plot the wing lift curve itself. The wing induced drag coefficient, C_{Di}, was also a given result, which was required to compute the maximum drag coefficient, C_{Dmax}.

The wing lift curve was used to locate the AoA at which the maximum wing lift coefficient existed, and by using the same AoA on the HTU's wing lift curve, the respective lift coefficient could be found. For the wing, this could be done for every boundary condition, however, for the HTU only the first boundary condition was used, for the aforementioned reason in the XFOIL's HTU section. It was necessary to compute different cases of the HTU having the elevator deflected at 0° and at 15° to study the case at which the highest lift is required [9].

For each boundary condition, Glauert III was set to solve for maximum lift conditions, $C_{Lwingmax}$, and for cruise conditions with $C_{Lcruise}$=0.2. Cruise condition was required for two main reasons; data range and resolution. Computing for cruise speeds wiould therefore allow for better wind-tunnel balance calibration, as well as aid in results by providing a wider range of conditions to be tested at the wind-tunnel.

4.4.1 Wing - $C_{Lwingmax}$

The first thing done in Glauert III was set the wing's parameters. Half of wingspan was set to 0.239, as measured on the generated CAD model, Geometric Twist was set to yes since there was found to be a twist, and number of breaking lines was set to 30, which represents sections along they y-axis of the wing.

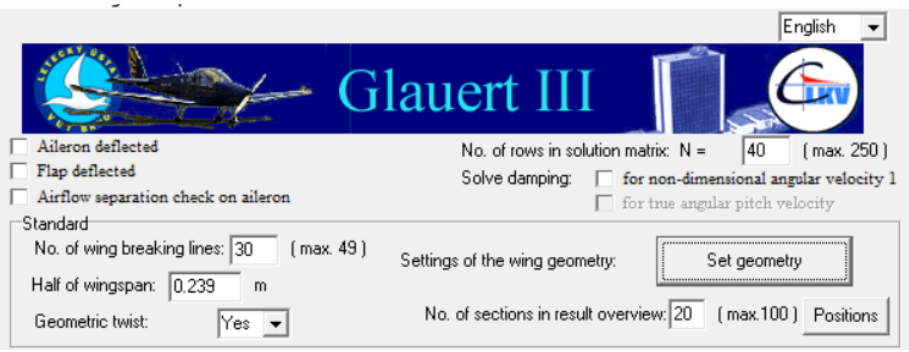

Figure 42 Glauert Screenshot of the wing's parameters

Set Geometry opened a new window, which prompts the user to input more detailed information regarding the wing, and here is where the XFOIL results were used.

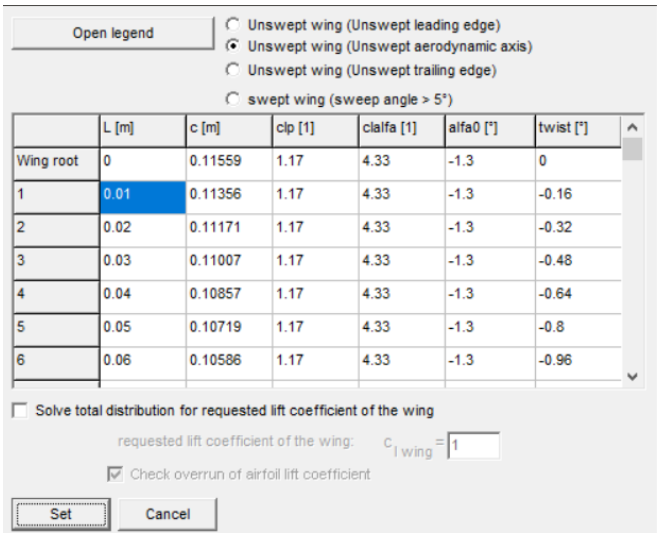

	L [m]	c [m]	clp [1]	clalfa [1]	alfa0 [°]	twist [°]
Wing root	0	0.11559	1.17	4.33	-1.3	0
1	0.01	0.11356	1.17	4.33	-1.3	-0.16
2	0.02	0.11171	1.17	4.33	-1.3	-0.32
3	0.03	0.11007	1.17	4.33	-1.3	-0.48
4	0.04	0.10857	1.17	4.33	-1.3	-0.64
5	0.05	0.10719	1.17	4.33	-1.3	-0.8
6	0.06	0.10586	1.17	4.33	-1.3	-0.96

Figure 43 Glauert Screenshot of Set Geometry window

L is the distance from the computational root to the current section, c is the chord at the current section. XFOIL's generated results are inputted here; clp is C_{Lmax}, clalfa is $C_{L}\alpha$ and alfa0 is α_0. Twist refers to the geometric twist, and here it was assumed that from the root to the tip the increment is uniform. The setting angle was ignored, and it was considered that the wing has 0 setting angle at the root. It was set in negative as requested by standard, described in the Figure 44 as provided by Glauert III [9].

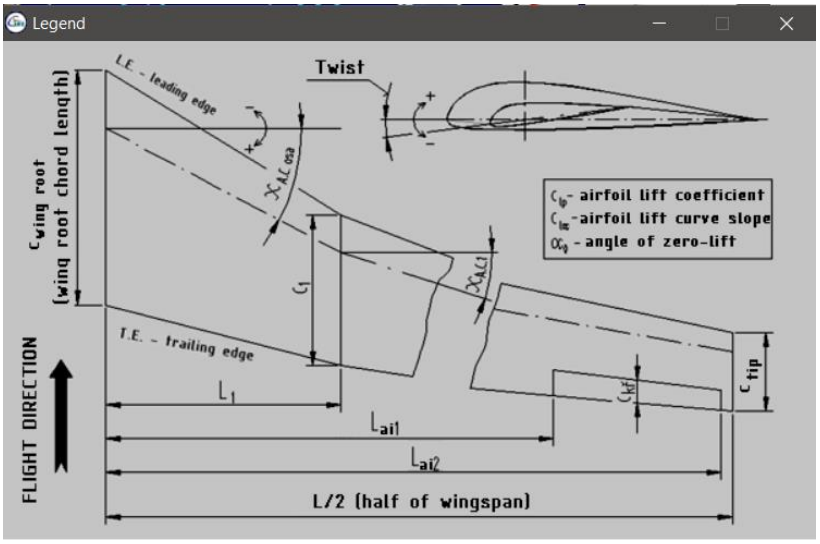

Figure 44 Glauert III Set Geometry Legend

Finally, clicking set and then solve opened the results window showing the Wing Planform as visualised by Glauert III. Figure 45 shows that Glauert' s depiction of the planform is relatively accurate, and satisfactory for this project [9].

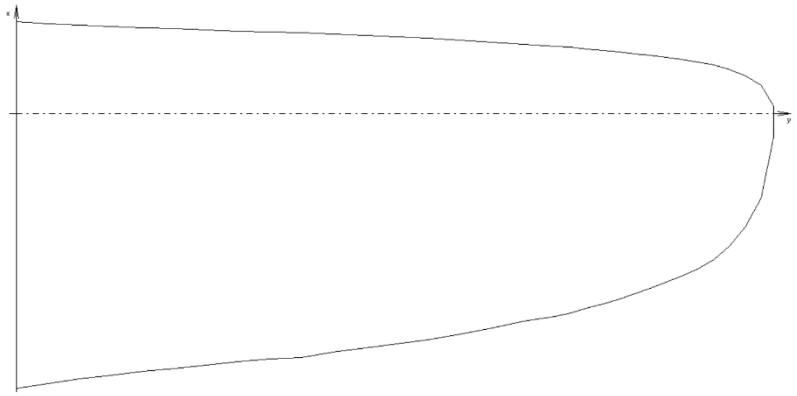

Figure 45 Wing Planform's result by Glauert III

Clicking on the Lift Distribution tab showed the graphs of lift coefficients against y-axis, from which the user can determine where the boundary layer separation occurs along the wing's span.

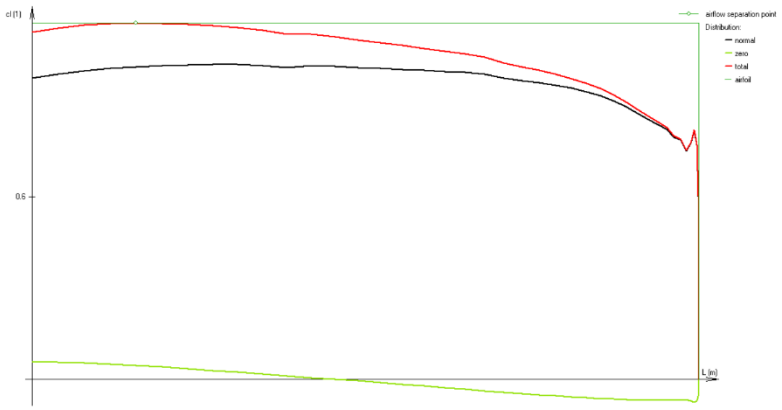

Figure 46 Wing Lift Distribution when solving for maximum lift coefficient

Figure 46 shows a point, close to the fuselage, where separation of flow occurs. The wing of the model is overall elliptical, and one would expect separation to occur across the whole span, making it susceptible to stalls. However, due to the modified planform, mainly the straight LE, as well as the geometric twist, the properties change to resemble a combination of a tapered and elliptical wing, thus improving the aerodynamic properties [5][6][9].

Finally, the Results tab effectively contained the data that is mostly required as can be observed in Figure 47. The results could be exported in text and imported in Excel, as in Table 5, for evaluation and further computations in a similar way the XFOIL results were manipulated.

Results overview:

Area of the wing S = 0.044 m2
Aspect ratio Lambda = 5.213
Max. lift coefficient of the wing is Clwingmax = 1.0944
Lift curve slope of the wing = 3.4121 rad-1
Angle of zero-lift coefficient (in the wing root) Alfa0wing = 0.3614 ° (without the influence of flaps and ailerons)
Glauert coefficient delta = 0.008 (for the calculation of induced drag - calculated from normal distribution)
Induced drag coefficient Cxi = 0.0737 (for the lift coefficient of the wing Clwing = 1.0944)

theta	z	c	cln	cl0	claisym	claiantis	clfl	cldam	clp	cltotal
0	0.239	0.01	0	0	0	0	0	0	1.17	0
4.737	0.238	0.015	0.7745	-0.0724	0	0	0	0	1.17	0.7752
9.474	0.236	0.03	0.7715	-0.071	0	0	0	0	1.17	0.7733
14.211	0.232	0.044	0.7893	-0.0705	0	0	0	0	1.17	0.7933
18.947	0.226	0.054	0.827	-0.0706	0	0	0	0	1.17	0.8344
23.684	0.219	0.062	0.8639	-0.0693	0	0	0	0	1.17	0.876
28.421	0.21	0.068	0.9067	-0.0671	0	0	0	0	1.17	0.9251
33.158	0.2	0.073	0.9417	-0.0628	0	0	0	0	1.17	0.9677
37.895	0.189	0.079	0.9652	-0.0563	0	0	0	0	1.17	0.9999
42.632	0.176	0.084	0.9813	-0.048	0	0	0	0	1.17	1.0258
47.368	0.162	0.087	1.0028	-0.0388	0	0	0	0	1.17	1.0586
52.105	0.147	0.091	1.0125	-0.028	0	0	0	0	1.17	1.08
56.842	0.131	0.095	1.0194	-0.0163	0	0	0	0	1.17	1.0993
61.579	0.114	0.098	1.0259	-0.004	0	0	0	0	1.17	1.1186
66.316	0.096	0.101	1.0276	0.0086	0	0	0	0	1.17	1.1331
71.053	0.078	0.104	1.0332	0.0214	0	0	0	0	1.17	1.1521
75.789	0.059	0.106	1.0334	0.0338	0	0	0	0	1.17	1.1647
80.526	0.039	0.109	1.0278	0.045	0	0	0	0	1.17	1.1698
85.263	0.02	0.112	1.0145	0.0538	0	0	0	0	1.17	1.164
90	0	0.116	0.9889	0.0575	0	0	0	0	1.17	1.1397

theta - angle defining the position of the section (see help)
z - position of the section on the half of wingspan (0 = wing root)
c - Airfoil chord length
cln - value of the lift coefficient of normal distribution
cl0 - value of the lift coefficient of zero distribution
claisym - value of the lift coefficient of aileron symetric distribution (zero)
claiantisym - value of the lift coefficient of aileron antisymetric distribution
clfl - value of the lift coefficient of flap distribution (zero)
cldam - value of local lift coefficient of aerodynamic damping
clp - value of airfoil lift coefficient
cltotal - value of total lift coefficient

Figure 47 Glauert II results for wing at RE=62868 for maximum lift coefficient

The maximum lift coefficient for the whole wing, $C_{Lwingmax}$, zero lift angle, α_{0wing}, slope of the wing lift curve, C_L-α, and the induced drag coefficient, C_{Di}, could be read directly from the results. Through the first three, the wing lift curve was constructed. $C_{Lwingmax}$ was used to compute the lift generated by the wing. The wing lift curve and HTU lift curve were related together in such a way that the corresponding AoA for the maximum wing lift coefficient was to locate the maximum HTU lift coefficient (C_{LHTU}).

The data available to generate the wing or wing lift curve was: the maximum point in the y-axis, $C_{Lwingmax}$, a point in x at which y=0, α_{0wing}, and the gradient of the line, m=C_L-α. It was assumed that the lift curve is a perfect straight line, and the change in slope towards a higher lift coefficient was neglected. The basics of a straight-line equation were brought to use, by employing the formula y=mx+c to find the y-intercept of the curve. When y=0, m and x were known, and c could easily be solved for, resulting finally in the wing lift curve equation. Then the equation was used to find C_{Lwing} for different values of α in the range of -10 to 25°. Once the values were obtained, a plot of C_{Lwing} vs α was possible. The angle of attack for $C_{Lwingmax}$ could then be obtained by direct reading through the curve, or by substituting y for $C_{Lwingmax}$ in the equation.

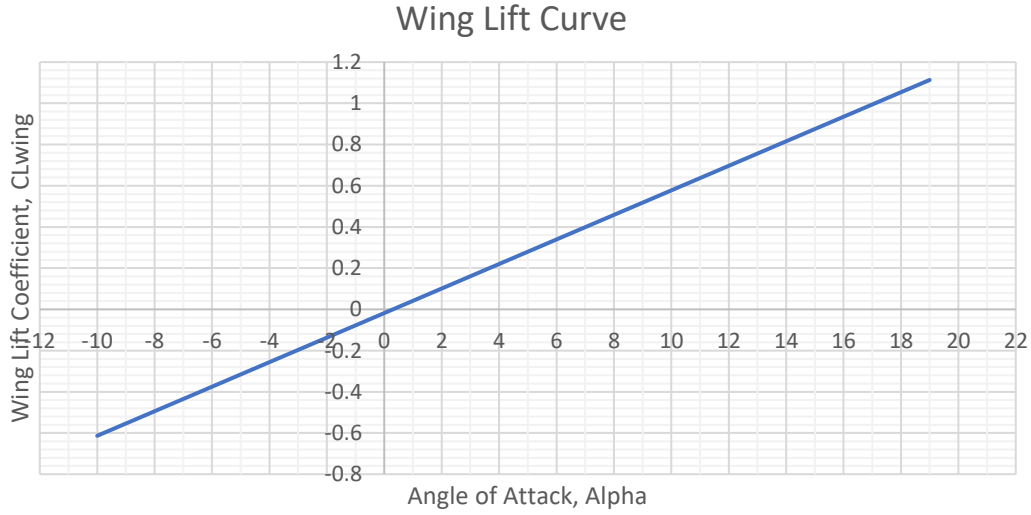

Figure 48 Wing's Lift Curve at Re=62868

The angle of attack for maximum wing lift coefficient was found to be 18.7°.

The next step was exporting the Glauert III results to Excel and integrating for the wing drag and wing moment coefficients distribution. For this part, cltotal was the column of the table that interests us. For each value of cltotal, at a point z along the y-axis, the corresponding values of C_D and C_M are obtained from the C_L-C_D and C_L-C_M graphs respectively. Each value of C_D and C_M was plotted against the respective location along

the span, resulting in the drag and pitching moment coefficients distributions as shown in Figures 50 and 51 respectively. Figure 49 shows a sample of a reading of C_D corresponding to the second value of cltotal in Table 5; as can be seen approximation to the closest value of cltotal has to be made as the resolution of the results given by XFOIL is different than the resolution of the results by Glauert III.

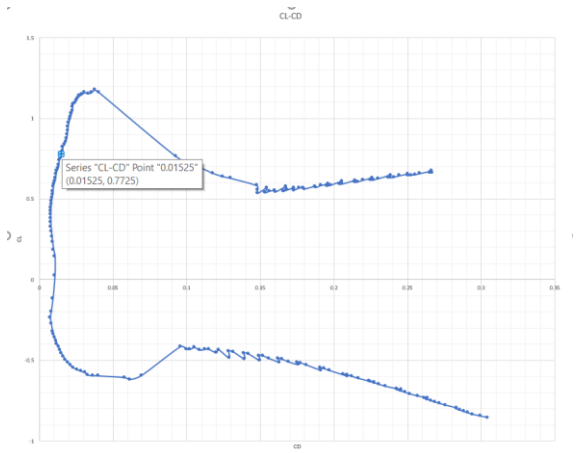

Figure 49 reading corresponding value of CD for the respective CL as given by Glauert III

Each drag coefficient obtained represents only the coefficient at a section at which the corresponding cltotal was read, therefore to generate the distribution across the whole wing, the following summation of integration was applied incrementally in a similar manner as the integration to locate C_{MAC} [5][6].

$$\sum_{0}^{0.239} \int_{z-1}^{z} CD(y) = \sum_{0}^{0.239} \text{CD.y}_{z-1}^{z}$$

Where z is the position along the wing span (y-axis on the Glauert results), and z-1 is the location of the previous position. Plotting each result of the individual integrations to the respective z position (y), gave a drag coefficient distribution along the wing span.

Similarly, for the moment coefficient [5][6];

$$\sum_{0}^{0.239} \int_{z-1}^{z} CM(y) = \sum_{0}^{0.239} \text{CM.y}_{z-1}^{z}$$

Finally, the summation of the integration results gave the Wing Drag coefficient, which for the first boundary condition at $C_{Lwingmax}$ resulted in C_{Dwing}=0.0101054137 and C_{Mwing}=-0.0059651.

Table 5 Glauert III results for wing at Re=62868 and maximum lift in Excel, with integration and summation for C_{Dwing} and C_{Mwing}

Z	CLAISYM	CLAIANTISYM	CLDAM	CLP	CLTOTAL	CD	CDWING(Z)	CM	CMWING(Z)
0.239	0	0	0	1.36	0	0.0241	0.0000241	-0.01	-0.00001
0.238	0	0	0	1.36	0.8586	0.02782	5.564E-05	-0.0522	-0.0001044
0.236	0	0	0	1.36	0.8583	0.0278	0.0001112	-0.0522	-0.0002088
0.232	0	0	0	1.36	0.8831	0.02887	0.00017322	-0.0513	-0.0003078
0.226	0	0	0	1.36	0.9335	0.02993	0.00020951	-0.0497	-0.0003479
0.219	0	0	0	1.36	0.9856	0.03106	0.00027954	-0.0477	-0.0004293
0.21	0	0	0	1.36	1.0471	0.03202	0.0003202	-0.0453	-0.000453
0.2	0	0	0	1.36	1.1013	0.03319	0.00036509	-0.0417	-0.0004587
0.189	0	0	0	1.36	1.1434	0.0337	0.0004381	-0.0394	-0.0005122
0.176	0	0	0	1.36	1.1777	0.03445	0.0004823	-0.0367	-0.0005138
0.162	0	0	0	1.36	1.2199	0.03546	0.0005319	-0.0309	-0.0004635
0.147	0	0	0	1.36	1.2481	0.03832	0.00061312	-0.0264	-0.0004224
0.131	0	0	0	1.36	1.2732	0.04162	0.00070754	-0.021	-0.000357
0.114	0	0	0	1.36	1.2979	0.04462	0.00080316	-0.0191	-0.0003438
0.096	0	0	0	1.36	1.3164	0.04718	0.00084924	-0.0171	-0.0003078
0.078	0	0	0	1.36	1.3397	0.05289	0.00100491	-0.0133	-0.0002527
0.059	0	0	0	1.36	1.3548	0.06034	0.0012068	-0.008	-0.00016
0.039	0	0	0	1.36	1.3599	0.061	0.001159	-0.008	-0.000152
0.02	0	0	0	1.36	1.3513	0.06034	0.0012068	-0.008	-0.00016
0	0	0	0	1.36	1.3213	0.0489	0	-0.016	0
						Cdwing	0.01054137	Cmwing	-0.0059651

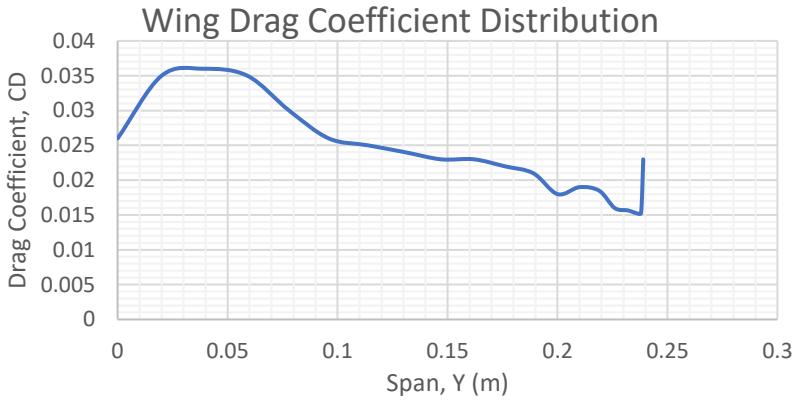

Figure 50 Wing drag coefficient (CD) distribution at Re=62868, at maximum lift condition

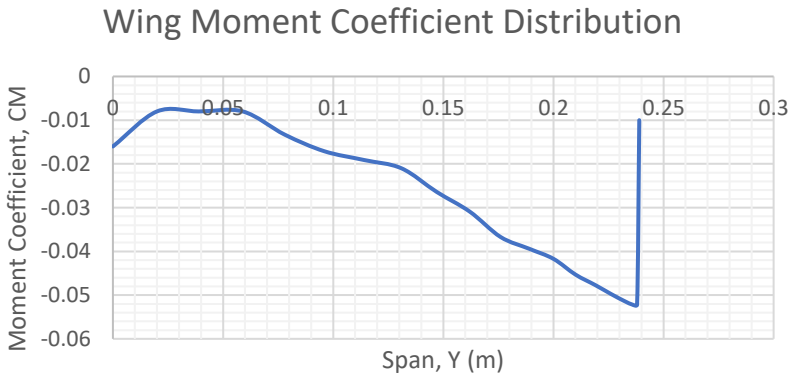

Figure 51 Wing moment coefficient (CM) distribution at Re=62868, at maximum lift condition

4.4.2 Wing – $C_{Lcruise}$

At the same boundary condition, it was necessary to find the wing's aerodynamic properties under cruise conditions, hence setting $C_{Lcruise}$=0.2 as an approximation and solving in Glauert III once more. This step could be done easily in GLUAERT by ticking the box 'Solve Total Distribution for Requested Lift Coefficient of The Wing', and setting C_{lwing} to the desired $C_{Lcruise}$.

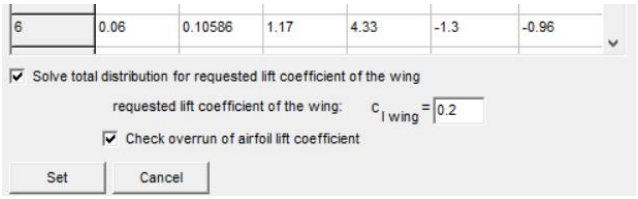

Figure 52 Glauert III screenshot to solve for cruise condition

Upon solving, the results window opened once more, showing an identical planform as before, however a slightly different Lift Distribution curve and results.

Area of the wing S = 0.044 m2
Aspect ratio Lambda = 5.213
Requested lift coefficient of the wing is Clwing = 0.2
Max. lift coefficient of the wing is Clwingmax = 1.0944
Lift curve slope of the wing = 3.4121 rad-1
Angle of zero-lift coefficient (in the wing root) Alfa0wing = 0.3614 ° (without the influence of flaps and ailerons)
Glauert coefficient delta = 0.008 (for the calculation of induced drag - calculated from normal distribution)
Induced drag coefficient Cxi = 0.0025 (for the lift coefficient of the wing Clwing = 0.2)

theta	z	c	cln	cl0	claisym	claiantis	clfl	cldam	clp	cltotal
0	0.239	0.01	0	0	0	0	0	0	1.17	0
4.737	0.238	0.015	0.7745	-0.0724	0	0	0	0	1.17	0.0825
9.474	0.236	0.03	0.7715	-0.071	0	0	0	0	1.17	0.0833
14.211	0.232	0.044	0.7893	-0.0705	0	0	0	0	1.17	0.0874
18.947	0.226	0.054	0.827	-0.0706	0	0	0	0	1.17	0.0948
23.684	0.219	0.062	0.8639	-0.0693	0	0	0	0	1.17	0.1034
28.421	0.21	0.068	0.9067	-0.0671	0	0	0	0	1.17	0.1142
33.158	0.2	0.073	0.9417	-0.0628	0	0	0	0	1.17	0.1255
37.895	0.189	0.079	0.9652	-0.0563	0	0	0	0	1.17	0.1367
42.632	0.176	0.084	0.9813	-0.048	0	0	0	0	1.17	0.1482
47.368	0.162	0.087	1.0028	-0.0388	0	0	0	0	1.17	0.1617
52.105	0.147	0.091	1.0125	-0.028	0	0	0	0	1.17	0.1744
56.842	0.131	0.095	1.0194	-0.0163	0	0	0	0	1.17	0.1875
61.579	0.114	0.098	1.0259	-0.004	0	0	0	0	1.17	0.2011
66.316	0.096	0.101	1.0276	0.0086	0	0	0	0	1.17	0.2141
71.053	0.078	0.104	1.0332	0.0214	0	0	0	0	1.17	0.228
75.789	0.059	0.106	1.0334	0.0338	0	0	0	0	1.17	0.2405
80.526	0.039	0.109	1.0278	0.045	0	0	0	0	1.17	0.2506
85.263	0.02	0.112	1.0145	0.0538	0	0	0	0	1.17	0.2567
90	0	0.116	0.9889	0.0575	0	0	0	0	1.17	0.2552

Figure 53 Glauert II results for wing at RE=62868 for cruise lift coefficient

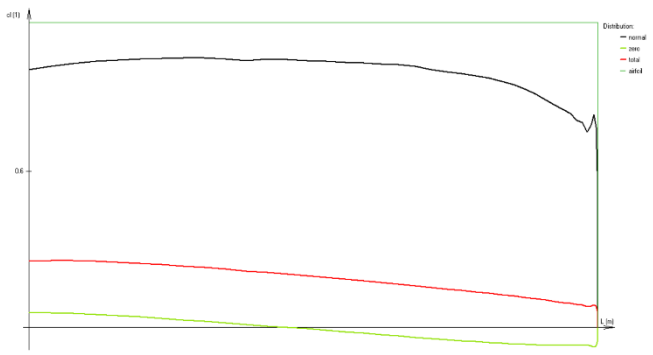

Figure 54 Wing Lift Distribution when solving for cruise lift coefficient

At this case, no separation of flow occured.

Using the same wing lift curve generated before and locating CL=0.2, for cruise condition, it was found that $\alpha_{wingcruise}$=3.57.

The following drag and moment coefficients distributions were obtained in excel following the procedure as explained for maximum lift condition.

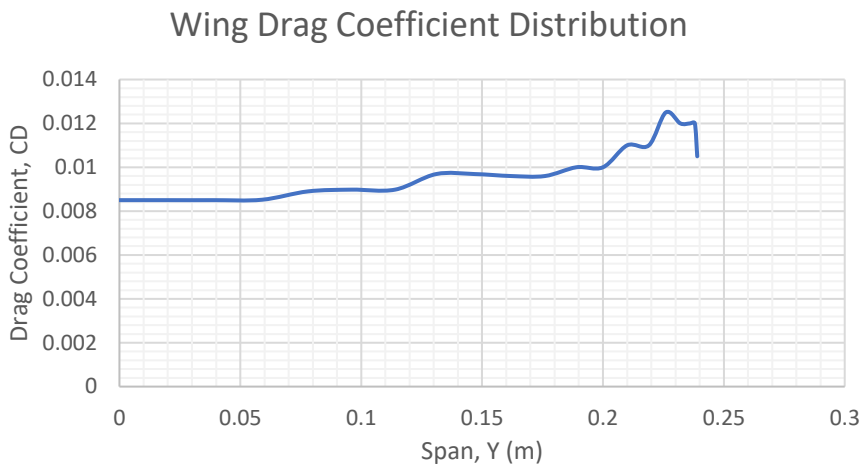

Figure 55 Wing drag coefficient (CD) distribution at Re=62868, at cruise lift condition

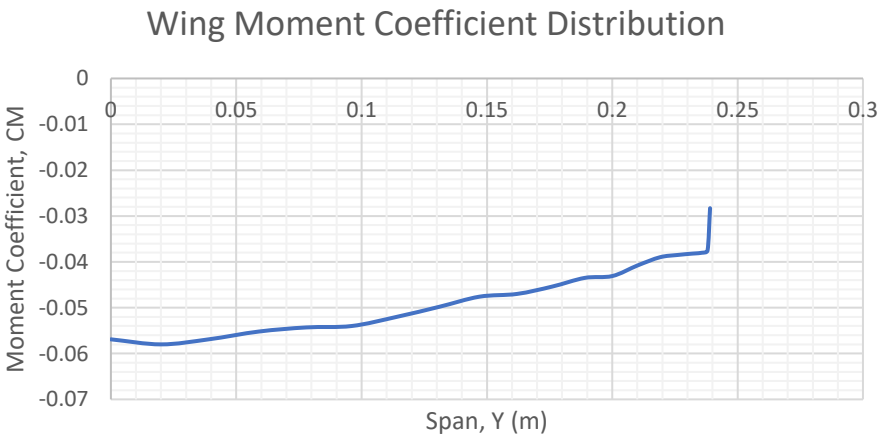

Figure 56 Wing moment coefficient (CM) distribution at Re=62868, at cruise lift condition

The summation of the integration results gives the Wing Drag coefficient, C_D=0.00576484, and Wing Moment Coefficient, C_M=-0.0117862

The procedures for both C_{LMAX} and $C_{Lcruise}$ was repeated for the three other boundary conditions, with Glauert III results tabulated and further Excel computations found in Appendix B.

Table 6 shows the Maximum Wing Lift Coefficients, Wing Moment Coefficients, Wing Drag coefficients and Wing Induced Drag coefficients obtained at all boundary conditions for the wing at both C_{Lmax} and $C_{Lcruise}$ conditions.

Table 6 Results for computation of Wing's Lift and Drag Coefficients

	C_{LMAX}					**$C_{LCRUISE}$**				
RE	**α_w**	**$C_{Lwingmax}$**	**C_{Mwing}**	**C_{Dwing}**	**C_{Di}**	**α_w**	**$C_{Lwingcruise}$**	**C_{Mwing}**	**C_{Dwing}**	**C_{Di}**
62868	**18.68**	1.2654	-0.00596	0.010541	0.0982	**3.57**	0.2	-0.0118	0.00576	0.0025
125736	**20.47**	1.2488	-0.00131	0.009268	0.0959	**3.33**	0.2	-0.0125	0.00344	0.0025
188604	**20.56**	1.3156	-0.00340	0.010134	0.1065	**2.84**	0.2	-0.0116	0.00265	0.0025
282926	**22.35**	1.3198	-0.00538	0.009894	0.1072	**3.02**	0.2	-0.0102	0.00212	0.0025

Under the cruise conditions, the wing drag coefficients vary however the max wing lift coefficient and induced drag is constant for any value of RE.

α_w is the angle of attack with of the root aerofoil, including the setting angle. The actual angle of attack with respect to the whole model, α is

$$\alpha = \alpha_w - 1.665$$

Given that the HTU has no setting angle, then

$$\alpha_H = \alpha$$

4.4.3 Horizontal Tail Unit – No Deflection

For the HTU without an activated elevator, C_{DHTU} and C_{MHTU} at both maximum and cruise conditions were computed in the same manner as for the wing. The main differences being that no geometric twist exists in the HTU and different spacings between sections were taken. Geometric parameters of the HTU were inputted into the software and then solved for.

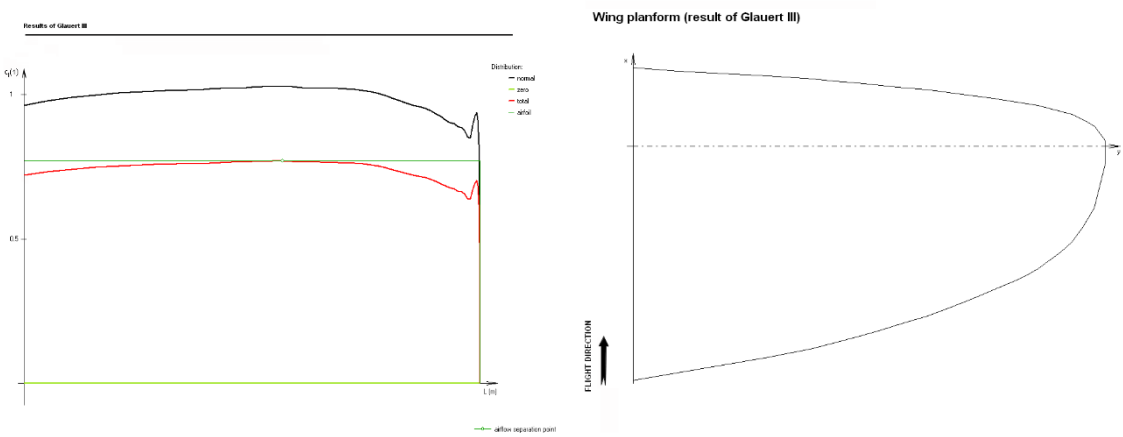

Figure 57 HTU Lift Distribution when solving for maximum lift coefficient and Planform

Results overview:

Area of the wing S = 0.011 m2
Aspect ratio Lambda = 4.036
Max. lift coefficient of the wing is Clwingmax = 0.6834
Lift curve slope of the wing = 3.1071 rad-1
Angle of zero-lift coefficient (in the wing root) Alfa0wing = 0 ° (without the influence of flaps and ailerons)
Glauert coefficient delta = 0.0012 (for the calculation of induced drag - calculated from normal distribution)
Induced drag coefficient Cxi = 0.0369 (for the lift coefficient of the wing Clwing = 0.6834)

theta	z	c	cln	cl0	claisym	claiantis	clfl	cldam	clp	cltotal
0	0.105	0.005	0	0	0	0	0	0	0.7	0
4.737	0.105	0.007	0.8562	0	0	0	0	0	0.7	0.5852
9.474	0.104	0.013	0.9309	0	0	0	0	0	0.7	0.6362
14.211	0.102	0.02	0.8784	0	0	0	0	0	0.7	0.6003
18.947	0.099	0.025	0.9086	0	0	0	0	0	0.7	0.621
23.684	0.096	0.03	0.9311	0	0	0	0	0	0.7	0.6363
28.421	0.092	0.034	0.9587	0	0	0	0	0	0.7	0.6552
33.158	0.088	0.038	0.9751	0	0	0	0	0	0.7	0.6664
37.895	0.083	0.041	0.9989	0	0	0	0	0	0.7	0.6827
42.632	0.077	0.044	1.0135	0	0	0	0	0	0.7	0.6926
47.368	0.071	0.047	1.0181	0	0	0	0	0	0.7	0.6958
52.105	0.064	0.051	1.0197	0	0	0	0	0	0.7	0.6969
56.842	0.057	0.053	1.0237	0	0	0	0	0	0.7	0.6996
61.579	0.05	0.057	1.0182	0	0	0	0	0	0.7	0.6958
66.316	0.042	0.059	1.0148	0	0	0	0	0	0.7	0.6935
71.053	0.034	0.061	1.0116	0	0	0	0	0	0.7	0.6914
75.789	0.026	0.063	1.0074	0	0	0	0	0	0.7	0.6885
80.526	0.017	0.065	0.9992	0	0	0	0	0	0.7	0.6829
85.263	0.009	0.067	0.9857	0	0	0	0	0	0.7	0.6737
90	0	0.069	0.9641	0	0	0	0	0	0.7	0.6589

theta - angle defining the position of the section (see help)
z - position of the section on the half of wingspan (0 = wing root)
c - Airfoil chord length
cln - value of the lift coefficient of normal distribution
cl0 - value of the lift coefficient of zero distribution
claisym - value of the lift coefficient of aileron symetric distribution (zero)
claiantisym - value of the lift coefficient of aileron antisymetric distribution
clfl - value of the lift coefficient of flap distribution (zero)
cldam - value of local lift coefficient of aerodynamic damping
clp - value of airfoil lift coefficient
cltotal - value of total lift coefficient

Figure 58 Glauert II results for HTU at Re=62868 for maximum lift coefficient, with no elevator deflection

Once the results were obtained, unlike for the wing, the maximum lift coefficient along the HTU could not be read directly through the results, as it has to be taken into consideration that the HTU is in flight at an AoA with respect to the wing's α at any point in time. This means that if, for example, the Wing is experiencing maximum lift coefficient at α=18.7°, under such condition the HTU will be at the same α minus the setting angle of the wing, i.

$$\alpha_H = \alpha - i$$

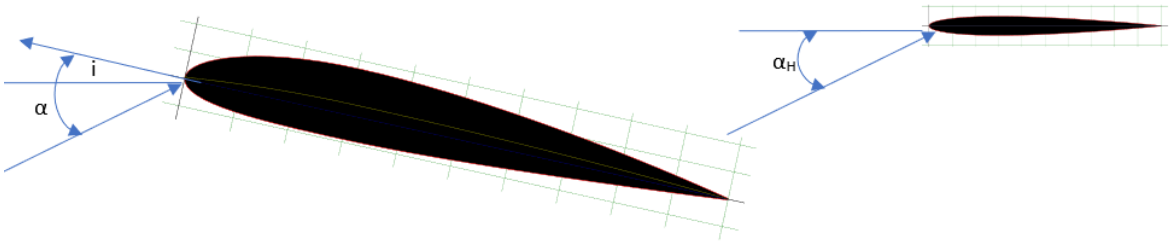

Figure 59 Angle of Attack on wing means different angle of attack on HTU

Hence, if the wing has a root setting of +1.665° and its maximum lift is at 18.7°, under that condition the HTU would be flying at an AoA=18.7 – 1.665, which is 17.04°. Although not impossible, such angle will most probably not be the same angle at which the HTU experiences maximum lift, and the lift at that angle needs to be found by relating the wing's and HTU's lift curves. As mentioned, for the wing's maximum lift coefficient of 18.7°, the HTU would be at 17.04° and by reading directly from the HTU's lift curve or by substitution in the curve's equation, the respective lift coefficient of the HTU would then be found. The HTU's lift curve is constructed in the same manner as done for the wing.

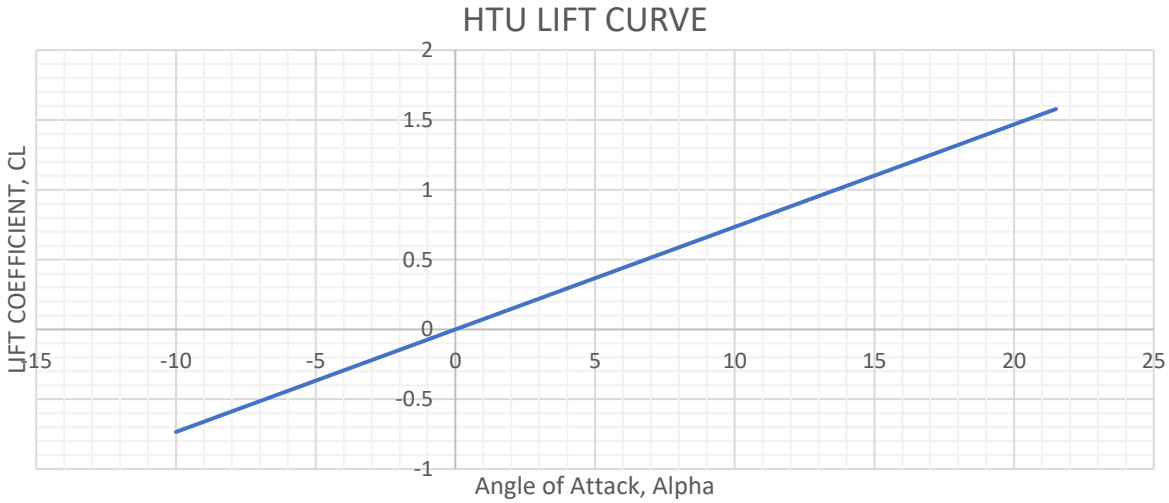

Figure 60 HTU's Lift Curve at Re=62868, no elevator deflection

Through the HTU Lift Curve, it was found that the HTU's lift coefficient at the instant when the wing is experiencing maximum lift is $C_{LHTUwmax}$=1.2504.

Just like for the wing, the corresponding C_{DHTU} and C_{MHTU} were read from the C_L-C_D and C_L-C_M curves generated through XFOIL's results, and then each value integrated as before. A summation of the integration results in the HTU's wing drag coefficient and HTU's pitching moment coefficient.

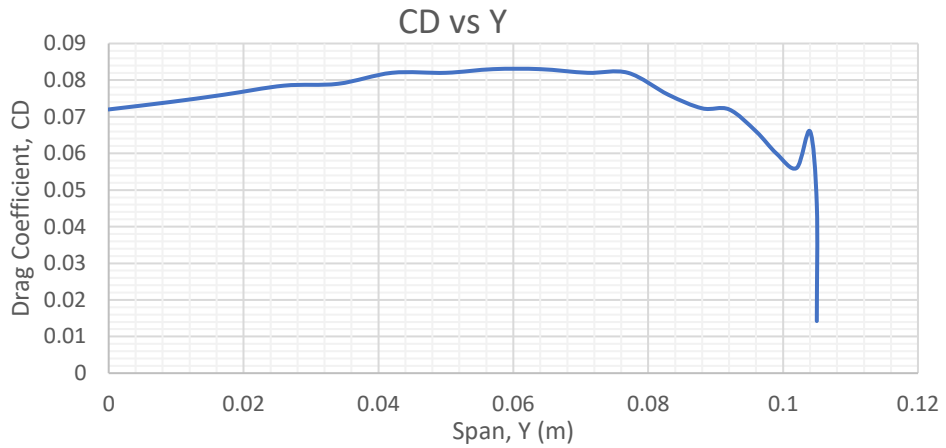

Figure 61 HTU drag coefficient (CD) distribution at Re=62868, at maximum lift condition, no elevator deflection

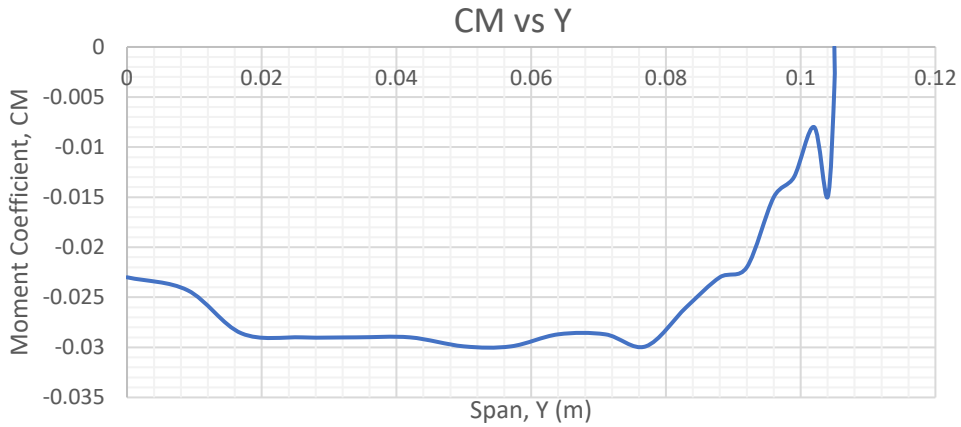

Figure 62 HTU moment coefficient (CM) distribution at Re=62868, at maximum lift condition, no elevator deflection

For cruise condition, $C_{LHTUcruise}$ with respect to $C_{LWingCruise}$ was obtained in the same way as mentioned above for maximum conditions, by locating the AoA of the wing at which C_L=0.2, and finding the corresponding C_L of the HTU at that same AoA. The drag and moment coefficients distributions and summations where obtained using also the same method.

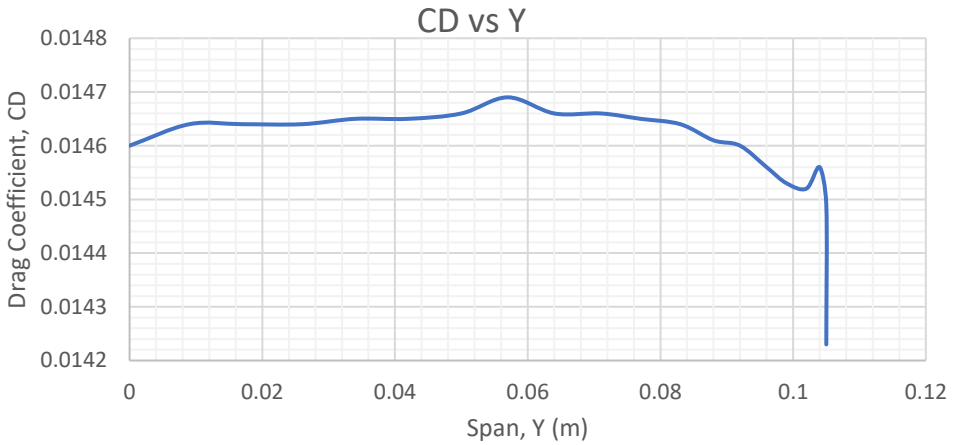

Figure 63 HTU drag coefficient (CD) distribution at Re=62868, at cruise lift condition, no elevator deflection

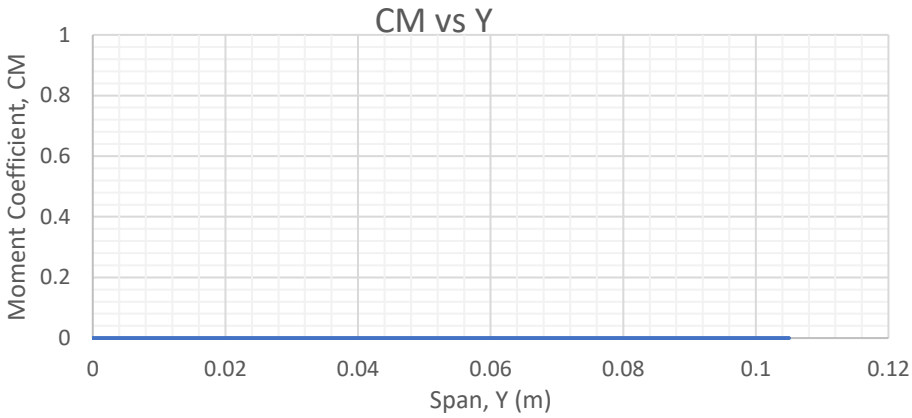

Figure 64 HTU moment coefficient (CM) distribution at Re=62868, at cruise lift condition, no elevator deflection

The moment coefficient distribution of the HTU was found to be zero, along all surface.

4.4.4 Horizontal Tail Unit – 15°

Whilst the procedure to compute for coefficients with a deflected flap or aileron was basically the same as for without deflection, a few parameters had to be inputted in Glauert III to teach the software how the deflection would occur physically.

Firstly, Aileron Deflected was ticked, and under Simplified Setting, the following were set. Aileron lift coefficient with aileron deflected up for root and tip were given the same C_{Lmax} as found through XFOIL's results for NACA0005 with deflection at -15°. Aileron Chord length, C_{fl}, was found to be 31% of the overall chord. Deflection Angle was set at -15°, as per the case required. Aileron root and tip positions were set at 0 and 0.105m respectively given that the elevator starts and ends at the root and tip of the HTU [9].

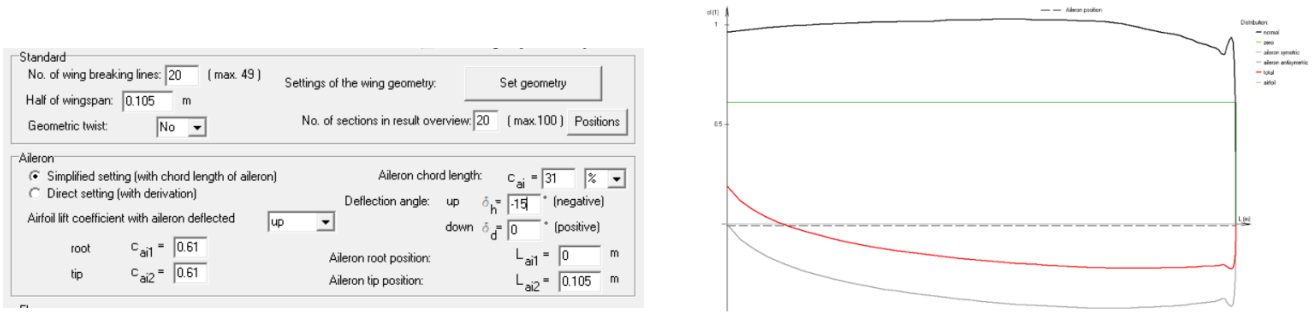

Figure 65 Screenshot of Glauert III showing parameters set for deflection of elevator (left) and the resulting wing-lift distribution (right)

Once this was done, solving would give results which were evaluated for both the C_{LHTU}, C_{MHTU} and $C_{DHTU\ in}$ the same manner as for the HTU without deflection.

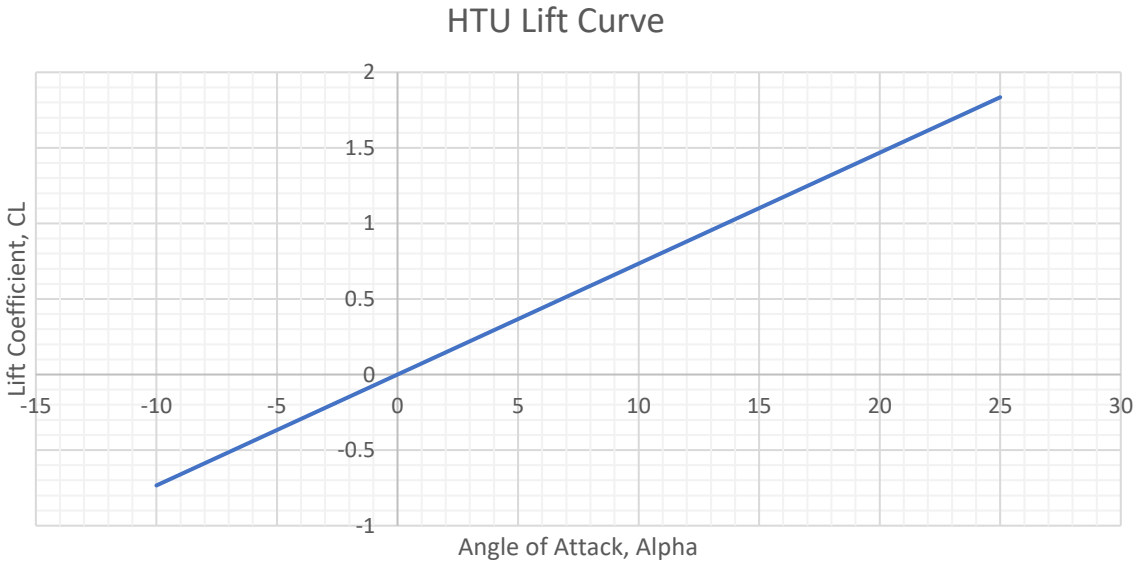

Figure 66 HTU lift curve with elevator deflection -15°

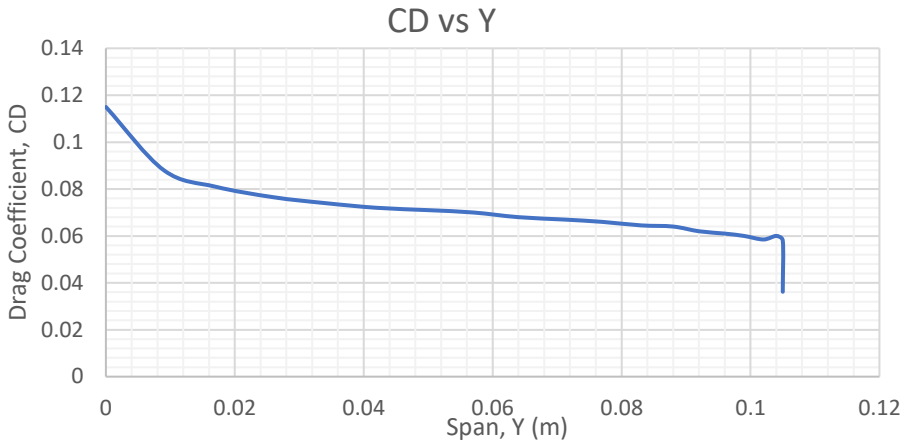

Figure 67 HTU drag coefficient (CD) distribution at Re=62868, at maximum lift condition, elevator deflection -15degrees

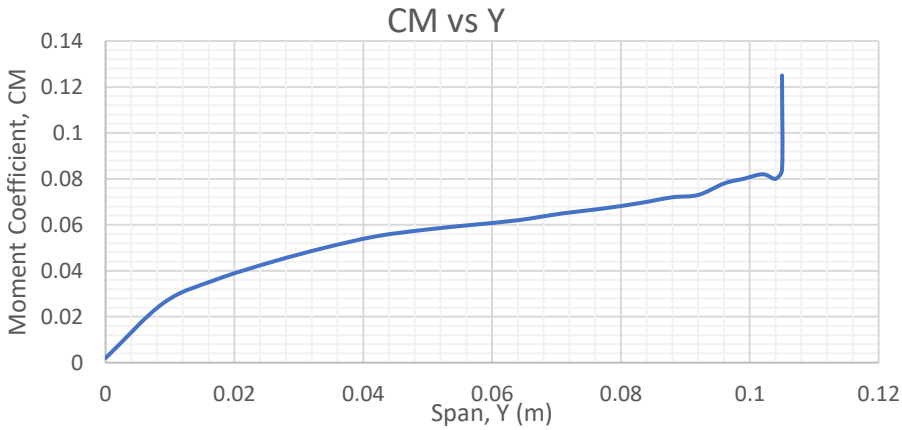

Figure 68 HTU moment coefficient (CM) distribution at Re=62868, at maximum lift condition, elevator deflection -15degrees

Once again, the same procedure was followed for cruise conditions, setting Glauert III to solve for requested lift coefficient of 0.2. The HTU's maximum lift coefficient was found again by locating the respective AoA given at the Wing's cruise condition.

Glauert III's results tabulated and further Excel computations for the HTU at maximum and cruise conditions, each case with 0 and 15°, can be found in Appendix B.

Both for this set-up and for without elevator deflected, the HTU lift curve was used to locate the respective C_{HTUmax} for $C_{LWingmax}$ at all four boundary conditions, max and cruise. This was made possible by using the different AoA of the lift coefficients of the wing at the different boundary conditions and applying them to the HTU's lift curve of the first boundary condition. It was expected to give a more accurate result in terms of lift. Since the moment and drag coefficients depend on the distributions given, it was not

possible to generate them as well since XFOIL failed to converge, so the HTU was assumed to have the same forces for all boundary conditions, except for lift.

Table 7 shows the results obtained through this section for the HTU, at both the maximum and cruise conditions and both for 0 and -15° deflection of the elevator. Table 8 shows the HTU's lift coefficients, maximum and cruise, with respect to the wing under different boundary conditions.

Table 7 HTU coefficients at maximum and cruise lift conditions with different deflections

RE=62868	**MAXIMUM LIFT CONDITION**				**CRUISE LIFT CONDITION**			
DEFLECTION	**$C_{LHTUmax}$**	**C_{MHTU}**	**C_{DHTU}**	**C_{Di}**	**$C_{LHTUcruise}$**	**C_{MHTU}**	**C_{DHTU}**	**C_{Di}**
0°	1.2489	-0.00272	0.00805	0.0443	0.2	0.0000	0.0015	0.32
15°	1.1976	0.00604	0.00743	0.0318	0.2	0.0123	0.0038	0.32

Table 8 HTU's maximum and cruise lift coefficients at different Reynolds Numbers with respect to the Wing

	$C_{LHTUMAX}$				**$C_{LCRUISE}$**			
DEFLECTION	**62868**	**125736**	**188604**	**282906**	**62868**	**125736**	**188604**	**282906**
0°	1.2489	1.3803	1.3869	1.5183	0.1352	0.1215	0.0858	0.0986
15°	1.1976	1.3239	1.3302	1.4562	0.1304	0.1172	0.0827	0.0951

4.4.5 Coefficients Tabulations

Tables 9-12 are categorized by lift condition and elevator set up and they include all the coefficients of the forces acting on the aircraft's components individually.

Table 9 Forces coefficients for maximum lift condition and no elevator deflection

MAXIMUM LIFT COEFFICIENT CONDITION - NO ELEVATOR

REYNOLDS NUMBER	Wing Lift Coefficient	HTU Lift Coefficient	Fuselage Lift Coefficient	Wing Drag Coefficient	Wing Induced Drag Coefficient	HTU Drag Coefficient	HTU Induced Drag Coefficient	Fuselage Drag Coefficient	Wing Pitching Moment Coefficient	HTU Pitching Moment Coefficient
RE	CLwing	CLhtu	CLfus	CDwing	CDiWing	CDhtu	CDiHTU	CDfus	CMwing	CMhtu
-	-	-	-	-	-	-	-	-	-	-
62868	1.2651	1.24889	0	0.0105414	0.0982	0.003887	0.0443	0.0081198	-0.00597	-0.002718
125736	1.2488	1.38028	0	0.0092679	0.0959	0.003887	0.0443	0.0070687	-0.00131	-0.002718
188604	1.3156	1.38689	0	0.0101343	0.1065	0.003887	0.0443	0.0065320	-0.00340	-0.002718
282906	1.3198	1.51828	0	0.0098940	0.1072	0.003887	0.0443	0.0060104	-0.00538	-0.002718

Table 10 Forces coefficients for maximum lift condition and -15degrees elevator deflection

MAXIMUM LIFT COEFFICIENT CONDITION - ELEVATOR -15°

REYNOLDS NUMBER	Wing Lift Coefficient	HTU Lift Coefficient	Fuselage Lift Coefficient	Wing Drag Coefficient	Wing Induced Drag Coefficient	HTU Drag Coefficient	HTU Induced Drag Coefficient	Fuselage Drag Coefficient	Wing Pitching Moment Coefficient	HTU Pitching Moment Coefficient
RE	CLwing	CLhtu	CLfus	CDwing	CDiWing	CDhtu	CDiHTU	CDfus	CMwing	CMhtu
-	-	-	-	-	-	-	-	-	-	-
62868	1.2651	1.1976	0	0.010541	0.0982	0.00743	0.0318	0.0081198	-0.00597	0.00604
125736	1.2488	1.3239	0	0.009268	0.0959	0.00743	0.0318	0.0070687	-0.00131	0.00604
188604	1.3156	1.3302	0	0.010134	0.1065	0.00743	0.0318	0.0065320	-0.00340	0.00604
282906	1.3198	1.4562	0	0.009894	0.1072	0.00743	0.0318	0.0060104	-0.00538	0.00604

Table 11 Forces coefficients for cruise lift condition and no elevator deflection

CRUISE CONDITION - NO ELEVATOR

REYNOLDS NUMBER	Wing Lift Coefficient	HTU Lift Coefficient	Fuselage Lift Coefficient	Wing Drag Coefficient	Wing Induced Drag Coefficient	HTU Drag Coefficient	HTU Induced Drag Coefficient	Fuselage Drag Coefficient	Wing Pitching Moment Coefficient	HTU Pitching Moment Coefficient
RE	CLwing	CLhtu	CLfus	CDwing	CDiWing	CDhtu	CDiHTU	CDfus	CMwing	CMhtu
-	-	-	-	-	-	-	-	-	-	-
62868	0.2	0.1352	0	0.005765	0.0025	0.0015366	0.0032	0.0081198	-0.01179	0
125736	0.2	0.1215	0	0.003442	0.0025	0.0015366	0.0032	0.0081198	-0.01252	0
188604	0.2	0.0858	0	0.002646	0.0025	0.0015366	0.0032	0.0081198	-0.01156	0
282906	0.2	0.0986	0	0.002123	0.0025	0.0015366	0.0032	0.0081198	-0.01024	0

Table 12 Forces coefficients for cruise lift condition and -15degrees elevator deflection

CRUISE CONDITION - ELEVATOR -15°

REYNOLDS NUMBER	Wing Lift Coefficient	HTU Lift Coefficient	Fuselage Lift Coefficient	Wing Drag Coefficient	Wing Induced Drag Coefficient	HTU Drag Coefficient	HTU Induced Drag Coefficient	Fuselage Drag Coefficient	Wing Pitching Moment Coefficient	HTU Pitching Moment Coefficient
RE	CLwing	CLhtu	CLfus	CDwing	CDiWing	CDhtu	CDiHTU	CDfus	CMwing	CMhtu
-	-	-	-	-	-	-	-	-	-	-
62868	0.2	0.1304	0	0.005765	0.0025	0.003834	0.0032	0.0081198	-0.01179	0.00044
125736	0.2	0.1172	0	0.003442	0.0025	0.003834	0.0032	0.0081198	-0.01252	0.00044
188604	0.2	0.0827	0	0.002646	0.0025	0.003834	0.0032	0.0081198	-0.01156	0.00044
282906	0.2	0.0951	0	0.002123	0.0025	0.003834	0.0032	0.0081198	-0.01024	0.00044

4.5 Individual Forces

The final step in computation was to evaluate the resulting lift and drag forces as well as the moments, all at the different boundary conditions and set-ups.

The first section deals with the computation of Lift, Drag and Pitching and Force Moments for both the wing and HTU at each boundary condition using maximum lift coefficient and cruise lift coefficient. It also contains computations for the drag generated by the fuselage. The fuselage's lift was neglected. This will show how all the forces are acting on the model's parts individually. The area used for computing the properties of the wings is the same value as given by the model's specs, since it was the effective area during testing.

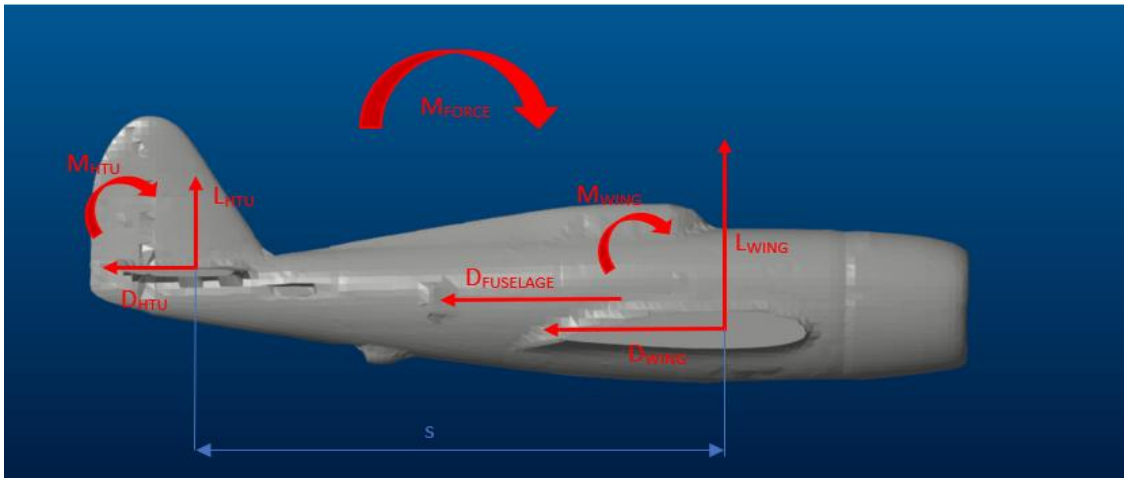

Figure 69 Model's depiction of individual loadings

4.5.1 Lift – Wing and HTU

Lift could be computed directly from the lift coefficients already obtained, both for $C_{Lwingmax}$ and $C_{Lwingcruise}$, using the formula [5]:

$$L = C_L.\frac{\rho.v^2}{2}.A$$

Where C_L represents the respective distributed lift coefficient, A is the aerodynamic part's surface area, ρ is the density of the fluid and v is the velocity.

Table 13 shows the lift acting on the wing and HTU at different conditions.

Table 13 Lift forces acting on the Wing and HTU at different conditions

	WING		HORIZONTAL TAIL UNIT			
REYNOLDS	$L_{wingmax}$	$L_{wingcruise}$	$L_{HTUmax0}$	$L_{HTUmax15}$	$L_{HTUcruise0}$	$L_{HTUcruise15}$
-	N	N	N	N	N	N
62868	3.352945	0.53007	0.818920	0.785288	0.090306	0.08710
125736	13.23898	2.12027	3.620299	3.472421	0.324622	0.313133
188604	31.38109	4.77061	8.184681	7.850127	0.515788	0.497152
282906	70.83285	10.7339	20.16017	19.33585	1.333654	1.286314

4.5.2 Drag – Wing and HTU

For drag, a small step was required prior to computing the final force. Both the induced drag and wing drag coefficients determined in the previous step needed to be combined for the maximum drag coefficient, C_{Dmax} [5][6].

$$C_{Dmax} = C_{Dwing} + C_{Di}$$

Finally, the following formula followed:

$$D = C_{Dmax}.\frac{\rho.v^2}{2}.A$$

Where C_{Dmax} represents the maximum drag coefficient under maximum lift condition, or cruise lift respectively.

Table 14 shows the drag acting on the wing and HTU at different conditions.

Table 14 Drag forces acting on the Wing and HTU at different conditions

	WING		HORIZONTAL TAIL UNIT			
REYNOLDS	$D_{wingmax}$	$D_{wingcruise}$	$D_{HTUmax0}$	$D_{HTUmax15}$	$D_{HTUcruise0}$	$D_{HTUcruise15}$
-	N	N	N	N	N	N
62868	0.2882016	0.021905	0.031597	0.024904	0.003164	0.004275
125736	1.1149228	0.062993	0.031597	0.024904	0.003164	0.004275
188604	2.7820850	0.122745	0.031597	0.024904	0.003164	0.004275
282906	6.2843630	0.248114	0.031597	0.024904	0.003164	0.004275

4.5.3 Pitching Moment – Wing and HTU

To compute the pitching moment, the following formula was used [5]:

$$M = C_M . c_{MAC} . \frac{\rho . v^2}{2} . A$$

It resembles the ones for Lift and Drag, with the inclusion of C_{MAC}.

Table 15 shows the pitching acting on the wing and HTU at different conditions.

Table 15 Pitching moments acting on the Wing and HTU at different conditions

	WING			**HORIZONTAL TAIL UNIT**		
REYNOLDS	$M_{wingmax}$	$M_{wingcruise}$	$M_{HTUmax0}$	$M_{HTUmax15}$	$M_{HTUcruise0}$	$M_{HTUcruise15}$
-	Nm	Nm	Nm	Nm	Nm	Nm
62868	-0.00151	-0.00298	-9.55E-5	0.00021	0	0.00044
125736	-0.00132	-0.01264	-9.55E-5	0.00021	0	0.00044
188604	-0.00773	-0.02627	-9.55E-5	0.00021	0	0.00044
282906	-0.02750	-0.05235	-9.55E-5	0.00021	0	0.00044

4.5.4 Force Moments – HTU about Wing

Both the Wing and HTU will generate pitching moment of their own, however, as the final results will be summed up to be equivalent as if acting on the wing's AC, the lift generated by the HTU will cause a force moment about the wing's MAC.

This force is computed by multiplying the lift generated by the HTU and the distance separating the MAC_{HTU} and MAC_{wing}. The distance, s, was found to be approximately 255 mm. The angle offset was ignored, as it is small and would result in a negligible difference in distance.

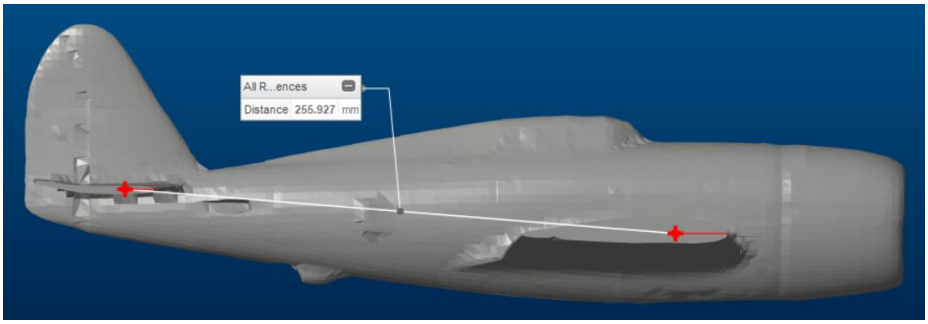

Figure 70 Distance between Wing's and HTU's MAC

$$M_{Force} = L \times s$$

Table 16 shows the force moments at different conditions

Table 16 Force Moments caused by the HTU forces acting around the wing's MAC

	FORCE MOMENTS (NM)			
REYNOLDS	0°, Maximum	15°, Maximum	0°, Cruise	15°, Cruise
62868	0.208825	0.200248	0.023028	0.022211
125736	0.923176	0.885467	0.082779	0.079849
188604	2.087094	2.001782	0.131526	0.126774
282906	5.140843	4.930642	0.340082	0.32801

4.5.5 Drag – Fuselage

The drag related to the fuselage was computed in terms of skin friction drag, because in order to compute the drag coefficient for the fuselage required complex computations and simulations, if done theoretically.

The wetted area of the fuselage, $A_{Fuselage}$ was obtained as explained in the section Model Geometry Acquisition.

By Von Karman's 1/7 Power Law, for turbulent flow, the Coefficient of Friction is [10]:

$$C_f = \frac{0.074}{Re^{0.2}}$$

It is important to note that in this case, this equals the Coefficient of Friction Drag, C_{Df}, unlike in the theory of plate flows where C_{Df} is twice C_f as it has to count for the area of the second face of the plate too. The wetted area of the fuselage includes the whole surface all around.

Followed by the drag formulation [5][6]:

$$D_f = C_{Df}.\frac{\rho.v^2}{2}.A_{Fuselage}$$

Table 17 Fuselage drag at different boundary conditions

REYNOLDS	**62868**	**125736**	**188604**	**182906**
C_{DF}	0.008120	0.007069	0.006532	0.006010
D_F (N)	0.066920	0.233281	0.485031	1.004171

At the lowest Reynolds number, the drag was close to negligible. It could therefore be assumed that under cruise conditions, the friction drag's change would be negligible. With this reasoning, the fuselage's drag under cruise conditions was taken as 0.06N throughout all computations.

Having obtained all individual forces and moments as acting on their relative components at different boundary conditions and set-ups, tables were created for each condition for a better understanding of the forces.

4.5.6 Individual Forces Tabulations

Table 18 Individual Forces for maximum lift condition and no elevator deflection

MAXIMUM LIFT CONDITION - NO ELEVATOR

REYNOLDS NUMBER	Wing Lift	HTU Lift	Fuselage Lift	Wing Drag	HTU Drag	Fuselage Drag	Wing Pitching Moment	HTU Pitching Moment	Force Moment
RE	Lwing	Lhtu	Lfus	Dwing	Dhtu	Dfus	Mwing	Mhtu	Mf
-	N	N	N	N	N	N	Nm	Nm	Nm
62868	3.35295	0.8189	0	0.28820	0.03160	0.06692	-0.00151	-9.55282E-05	0.20882
125736	13.2390	3.6203	0	1.11492	0.03160	0.23328	-0.00132	-9.55282E-05	0.92317
188604	31.3811	8.1847	0	2.78209	0.03160	0.48503	-0.00773	-9.55282E-05	2.08709
282906	70.8329	20.160	0	6.28436	0.03160	1.00417	-0.02750	-9.55282E-05	5.14084

Table 19 Individual Forces for maximum lift condition and -15degrees elevator deflection

MAXIMUM LIFT CONDITION - ELEVATOR 15°

REYNOLDS NUMBER	Wing Lift	HTU Lift	Fuselage Lift	Wing Drag	HTU Drag	Fuselage Drag	Wing Pitching Moment	HTU Pitching Moment	Force Moment
RE	Lwing	Lhtu	Lfus	Dwing	Dhtu	Dfus	Mwing	Mhtu	Mf
-	N	N	N	N	N	N	Nm	Nm	Nm
62868	3.35295	0.78529	0	0.28820	0.02490	0.06692	-0.00151	0.0002123	0.200248
125736	13.2390	3.47242	0	1.11492	0.02490	0.23328	-0.00132	0.0002123	0.885467
188604	31.3811	7.85013	0	2.78209	0.02490	0.48503	-0.00773	0.0002123	2.001782
282906	70.8329	19.3359	0	6.28436	0.02490	1.00417	-0.02750	0.0002123	4.930642

Table 20 Individual Forces for cruise lift condition and no elevator deflection

CRUISE CONDITION - NO ELEVATOR

REYNOLDS NUMBER	Wing Lift	HTU Lift	Fuselage Lift	Wing Drag	HTU Drag	Fuselage Drag	Wing Pitching Moment	HTU Pitching Moment	Force Moment
RE	Lwing	Lhtu	Lfus	Dwing	Dhtu	Dfus	Mwing	Mhtu	Mf
-	N	N	N	N	N	N	Nm	Nm	Nm
62868	0.53007	0.090306	0	0.021905	0.003164	0.06692	-0.00298	0	0.023028
125736	2.12027	0.324622	0	0.062993	0.003164	0.233281	-0.01264	0	0.082779
188604	4.77061	0.515788	0	0.122745	0.003164	0.485031	-0.02627	0	0.131526
282906	10.7339	1.333654	0	0.248114	0.003164	1.004171	-0.05235	0	0.340082

Table 21Individual Forces for cruise lift condition and -15 degrees elevator deflection

CRUISE CONDITION - ELEVATOR 15°

REYNOLDS NUMBER	Wing Lift	HTU Lift	Fuselage Lift	Wing Drag	HTU Drag	Fuselage Drag	Wing Pitching Moment	HTU Pitching Moment	Force Moment
RE	Lwing	Lhtu	Lfus	Dwing	Dhtu	Dfus	Mwing	Mhtu	Mf
-	N	N	N	N	N	N	Nm	Nm	Nm
62868	0.53007	0.087100	0	0.021905	0.004275	0.06692	-0.00298	0.00044	0.022211
125736	2.12027	0.313133	0	0.062993	0.004275	0.06692	-0.01264	0.00044	0.079849
188604	4.77061	0.497152	0	0.122745	0.004275	0.06692	-0.02627	0.00044	0.126774
282906	10.7339	1.286314	0	0.248114	0.004275	0.06692	-0.05235	0.00044	0.328010

4.6 Total Forces

Finally, all forces generated were combined together to evaluate the total lift, drag and moments generated by the model aircraft as acting on the AC of the wing. The AC of the wing, positioned at 25% of the chord from the LE, is the position where all forces acting on the model were assumed to act.

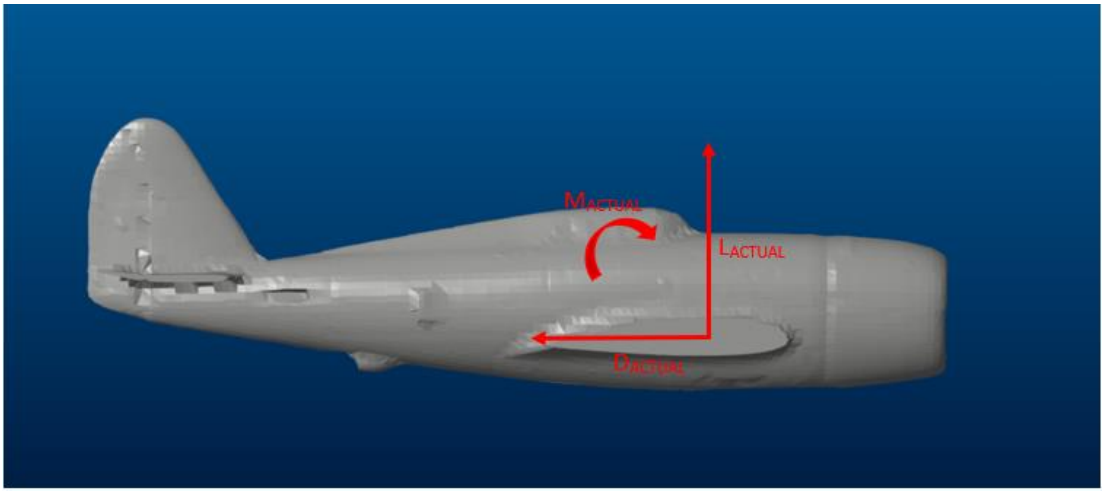

Figure 71 Model's depiction of actual loadings

This step was very straight forward, and it only required adding up together all the respective forces, such that:

$$L_{ACTUAL} = L_{wing} + L_{HTU}$$

$$D_{ACTUAL} = D_{wing} + D_{HTU} + D_{Fuselage}$$

$$M_{ACTUAL} = M_{wing} + M_{HTU} + M_{Forces}$$

The forces tabulated in Tables 22-25 are the forces read by the wind tunnel's balance during testing [5][6].

4.6.1 Total Forces Tabulations

Table 22 Summed Forces for maximum lift condition and no elevator deflection

MAXIMUM LIFT CONDITION - NO ELEVATOR

REYNOLDS NUMBER	Velocity	Total Lift	Total Drag	Total Pitching Moment	Force Moment
RE	v	L	D	M	Mf
-	m/s	N	N	Nm	Nm
62868	10	4.171865	0.386719	-0.001605528	0.208825
125736	20	16.85928	1.379801	-0.001415528	0.923176
188604	30	39.56577	3.298713	-0.007825528	2.087094
282906	45	90.99302	7.320131	-0.027595528	5.140843

Table 23 Summed Forces for maximum lift condition and -15degrees elevator deflection

MAXIMUM LIFT CONDITION – ELEVATOR AT 15°

REYNOLDS NUMBER	Velocity	Total Lift	Total Drag	Total Pitching Moment	Force Moment
RE	v	L	D	M	Mf
-	m/s	N	N	Nm	Nm
62868	10	4.138233	0.380026	-0.001297715	0.200248
125736	20	16.71140	1.373108	-0.001107715	0.885467
188604	30	39.23122	3.292020	-0.007517715	2.001782
282906	45	90.16870	7.3134380	-0.027287715	4.930642

Table 24 Summed Forces for cruise lift condition and no elevator deflection

CRUISE LIFT CONDITION - NO ELEVATOR

REYNOLDS NUMBER	Velocity	Total Lift	Total Drag	Total Pitching Moment	Force Moment
RE	v	L	D	M	Mf
-	m/s	N	N	Nm	Nm
62868	10	0.620376	0.091989	-0.002975	0.023028
125736	20	2.444892	0.299438	-0.012642	0.082779
188604	30	5.286398	0.610940	-0.026266	0.131526
282906	45	12.06755	1.255449	-0.052347	0.340082

Table 25 Summed Forces for cruise lift condition and -15degrees elevator deflection

CRUISE LIFT CONDITION – ELEVATOR AT 15°

REYNOLDS NUMBER	Velocity	Total Lift	Total Drag	Total Pitching Moment	Force Moment
RE	v	L	D	M	Mf
-	m/s	N	N	Nm	Nm
62868	10	0.617170	0.093100	-0.002535	0.022211
125736	20	2.433403	0.134188	-0.012202	0.079849
188604	30	5.267762	0.193940	-0.025826	0.126774
282906	45	12.02021	0.319309	-0.051907	0.328010

5 Wind-Tunnel Testing

This section deals with the practical part of the experiment created, which will serve as both validation of the results, as well as a guide to show whether the methodological process was done correctly or not. It will also introduce the students to wind-tunnel usage, which is of high importance in the aerospace industry.

The first part includes the design of the fixture between model and balance rod and the calibration of the whole balance. The second part is the testing itself, including reading the forces generated by the model mounted on the balance.

5.1 Balance & Fixture

The balance provided, shown in Figure 72, is a 2-axis balance which works by measuring the bending moments acting on the base of the rod. Since it does not measure torsional moments, the pitching moments and force moments computed in the theoretical part could not be tested for here.

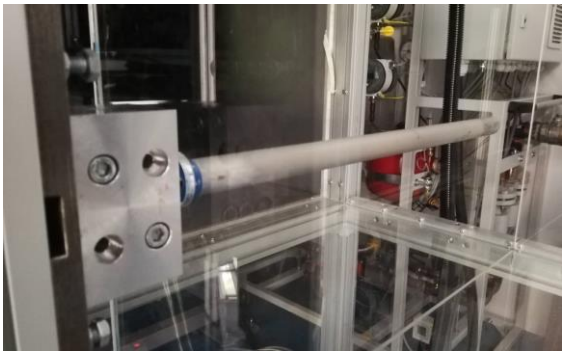

Figure 72 The balance mounted in the test-chamber, without the clamp and fixture

The overall balance consists of the measuring part itself, a rod which will extrude into the wind-tunnel test section, a clamp to join the balance rod to the intermediate fixture and the fixture itself. An intermediate fixture between the model and the balance was designed on Creo Parametric 3.0, Figure 73, and 3D printed.

The design process involved locating the C_{MAC} and MAC on the actual model and finding where this intersected with the centreline of the fuselage. This point lied on the battery slot; therefore, the model was to be mounted there in such a way that the vertical fixture lies on the same point.

Figure 73 CAD Model of the intermediate fixture for balance mounting

The clamp shown in Figure 74 was used as the connection between the balance and the intermediate mounting piece. The intermediate mounting was designed such that its base fixes to the clamp through the use of four screws. The clamp's design allowed for the model to be set at different angles to the horizontal by simply rotating the clamp itself around the balance rod before tightening. The vertical part of the fixture was designed with an aerofoil profile to reduce its influence on the measurements during testing and was printed as one piece with the base. The top part of the fixture was printed separately and has a hole in which the vertical fixture will be glued. Glue was used to fix the insert in the battery slot.

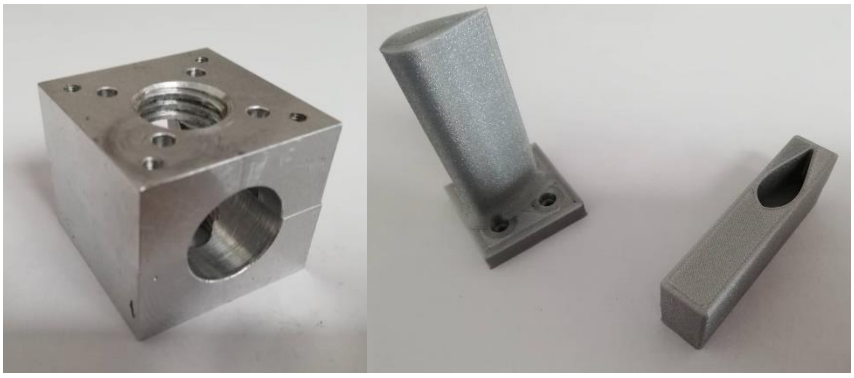

Figure 74 The clamp (left) used and the two 3D printed parts (right) of the intermediate fixture.

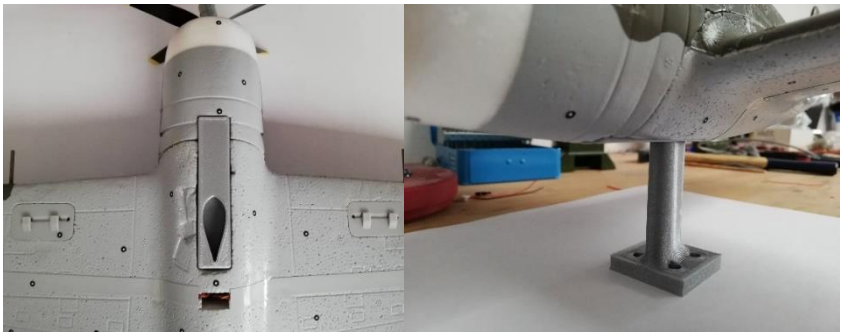

Figure 75 Fitting the fixture's insert in the battery slot (left) and the model mounted to the vertical fixture and base (right).

The balance was calibrated by first taking a reading with zero loading and then taking a reading with a known added load of 20N. When the balance was unloaded, the software was set to read at 0 N, and when it was loaded, it was set to read 20 N. The fixture with the model was then assembled in the test-chamber and set again to read at zero. The software used was DEWESoft X.

Figure 76 The model mounted in the test chamber before testing at AoA of 17 degrees

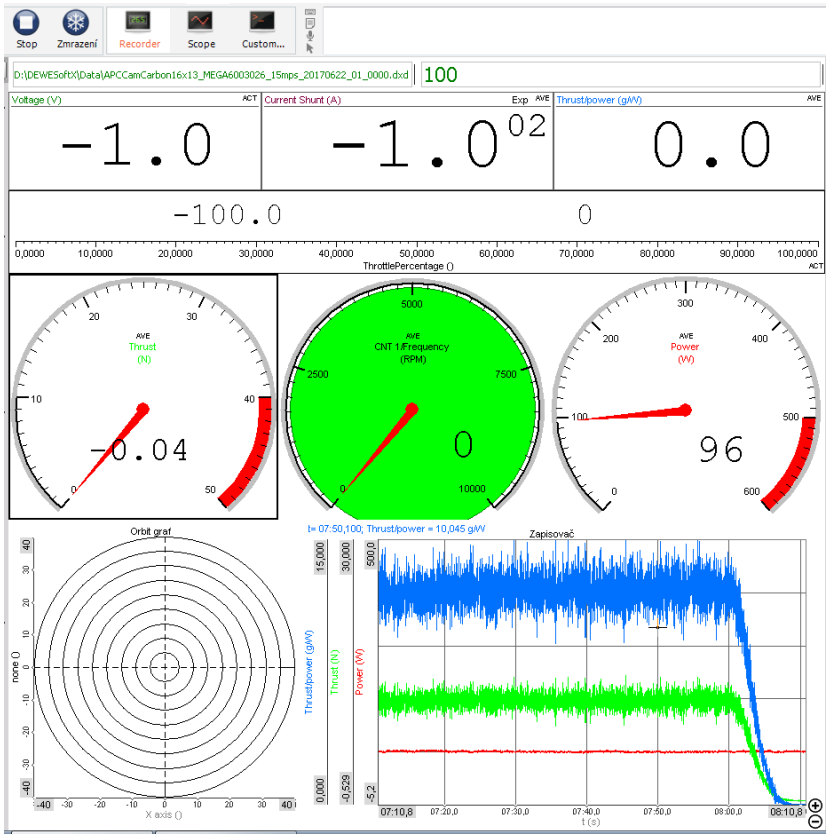

Figure 77 Screenshot of DEWESoft X showing a reading of 0 N Lift

5.2 Testing

The next step was to start the actual testing. The balance was meant to read lift and drag, however due to technical issues, the drag measurement was not possible. It was decided to follow through with the practical as it would be sufficient to obtain the readings for lift only given that the procedure is unchanged and the only difference is in reading one less value.

When the balance reads the forces generated in testing, it is measuring the forces generated by flow around the model as well as around itself. It would be ideal to actually measure the forces generated by the flow around itself by running the test without the model attached and then subtracting these forces from the reading given by the model and balance together. This was the original intention, however due to the time limitation brought about by the issue mentioned, it was decided to skip this step and take the balance effects on the results into considerations when analysing the results.

From the results obtained in the section Total Forces (p.73-4), it was decided that the best set-up to use would be without an elevator deflection and using the condition for maximum lift. The differences between the elevator being deflected and not seem to be negligible, therefore it is best to keep the set-up as simple as possible. At maximum lift conditions, the forces are naturally greater, and it is easier and more accurate for the balance to read larger forces than smaller ones.

From Table 6, it can be seen that at each boundary condition, the maximum lift occurs at a range of AoA between 18° and 22°. The angle of attack for maximum wing lift coefficient is given with respect to the wing, however it was necessary to subtract the setting angle of 1.665° so that the testing is done with respect to the fuselage. Due to these results, it was decided that the model should be tested at a range of AoA covering all these angles for different boundary conditions. This allowed for the possibility of achieving a lift curve, Figure 80, for the whole model for better result analysis. The angles tested in the wind tunnel were 0, 10, 15, 16, 17, 18 and 21 degrees and for each AoA two velocities, 10 and 20 m/s were tested. During testing it was visible that velocities greater than 20 m/s put the model under extreme physical stresses. Hence, it was decided not to use higher velocities. Should the model be 3D printed in the future, it could be possible to test at 30 and 45 m/s too.

A digital level was used to set the angles during different runs, and once the angles were set, the wind tunnel's velocity was increased through the knob control in a slow and steady manner. Once 10m/s was reached, the tunnel was given time to stabilize and then the lift reading was read from the computer. The velocity was increased to 20m/s, and once stabilized again, the new lift was read. The wind tunnel was turned off, the model adjusted to the next AoA and the procedure repeated, until all AoAs where covered.

Figure 78 The model mounted in the test chamber during testing at AoA of 0 degrees

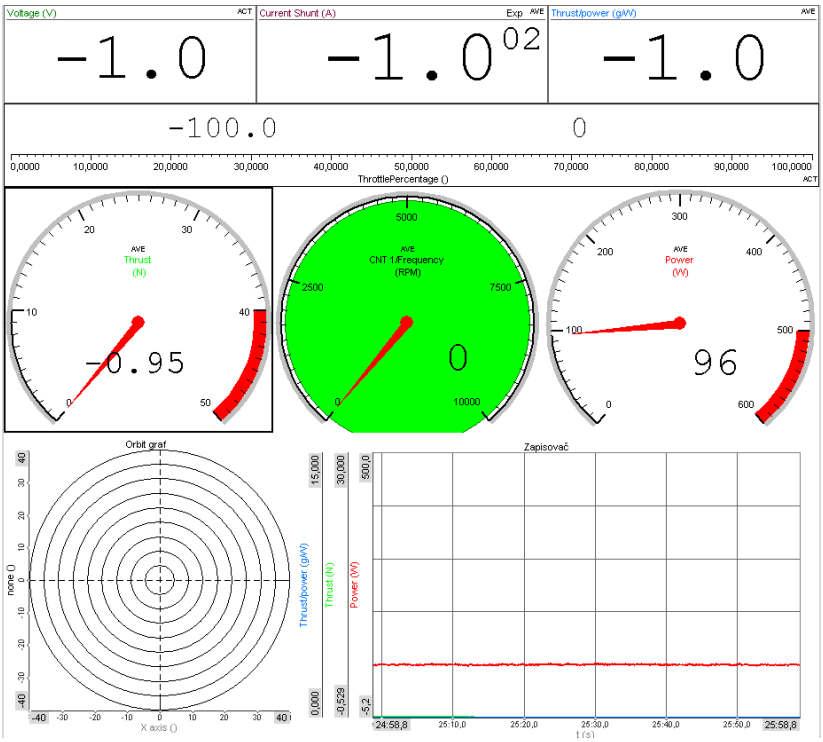

Figure 79 Screenshot of DEWESoft X for AoA 0 degrees at 20 m/s

The density of air during testing was noted to be 1.14285kg/m^3 which varies from the 1.2047 considered during the computations. The lift equation was reversed to solve for the lift coefficients at the current air density. The area considered was only that of the wings, as the HTU was too disruptive, via extreme vibrations, during testing that it was deemed ineffective compared to the wing.

Table 26 shows the results obtained from the wind-tunnel test at 10 and 20 m/s and for different AoAs.

Table 26 Wind-Tunnel results

10 m/s			20 m/s		
AoA	**LIFT**	**C_{LModel}**	**AoA**	**LIFT**	**C_{LModel}**
°	N	-	°	N	-
0	-0.38	-0.151	0	-0.95	-0.09438
10	1.72	0.683496	10	6.98	0.69343
15	2.37	0.941793	15	9.42	0.935833
16	2.41	0.957689	16	9.42	0.935833
17	2.43	0.965636	17	9.74	0.967623
17	2.48	0.985505	17	9.7	0.963649
18	2.46	0.977558	18	9.54	0.947754
21	2.37	0.941793	21	9.58	0.951728

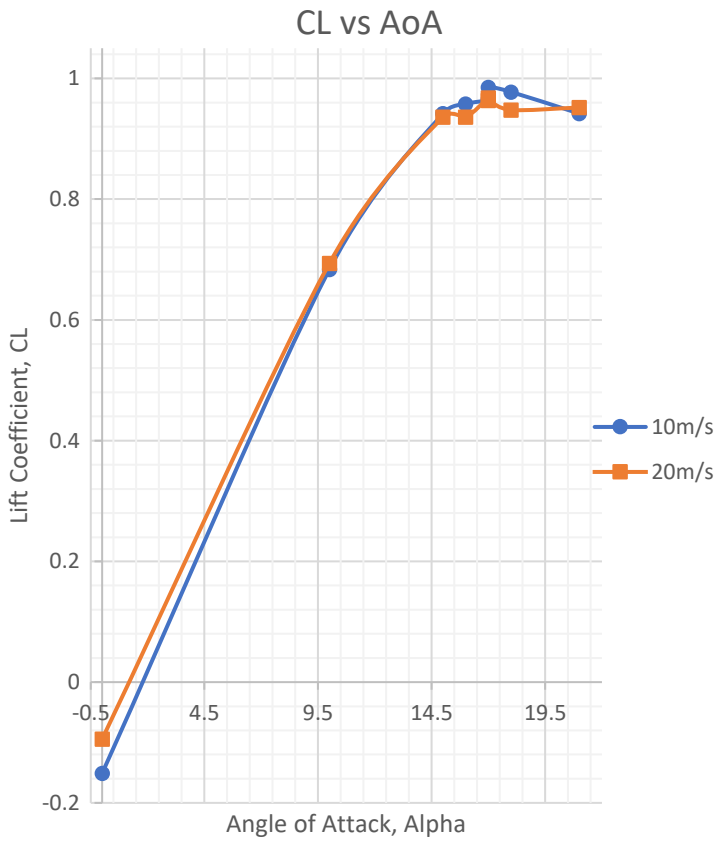

Figure 80 Lift curves generated for the model through testing

At the first boundary condition in the computational part, RE=62868, the AoA for maximum lift of the wing occurred at 17° with respect to the fuselage, and at this angle the test was run twice for more accurate results. The AoA for the largest lift at 10 m/s was found to be 17°, in accordance with the computational part, however at 20 m/s it was found to be also 17°, rather than the 18° computational counterpart. This was still satisfactory when the systematic errors are taken into consideration. At an AoA of zero degrees, the model generated negative lift.

The lift values obtained for the model at 17° during the two different runs of 10 and 20 m/s were then compared to the theoretical ones, tabulated in Table 27.

Table 27 Comparison between theoretical and practical Lift results at 17° for 10 and 20 m/s

	Lift	
	N	
17°	Theoretical	Practical
10 m/s	4.171865	2.46
20 m/s	16.85928	9.72

By first inspection, it appears that the difference is significant. The practical part resulted in almost half the theoretical value at 10 m/s, however the difference seems to be slightly reduced at 20 m/s. Taking percentages, at 10 m/s, the practical result is 60 % of the theoretical and at 20 m/s, the practical result is also around 60 % of the theoretical. This means there is consistency in the error. The same difference can be observed when comparing the maximum lift coefficient of the wings, to those of resulted here. The wing had $C_{Lwingmax}$ of 1.265 and 1.248 at 10 and 20 m/s respectively, whereas here C_{Lmodel} are 0.975 and 0.965 respectively. It is good to note that due to some occurrence, during the practical, the lift coefficient was greater at the lower velocity.

Prior to testing, it was well known that errors will exist. The main error is that the wind-tunnel is designed for models of scale up to 1:48, whereas the model used has a scale of approximately 1:25. The wing tips are too close to the walls, and wall influence plays a major part in the outcome. During testing it was also noted that the wing and HTU were vibrating, with the latter vibrating quite vigorously. This meant that the flow around the HTU was probably separating. The flow to the HTU was disrupted significantly by the wings and balance, both of which were directly in the path of incoming flow. Figure 81 shows the vibration effects on the HTU and wings during testing at 20 m/s.

Figure 81 Vibrations' distortions at the HTU and wing tips

Considering that the HTU was computed to generate 0.82 N at 10 m/s and 3.62 N at 20 m/s, and assuming that these are rendered ineffective during the testing, the practical results were quite accurate. If the HTU was not ineffective during testing, and it was performing properly, then these forces would be added to the output. If these are added to their respective outputs, at 10 m/s the total would be 3.28 N and at 20 m/s the total would be 13.34 N which are very close to those computed. As there is no evidence that the HTU was ineffective, however, this assumption could not be taken.

Other sources of error include the misalignment of the AoA, vibrations in the balance, geometric imperfections in the model, surface imperfections in the model, physical details that were unaccounted for during computations such as the mountings for the wheels and servo mechanisms, and body rigidity of the whole model.

6 Conclusion

The goal of the thesis project was to create an experiment highlighting the main practical topics covered throughout the course Aerodynamics I to analyse aerofoils and finite wings, as well as give a better understanding of wind-tunnels in one main project.

Starting with 2D analysis of aerofoils, through the use of XFOIL, helped in learning to work with XFOIL or similar software to analyse 2D aerofoil characteristics and process the output data. It brought about the use of curves of aerodynamic properties of the said 2D aerofoils; C_L-α, C_L-C_D and C_L-C_M. Having obtained the curves for different aerofoils, different boundary conditions and different set-ups would help students to recognise how these variants affect the properties.

The use of Glauert III was made to then convert the 2D characteristics over a finite wing (3D) resulting in the forces' distributions along the span. Glauert III outputs visualisation of the lift coefficient distribution, and a set of results which could be used alongside the curves generated by XFOIL to obtain the distribution for the drag and pitching moments. This step helped in understanding better the relation between the lift, drag and pitching moments coefficients, and how the latter two vary with different lift characteristics and different set-ups.

Basic computations of general aerodynamic properties of a finite wing were done next. These were covered throughout the course, and involve formulations to convert the coefficients into forces, as well as independent formulae to compute for the moments generated by the HTU's lift with respect to the wing's MAC as well as formulation for the friction drag around a body of a complex geometry using the Von Karman's $1/7^{th}$ power law.

To close the theoretical part, the computed forces were depicted visually to show where and how they are acting on the model individually (realistically), followed by their summation and depiction of how they are acting around the mounting point (MAC_{wing}) in the wind-tunnel.

Wind-Tunnel testing is quite straightforward in its own respect; the main goal here was to familiarise with the setting up and usage of wind-tunnels and actual testing, as well as analysing the output data. Essentially a crucial part in the whole experiment, this step can show any errors done during the theoretical part or even during the testing itself, as it serves also as data validation.

The results obtained through the wind-tunnel varied a bit from the theoretical ones, and although mistakes in theoretical part are not to be excluded, sources of error mentioned in both the Testing section and in the Sources of Error are considered primary reasons why the results were off. Overall, the results obtained were quite satisfactory.

The main project followed through all the essential steps necessary to get a hands-on experience of the aerodynamic world through computations and practical sessions. Working directly on a model of any aircraft makes for a more interesting approach to learn and understand the subject better.

Along the path of the experiment creation, modern technologies such as 3D scanning and 3D printing were also put to use, which adds to the equation a modern engineering approach in problem solving.

At the end of the project, there still exist possibilities for future work and expansion on the problem, for instance 3D printing the whole model and testing at greater speeds with better body rigidity for more accurate results, and CFD can be used for validation too.

7 Sources of Error

- Manufacturing defects might alter the model's geometry and consequently aerodynamic properties.
- 3D scanning; mainly due to the lens effect, low scan quality due to reflective surface which leads to holes in the resulting mesh and effectively altering the actual geometries such as aerofoil shapes, angles in the geometry and other dimensions.
- CAD processing; inaccurate readings of measurements due to graphics limitations of tiny details, such as very sharp edges or notches in the actual model. This might affect all of the geometry acquisition section.
- XFOIL; results were varying between runs, and even if the difference was close to negligible, it still alters the final results. Some cases were even failing to converge.
- Assumptions; negligible differences caused by dihedral angle, geometric twist assumed to be distributed evenly along wing span, HTU results at different boundary conditions considered to be relevantly equal due to failed convergence on XFOIL, negligible lift caused by the fuselage amongst others, wing and HTU lift curves assumed to be a perfect straight line.
- Difference in properties of air between the conditions taken for theory to the actual ones during the wind-tunnel testing.
- Systematic Errors; Inaccuracies in the wind-tunnel testing which might include unstable flow, non-accurate angle of attack, wall influence, inaccurate calibration of the balance, vibrations in the balance and vibrations within the model.
- Human error; computations, measurement readings and set-ups.

8 Bibliography

[1] E-flite® UMX™ P-47 BL BNF Basic Brushless Ultra Micro Scale RC Airplane Warbird | Horizon Hobby. (n.d.). Retrieved February 11, 2019, from https://www.horizonhobby.com/umx-p-47-bl-bnf-basic-eflu3250

[2] Republic P-47 Thunderbolt. (n.d.). Retrieved February 11, 2019, from http://www.aviation-history.com/republic/p47.html

[3] NACA 4-digit airfoil generator (NACA 2412 AIRFOIL). (n.d.). Retrieved March 13, 2019, from http://airfoiltools.com/airfoil/naca4digit

[4] Vogeltanz, T. (2016). Application for calculation of mean aerodynamic chord of arbitrary wing planform. *AIP Conference Proceedings*, *1738*, 10–14.

[5] Valentine, D. T., Collicott, S. H., Carpenter, P. W., & Houghton, E. L. (2016). Aerodynamics for Engineering Students. In *Aerodynamics for Engineering Students*.

[6] POPE, A., BARLOW, J., RAE, H., Low-Speed Wind Tunnel Testing, Wiley and sons, ISBN 0-47-55774-9.

[7] Fluid Properties Calculator. (n.d.). Retrieved March 5, 2019, from http://www.mhtl.uwaterloo.ca/old/onlinetools/airprop/airprop.html

[8] Drela, M. (2001). *XFOIL 6.94 User Guide*. 33.

[9] Vanek, F., Hlinka, J., & Bartonek, J. (2010). *Glauert III (user's guide)*. 1–26.

[10] Kudela, H. (n.d.). *Turbulent flow*. Retrieved March 11, 2019, from http://www.itcmp.pwr.wroc.pl/~znmp/dydaktyka/fundam_FM/Lecture_no3_Turbulent_flow_Modelling.pdf

[11] Velazquez, L. (2009). Low-Speed Wind Tunnel Testing For an Unmanned Aerial Vehicle Airfoil. *Colloquium Fluid Dynamics*, pp. 1–4.

[12] Gonzalez, M., Ezquerro, J. M., Lapuerta, V., Laveron, A., & Rodriguez, J. (2012). Components of a Wind Tunnel Balance: Design and Calibration. *Wind Tunnels and Experimental Fluid Dynamics Research*.

[13] Manual, I. (n.d.). *UMX P-47 Thunderbolt*.

9 Nomenclature

ρ	Density
μ	Dynamic Viscosity
ν	Kinematic Viscosity
2D	Two Dimensional
3D	Three Dimensional
A	Area
AoA, α	Angle of Attack
CAD	Computer Aided Design
CFD	Computational Fluid Dynamics
C_D	Drag Coefficient
C_F	Friction Coefficient
C_L	Lift Coefficient
C_M	Pitching Moment Coefficient
C_{MAC}	Mean Aerodynamic Chord Length
D	Drag
HTU	Horizontal Tail Unit
L	Lift
LE	Leading Edge
M	Moments
MAC	Mean Aerodynamic Centre
NACA	National Advisory Committee for Aeronautics
RE	Reynolds Number
TE	Trailing Edge
v	Velocity

10 List of Figures

11 List of Tables

12 List of Appendices

- Appendix A – XFOIL Results
- Appendix B – GLAUERT III Results

13 Appendix A – XFOIL Results

This section contains the curves of lift coefficients versus angle of attack, drag coefficient and pitching moment coefficient for both aerofoils at different boundary conditions and set-ups as obtained through XFOIL's results. The first part contains the wing's NACA2313 aerofoil's 2-D characteristics, with each of the three plots for each boundary condition. The second part holds the 2-D characteristics for the HTU's NACA0005 aerofoil, with each of the plots for elevator without deflection and with -15° deflection (Upwards).

The tables generated by XFOIL are not displayed, as they are quite large and not really necessary; however, it is good to note that XFOIL's values might vary between different runs for the same conditions.

The CL vs Alpha (α) was used to obtain values required as inputs in Glauert III, which include maximum lift coefficient, C_{Lmax}, Zero-Lift Angle, α_0, and the Curve Slope, C_L-α.

C_L vs C_D and C_L vs C_M curves were used to find the Drag and Pitching Moment coefficient distributions along the wing and HTU, once Glauert III's results were obtained.

13.1 NACA2313

13.1.1 Re=62868

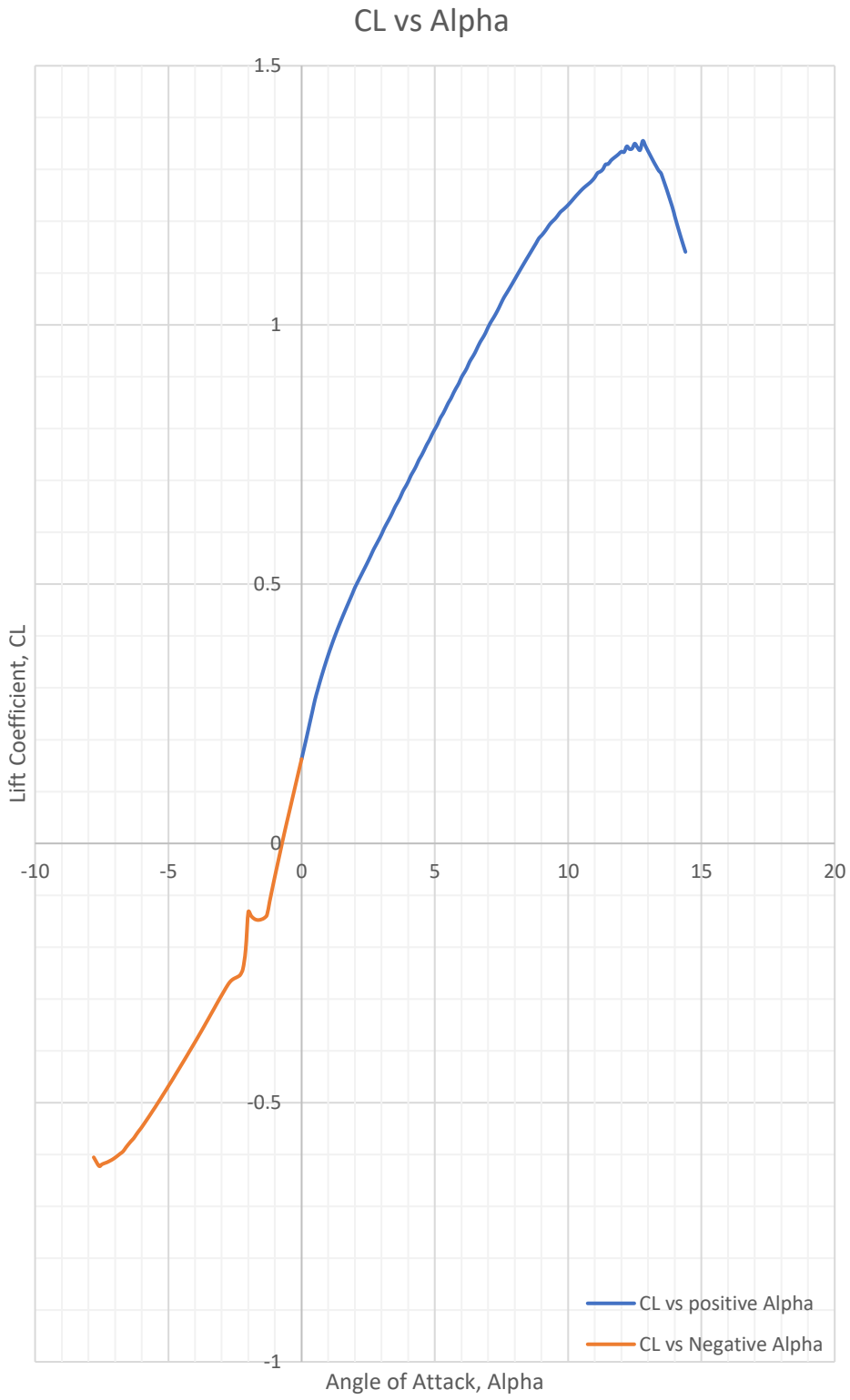

Figure 82 NACA2313's C_L vs Alpha graph at Re=62868

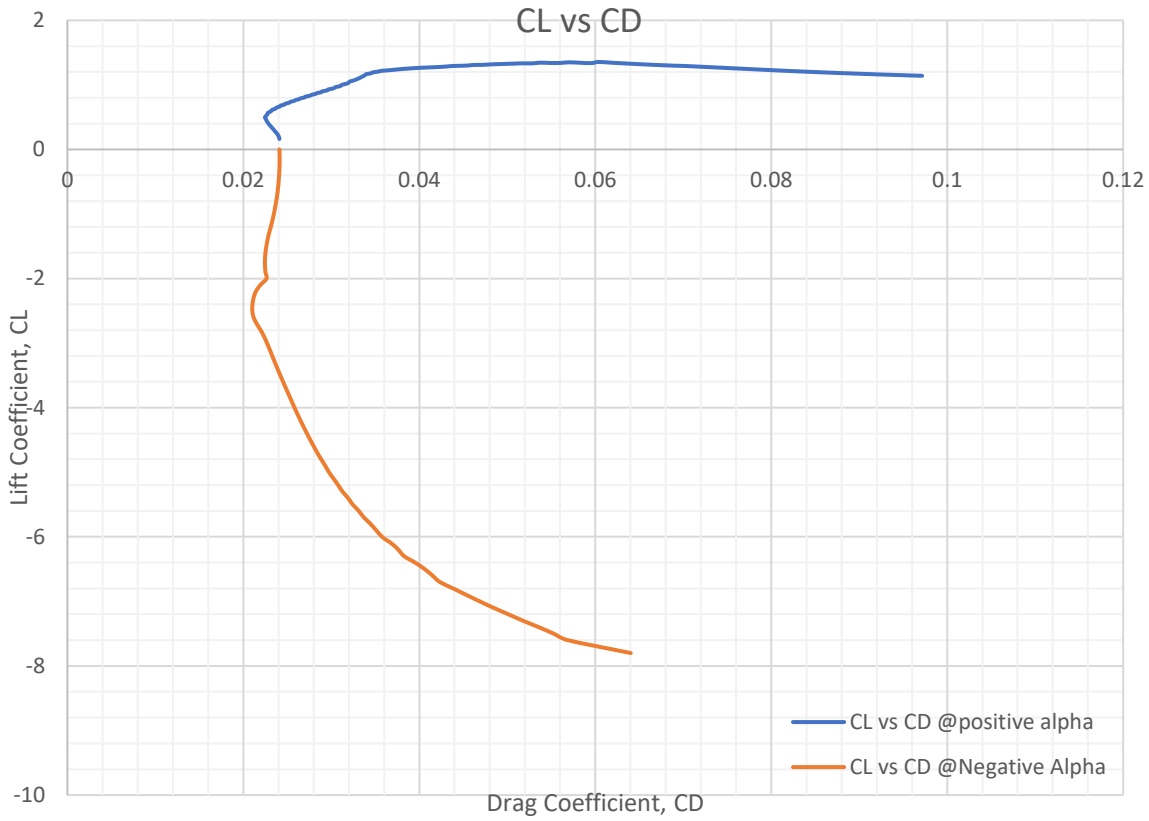

Figure 84 NACA2313's C_L vs C_D graph at Re=62868

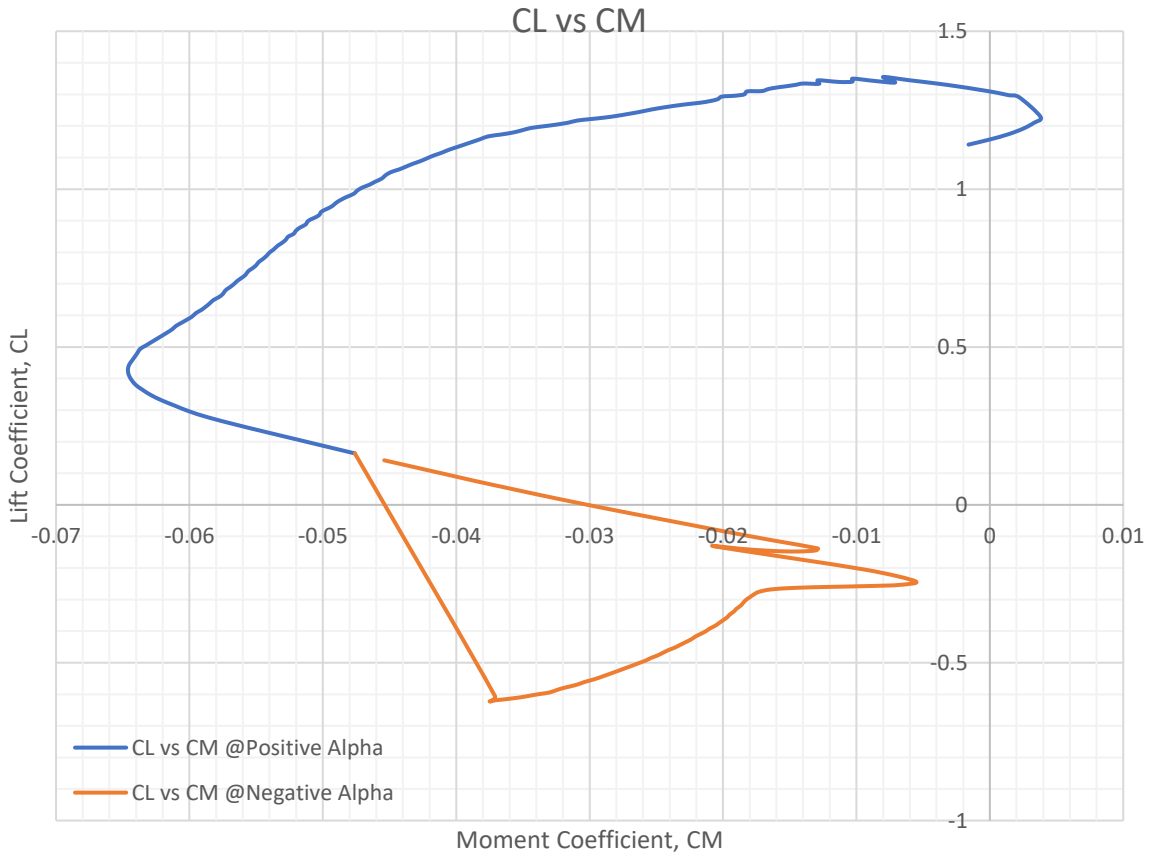

Figure 83 NACA2313's C_L vs C_M graph at Re=62868

13.1.2 Re=125736

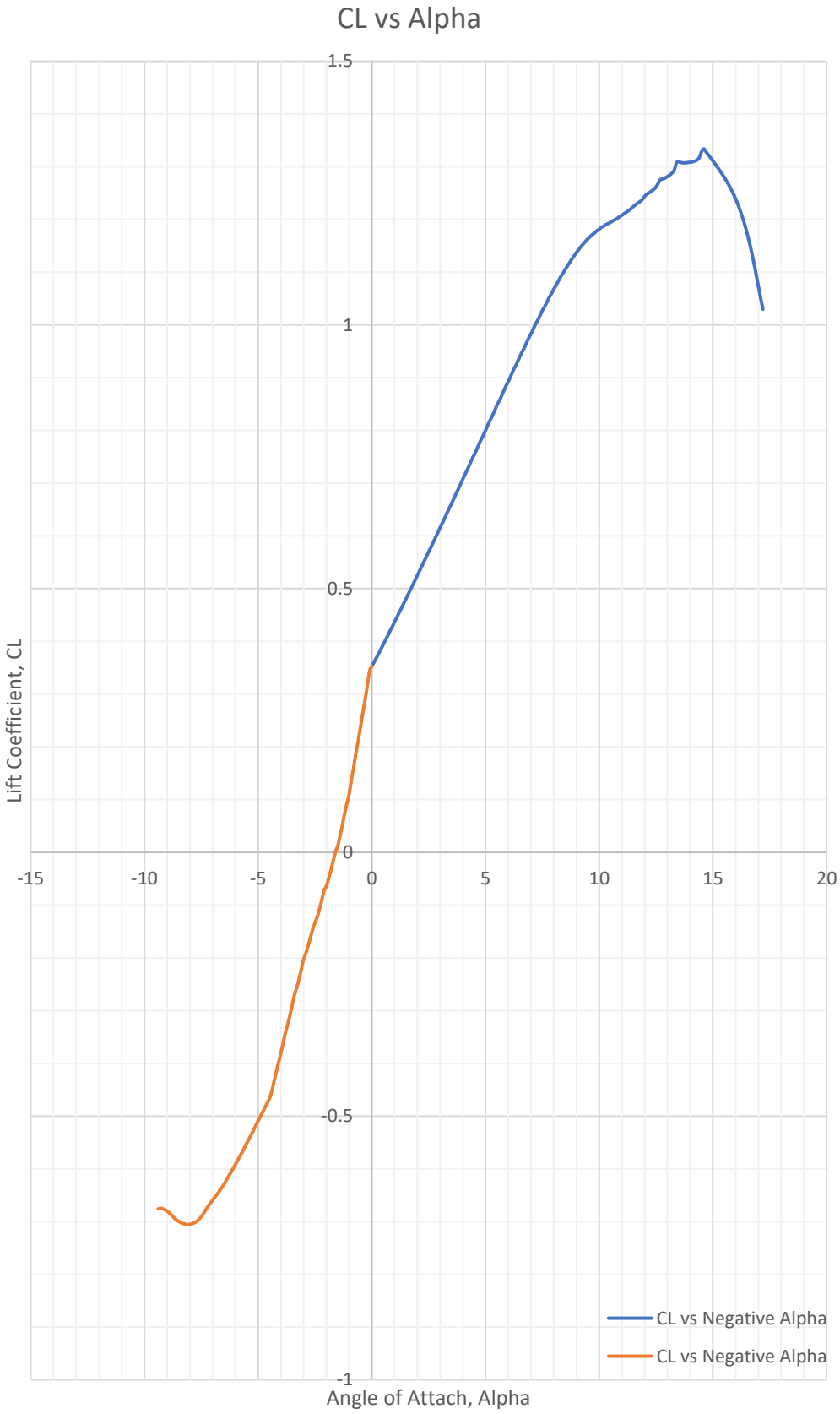

Figure 85 NACA2313's CL vs Alpha graph at Re=125736

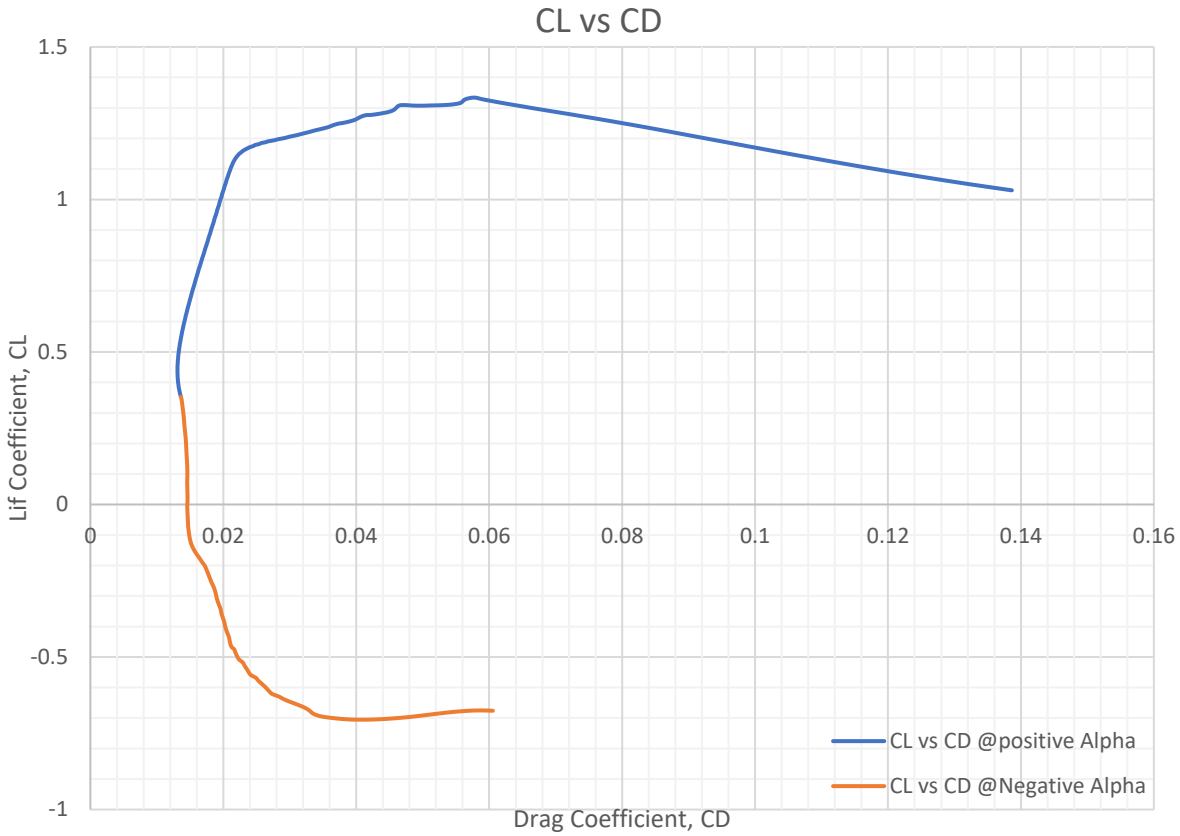

Figure 87NACA2313's C_L vs C_D graph at Re=125736

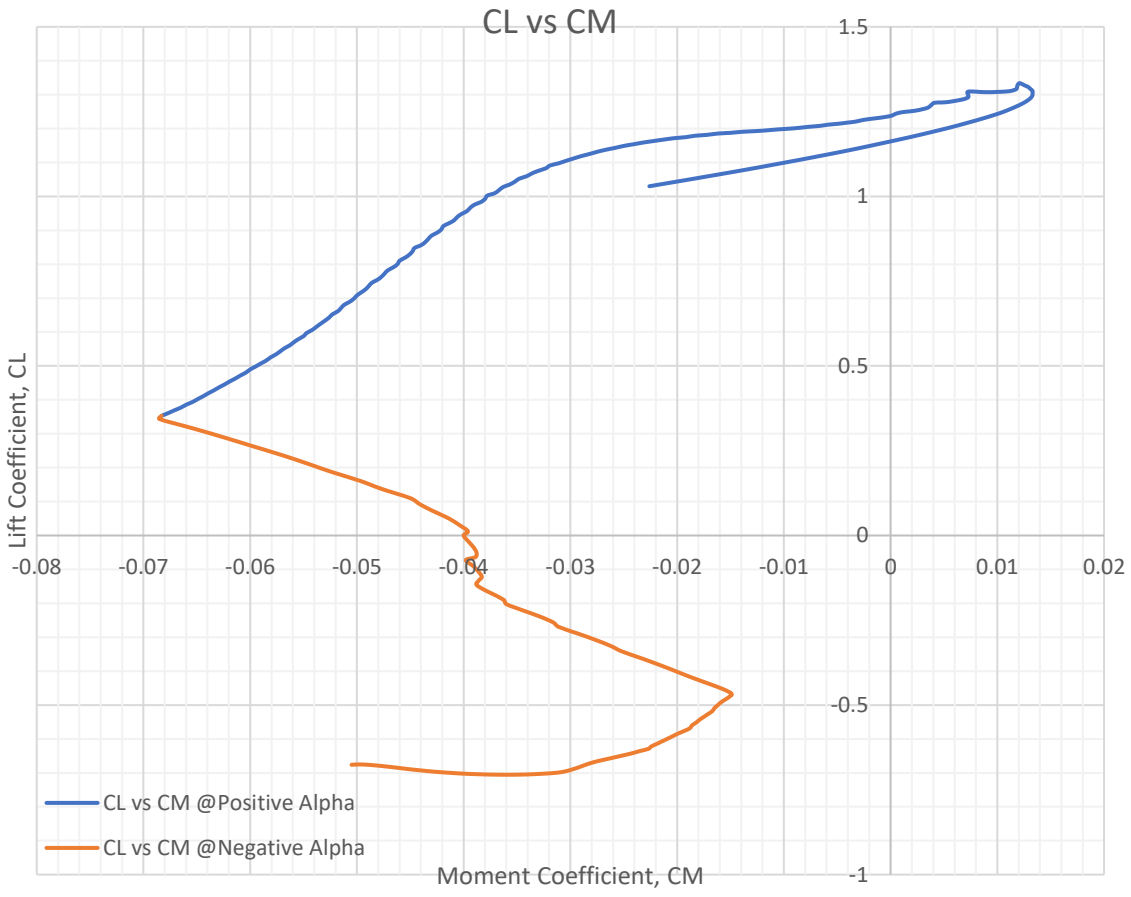

Figure 86NACA2313's C_L vs C_M graph at Re=125736

13.1.3 Re=188604

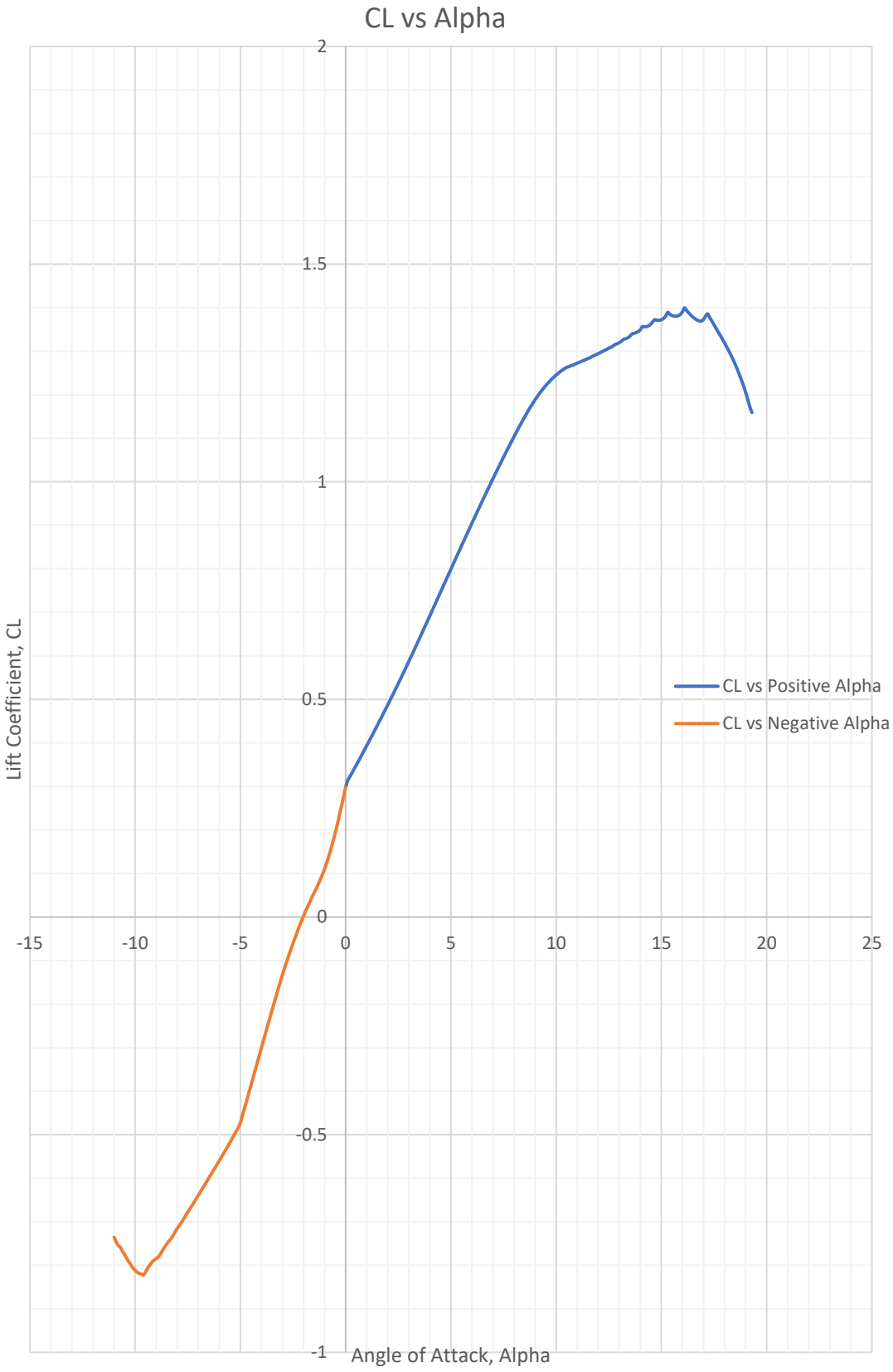

Figure 88NACA2313's CL vs Alpha graph at Re=188604

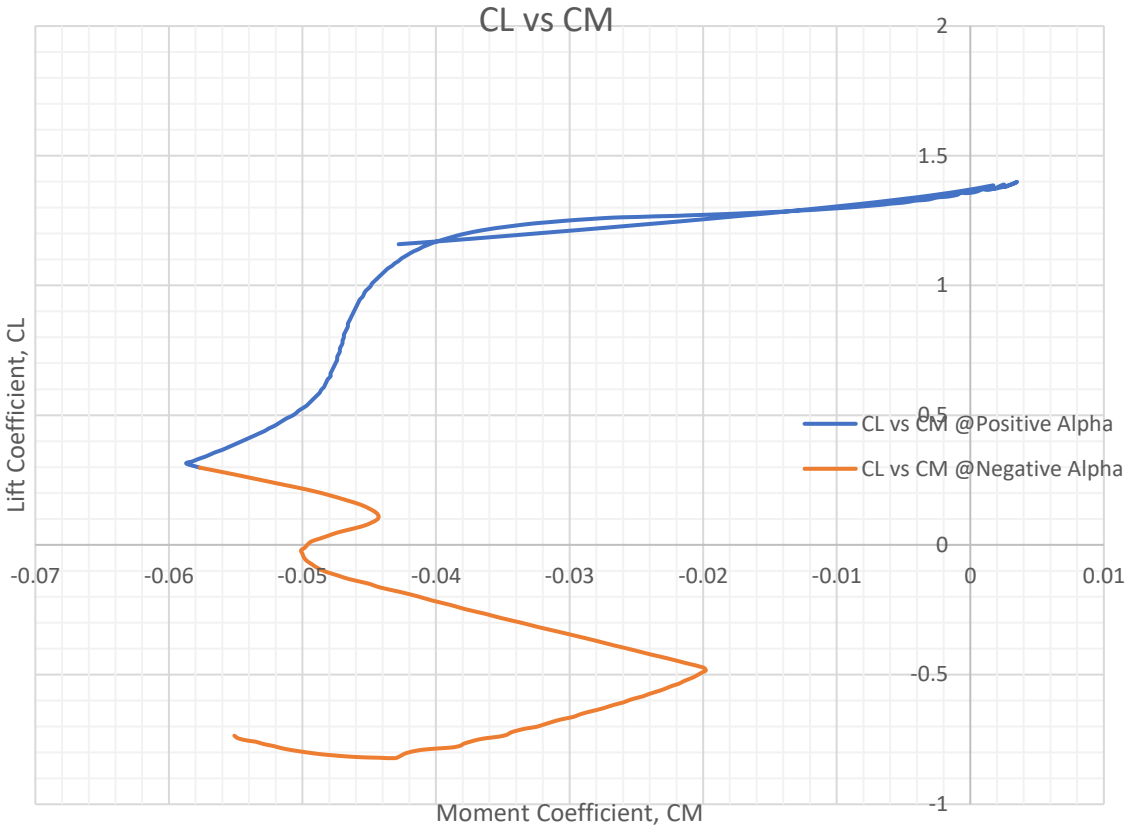

Figure 90 NACA2313's C_L vs C_D graph at Re=188604

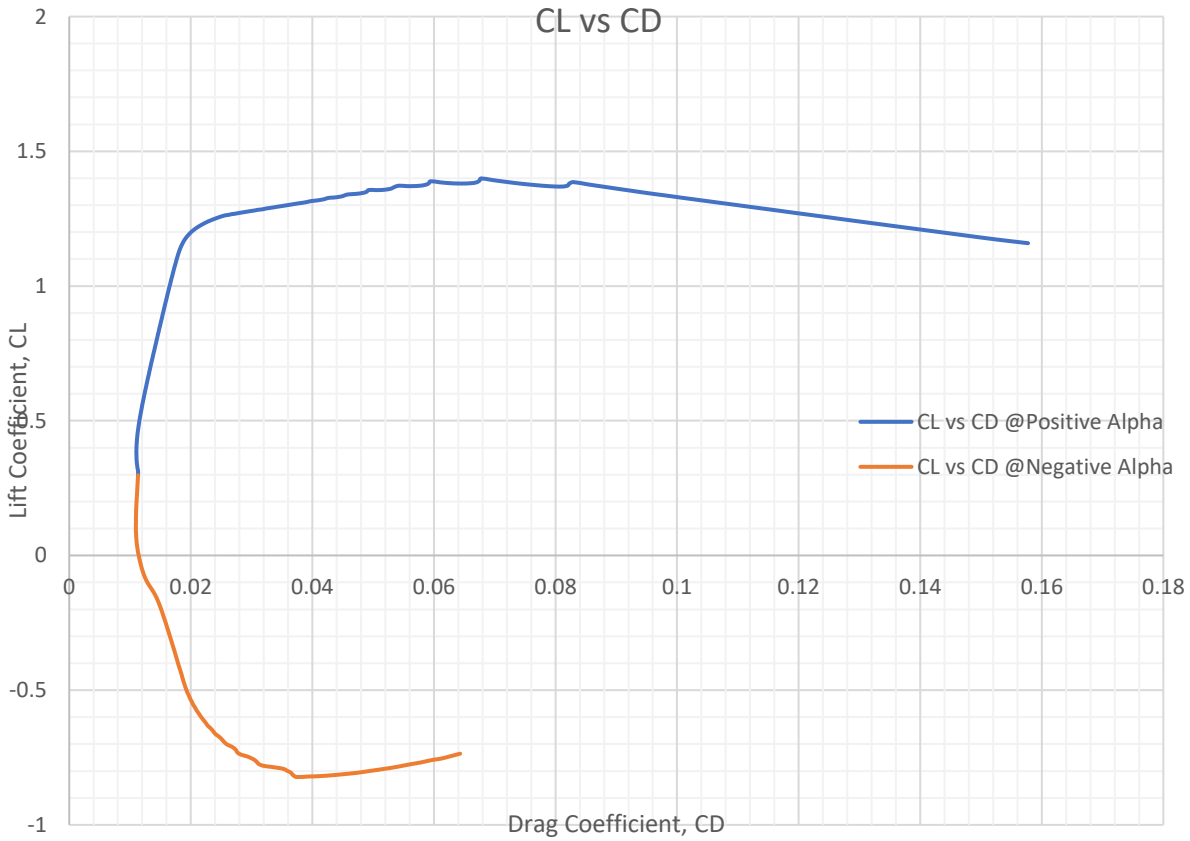

Figure 89 NACA2313's C_L vs C_M graph at Re=188604

13.1.4 Re=282906

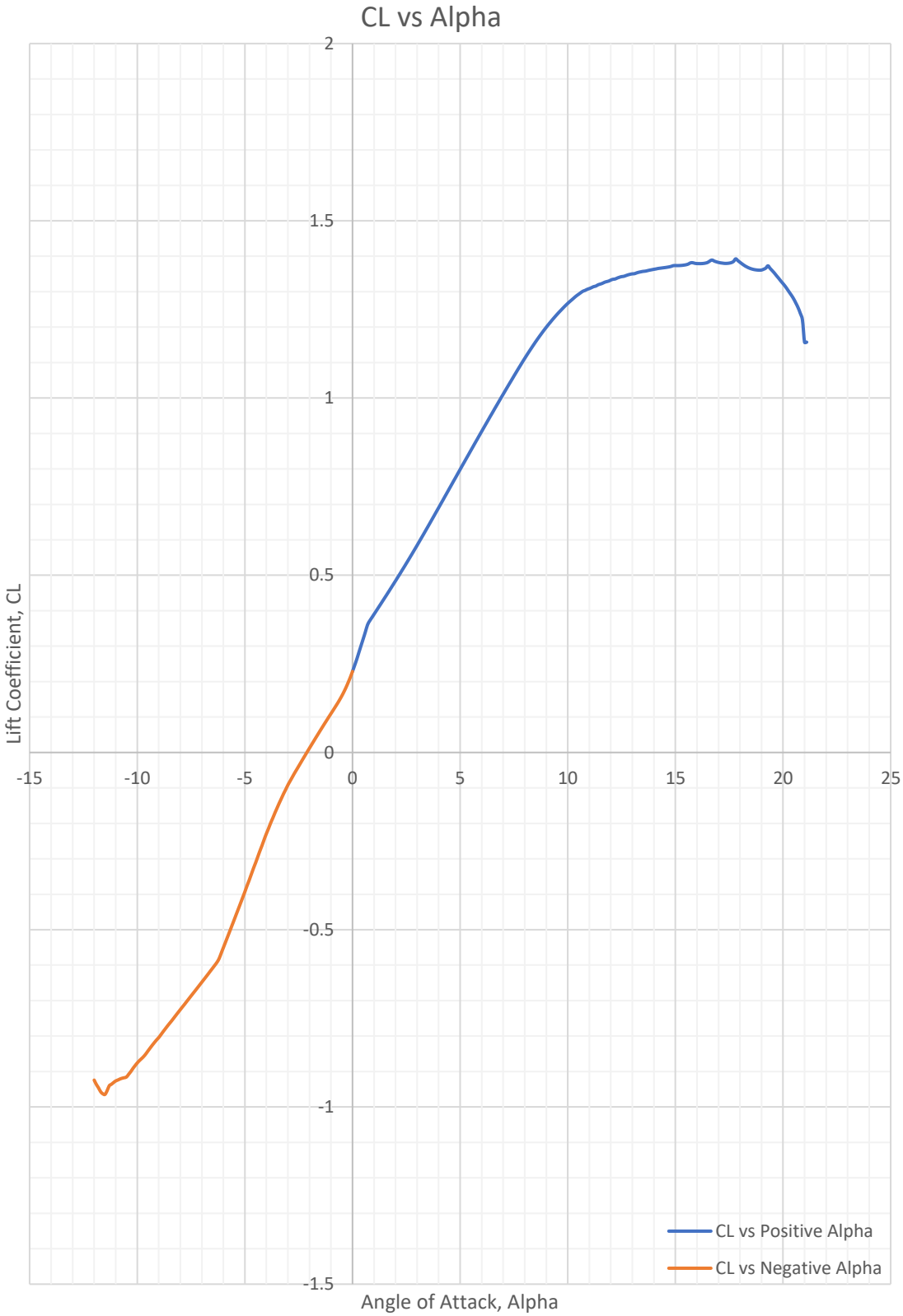

Figure 91 NACA2313's C_L vs Alpha graph at Re=282906

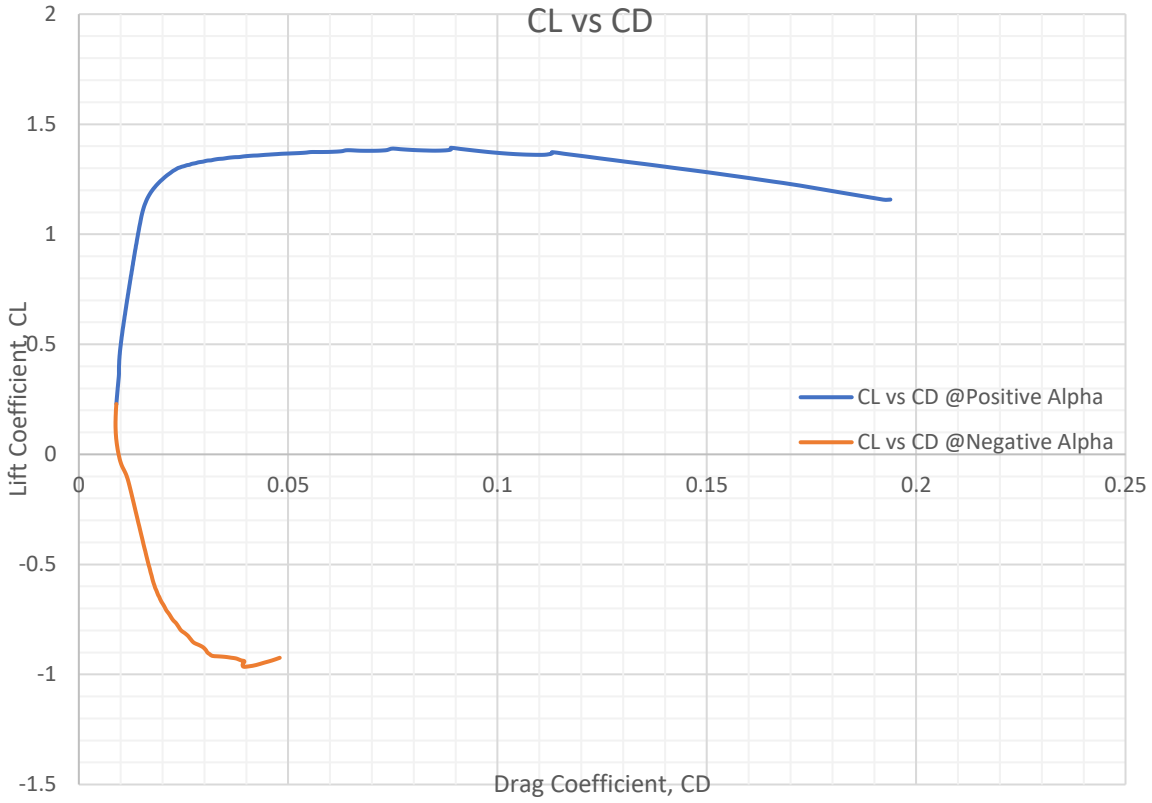

Figure 93 NACA2313's C_L vs C_D graph at Re=282906

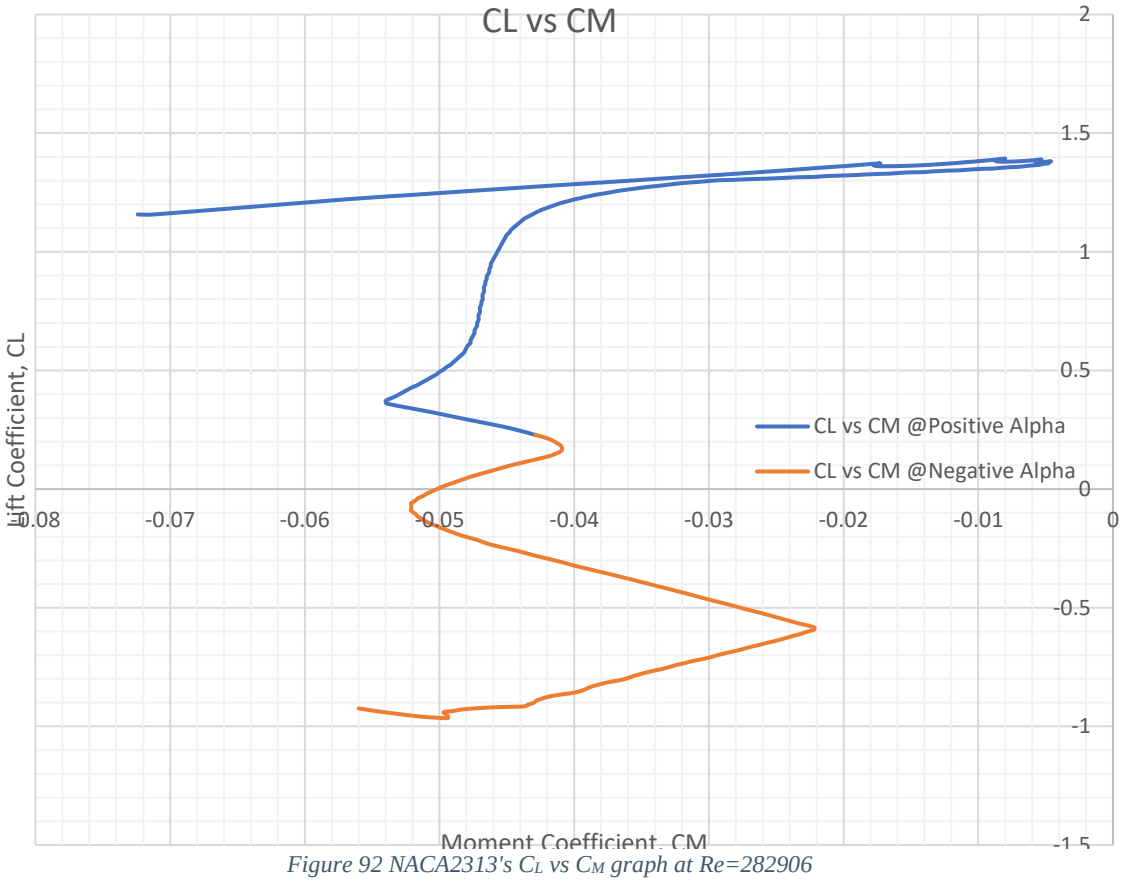

Figure 92 NACA2313's C_L vs C_M graph at Re=282906

13.2 NACA0005

13.2.1 Re=62868; No Elevator Deflection

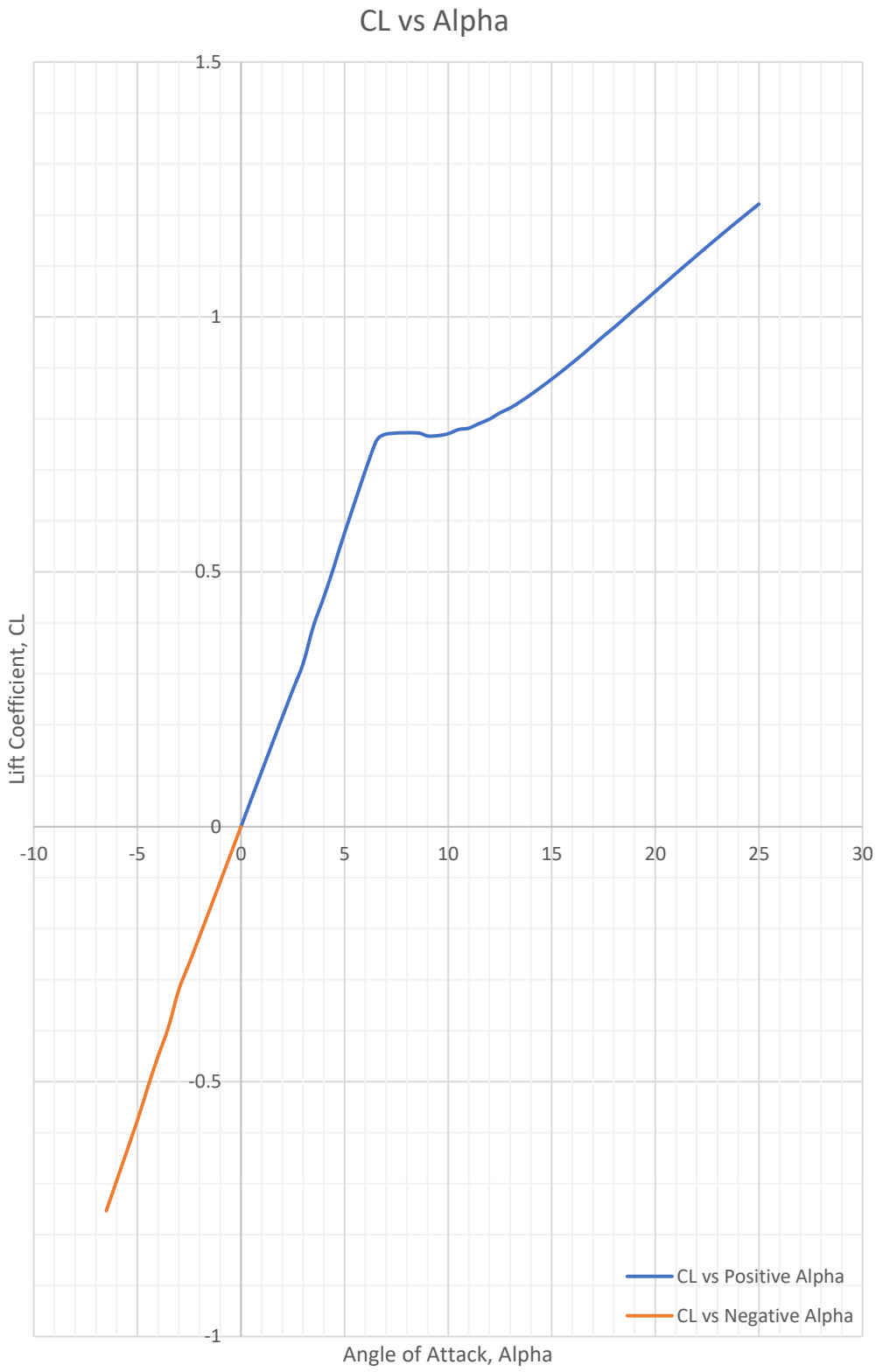

Figure 94 NACA0005's C_L vs Alpha graph at Re=62868 [No Elevator Deflection]

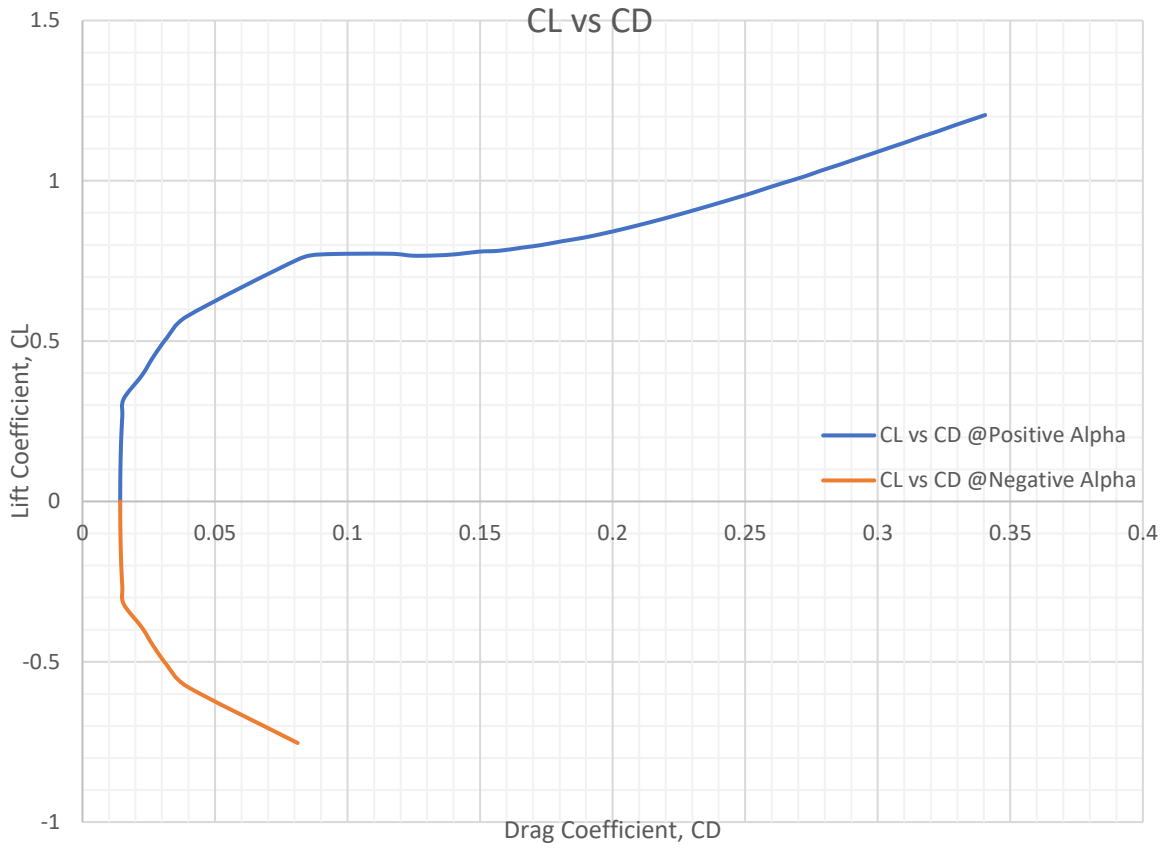

Figure 96 NACA0005's C_L vs C_D graph at Re=62868 [No Elevator Deflection]

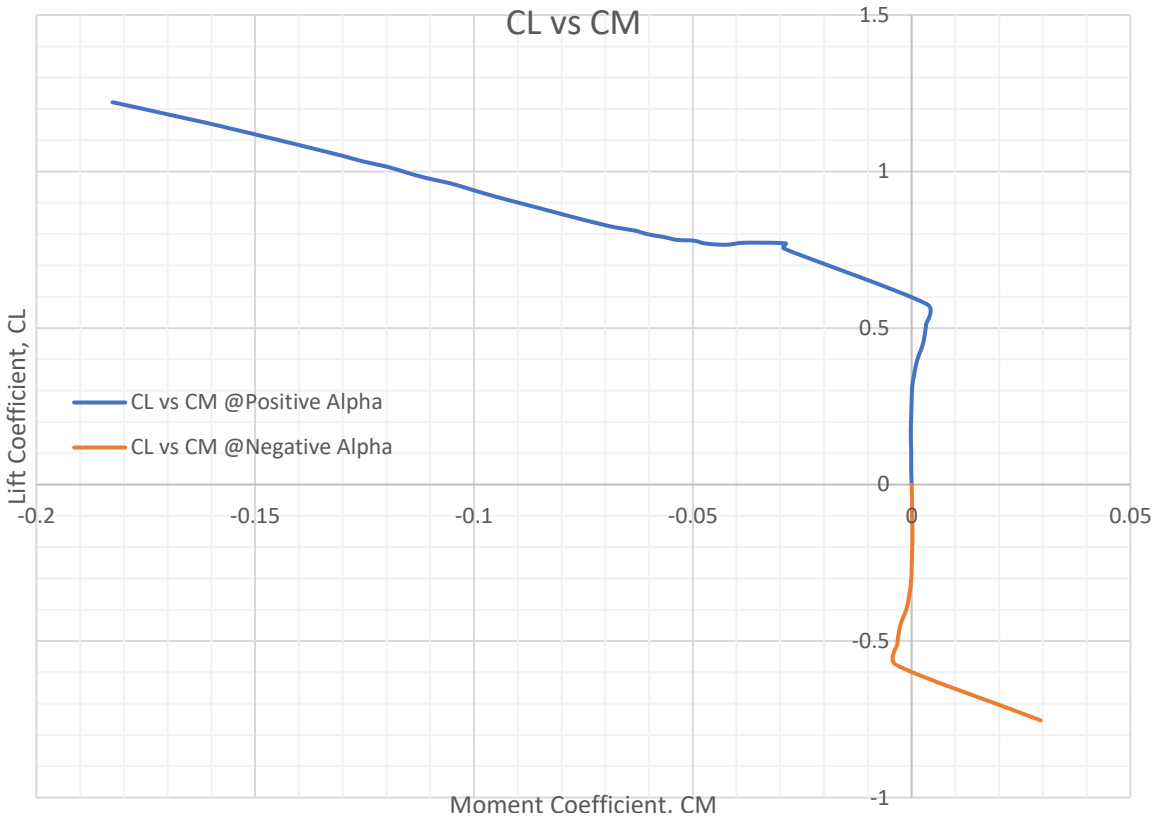

Figure 95 NACA0005's C_L vs C_M graph at Re=62868 [No Elevator]

13.2.2 Re=62868; Elevator Deflection -15°

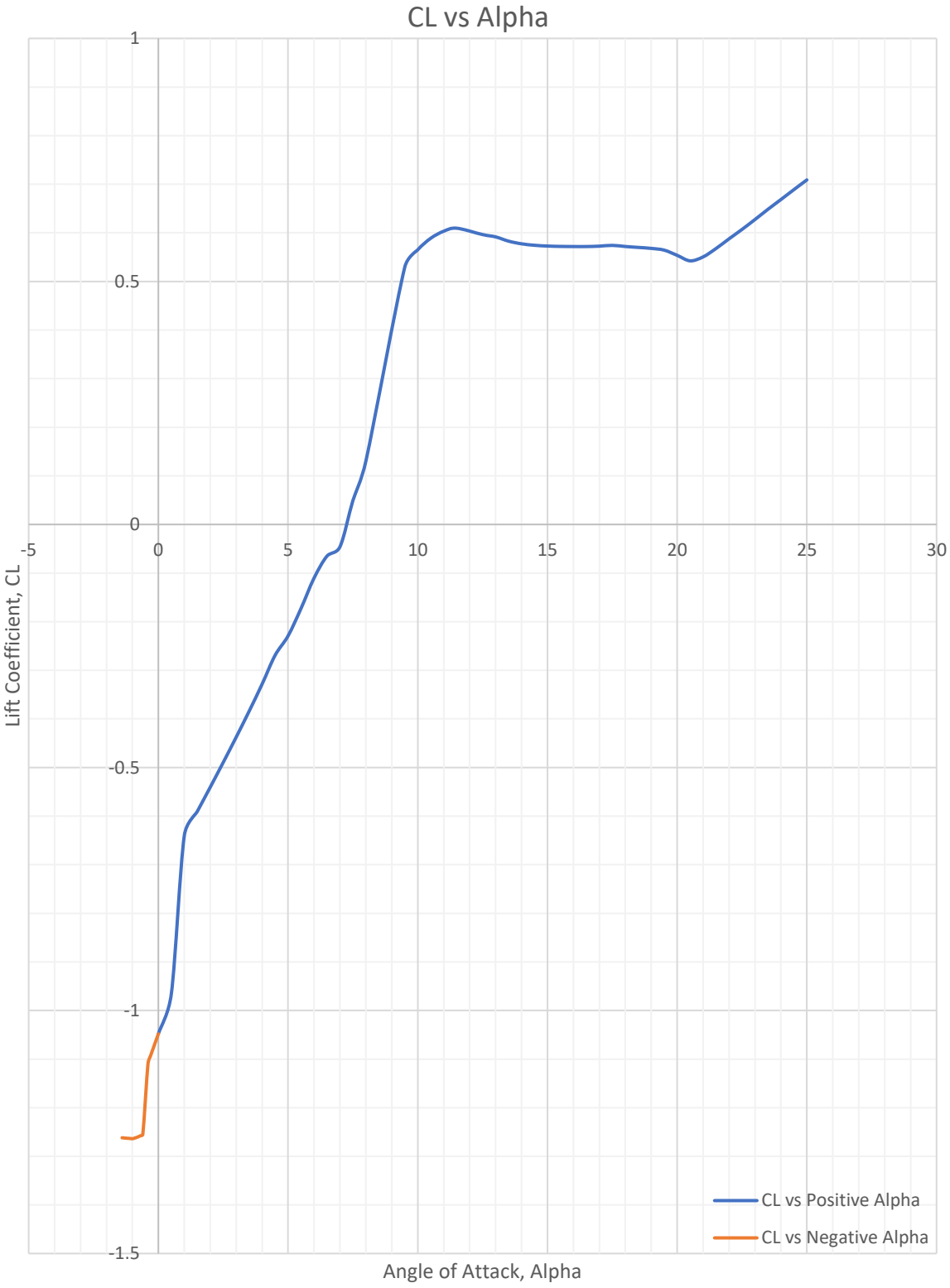

Figure 97 NACA0005's C_L vs Alpha graph at Re=62868 [Elevator Deflection -15°]

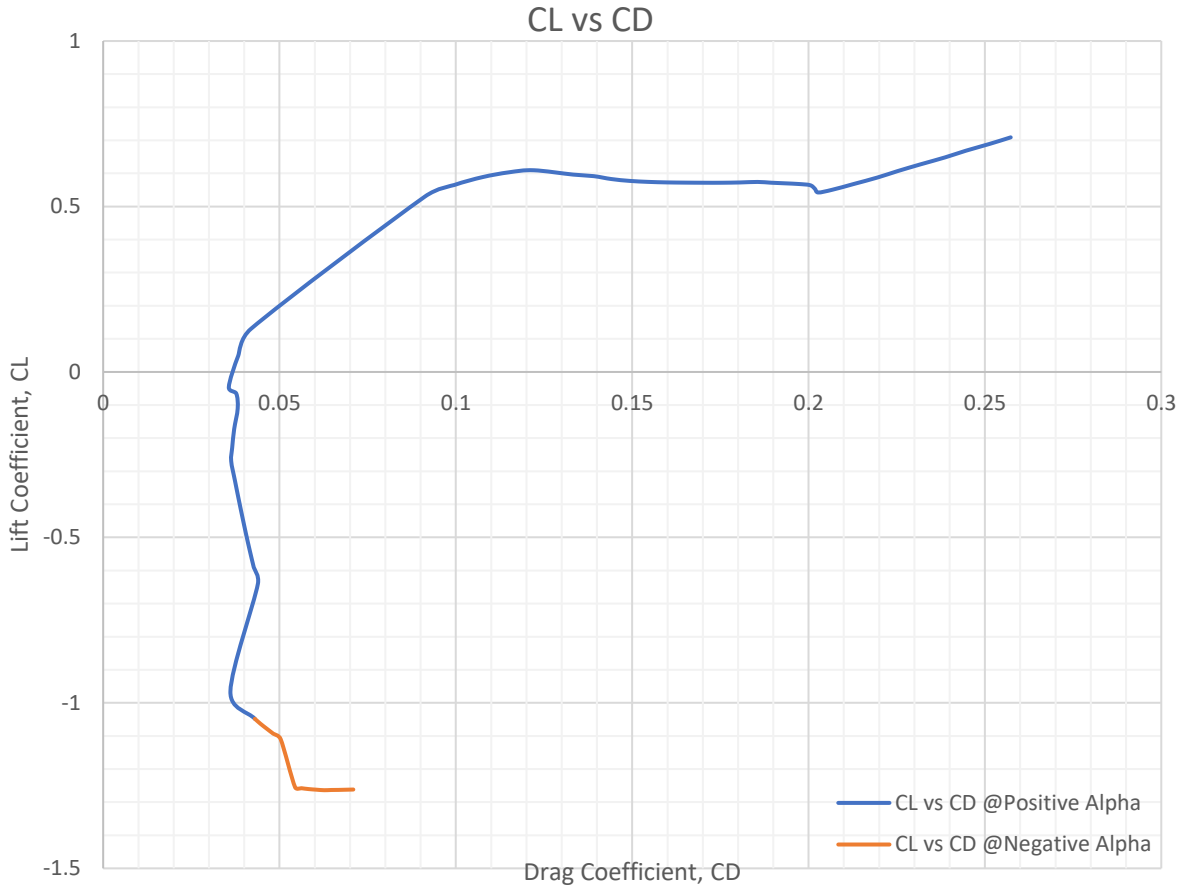

Figure 99 NACA0005's C_L vs C_D graph at Re=62868 [Elevator Deflection -15°]

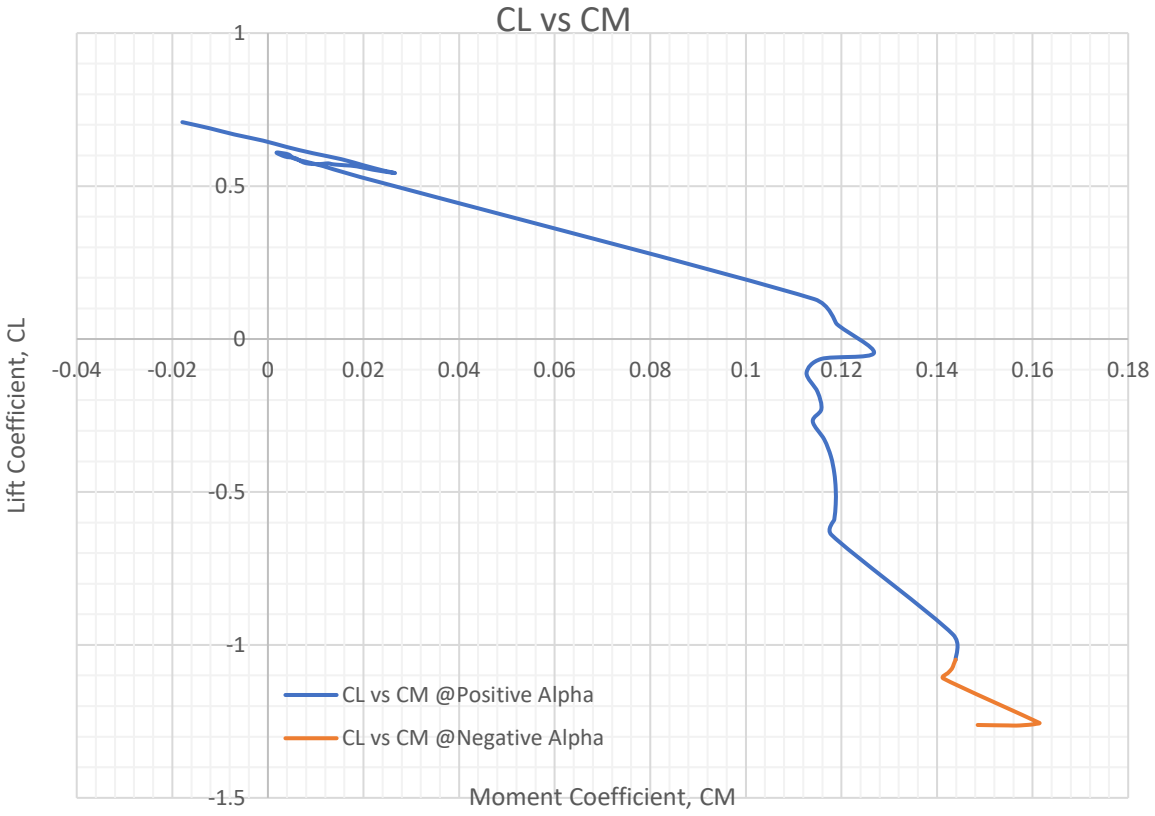

Figure 98 NACA0005's C_L vs C_M graph at Re=62868 [Elevator Deflection -15°]

14 Appendix B – Glauert III Results

This appendix deals with publishing the results given by Glauert III and the results computed on Excel for the respective Drag and Pitching Moment Coefficients. The first part contains the wing's 3-D characteristics, with each set of Glauert III results, tabulations and resulting distributions for each boundary condition. The second part holds the 3-D characteristics for the HTU, with each set of results, tabulations and resulting distributions for elevator without deflection and with -15° deflection (Upwards). For both parts, and for all boundary conditions and set-ups, Glauert III was used to solve for maximum lift coefficient, C_{Lmax}, and for a given cruise coefficient, $C_{Lcruise}$=0.2.

The wing's maximum lift coefficient, $C_{Lwingmax}$, and induced drag coefficient, $C_{Di,}$ were read directly from the results overview. A Wing's lift curve was constructed using $C_{Lwingmax}$, Lift Curve Slope of the wing, and angle of zero-lift given in the results overview too. Through this curve, the angle of attack at which $C_{Lwingmax}$ occurs was read. In the HTU's wing lift curve, the respective C_{LHTU}, was read by following the respective AoA to the wing. This means subtracting the wing's AoA for $C_{Lwingmas}$ by the wing's setting angle.

For both the wing and HTU, the Drag and Pitching Moment Coefficients (C_D and C_M) were read directly from the C_L vs C_D and C_L vs C_M curves generated through XFOIL's results, as in Appendix A. The coefficient distributions $C_{Dwing}(z)$ and $C_{Mwing}(z)$ were generated through the following integrations, and then summed up to obtain total values C_{Dwing} and $C_{Mwing.}$

Drag Coefficient Distribution:

$$\sum_{0}^{0.239} \int_{z-1}^{z} CD(y) = \sum_{0}^{0.239} \text{CD.y}_{\,z-1}^{\,z}$$

Pitching Moment Coefficient Distribution:

$$\sum_{0}^{0.239} \int_{z-1}^{z} CM(y) = \sum_{0}^{0.239} \text{CM.y}_{\,z-1}^{\,z}$$

14.1 Wing – NACA2313

14.1.1 Reynolds Number 62868

14.1.1.1 Maximum Lift Coefficient

Results overview:

Area of the wing S = 0.044 m2
Aspect ratio Lambda = 5.213
Max. lift coefficient of the wing is Clwingmax = 1.2651
Lift curve slope of the wing = 4.4379 rad-1
Angle of zero-lift coefficient (in the wing root) Alfa0wing = 0.9549 ° (without the influence of flaps and ailerons)
Glauert coefficient delta = 0.0054 (for the calculation of induced drag - calculated from normal distribution)
Induced drag coefficient Cxi = 0.0982 (for the lift coefficient of the wing Clwing = 1.2651)

theta	z	c	cln	cl0	claisym	claiantis	clfl	cldam	clp	cltotal
0	0.239	0.01	0	0	0	0	0	0	1.36	0
4.737	0.238	0.015	0.7454	-0.0843	0	0	0	0	1.36	0.8586
9.474	0.236	0.03	0.7439	-0.0828	0	0	0	0	1.36	0.8583
14.211	0.232	0.044	0.7632	-0.0824	0	0	0	0	1.36	0.8831
18.947	0.226	0.054	0.8035	-0.0828	0	0	0	0	1.36	0.9335
23.684	0.219	0.062	0.8438	-0.0817	0	0	0	0	1.36	0.9856
28.421	0.21	0.068	0.8906	-0.0795	0	0	0	0	1.36	1.0471
33.158	0.2	0.073	0.9297	-0.0747	0	0	0	0	1.36	1.1013
37.895	0.189	0.079	0.9569	-0.0671	0	0	0	0	1.36	1.1434
42.632	0.176	0.084	0.9763	-0.0574	0	0	0	0	1.36	1.1777
47.368	0.162	0.087	1.001	-0.0464	0	0	0	0	1.36	1.2199
52.105	0.147	0.091	1.0131	-0.0335	0	0	0	0	1.36	1.2481
56.842	0.131	0.095	1.0219	-0.0194	0	0	0	0	1.36	1.2732
61.579	0.114	0.098	1.0297	-0.0047	0	0	0	0	1.36	1.2979
66.316	0.096	0.101	1.0323	0.0105	0	0	0	0	1.36	1.3164
71.053	0.078	0.104	1.0386	0.0258	0	0	0	0	1.36	1.3397
75.789	0.059	0.106	1.0389	0.0404	0	0	0	0	1.36	1.3548
80.526	0.039	0.109	1.0327	0.0535	0	0	0	0	1.36	1.3599
85.263	0.02	0.112	1.0181	0.0634	0	0	0	0	1.36	1.3513
90	0	0.116	0.9913	0.0673	0	0	0	0	1.36	1.3213

theta - angle defining the position of the section (see help)
z - position of the section on the half of wingspan (0 = wing root)
c - Airfoil chord length
cln - value of the lift coefficient of normal distribution
cl0 - value of the lift coefficient of zero distribution
claisym - value of the lift coefficient of aileron symetric distribution (zero)
claiantisym - value of the lift coefficient of aileron antisymetric distribution
clfl - value of the lift coefficient of flap distribution (zero)
cldam - value of local lift coefficient of aerodynamic damping
clp - value of airfoil lift coefficient
cltotal - value of total lift coefficient

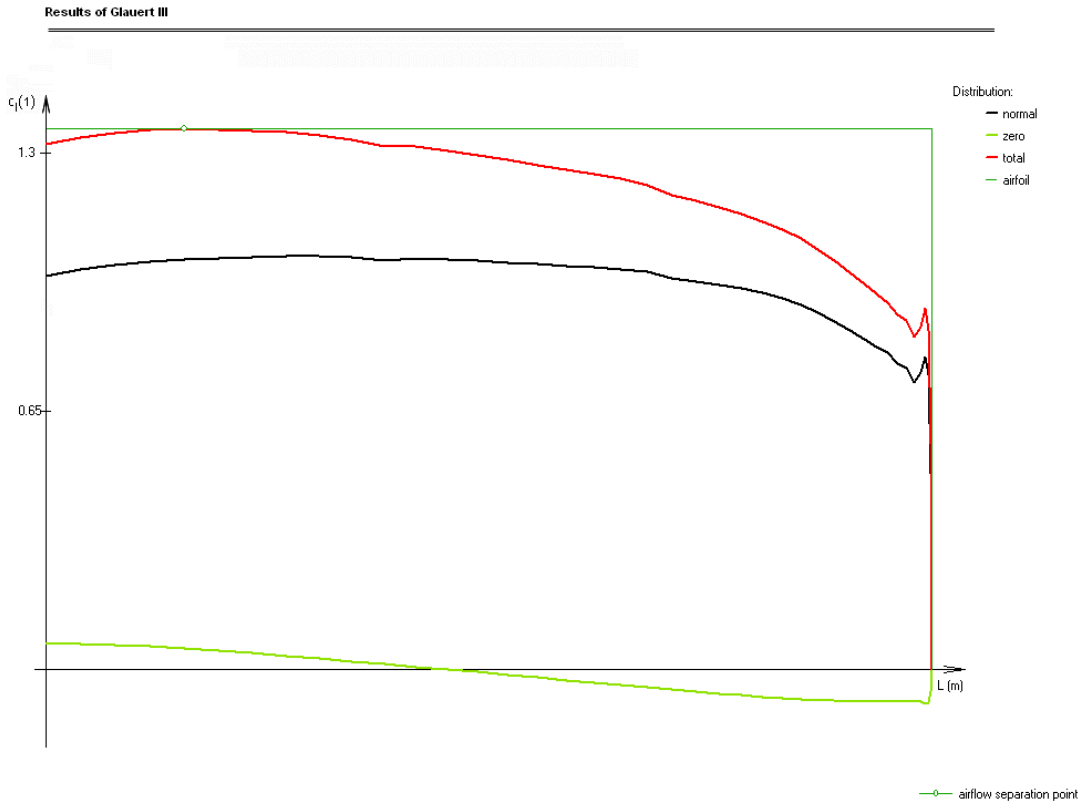
Results of Glauert III
$c_l(1)$
1.3
0.65
L (m)
Distribution:
normal
zero
total
airfoil
airflow separation point

Z	CLAISYM	CLAIANTISYM	CLDAM	CLP	CLTOTAL	CD	CDWING(Z)	CM	CMWING(Z)
0.239	0	0	0	1.36	0	0.0241	0.0000241	-0.01	-0.00001
0.238	0	0	0	1.36	0.8586	0.02782	5.564E-05	-0.0522	-0.0001044
0.236	0	0	0	1.36	0.8583	0.0278	0.0001112	-0.0522	-0.0002088
0.232	0	0	0	1.36	0.8831	0.02887	0.00017322	-0.0513	-0.0003078
0.226	0	0	0	1.36	0.9335	0.02993	0.00020951	-0.0497	-0.0003479
0.219	0	0	0	1.36	0.9856	0.03106	0.00027954	-0.0477	-0.0004293
0.21	0	0	0	1.36	1.0471	0.03202	0.0003202	-0.0453	-0.000453
0.2	0	0	0	1.36	1.1013	0.03319	0.00036509	-0.0417	-0.0004587
0.189	0	0	0	1.36	1.1434	0.0337	0.0004381	-0.0394	-0.0005122
0.176	0	0	0	1.36	1.1777	0.03445	0.0004823	-0.0367	-0.0005138
0.162	0	0	0	1.36	1.2199	0.03546	0.0005319	-0.0309	-0.0004635
0.147	0	0	0	1.36	1.2481	0.03832	0.00061312	-0.0264	-0.0004224
0.131	0	0	0	1.36	1.2732	0.04162	0.00070754	-0.021	-0.000357
0.114	0	0	0	1.36	1.2979	0.04462	0.00080316	-0.0191	-0.0003438
0.096	0	0	0	1.36	1.3164	0.04718	0.00084924	-0.0171	-0.0003078
0.078	0	0	0	1.36	1.3397	0.05289	0.00100491	-0.0133	-0.0002527
0.059	0	0	0	1.36	1.3548	0.06034	0.0012068	-0.008	-0.00016
0.039	0	0	0	1.36	1.3599	0.061	0.001159	-0.008	-0.000152
0.02	0	0	0	1.36	1.3513	0.06034	0.0012068	-0.008	-0.00016
0	0	0	0	1.36	1.3213	0.0489	0	-0.016	0
						Cdwing	**0.01054137**	**Cmwing**	**-0.0059651**

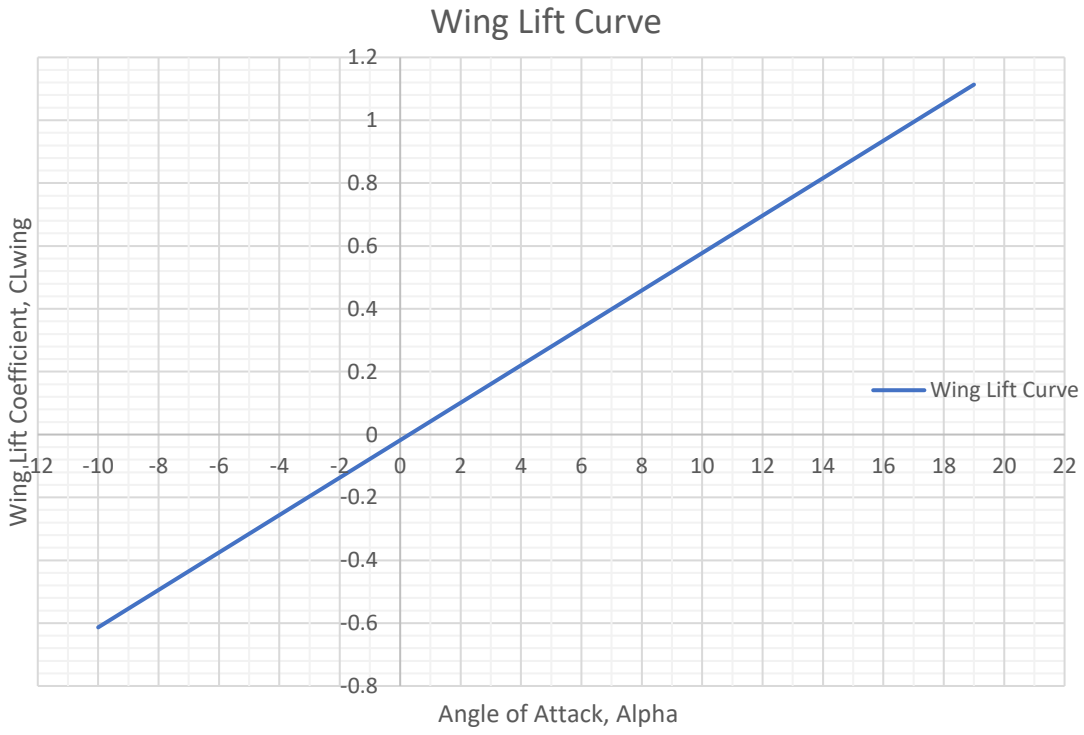

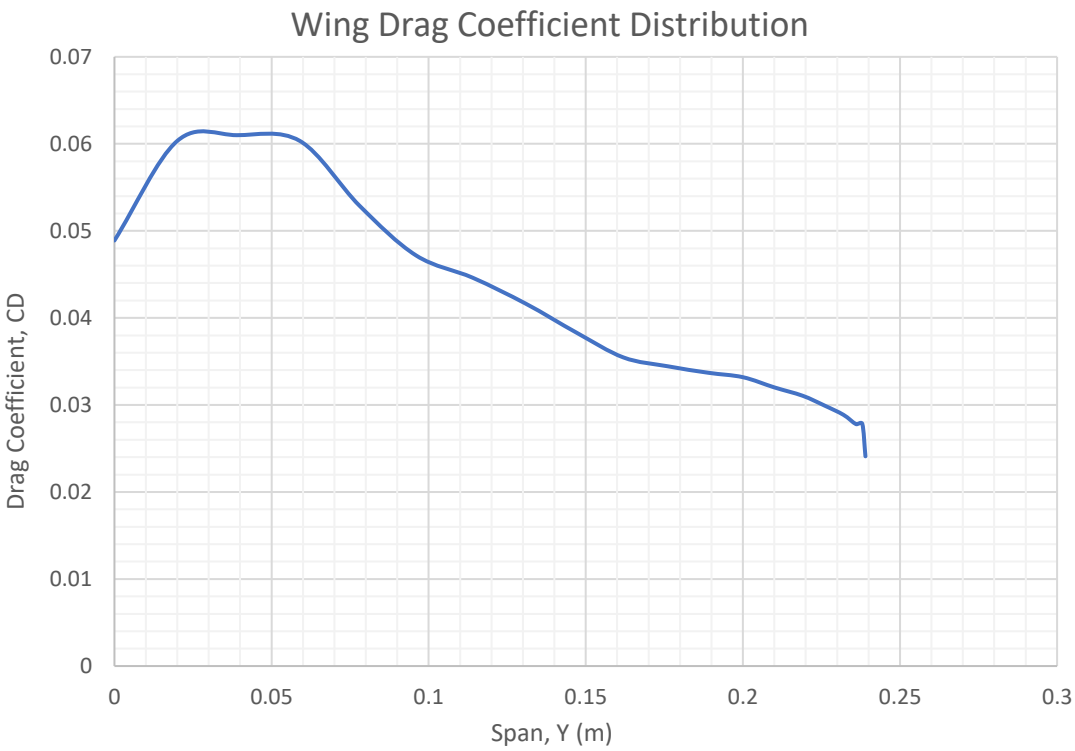
Wing Drag Coefficient Distribution
Drag Coefficient, CD
0.07
0.06
0.05
0.04
0.03
0.02
0.01
0
0
0.05
0.1
0.15
0.2
0.25
0.3
Span, Y (m)

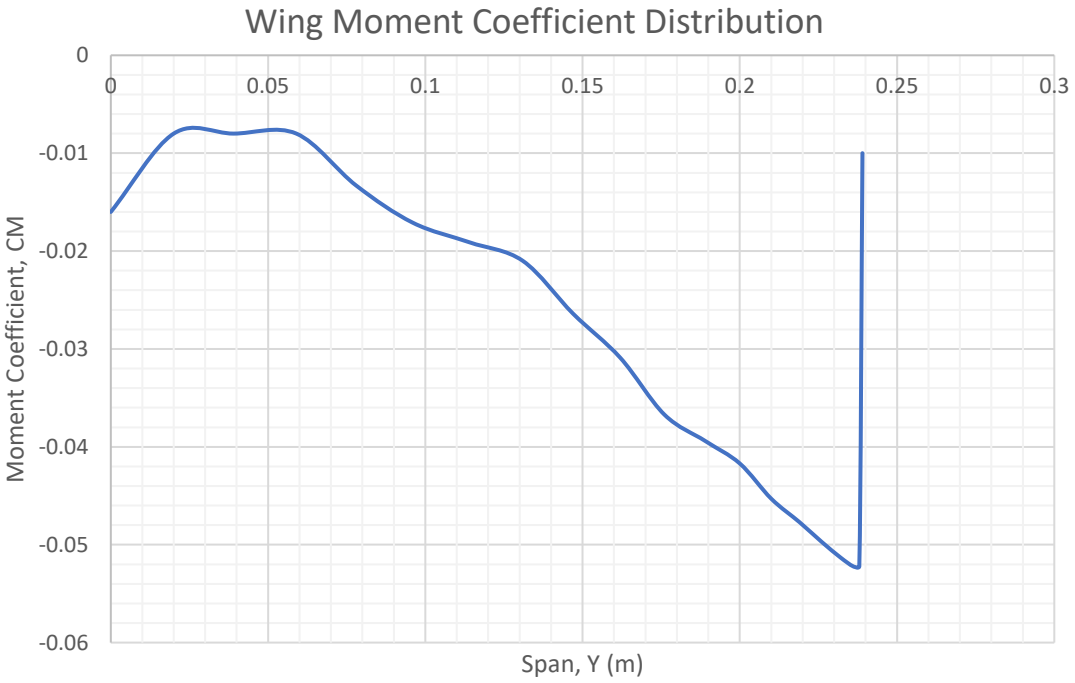
Wing Moment Coefficient Distribution
Moment Coefficient, CM
0
-0.01
-0.02
-0.03
-0.04
-0.05
-0.06
0
0.05
0.1
0.15
0.2
0.25
0.3
Span, Y (m)

14.1.1.2 Cruise Lift Coefficient

Results overview:

Area of the wing S = 0.044 m2
Aspect ratio Lambda = 5.213
Requested lift coefficient of the wing is Clwing = 0.2
Max. lift coefficient of the wing is Clwingmax = 1.2651
Lift curve slope of the wing = 4.4379 rad-1
Angle of zero-lift coefficient (in the wing root) Alfa0wing = 0.9549 ° (without the influence of flaps and ailerons)
Glauert coefficient delta = 0.0054 (for the calculation of induced drag - calculated from normal distribution)
Induced drag coefficient Cxi = 0.0025 (for the lift coefficient of the wing Clwing = 0.2)

theta	z	c	cln	cl0	claisym	claiantis	clfl	cldam	clp	cltotal
0	0.239	0.01	0	0	0	0	0	0	1.36	0
4.737	0.238	0.015	0.7454	-0.0843	0	0	0	0	1.36	0.0647
9.474	0.236	0.03	0.7439	-0.0828	0	0	0	0	1.36	0.066
14.211	0.232	0.044	0.7632	-0.0824	0	0	0	0	1.36	0.0702
18.947	0.226	0.054	0.8035	-0.0828	0	0	0	0	1.36	0.0778
23.684	0.219	0.062	0.8438	-0.0817	0	0	0	0	1.36	0.087
28.421	0.21	0.068	0.8906	-0.0795	0	0	0	0	1.36	0.0986
33.158	0.2	0.073	0.9297	-0.0747	0	0	0	0	1.36	0.1112
37.895	0.189	0.079	0.9569	-0.0671	0	0	0	0	1.36	0.1242
42.632	0.176	0.084	0.9763	-0.0574	0	0	0	0	1.36	0.1378
47.368	0.162	0.087	1.001	-0.0464	0	0	0	0	1.36	0.1537
52.105	0.147	0.091	1.0131	-0.0335	0	0	0	0	1.36	0.1691
56.842	0.131	0.095	1.0219	-0.0194	0	0	0	0	1.36	0.1849
61.579	0.114	0.098	1.0297	-0.0047	0	0	0	0	1.36	0.2012
66.316	0.096	0.101	1.0323	0.0105	0	0	0	0	1.36	0.2169
71.053	0.078	0.104	1.0386	0.0258	0	0	0	0	1.36	0.2335
75.789	0.059	0.106	1.0389	0.0404	0	0	0	0	1.36	0.2482
80.526	0.039	0.109	1.0327	0.0535	0	0	0	0	1.36	0.26
85.263	0.02	0.112	1.0181	0.0634	0	0	0	0	1.36	0.267
90	0	0.116	0.9913	0.0673	0	0	0	0	1.36	0.2656

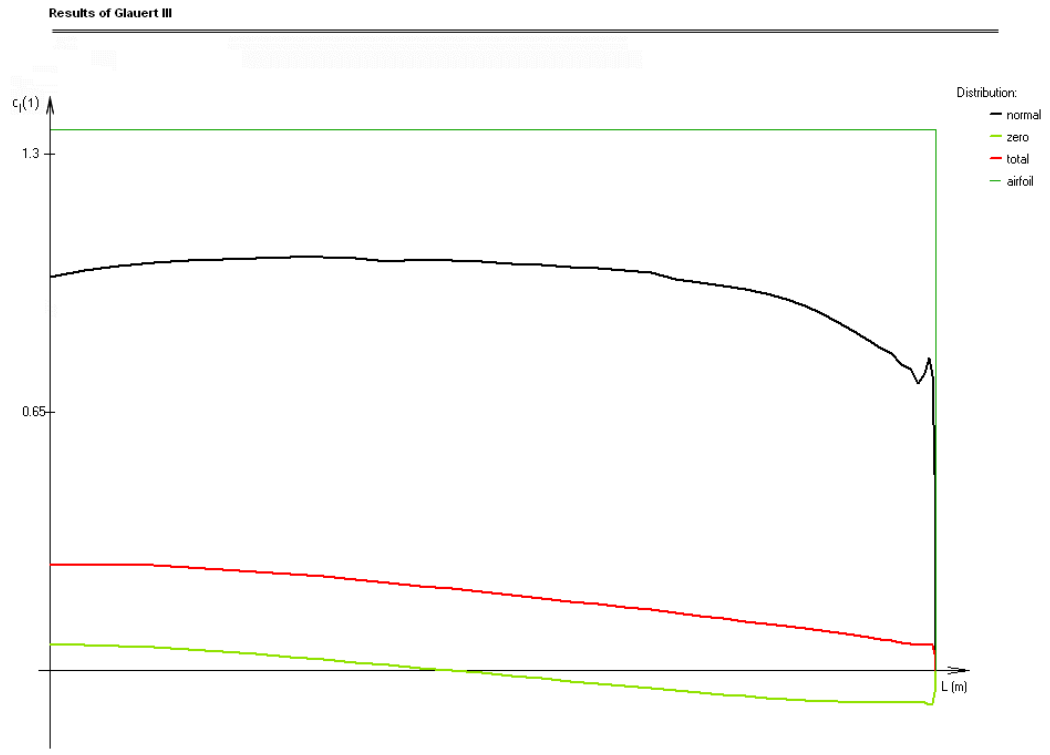

Z	CLAISYM	CLAIANTISYM	CLDAM	CLP	CLTOTAL	CD	CDWING(Z)	CM	CMWING(Z)
0.239	0	0	0	1.36	0	0.0241	0	-0.0283	-0.0000283
0.238	0	0	0	1.36	0.0647	0.025	0.00005	-0.0375	-7.5E-05
0.236	0	0	0	1.36	0.066	0.0255	0.000102	-0.038	-0.000152
0.232	0	0	0	1.36	0.0702	0.0255	0.000153	-0.0382	-0.0002292
0.226	0	0	0	1.36	0.0778	0.025	0.000175	-0.0385	-0.0002695
0.219	0	0	0	1.36	0.087	0.0252	0.0002268	-0.039	-0.000351
0.21	0	0	0	1.36	0.0986	0.0249	0.000249	-0.0408	-0.000408
0.2	0	0	0	1.36	0.1112	0.0247	0.0002717	-0.0431	-0.0004741
0.189	0	0	0	1.36	0.1242	0.0246	0.0003198	-0.0435	-0.0005655
0.176	0	0	0	1.36	0.1378	0.0243	0.0003402	-0.0454	-0.0006356
0.162	0	0	0	1.36	0.1537	0.0242	0.000363	-0.047	-0.000705
0.147	0	0	0	1.36	0.1691	0.0241	0.0003856	-0.0476	-0.0007616
0.131	0	0	0	1.36	0.1849	0.02406	0.00040902	-0.0498	-0.0008466
0.114	0	0	0	1.36	0.2012	0.024	0.000432	-0.052	-0.000936
0.096	0	0	0	1.36	0.2169	0.024	0.000432	-0.054	-0.000972
0.078	0	0	0	1.36	0.2335	0.0239	0.0004541	-0.0543	-0.0010317
0.059	0	0	0	1.36	0.2482	0.0238	0.000476	-0.0552	-0.001104
0.039	0	0	0	1.36	0.26	0.02378	0.00045182	-0.0569	-0.0010811
0.02	0	0	0	1.36	0.267	0.02369	0.0004738	-0.058	-0.00116
0	0	0	0	1.36	0.2656	0.0236	0	-0.0569	0
						CDwing	0.00576484	Cmwing	-0.0117862

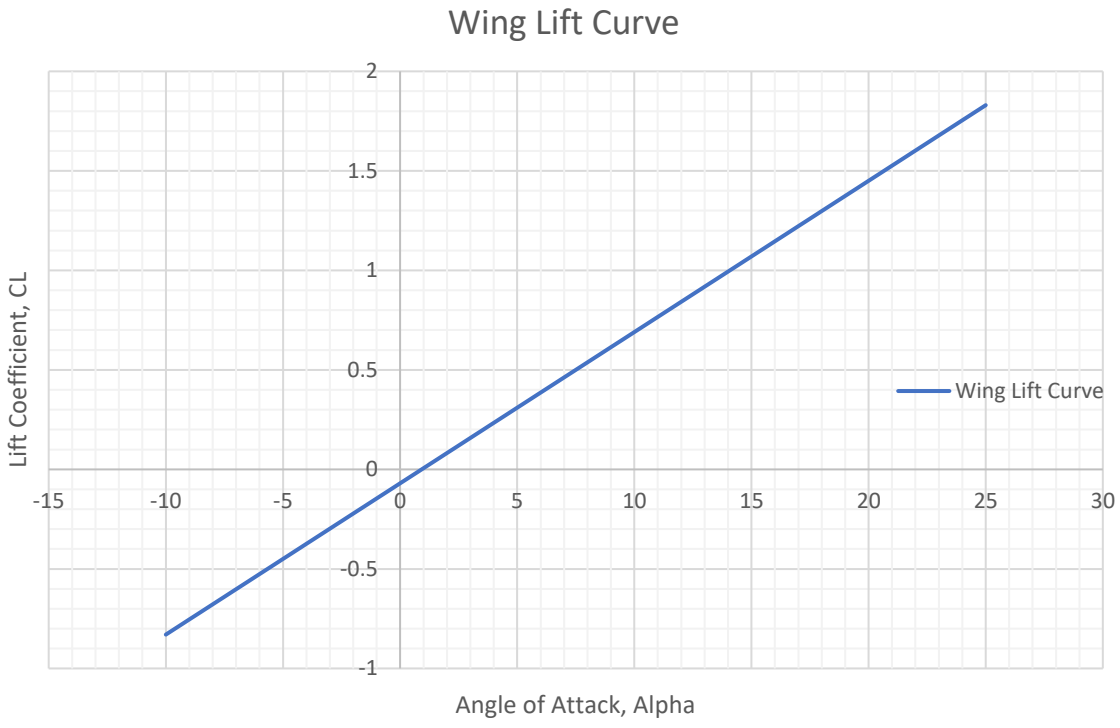

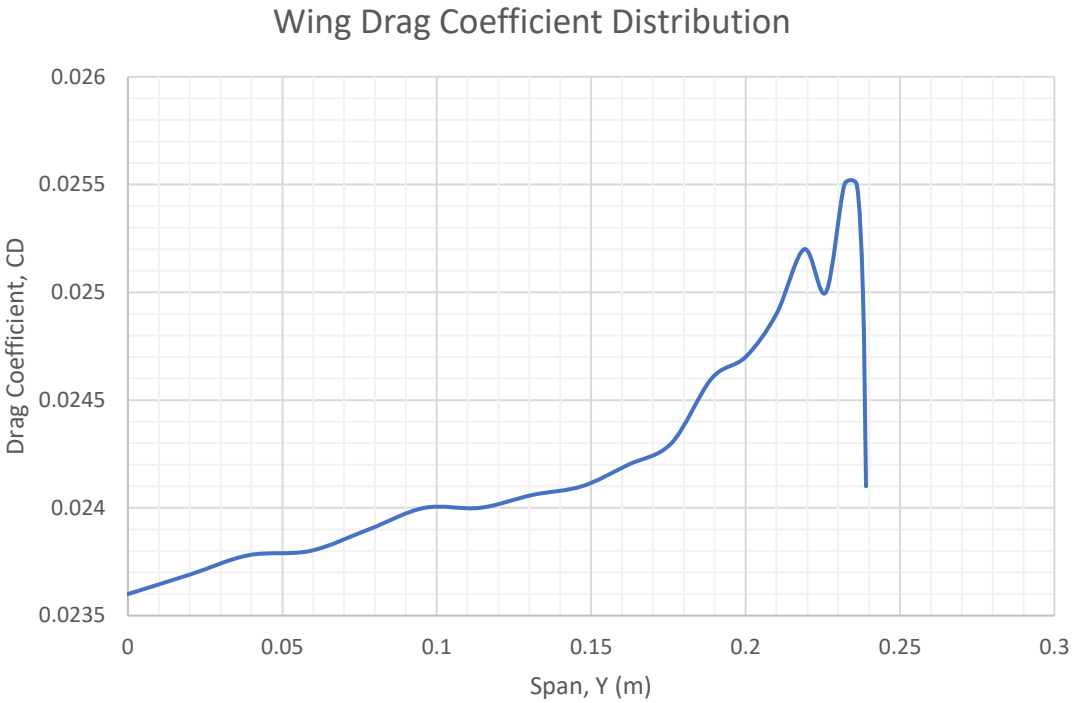
Wing Drag Coefficient Distribution
0.026
0.0255
0.025
0.0245
0.024
0.0235
Drag Coefficient, CD
0
0.05
0.1
0.15
0.2
0.25
0.3
Span, Y (m)

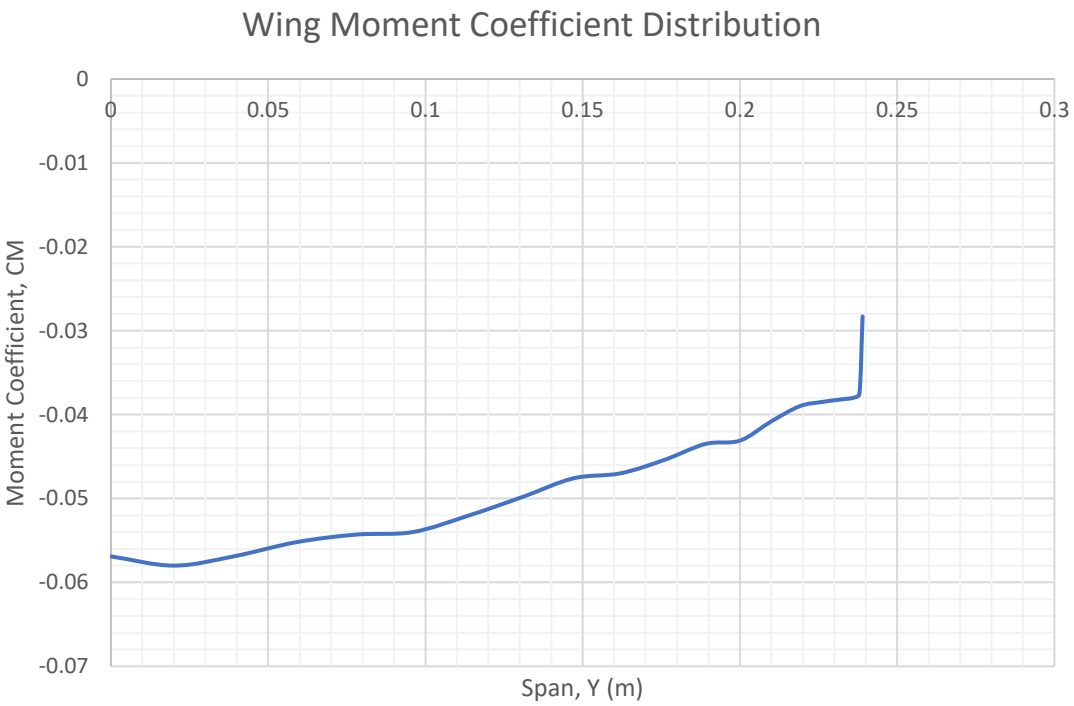
Wing Moment Coefficient Distribution
0
-0.01
-0.02
-0.03
-0.04
-0.05
-0.06
-0.07
Moment Coefficient, CM
0
0.05
0.1
0.15
0.2
0.25
0.3
Span, Y (m)

14.1.2 Reynolds Number 125736

14.1.2.1 Maximum Lift Coefficient

Results overview:

Area of the wing S = 0.044 m2
Aspect ratio Lambda = 5.213
Max. lift coefficient of the wing is Clwingmax = 1.2488
Lift curve slope of the wing = 3.5048 rad-1
Angle of zero-lift coefficient (in the wing root) Alfa0wing = 0.0607 ° (without the influence of flaps and ailerons)
Glauert coefficient delta = 0.0077 (for the calculation of induced drag - calculated from normal distribution)
Induced drag coefficient Cxi = 0.0959 (for the lift coefficient of the wing Clwing = 1.2488)

theta	z	c	cln	cl0	claisym	claiantis	clfl	cldam	clp	cltotal
0	0.239	0.01	0	0	0	0	0	0	1.33	0
4.737	0.238	0.015	0.7715	-0.0735	0	0	0	0	1.33	0.8898
9.474	0.236	0.03	0.7687	-0.0721	0	0	0	0	1.33	0.8878
14.211	0.232	0.044	0.7866	-0.0716	0	0	0	0	1.33	0.9106
18.947	0.226	0.054	0.8246	-0.0718	0	0	0	0	1.33	0.9579
23.684	0.219	0.062	0.8619	-0.0706	0	0	0	0	1.33	1.0057
28.421	0.21	0.068	0.9051	-0.0684	0	0	0	0	1.33	1.0619
33.158	0.2	0.073	0.9405	-0.064	0	0	0	0	1.33	1.1104
37.895	0.189	0.079	0.9644	-0.0574	0	0	0	0	1.33	1.1469
42.632	0.176	0.084	0.9809	-0.049	0	0	0	0	1.33	1.1758
47.368	0.162	0.087	1.0027	-0.0396	0	0	0	0	1.33	1.2125
52.105	0.147	0.091	1.0126	-0.0286	0	0	0	0	1.33	1.2358
56.842	0.131	0.095	1.0197	-0.0167	0	0	0	0	1.33	1.2567
61.579	0.114	0.098	1.0262	-0.0041	0	0	0	0	1.33	1.2774
66.316	0.096	0.101	1.028	0.0088	0	0	0	0	1.33	1.2925
71.053	0.078	0.104	1.0337	0.0218	0	0	0	0	1.33	1.3127
75.789	0.059	0.106	1.034	0.0344	0	0	0	0	1.33	1.3256
80.526	0.039	0.109	1.0283	0.0458	0	0	0	0	1.33	1.3299
85.263	0.02	0.112	1.0148	0.0547	0	0	0	0	1.33	1.322
90	0	0.116	0.9891	0.0584	0	0	0	0	1.33	1.2936

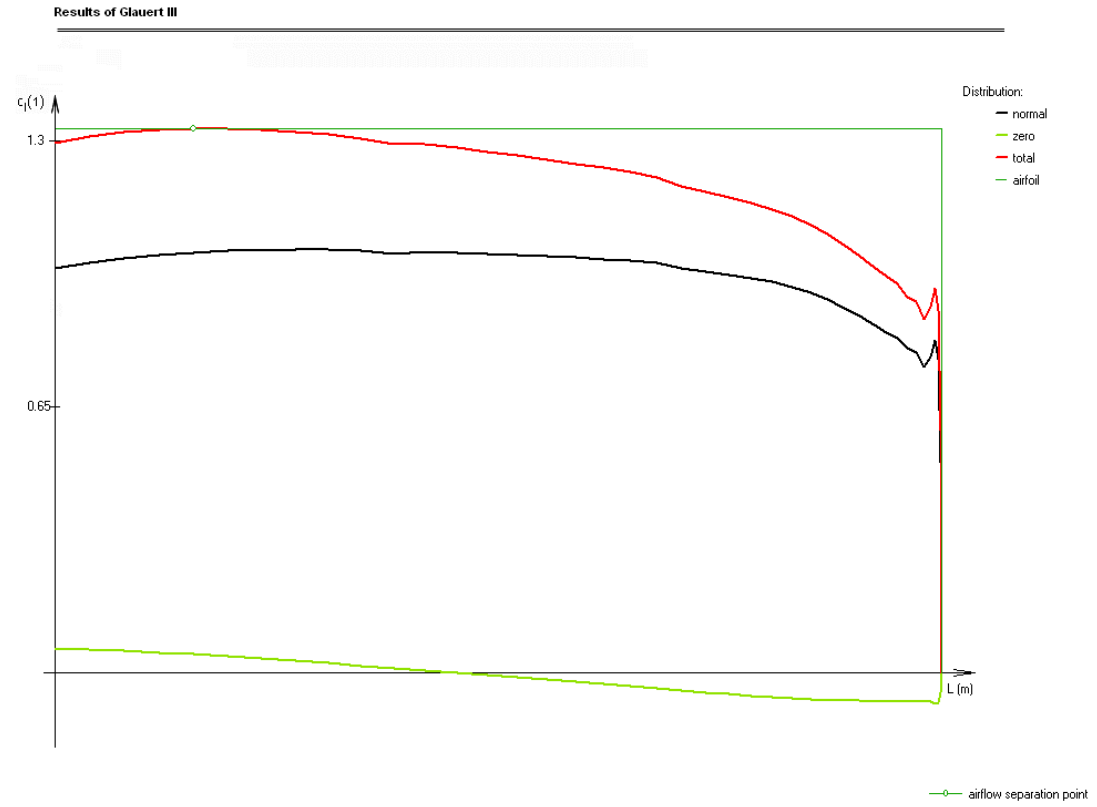

Z	CLAISYM	CLAIANTISYM	CLDAM	CLP	CLTOTAL	CD	CDWING(Z)	CM	CMWING(Z)
0.239	0	0	0	1.33	0	0.01458	0.00001458	-0.04	-0.00004
0.238	0	0	0	1.33	0.8898	0.018	0.000036	-0.043	-8.6E-05
0.236	0	0	0	1.33	0.8878	0.01795	7.18E-05	-0.043	-0.000172
0.232	0	0	0	1.33	0.9106	0.01834	0.00011004	-0.0421	-0.0002526
0.226	0	0	0	1.33	0.9579	0.01898	0.00013286	-0.0397	-0.0002779
0.219	0	0	0	1.33	1.0057	0.01973	0.00017757	-0.0378	-0.0003402
0.21	0	0	0	1.33	1.0619	0.02044	0.0002044	-0.0341	-0.000341
0.2	0	0	0	1.33	1.1104	0.0213	0.0002343	-0.0304	-0.0003344
0.189	0	0	0	1.33	1.1469	0.02213	0.00028769	-0.0258	-0.0003354
0.176	0	0	0	1.33	1.1758	0.024	0.000336	-0.0192	-0.0002688
0.162	0	0	0	1.33	1.2125	0.03167	0.00047505	-0.0049	-7.35E-05
0.147	0	0	0	1.33	1.2358	0.03589	0.00057424	0.0001	0.0000016
0.131	0	0	0	1.33	1.2567	0.03924	0.00066708	0.0018	0.0000306
0.114	0	0	0	1.33	1.2774	0.04135	0.0007443	0.0048	0.0000864
0.096	0	0	0	1.33	1.2925	0.04568	0.00082224	0.0073	0.0001314
0.078	0	0	0	1.33	1.3127	0.05495	0.00104405	0.0118	0.0002242
0.059	0	0	0	1.33	1.3256	0.05643	0.0011286	0.0125	0.00025
0.039	0	0	0	1.33	1.3299	0.0569	0.0010811	0.0125	0.0002375
0.02	0	0	0	1.33	1.322	0.0563	0.001126	0.0125	0.00025
0	0	0	0	1.33	1.2936	0.04568	0	0.0073	0
						CDwing	0.0092679	Cmwing	-0.0013101

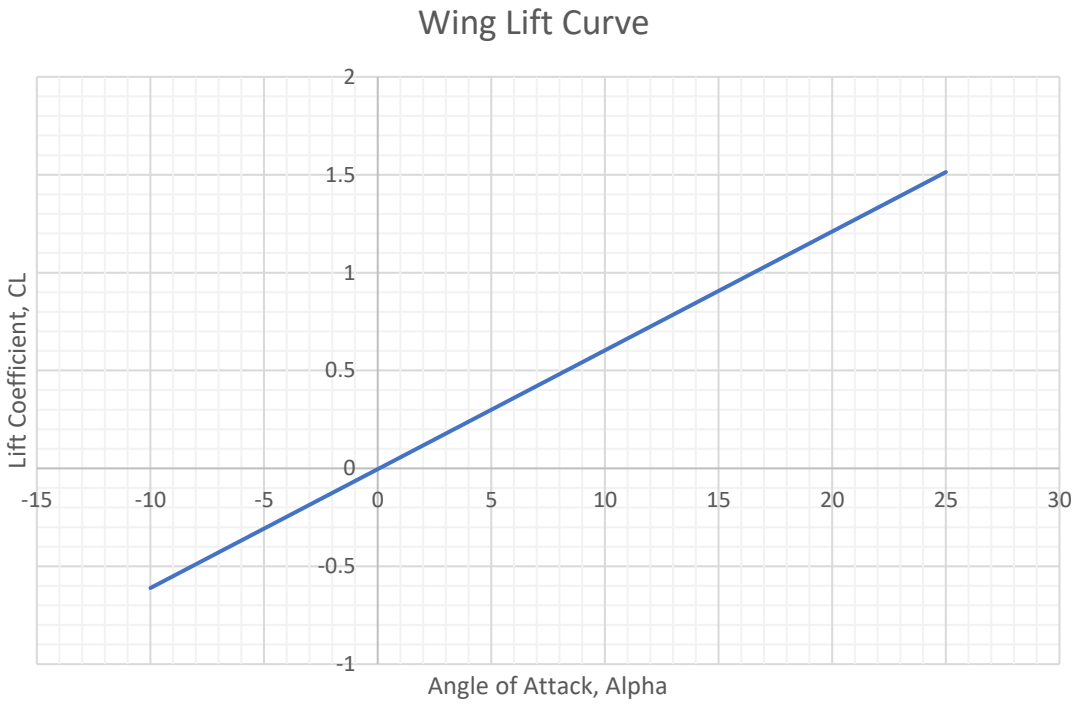

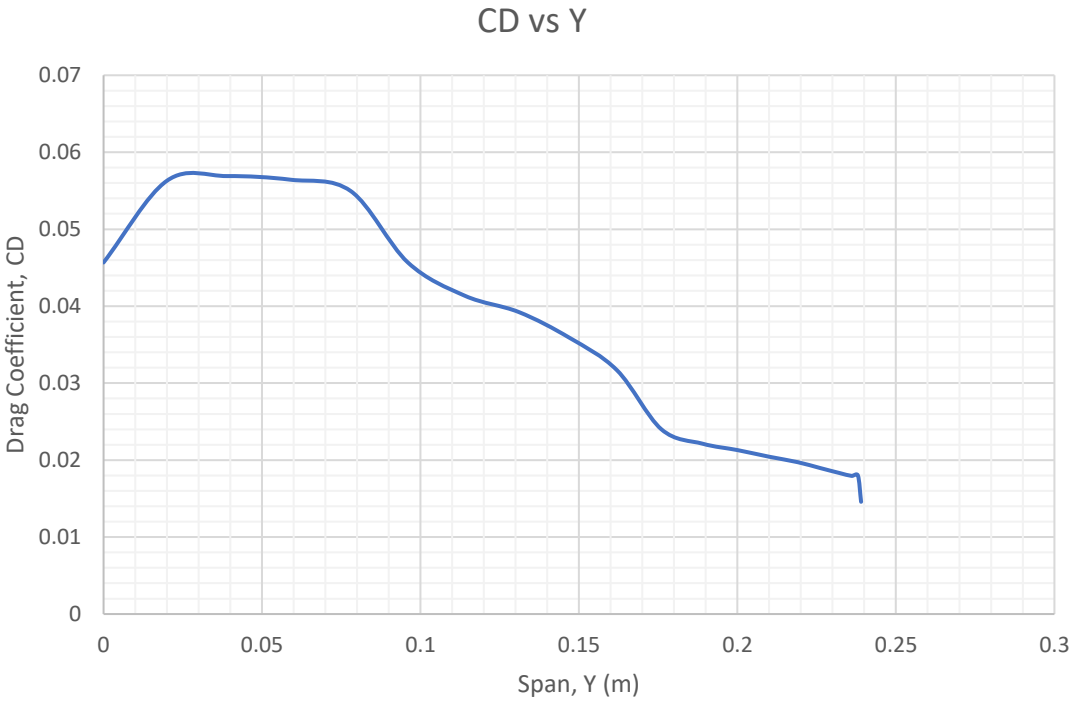
CD vs Y
Drag Coefficient, CD
0.07
0.06
0.05
0.04
0.03
0.02
0.01
0
0
0.05
0.1
0.15
0.2
0.25
0.3
Span, Y (m)

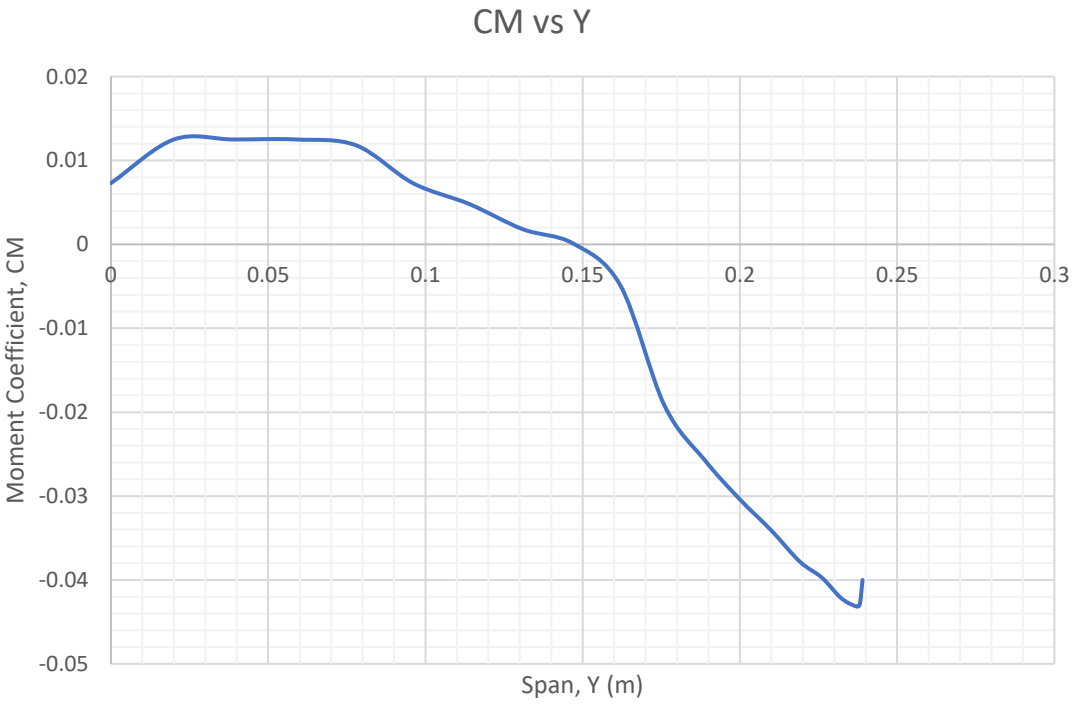
CM vs Y
Moment Coefficient, CM
0.02
0.01
0
-0.01
-0.02
-0.03
-0.04
-0.05
0
0.05
0.1
0.15
0.2
0.25
0.3
Span, Y (m)

14.1.2.2 Cruise Lift Coefficient

Results overview:

Area of the wing S = 0.044 m2
Aspect ratio Lambda = 5.213
Requested lift coefficient of the wing is Clwing = 0.2
Max. lift coefficient of the wing is Clwingmax = 1.2488
Lift curve slope of the wing = 3.5048 rad-1
Angle of zero-lift coefficient (in the wing root) Alfa0wing = 0.0607 ° (without the influence of flaps and ailerons)
Glauert coefficient delta = 0.0077 (for the calculation of induced drag - calculated from normal distribution)
Induced drag coefficient Cxi = 0.0025 (for the lift coefficient of the wing Clwing = 0.2)

theta	z	c	cln	cl0	claisym	claiantis	clfl	cldam	clp	cltotal
0	0.239	0.01	0	0	0	0	0	0	1.33	0
4.737	0.238	0.015	0.7715	-0.0735	0	0	0	0	1.33	0.0807
9.474	0.236	0.03	0.7687	-0.0721	0	0	0	0	1.33	0.0816
14.211	0.232	0.044	0.7866	-0.0716	0	0	0	0	1.33	0.0856
18.947	0.226	0.054	0.8246	-0.0718	0	0	0	0	1.33	0.0931
23.684	0.219	0.062	0.8619	-0.0706	0	0	0	0	1.33	0.1018
28.421	0.21	0.068	0.9051	-0.0684	0	0	0	0	1.33	0.1126
33.158	0.2	0.073	0.9405	-0.064	0	0	0	0	1.33	0.1241
37.895	0.189	0.079	0.9644	-0.0574	0	0	0	0	1.33	0.1355
42.632	0.176	0.084	0.9809	-0.049	0	0	0	0	1.33	0.1472
47.368	0.162	0.087	1.0027	-0.0396	0	0	0	0	1.33	0.1609
52.105	0.147	0.091	1.0126	-0.0286	0	0	0	0	1.33	0.1739
56.842	0.131	0.095	1.0197	-0.0167	0	0	0	0	1.33	0.1872
61.579	0.114	0.098	1.0262	-0.0041	0	0	0	0	1.33	0.2011
66.316	0.096	0.101	1.028	0.0088	0	0	0	0	1.33	0.2144
71.053	0.078	0.104	1.0337	0.0218	0	0	0	0	1.33	0.2286
75.789	0.059	0.106	1.034	0.0344	0	0	0	0	1.33	0.2412
80.526	0.039	0.109	1.0283	0.0458	0	0	0	0	1.33	0.2515
85.263	0.02	0.112	1.0148	0.0547	0	0	0	0	1.33	0.2577
90	0	0.116	0.9891	0.0584	0	0	0	0	1.33	0.2563

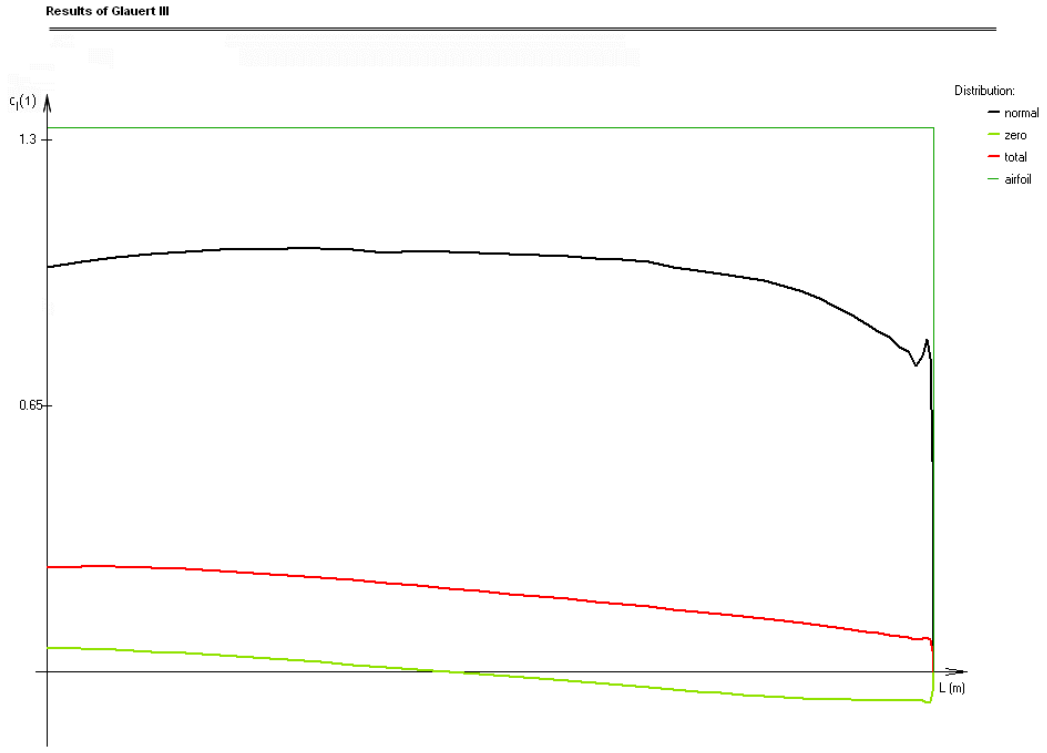

Z	CLAISYM	CLAIANTISYM	CLDAM	CLP	CLTOTAL	CD	CDWING(Z)	CM	CMWING(Z)
0.239	0	0	0	1.33	0	0.01458	1.458E-05	-0.04	-0.00004
0.238	0	0	0	1.33	0.0807	0.01456	2.912E-05	-0.0432	-8.64E-05
0.236	0	0	0	1.33	0.0816	0.01456	5.824E-05	-0.0435	-0.000174
0.232	0	0	0	1.33	0.0856	0.01457	8.742E-05	-0.0439	-0.0002634
0.226	0	0	0	1.33	0.0931	0.01459	0.0001021	-0.044	-0.000308
0.219	0	0	0	1.33	0.1018	0.01459	0.0001313	-0.0445	-0.0004005
0.21	0	0	0	1.33	0.1126	0.01459	0.0001459	-0.045	-0.00045
0.2	0	0	0	1.33	0.1241	0.01457	0.0001603	-0.046	-0.000506
0.189	0	0	0	1.33	0.1355	0.01455	0.0001892	-0.0476	-0.0006188
0.176	0	0	0	1.33	0.1472	0.0145	0.000203	-0.0485	-0.000679
0.162	0	0	0	1.33	0.1609	0.01448	0.0002172	-0.0495	-0.0007425
0.147	0	0	0	1.33	0.1739	0.01445	0.0002312	-0.057	-0.000912
0.131	0	0	0	1.33	0.1872	0.01442	0.0002451	-0.053	-0.000901
0.114	0	0	0	1.33	0.2011	0.01439	0.000259	-0.0535	-0.000963
0.096	0	0	0	1.33	0.2144	0.01436	0.0002585	-0.0545	-0.000981
0.078	0	0	0	1.33	0.2286	0.0143	0.0002717	-0.0561	-0.0010659
0.059	0	0	0	1.33	0.2412	0.01423	0.0002846	-0.0575	-0.00115
0.039	0	0	0	1.33	0.2515	0.01419	0.0002696	-0.0584	-0.0011096
0.02	0	0	0	1.33	0.2577	0.01418	0.0002836	-0.0584	-0.001168
0	0	0	0	1.33	0.2563	0.01416	0	-0.0584	0
						CDwing	0.0034417	Cmwing	-0.0125191

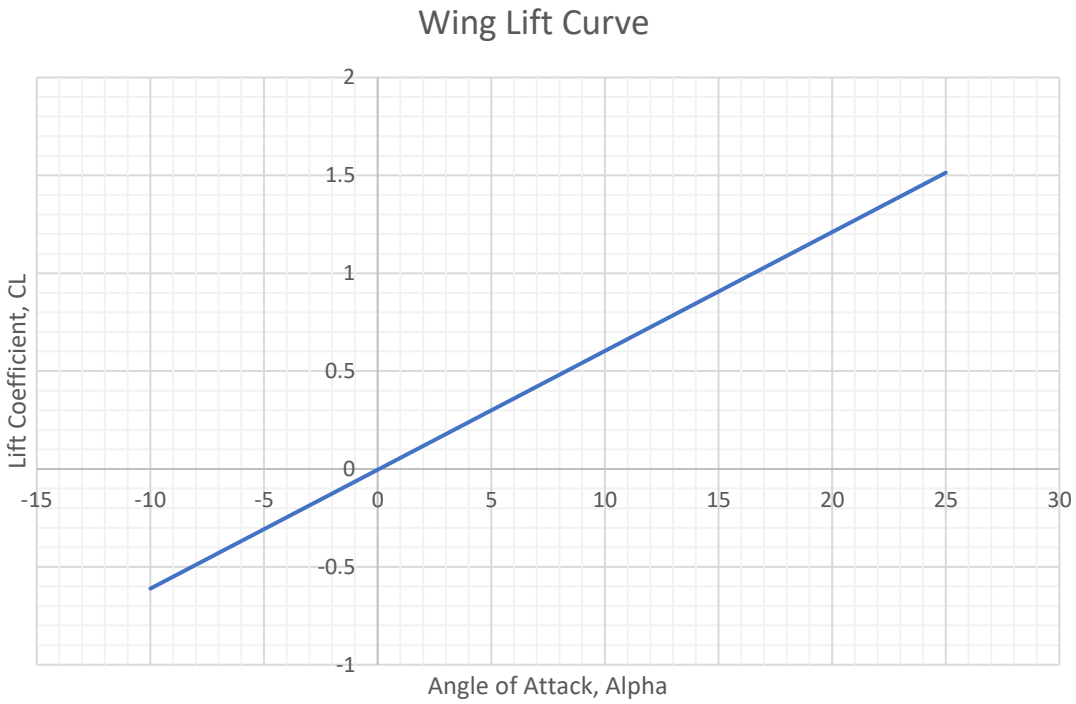

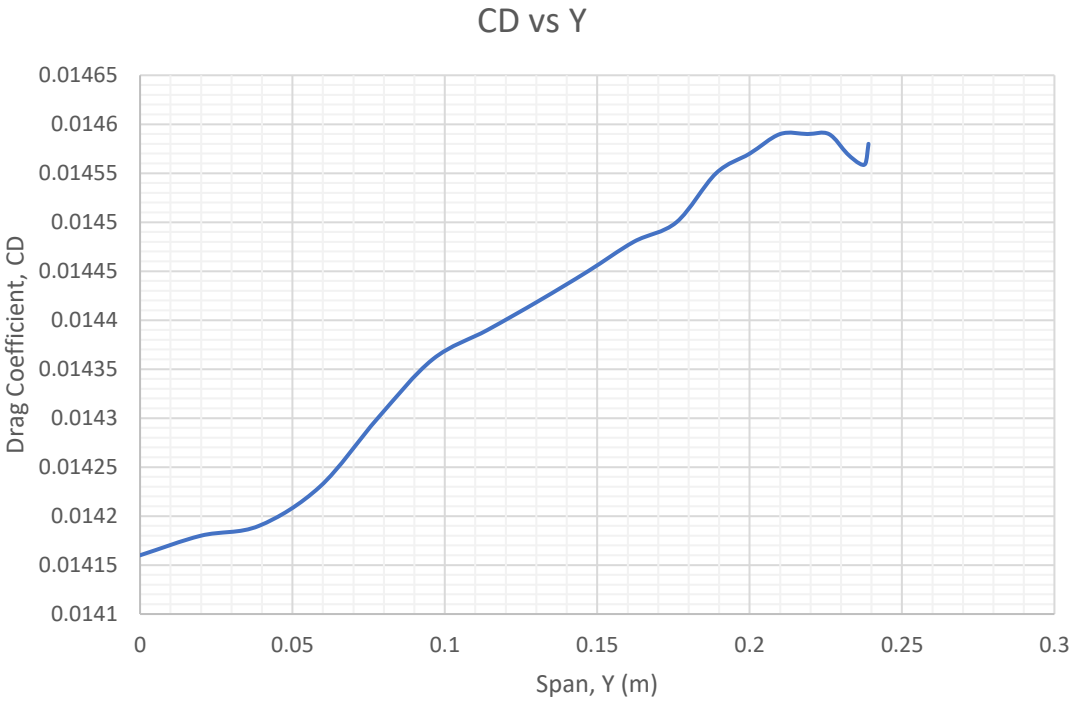
CD vs Y
Drag Coefficient, CD
0.01465
0.0146
0.01455
0.0145
0.01445
0.0144
0.01435
0.0143
0.01425
0.0142
0.01415
0.0141
0
0.05
0.1
0.15
0.2
0.25
0.3
Span, Y (m)

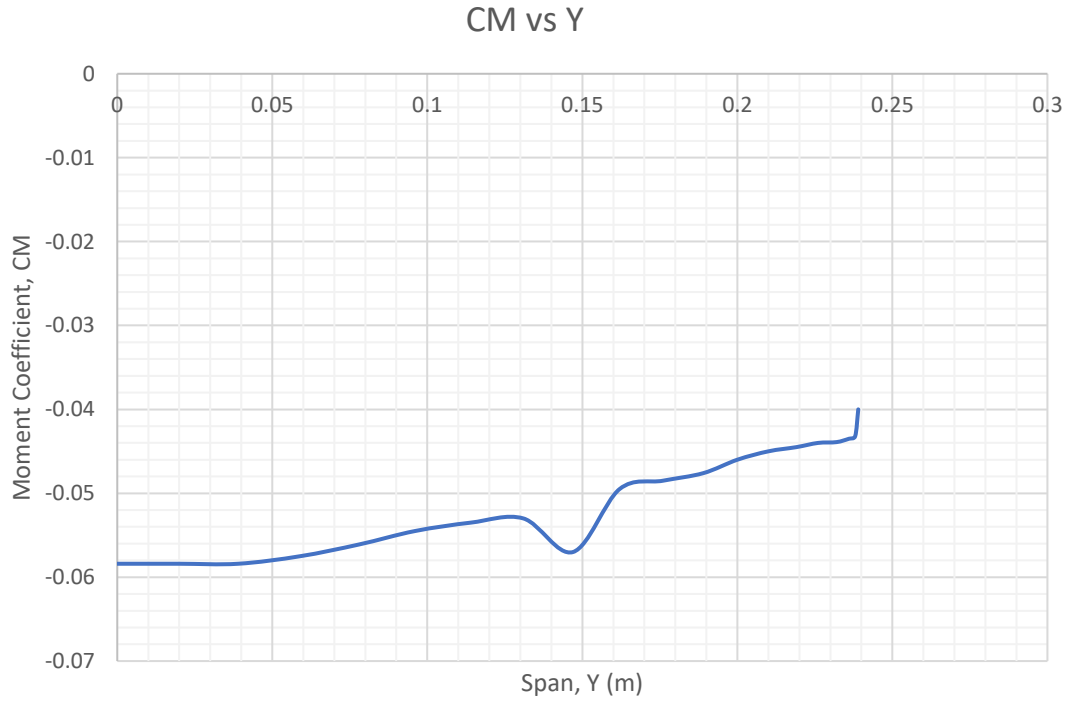
CM vs Y
Moment Coefficient, CM
0
-0.01
-0.02
-0.03
-0.04
-0.05
-0.06
-0.07
0
0.05
0.1
0.15
0.2
0.25
0.3
Span, Y (m)

14.1.3 Reynolds Number 188604

Results overview:

Area of the wing S = 0.044 m2
Aspect ratio Lambda = 5.213
Max. lift coefficient of the wing is Clwingmax = 1.3156
Lift curve slope of the wing = 3.5901 rad-1
Angle of zero-lift coefficient (in the wing root) Alfa0wing = -0.3398 ° (without the influence of flaps and ailerons)
Glauert coefficient delta = 0.0074 (for the calculation of induced drag - calculated from normal distribution)
Induced drag coefficient Cxi = 0.1065 (for the lift coefficient of the wing Clwing = 1.3156)

theta	z	c	cln	cl0	claisym	claiantis	clfl	cldam	clp	cltotal
0	0.239	0.01	0	0	0	0	0	0	1.4	0
4.737	0.238	0.015	0.7688	-0.0746	0	0	0	0	1.4	0.9368
9.474	0.236	0.03	0.7662	-0.0732	0	0	0	0	1.4	0.9347
14.211	0.232	0.044	0.7842	-0.0727	0	0	0	0	1.4	0.959
18.947	0.226	0.054	0.8224	-0.0729	0	0	0	0	1.4	1.0091
23.684	0.219	0.062	0.86	-0.0717	0	0	0	0	1.4	1.0598
28.421	0.21	0.068	0.9037	-0.0695	0	0	0	0	1.4	1.1194
33.158	0.2	0.073	0.9394	-0.065	0	0	0	0	1.4	1.1708
37.895	0.189	0.079	0.9637	-0.0583	0	0	0	0	1.4	1.2094
42.632	0.176	0.084	0.9804	-0.0498	0	0	0	0	1.4	1.24
47.368	0.162	0.087	1.0025	-0.0402	0	0	0	0	1.4	1.2786
52.105	0.147	0.091	1.0126	-0.029	0	0	0	0	1.4	1.3031
56.842	0.131	0.095	1.0199	-0.0169	0	0	0	0	1.4	1.3248
61.579	0.114	0.098	1.0266	-0.0042	0	0	0	0	1.4	1.3464
66.316	0.096	0.101	1.0285	0.0089	0	0	0	0	1.4	1.362
71.053	0.078	0.104	1.0342	0.0222	0	0	0	0	1.4	1.3828
75.789	0.059	0.106	1.0345	0.035	0	0	0	0	1.4	1.396
80.526	0.039	0.109	1.0287	0.0466	0	0	0	0	1.4	1.4
85.263	0.02	0.112	1.0151	0.0556	0	0	0	0	1.4	1.3911
90	0	0.116	0.9893	0.0593	0	0	0	0	1.4	1.3609

14.1.3.1 Maximum Lift Coefficient

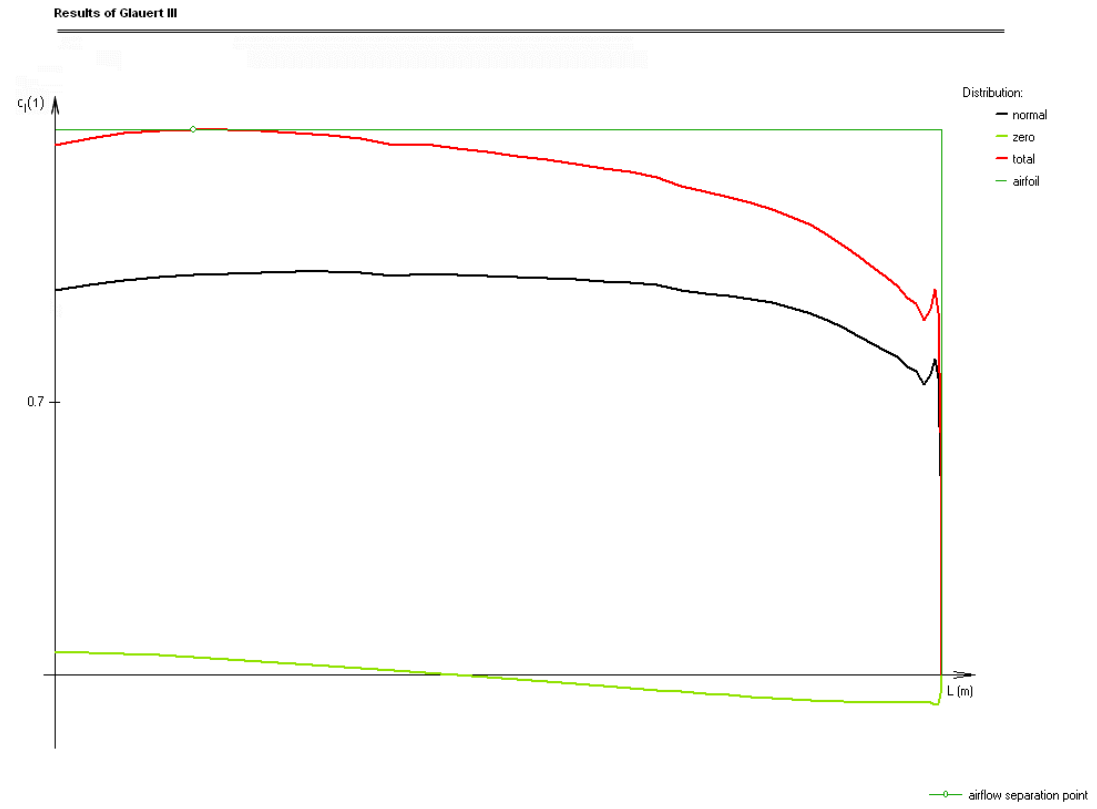

Z	CLAISYM	CLAIANTISYM	CLDAM	CLP	CLTOTAL	CD	CDWING(Z)	CM	CMWING(Z)
0.239	0	0	0	1.4	0	0.011	0.000011	-0.06	-0.00006
0.238	0	0	0	1.4	0.9368	0.01581	0.00003162	-0.0458	-9.2E-05
0.236	0	0	0	1.4	0.9347	0.0156	6.24E-05	-0.0458	-0.00018
0.232	0	0	0	1.4	0.959	0.01637	9.822E-05	-0.0458	-0.00027
0.226	0	0	0	1.4	1.0091	0.0166	0.0001162	-0.0448	-0.00031
0.219	0	0	0	1.4	1.0598	0.01715	0.00015435	-0.0438	-0.00039
0.21	0	0	0	1.4	1.1194	0.01785	0.0001785	-0.042	-0.00042
0.2	0	0	0	1.4	1.1708	0.01902	0.00020922	-0.0397	-0.00044
0.189	0	0	0	1.4	1.2094	0.0205	0.0002665	-0.037	-0.00048
0.176	0	0	0	1.4	1.24	0.02296	0.00032144	-0.0304	-0.00043
0.162	0	0	0	1.4	1.2786	0.02992	0.0004488	-0.0188	-0.00028
0.147	0	0	0	1.4	1.3031	0.03629	0.00058064	-0.0102	-0.00016
0.131	0	0	0	1.4	1.3248	0.04264	0.00072488	-0.0055	-9.4E-05
0.114	0	0	0	1.4	1.3464	0.04818	0.00086724	-0.0014	-2.5E-05
0.096	0	0	0	1.4	1.362	0.05303	0.00095454	0.0002	3.6E-06
0.078	0	0	0	1.4	1.3828	0.0591	0.0011229	0.0026	4.94E-05
0.059	0	0	0	1.4	1.396	0.06745	0.001349	0.0035	0.00007
0.039	0	0	0	1.4	1.4	0.06778	0.00128782	0.0035	6.65E-05
0.02	0	0	0	1.4	1.3911	0.06745	0.001349	0.003	0.00006
0	0	0	0	1.4	1.3609	0.05303	0	0.0002	0
						CDwing	0.01013427	Cmwing	-0.0034

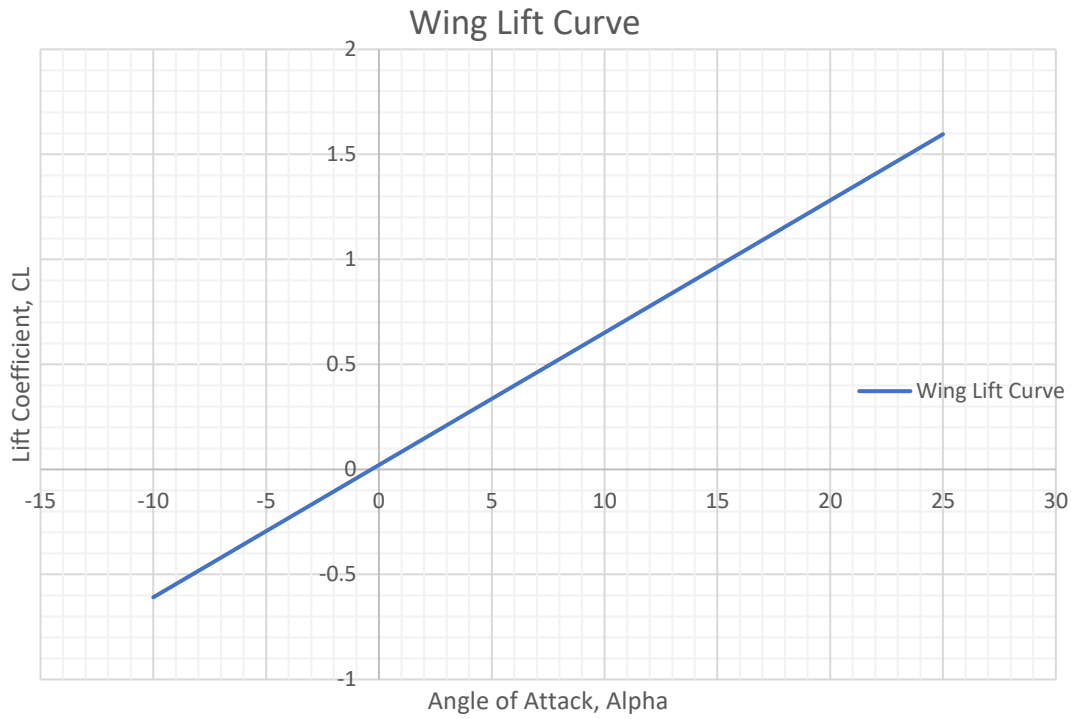

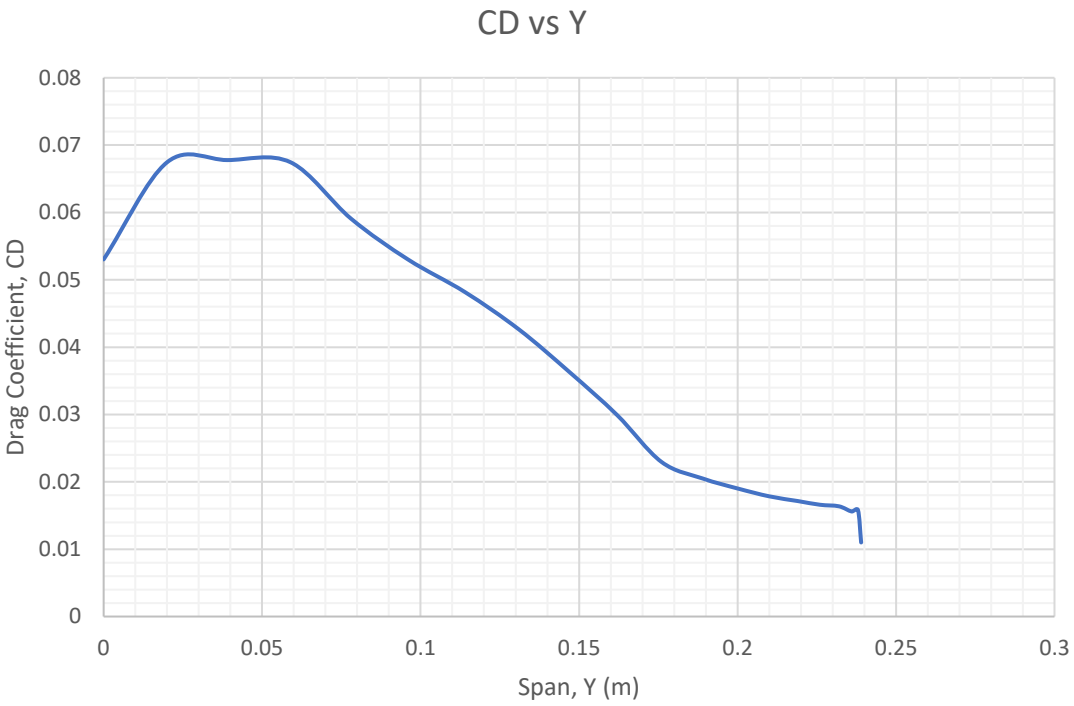
CD vs Y
Drag Coefficient, CD
0.08
0.07
0.06
0.05
0.04
0.03
0.02
0.01
0
0
0.05
0.1
0.15
0.2
0.25
0.3
Span, Y (m)

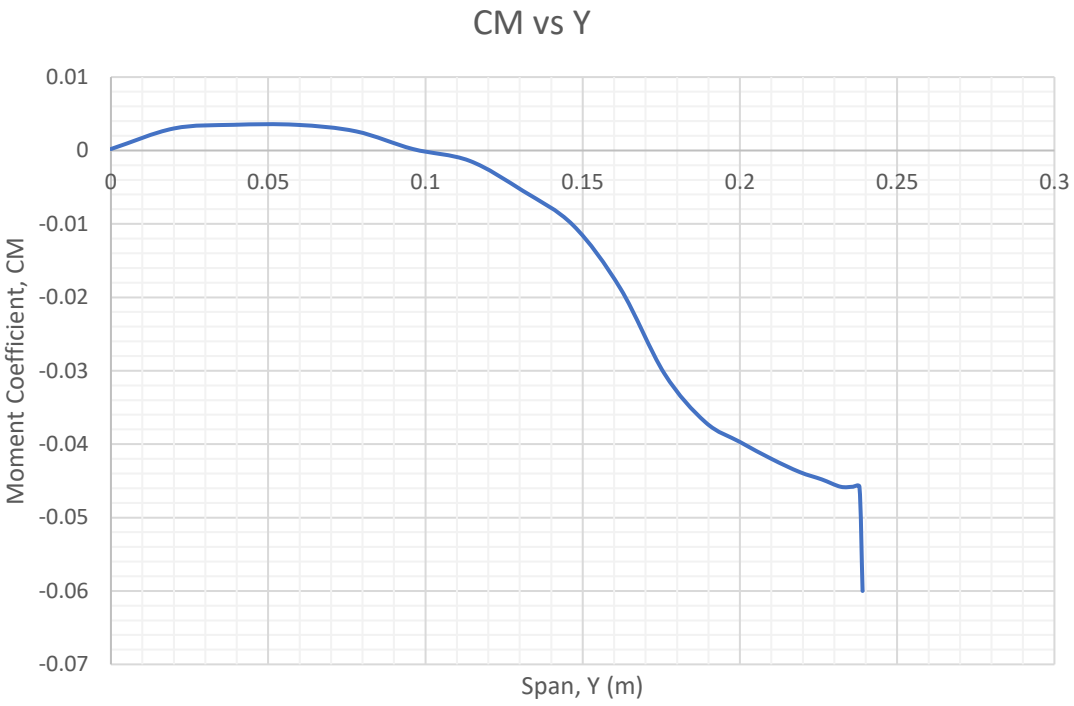
CM vs Y
Moment Coefficient, CM
0.01
0
-0.01
-0.02
-0.03
-0.04
-0.05
-0.06
-0.07
0
0.05
0.1
0.15
0.2
0.25
0.3
Span, Y (m)

14.1.3.2 Cruise Lift Coefficient

Results overview:

Area of the wing S = 0.044 m2
Aspect ratio Lambda = 5.213
Requested lift coefficient of the wing is Clwing = 0.2
Max. lift coefficient of the wing is Clwingmax = 1.3156
Lift curve slope of the wing = 3.5901 rad-1
Angle of zero-lift coefficient (in the wing root) Alfa0wing = -0.3398 ° (without the influence of flaps and ailerons)
Glauert coefficient delta = 0.0074 (for the calculation of induced drag - calculated from normal distribution)
Induced drag coefficient Cxi = 0.0025 (for the lift coefficient of the wing Clwing = 0.2)

theta	z	c	cln	cl0	claisym	claiantis	clfl	cldam	clp	cltotal
0	0.239	0.01	0	0	0	0	0	0	1.4	0
4.737	0.238	0.015	0.7688	-0.0746	0	0	0	0	1.4	0.0791
9.474	0.236	0.03	0.7662	-0.0732	0	0	0	0	1.4	0.08
14.211	0.232	0.044	0.7842	-0.0727	0	0	0	0	1.4	0.0841
18.947	0.226	0.054	0.8224	-0.0729	0	0	0	0	1.4	0.0915
23.684	0.219	0.062	0.86	-0.0717	0	0	0	0	1.4	0.1003
28.421	0.21	0.068	0.9037	-0.0695	0	0	0	0	1.4	0.1112
33.158	0.2	0.073	0.9394	-0.065	0	0	0	0	1.4	0.1228
37.895	0.189	0.079	0.9637	-0.0583	0	0	0	0	1.4	0.1344
42.632	0.176	0.084	0.9804	-0.0498	0	0	0	0	1.4	0.1462
47.368	0.162	0.087	1.0025	-0.0402	0	0	0	0	1.4	0.1602
52.105	0.147	0.091	1.0126	-0.029	0	0	0	0	1.4	0.1734
56.842	0.131	0.095	1.0199	-0.0169	0	0	0	0	1.4	0.187
61.579	0.114	0.098	1.0266	-0.0042	0	0	0	0	1.4	0.2011
66.316	0.096	0.101	1.0285	0.0089	0	0	0	0	1.4	0.2146
71.053	0.078	0.104	1.0342	0.0222	0	0	0	0	1.4	0.2291
75.789	0.059	0.106	1.0345	0.035	0	0	0	0	1.4	0.2419
80.526	0.039	0.109	1.0287	0.0466	0	0	0	0	1.4	0.2523
85.263	0.02	0.112	1.0151	0.0556	0	0	0	0	1.4	0.2586
90	0	0.116	0.9893	0.0593	0	0	0	0	1.4	0.2572

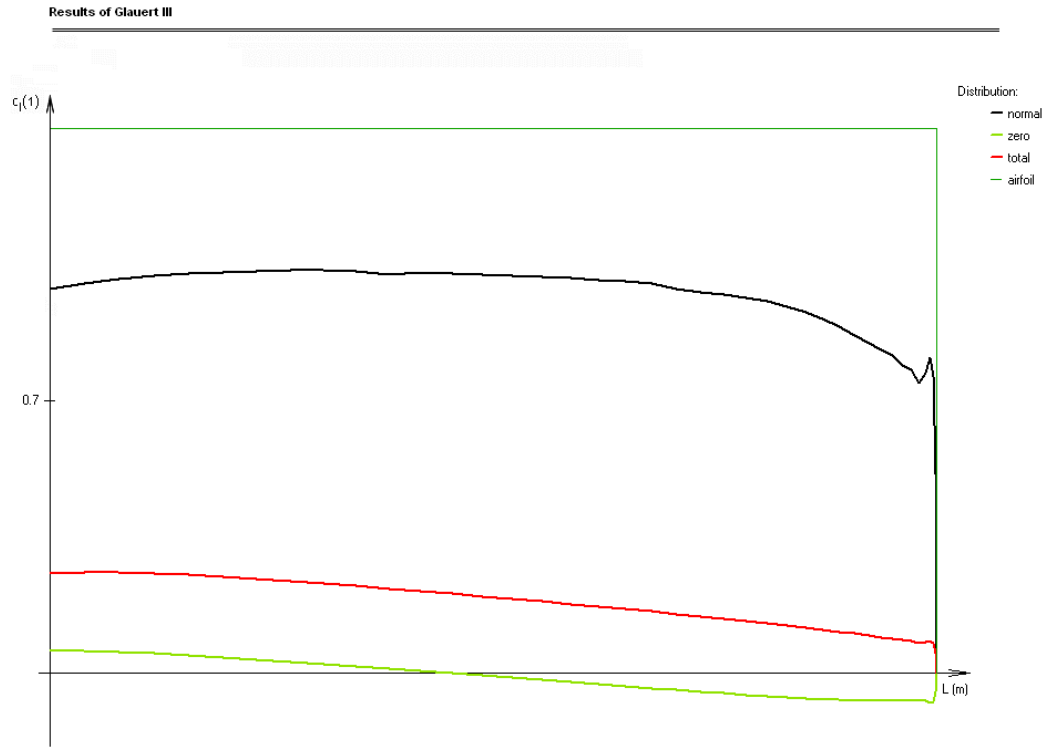

Z	CLAISYM	CLAIANTISYM	CLDAM	CLP	CLTOTAL	CD	CDWING(Z)	CM	CMWING(Z)
0.239	0	0	0	1.4	0	0.011	0.000011	-0.0498	-0.0000498
0.238	0	0	0	1.4	0.0791	0.011	0.000022	-0.0453	-9.06E-05
0.236	0	0	0	1.4	0.08	0.01098	4.392E-05	-0.045	-0.00018
0.232	0	0	0	1.4	0.0841	0.01098	6.588E-05	-0.0448	-0.0002688
0.226	0	0	0	1.4	0.0915	0.01096	7.672E-05	-0.0444	-0.0003108
0.219	0	0	0	1.4	0.1003	0.01096	9.864E-05	-0.0443	-0.0003987
0.21	0	0	0	1.4	0.1112	0.01098	0.0001098	-0.0443	-0.000443
0.2	0	0	0	1.4	0.1228	0.01097	0.00012067	-0.0445	-0.0004895
0.189	0	0	0	1.4	0.1344	0.01097	0.00014261	-0.04455	-0.00057915
0.176	0	0	0	1.4	0.1462	0.01098	0.00015372	-0.045	-0.00063
0.162	0	0	0	1.4	0.1602	0.01099	0.00016485	-0.0457	-0.0006855
0.147	0	0	0	1.4	0.1734	0.01101	0.00017616	-0.0468	-0.0007488
0.131	0	0	0	1.4	0.187	0.01105	0.00018785	-0.048	-0.000816
0.114	0	0	0	1.4	0.2011	0.01109	0.00019962	-0.0485	-0.000873
0.096	0	0	0	1.4	0.2146	0.0111	0.0001998	-0.0495	-0.000891
0.078	0	0	0	1.4	0.2291	0.01114	0.00021166	-0.0505	-0.0009595
0.059	0	0	0	1.4	0.2419	0.01119	0.0002238	-0.0525	-0.00105
0.039	0	0	0	1.4	0.2523	0.01121	0.00021299	-0.0535	-0.0010165
0.02	0	0	0	1.4	0.2586	0.01121	0.0002242	-0.054	-0.00108
0	0	0	0	1.4	0.2572	0.01121	0	-0.054	0
						CDwing	0.00264589	Cmwing	-0.01156065

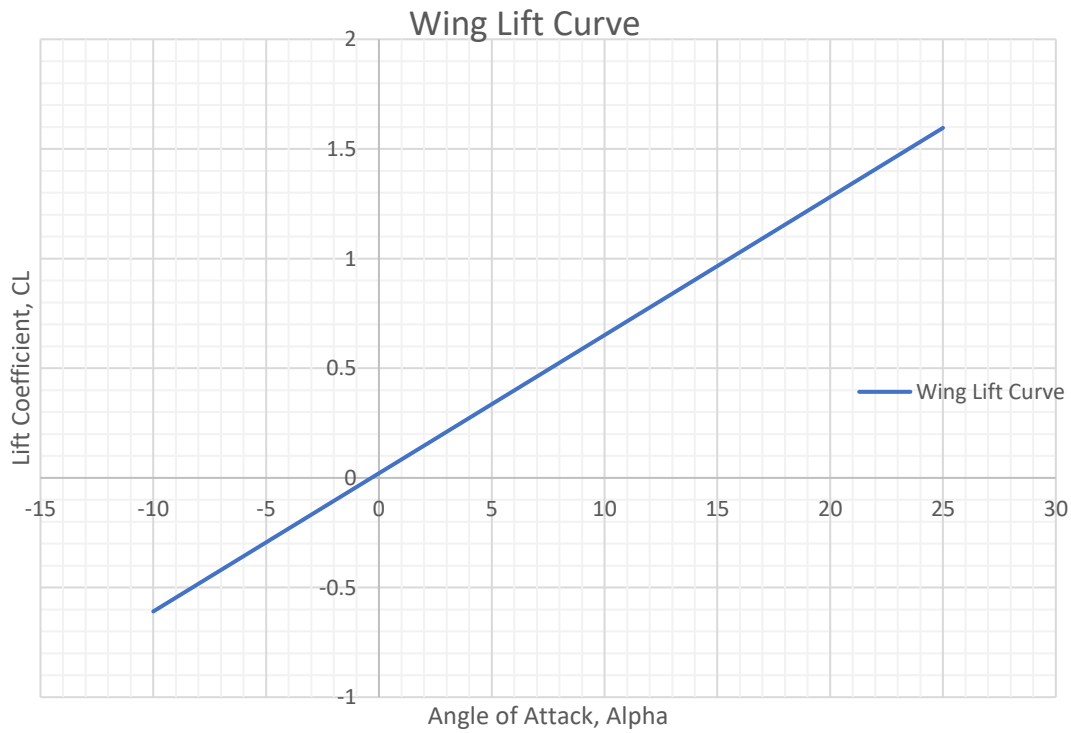

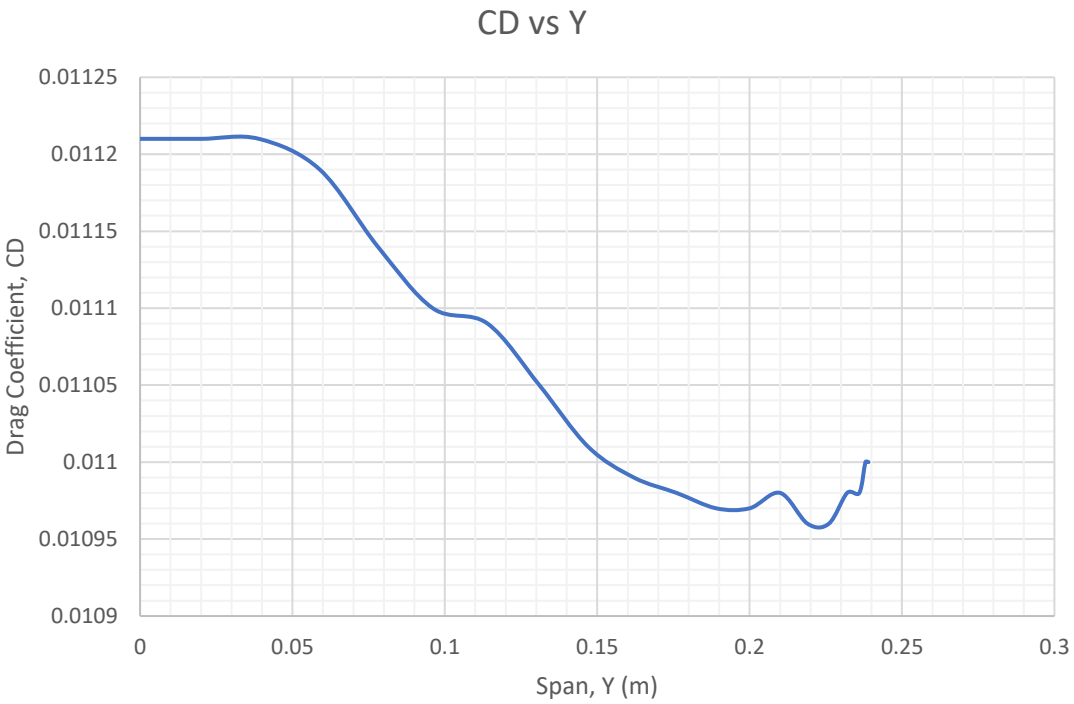
CD vs Y
0.01125
0.0112
0.01115
0.0111
0.01105
0.011
0.01095
0.0109
Drag Coefficient, CD
0
0.05
0.1
0.15
0.2
0.25
0.3
Span, Y (m)

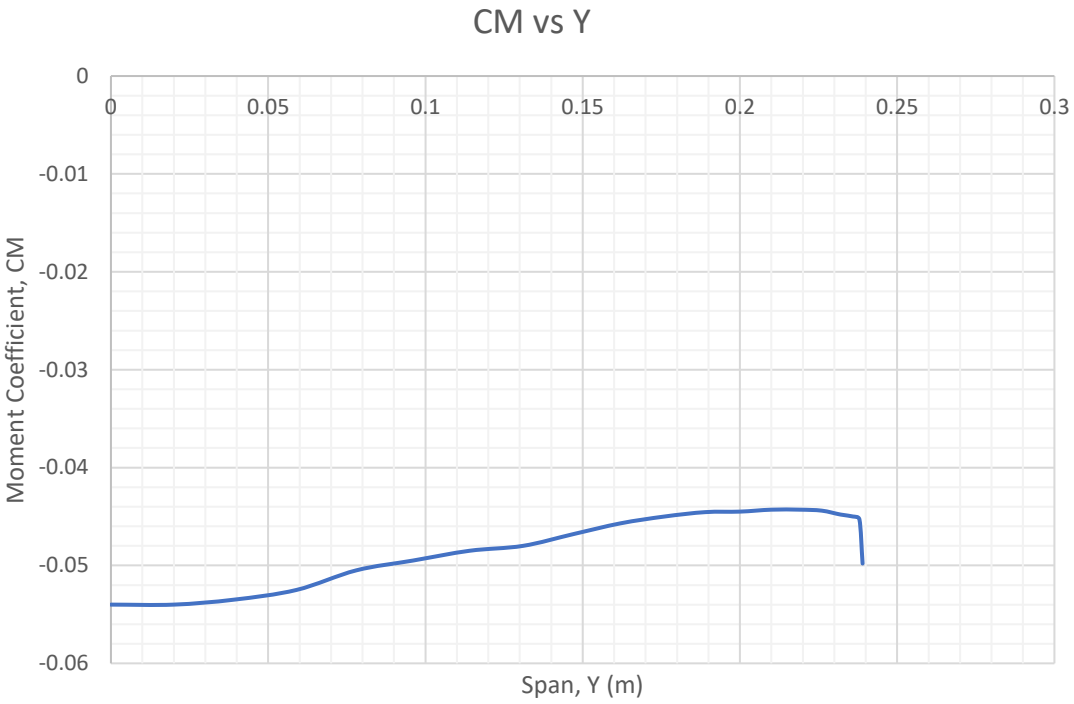
CM vs Y
0
-0.01
-0.02
-0.03
-0.04
-0.05
-0.06
Moment Coefficient, CM
0
0.05
0.1
0.15
0.2
0.25
0.3
Span, Y (m)

14.1.4 Reynolds Number 282906

14.1.4.1 Maximum Lift Coefficient

Results overview:

Area of the wing S = 0.044 m2
Aspect ratio Lambda = 5.213
Max. lift coefficient of the wing is Clwingmax = 1.3198
Lift curve slope of the wing = 3.318 rad-1
Angle of zero-lift coefficient (in the wing root) Alfa0wing = -0.4379 ° (without the influence of flaps and ailerons)
Glauert coefficient delta = 0.0083 (for the calculation of induced drag - calculated from normal distribution)
Induced drag coefficient Cxi = 0.1072 (for the lift coefficient of the wing Clwing = 1.3198)

theta	z	c	cln	cl0	claisym	claiantis	clfl	cldam	clp	cltotal
0	0.239	0.01	0	0	0	0	0	0	1.4	0
4.737	0.238	0.015	0.7776	-0.0711	0	0	0	0	1.4	0.9551
9.474	0.236	0.03	0.7745	-0.0697	0	0	0	0	1.4	0.9524
14.211	0.232	0.044	0.7921	-0.0692	0	0	0	0	1.4	0.9761
18.947	0.226	0.054	0.8295	-0.0693	0	0	0	0	1.4	1.0253
23.684	0.219	0.062	0.866	-0.0681	0	0	0	0	1.4	1.0748
28.421	0.21	0.068	0.9084	-0.0659	0	0	0	0	1.4	1.133
33.158	0.2	0.073	0.9429	-0.0616	0	0	0	0	1.4	1.1828
37.895	0.189	0.079	0.966	-0.0552	0	0	0	0	1.4	1.2197
42.632	0.176	0.084	0.9818	-0.0471	0	0	0	0	1.4	1.2486
47.368	0.162	0.087	1.003	-0.038	0	0	0	0	1.4	1.2856
52.105	0.147	0.091	1.0124	-0.0275	0	0	0	0	1.4	1.3086
56.842	0.131	0.095	1.0192	-0.016	0	0	0	0	1.4	1.329
61.579	0.114	0.098	1.0254	-0.004	0	0	0	0	1.4	1.3494
66.316	0.096	0.101	1.0271	0.0084	0	0	0	0	1.4	1.3639
71.053	0.078	0.104	1.0326	0.021	0	0	0	0	1.4	1.3838
75.789	0.059	0.106	1.0329	0.0331	0	0	0	0	1.4	1.3963
80.526	0.039	0.109	1.0273	0.0441	0	0	0	0	1.4	1.4
85.263	0.02	0.112	1.0141	0.0528	0	0	0	0	1.4	1.3912
90	0	0.116	0.9887	0.0565	0	0	0	0	1.4	1.3613

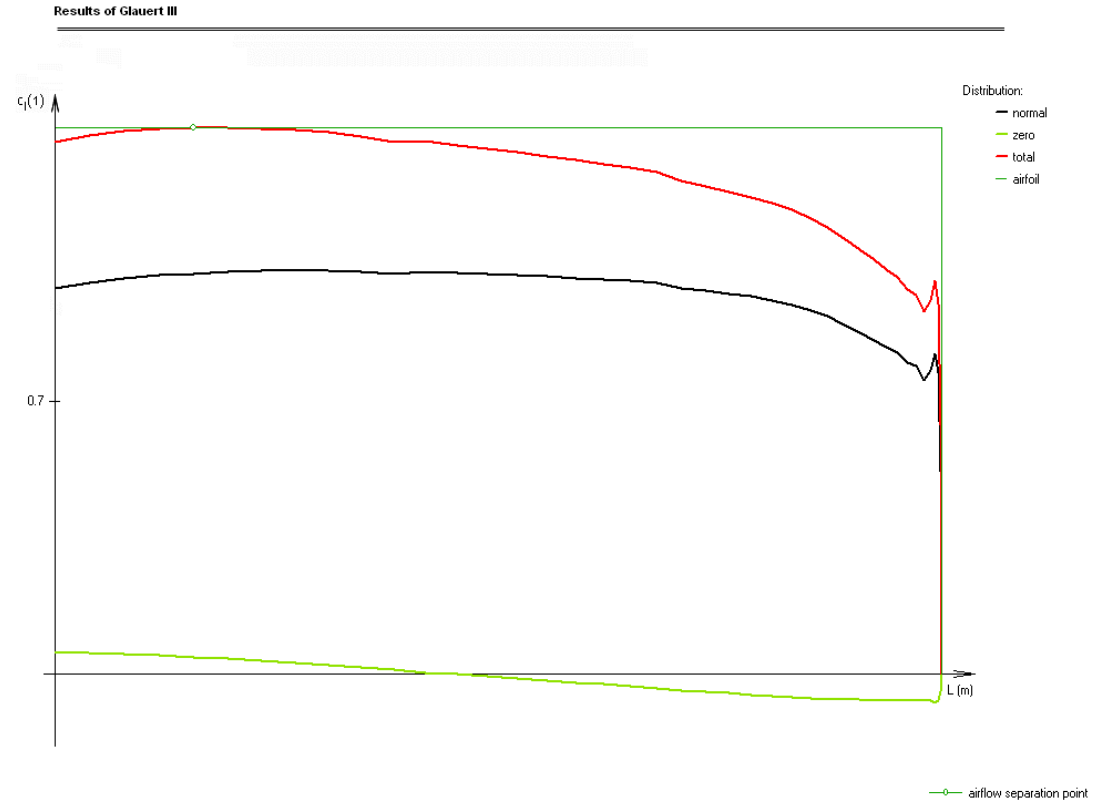

Z	CLAISYM	CLAIANTISYM	CLDAM	CLP	CLTOTAL	CD	CDWING(Z)	CM	CMWING(Z)
0.239	0	0	0	1.4	0	0.00959	9.59E-06	-0.05	-0.00005
0.238	0	0	0	1.4	0.9551	0.01376	2.75E-05	-0.046	-9.2E-05
0.236	0	0	0	1.4	0.9524	0.01364	5.46E-05	-0.046	-0.000184
0.232	0	0	0	1.4	0.9761	0.01394	8.36E-05	-0.0459	-0.000275
0.226	0	0	0	1.4	1.0253	0.01434	0.0001	-0.0455	-0.000319
0.219	0	0	0	1.4	1.0748	0.01485	0.000134	-0.045	-0.000405
0.21	0	0	0	1.4	1.133	0.01566	0.000157	-0.0439	-0.000439
0.2	0	0	0	1.4	1.1828	0.01697	0.000187	-0.0421	-0.000463
0.189	0	0	0	1.4	1.2197	0.01817	0.000236	-0.0404	-0.000525
0.176	0	0	0	1.4	1.2486	0.01992	0.000279	-0.0375	-0.000525
0.162	0	0	0	1.4	1.2856	0.02254	0.000338	-0.033	-0.000495
0.147	0	0	0	1.4	1.3086	0.02455	0.000393	-0.0281	-0.00045
0.131	0	0	0	1.4	1.329	0.02795	0.000475	-0.0165	-0.000281
0.114	0	0	0	1.4	1.3494	0.03506	0.000631	-0.0104	-0.000187
0.096	0	0	0	1.4	1.3639	0.04932	0.000888	-0.0062	-0.000112
0.078	0	0	0	1.4	1.3838	0.06373	0.001211	-0.0055	-0.000105
0.059	0	0	0	1.4	1.3963	0.07504	0.001501	-0.008	-0.00016
0.039	0	0	0	1.4	1.4	0.08888	0.001689	-0.008	-0.000152
0.02	0	0	0	1.4	1.3912	0.07504	0.001501	-0.008	-0.00016
0	0	0	0	1.4	1.3613	0.04932	0	0.0062	0
						CDwing	0.009894	Cmwing	-0.005378

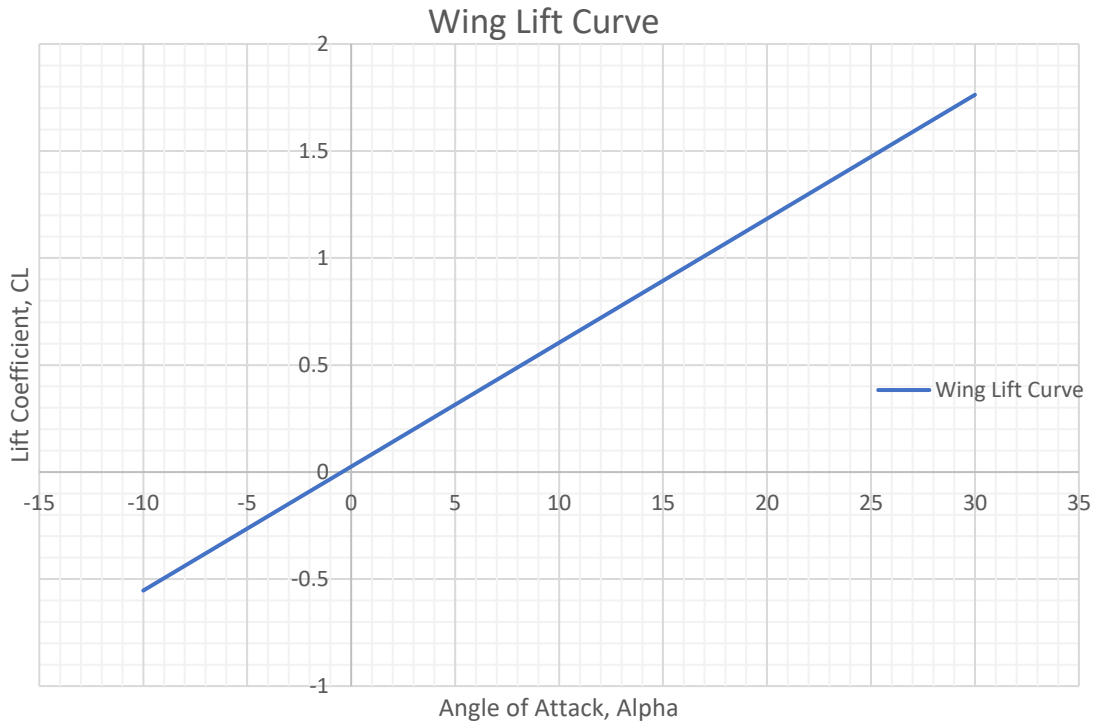

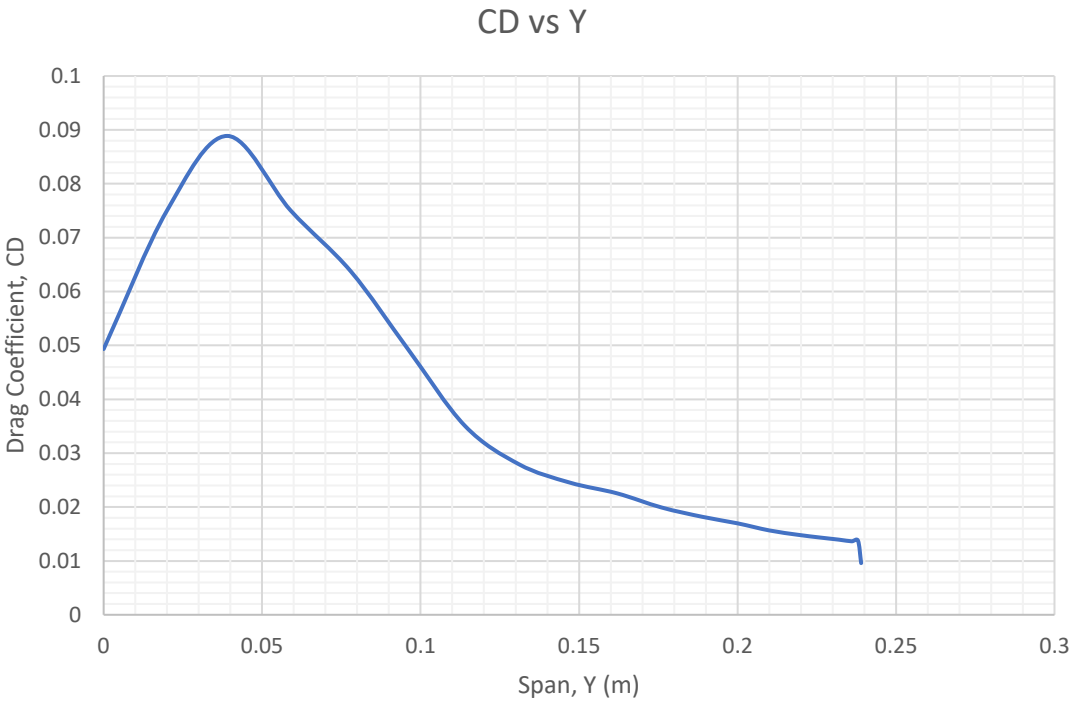
CD vs Y
Drag Coefficient, CD
0.1
0.09
0.08
0.07
0.06
0.05
0.04
0.03
0.02
0.01
0
0
0.05
0.1
0.15
0.2
0.25
0.3
Span, Y (m)

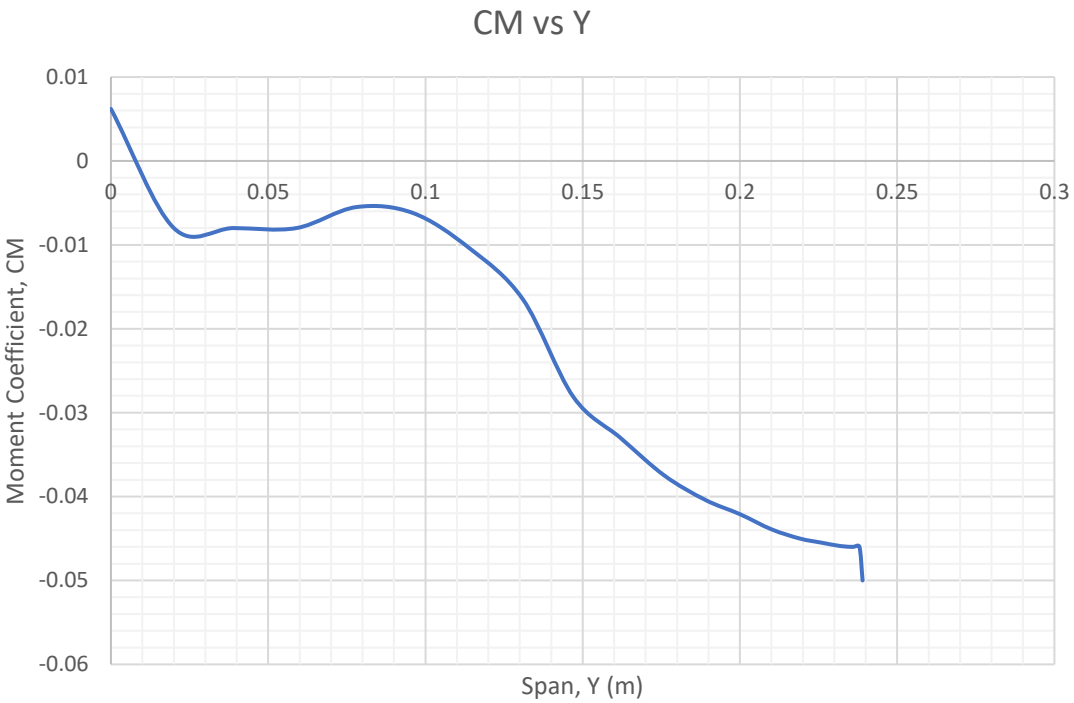
CM vs Y
Moment Coefficient, CM
0.01
0
-0.01
-0.02
-0.03
-0.04
-0.05
-0.06
0
0.05
0.1
0.15
0.2
0.25
0.3
Span, Y (m)

14.1.4.2 Cruise Lift Coefficient

Results overview:

Area of the wing S = 0.044 m2
Aspect ratio Lambda = 5.213
Requested lift coefficient of the wing is Clwing = 0.2
Max. lift coefficient of the wing is Clwingmax = 1.3198
Lift curve slope of the wing = 3.318 rad-1
Angle of zero-lift coefficient (in the wing root) Alfa0wing = -0.4379 ° (without the influence of flaps and ailerons)
Glauert coefficient delta = 0.0083 (for the calculation of induced drag - calculated from normal distribution)
Induced drag coefficient Cxi = 0.0025 (for the lift coefficient of the wing Clwing = 0.2)

theta	z	c	cln	cl0	claisym	claiantis	clfl	cldam	clp	cltotal
0	0.239	0.01	0	0	0	0	0	0	1.4	0
4.737	0.238	0.015	0.7776	-0.0711	0	0	0	0	1.4	0.0843
9.474	0.236	0.03	0.7745	-0.0697	0	0	0	0	1.4	0.0851
14.211	0.232	0.044	0.7921	-0.0692	0	0	0	0	1.4	0.0891
18.947	0.226	0.054	0.8295	-0.0693	0	0	0	0	1.4	0.0965
23.684	0.219	0.062	0.866	-0.0681	0	0	0	0	1.4	0.1051
28.421	0.21	0.068	0.9084	-0.0659	0	0	0	0	1.4	0.1158
33.158	0.2	0.073	0.9429	-0.0616	0	0	0	0	1.4	0.1269
37.895	0.189	0.079	0.966	-0.0552	0	0	0	0	1.4	0.138
42.632	0.176	0.084	0.9818	-0.0471	0	0	0	0	1.4	0.1492
47.368	0.162	0.087	1.003	-0.038	0	0	0	0	1.4	0.1625
52.105	0.147	0.091	1.0124	-0.0275	0	0	0	0	1.4	0.175
56.842	0.131	0.095	1.0192	-0.016	0	0	0	0	1.4	0.1878
61.579	0.114	0.098	1.0254	-0.004	0	0	0	0	1.4	0.2011
66.316	0.096	0.101	1.0271	0.0084	0	0	0	0	1.4	0.2138
71.053	0.078	0.104	1.0326	0.021	0	0	0	0	1.4	0.2275
75.789	0.059	0.106	1.0329	0.0331	0	0	0	0	1.4	0.2397
80.526	0.039	0.109	1.0273	0.0441	0	0	0	0	1.4	0.2496
85.263	0.02	0.112	1.0141	0.0528	0	0	0	0	1.4	0.2556
90	0	0.116	0.9887	0.0565	0	0	0	0	1.4	0.2542

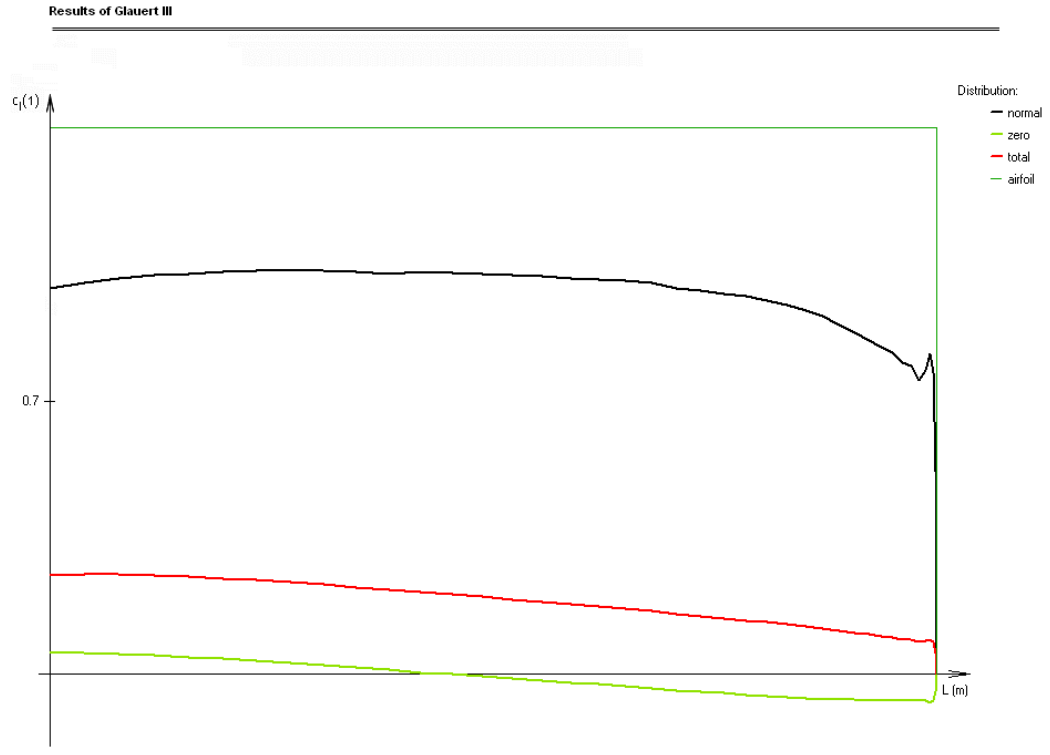

Z	CLAISYM	CLAIANTISYM	CLDAM	CLP	CLTOTAL	CD	CDWING(Z)	CM	CMWING(Z)
0.239	0	0	0	1.4	0	0.00959	9.59E-06	-0.05	-0.00005
0.238	0	0	0	1.4	0.0843	0.00887	1.774E-05	-0.0459	-9.18E-05
0.236	0	0	0	1.4	0.0851	0.00889	3.554E-05	-0.0459	-0.000184
0.232	0	0	0	1.4	0.0891	0.00885	5.31E-05	-0.0453	-0.000272
0.226	0	0	0	1.4	0.0965	0.00883	6.181E-05	-0.0453	-0.000317
0.219	0	0	0	1.4	0.1051	0.00881	7.929E-05	-0.044	-0.000396
0.21	0	0	0	1.4	0.1158	0.00879	8.79E-05	-0.0433	-0.000433
0.2	0	0	0	1.4	0.1269	0.00876	9.636E-05	-0.0426	-0.000469
0.189	0	0	0	1.4	0.138	0.00876	0.0001139	-0.0419	-0.000545
0.176	0	0	0	1.4	0.1492	0.00876	0.0001226	-0.0414	-0.00058
0.162	0	0	0	1.4	0.1625	0.00878	0.0001317	-0.041	-0.000615
0.147	0	0	0	1.4	0.175	0.00879	0.0001406	-0.0409	-0.000654
0.131	0	0	0	1.4	0.1878	0.00882	0.0001499	-0.041	-0.000697
0.114	0	0	0	1.4	0.2011	0.00885	0.0001593	-0.0414	-0.000745
0.096	0	0	0	1.4	0.2138	0.0089	0.0001602	-0.0419	-0.000754
0.078	0	0	0	1.4	0.2275	0.00896	0.0001702	-0.0429	-0.000815
0.059	0	0	0	1.4	0.2397	0.00899	0.0001798	-0.044	-0.00088
0.039	0	0	0	1.4	0.2496	0.00903	0.0001716	-0.044	-0.000836
0.02	0	0	0	1.4	0.2556	0.00908	0.0001816	-0.0453	-0.000906
0	0	0	0	1.4	0.2542	0.00908	0	-0.0453	0
						CDwing	0.0021228	Cmwing	-0.010239

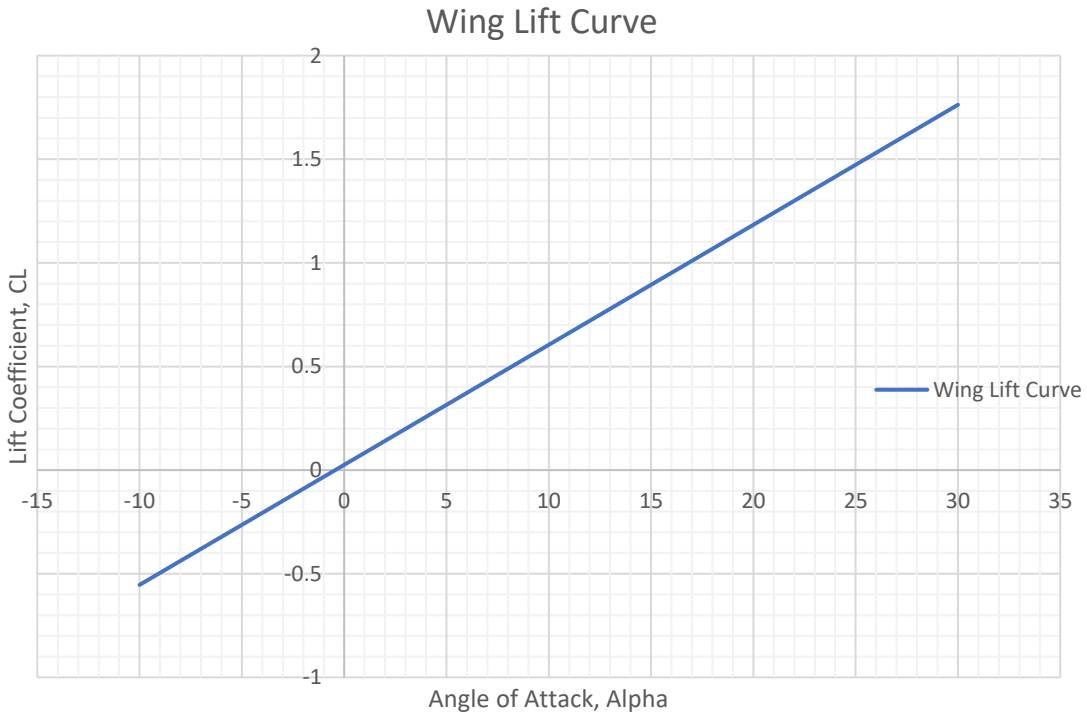

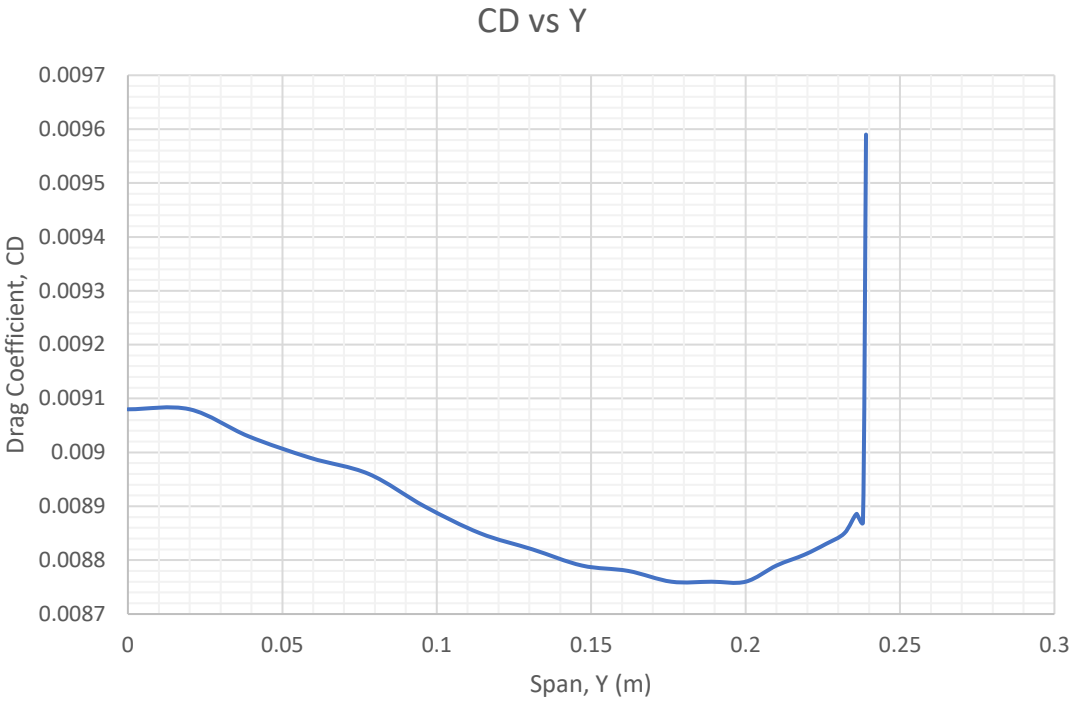
CD vs Y
Drag Coefficient, CD
0.0097
0.0096
0.0095
0.0094
0.0093
0.0092
0.0091
0.009
0.0089
0.0088
0.0087
0
0.05
0.1
0.15
0.2
0.25
0.3
Span, Y (m)

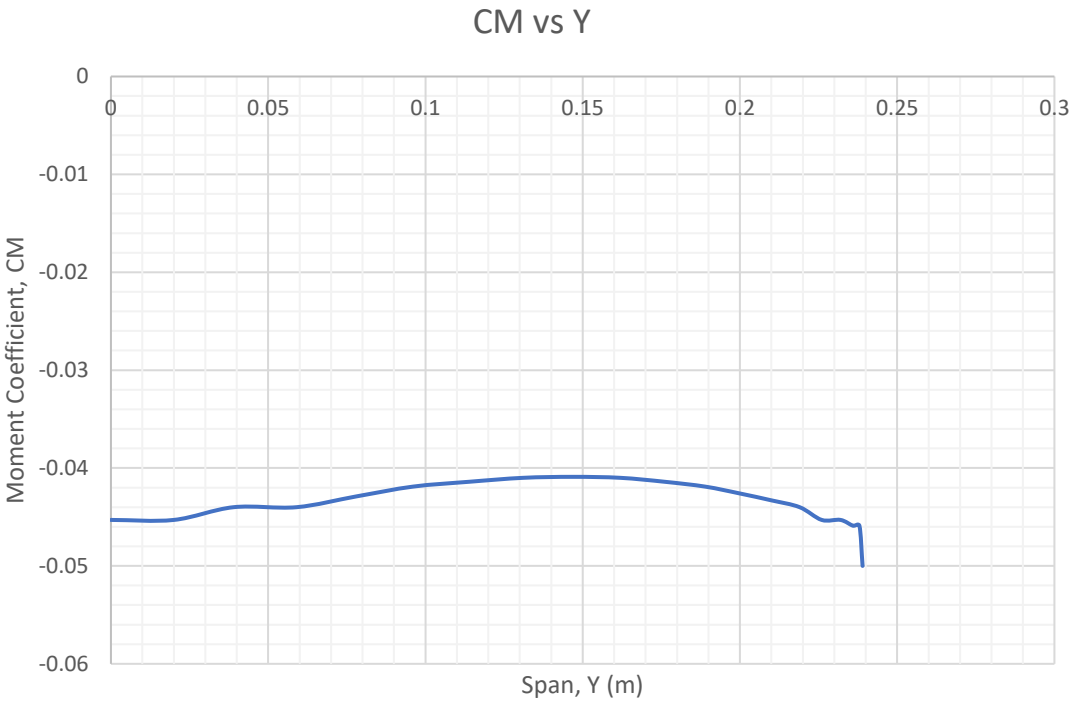
CM vs Y
Moment Coefficient, CM
0
-0.01
-0.02
-0.03
-0.04
-0.05
-0.06
0
0.05
0.1
0.15
0.2
0.25
0.3
Span, Y (m)

14.2 Horizontal Tail Unit – NACA0005

14.2.1 No Elevator Deflection

14.2.1.1 Maximum Lift Coefficient

Results overview:

Area of the wing S = 0.011 m2
Aspect ratio Lambda = 4.036
Max. lift coefficient of the wing is Clwingmax = 0.7492
Lift curve slope of the wing = 4.2054 rad-1
Angle of zero-lift coefficient (in the wing root) Alfa0wing = 0 ° (without the influence of flaps and ailerons)
Glauert coefficient delta = 0.0007 (for the calculation of induced drag - calculated from normal distribution)
Induced drag coefficient Cxi = 0.0443 (for the lift coefficient of the wing Clwing = 0.7492)

theta	z	c	cln	cl0	claisym	claiantis	clfl	cldam	clp	cltotal
0	0.105	0.005	0	0	0	0	0	0	0.77	0
4.737	0.105	0.007	0.8386	0	0	0	0	0	0.77	0.6283
9.474	0.104	0.013	0.9148	0	0	0	0	0	0.77	0.6854
14.211	0.102	0.02	0.8629	0	0	0	0	0	0.77	0.6465
18.947	0.099	0.025	0.8952	0	0	0	0	0	0.77	0.6707
23.684	0.096	0.03	0.9204	0	0	0	0	0	0.77	0.6896
28.421	0.092	0.034	0.9512	0	0	0	0	0	0.77	0.7127
33.158	0.088	0.038	0.9707	0	0	0	0	0	0.77	0.7273
37.895	0.083	0.041	0.9975	0	0	0	0	0	0.77	0.7474
42.632	0.077	0.044	1.0145	0	0	0	0	0	0.77	0.7601
47.368	0.071	0.047	1.0204	0	0	0	0	0	0.77	0.7645
52.105	0.064	0.051	1.0228	0	0	0	0	0	0.77	0.7663
56.842	0.057	0.053	1.0272	0	0	0	0	0	0.77	0.7696
61.579	0.05	0.057	1.0213	0	0	0	0	0	0.77	0.7652
66.316	0.042	0.059	1.0173	0	0	0	0	0	0.77	0.7622
71.053	0.034	0.061	1.0134	0	0	0	0	0	0.77	0.7593
75.789	0.026	0.063	1.0083	0	0	0	0	0	0.77	0.7554
80.526	0.017	0.065	0.9988	0	0	0	0	0	0.77	0.7484
85.263	0.009	0.067	0.984	0	0	0	0	0	0.77	0.7372
90	0	0.069	0.9614	0	0	0	0	0	0.77	0.7203

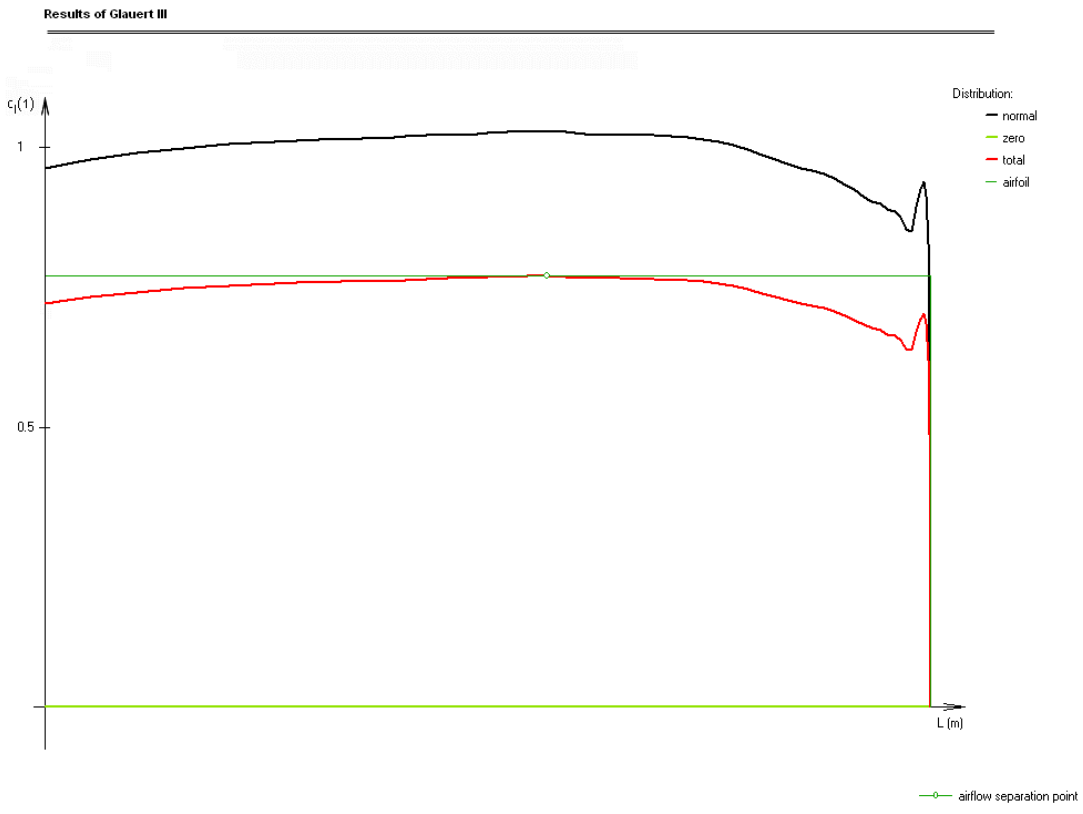

Z	CLAISYM	CLAIANTISYM	CLDAM	CLP	CLTOTAL	CD	CDWING(Z)	CM	CMWING(Z)
0.105	0	0	0	0.77	0	0.01423	0	0	0
0.105	0	0	0	0.77	0.6283	0.046	0.000046	-0.004	-0.000004
0.104	0	0	0	0.77	0.6854	0.066	0.000132	-0.015	-0.00003
0.102	0	0	0	0.77	0.6465	0.056	0.000168	-0.008	-2.4E-05
0.099	0	0	0	0.77	0.6707	0.06	0.00018	-0.013	-0.000039
0.096	0	0	0	0.77	0.6896	0.066	0.000264	-0.015	-0.00006
0.092	0	0	0	0.77	0.7127	0.072	0.000288	-0.022	-8.8E-05
0.088	0	0	0	0.77	0.7273	0.0723	0.0003615	-0.023	-0.000115
0.083	0	0	0	0.77	0.7474	0.076	0.000456	-0.026	-0.000156
0.077	0	0	0	0.77	0.7601	0.082	0.000492	-0.0299	-0.0001794
0.071	0	0	0	0.77	0.7645	0.082	0.000574	-0.0287	-0.0002009
0.064	0	0	0	0.77	0.7663	0.083	0.000581	-0.0287	-0.0002009
0.057	0	0	0	0.77	0.7696	0.083	0.000581	-0.0299	-0.0002093
0.05	0	0	0	0.77	0.7652	0.082	0.000656	-0.0299	-0.0002392
0.042	0	0	0	0.77	0.7622	0.082	0.000656	-0.029	-0.000232
0.034	0	0	0	0.77	0.7593	0.079	0.000632	-0.029	-0.000232
0.026	0	0	0	0.77	0.7554	0.0785	0.0007065	-0.029	-0.000261
0.017	0	0	0	0.77	0.7484	0.076	0.000608	-0.0286	-0.0002288
0.009	0	0	0	0.77	0.7372	0.074	0.000666	-0.0243	-0.0002187
0	0	0	0	0.77	0.7203	0.072	0	-0.023	0
						Cdwing	0.008048	Cmwing	-0.0027182

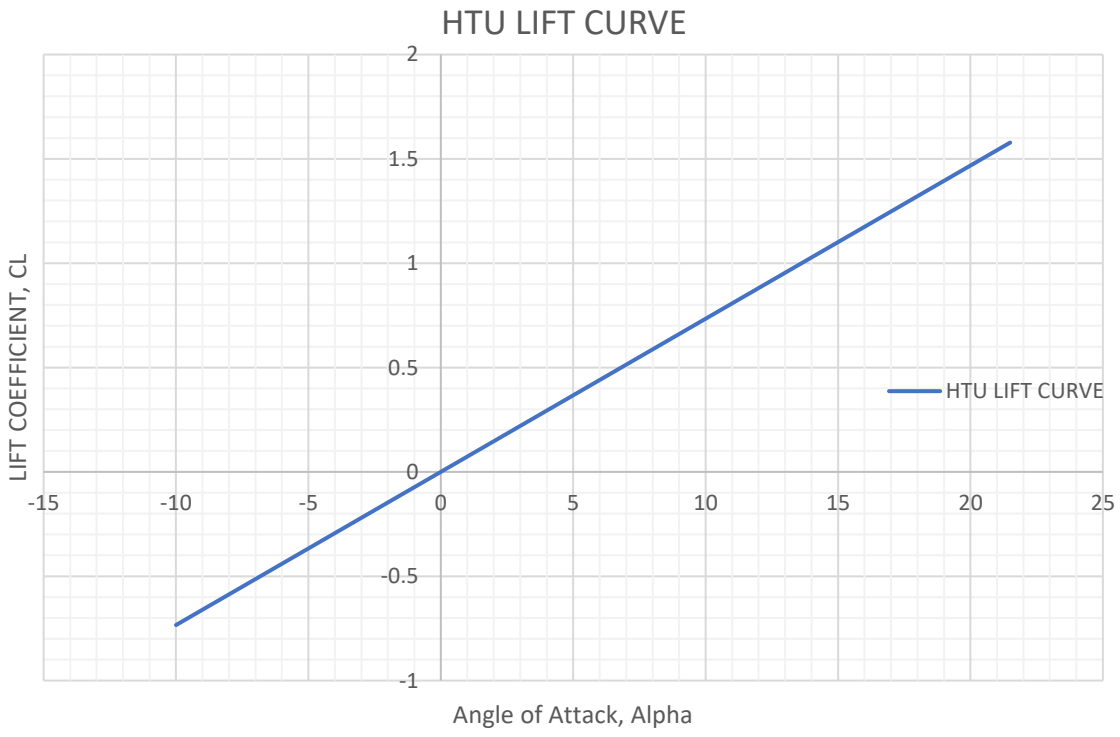

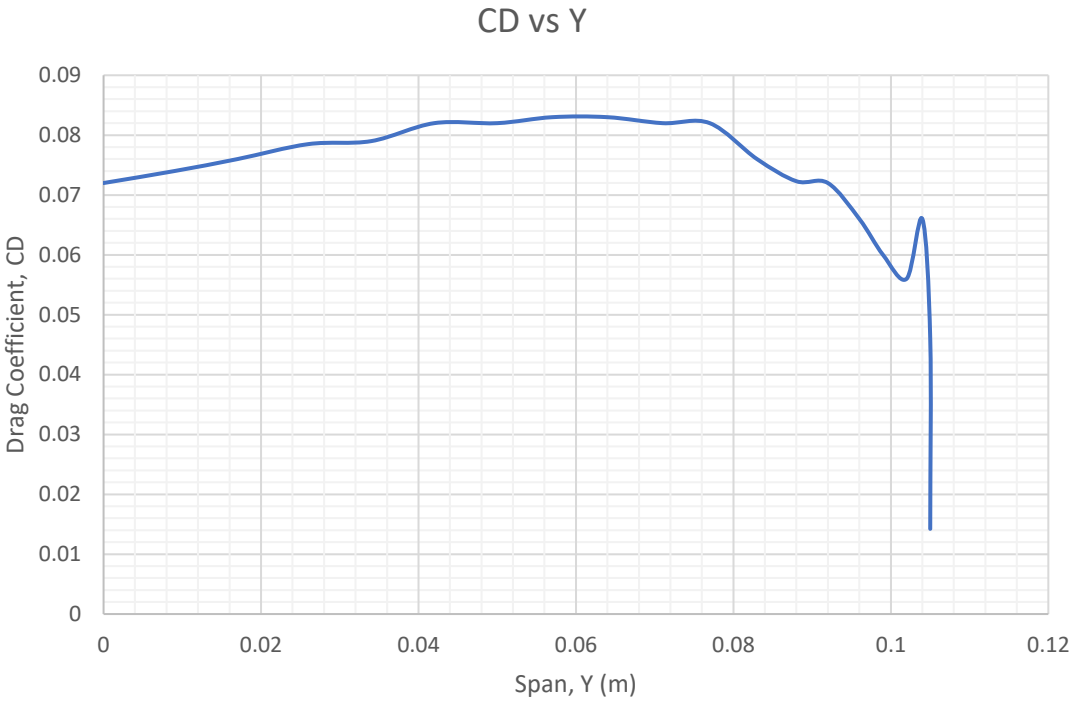
CD vs Y
Drag Coefficient, CD
0.09
0.08
0.07
0.06
0.05
0.04
0.03
0.02
0.01
0
0
0.02
0.04
0.06
0.08
0.1
0.12
Span, Y (m)

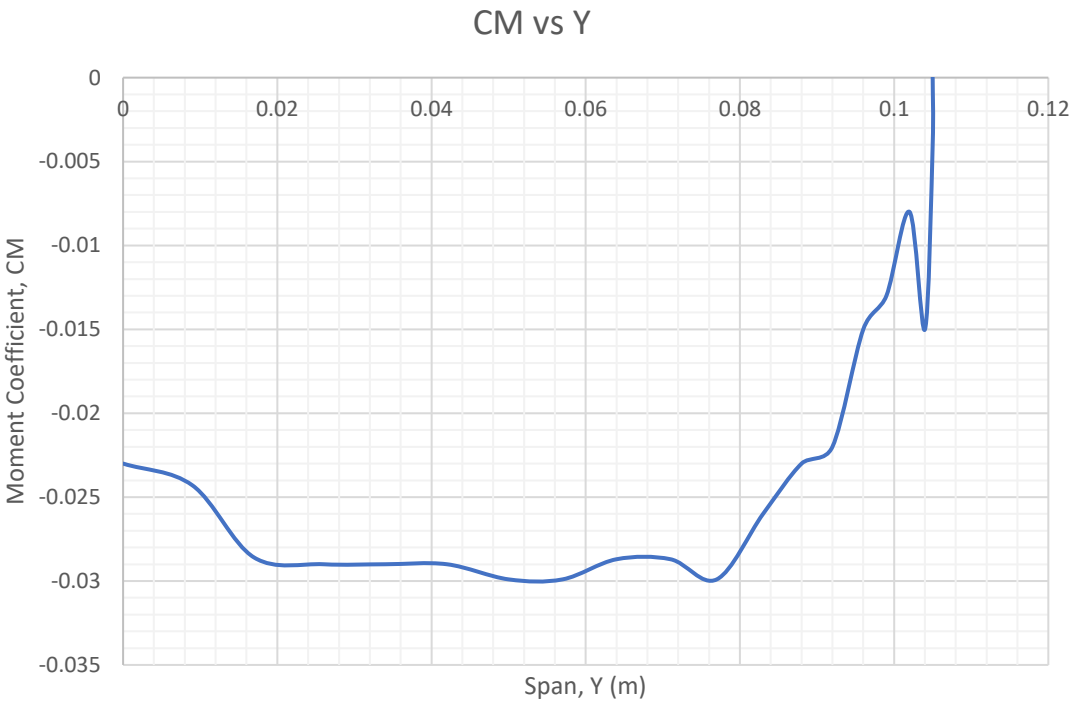
CM vs Y
Moment Coefficient, CM
0
-0.005
-0.01
-0.015
-0.02
-0.025
-0.03
-0.035
0
0.02
0.04
0.06
0.08
0.1
0.12
Span, Y (m)

14.2.1.2 Cruise Lift Coefficient

Results overview:

Area of the wing S = 0.011 m2
Aspect ratio Lambda = 4.036
Requested lift coefficient of the wing is Clwing = 0.2
Max. lift coefficient of the wing is Clwingmax = 0.7492
Lift curve slope of the wing = 4.2054 rad-1
Angle of zero-lift coefficient (in the wing root) Alfa0wing = 0 ° (without the influence of flaps and ailerons)
Glauert coefficient delta = 0.0007 (for the calculation of induced drag - calculated from normal distribution)
Induced drag coefficient Cxi = 0.0032 (for the lift coefficient of the wing Clwing = 0.2)

theta	z	c	cln	cl0	claisym	claiantis	clfl	cldam	clp	cltotal
0	0.105	0.005	0	0	0	0	0	0	0.77	0
4.737	0.105	0.007	0.8386	0	0	0	0	0	0.77	0.1677
9.474	0.104	0.013	0.9148	0	0	0	0	0	0.77	0.183
14.211	0.102	0.02	0.8629	0	0	0	0	0	0.77	0.1726
18.947	0.099	0.025	0.8952	0	0	0	0	0	0.77	0.179
23.684	0.096	0.03	0.9204	0	0	0	0	0	0.77	0.1841
28.421	0.092	0.034	0.9512	0	0	0	0	0	0.77	0.1902
33.158	0.088	0.038	0.9707	0	0	0	0	0	0.77	0.1941
37.895	0.083	0.041	0.9975	0	0	0	0	0	0.77	0.1995
42.632	0.077	0.044	1.0145	0	0	0	0	0	0.77	0.2029
47.368	0.071	0.047	1.0204	0	0	0	0	0	0.77	0.2041
52.105	0.064	0.051	1.0228	0	0	0	0	0	0.77	0.2046
56.842	0.057	0.053	1.0272	0	0	0	0	0	0.77	0.2054
61.579	0.05	0.057	1.0213	0	0	0	0	0	0.77	0.2043
66.316	0.042	0.059	1.0173	0	0	0	0	0	0.77	0.2035
71.053	0.034	0.061	1.0134	0	0	0	0	0	0.77	0.2027
75.789	0.026	0.063	1.0083	0	0	0	0	0	0.77	0.2017
80.526	0.017	0.065	0.9988	0	0	0	0	0	0.77	0.1998
85.263	0.009	0.067	0.984	0	0	0	0	0	0.77	0.1968
90	0	0.069	0.9614	0	0	0	0	0	0.77	0.1923

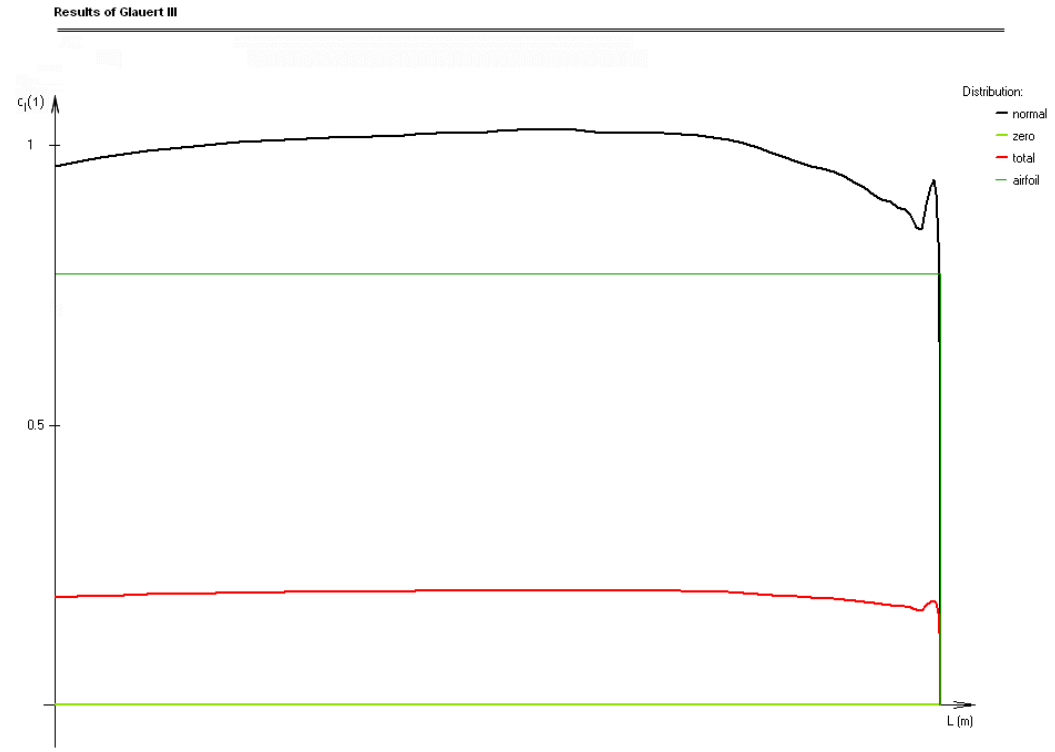

Z	CLAISYM	CLAIANTISYM	CLDAM	CLP	CLTOTAL	CD	CDWING(Z)	CM	CMWING(Z)
0.105	0	0	0	0.77	0	0.01423	0	0	0
0.105	0	0	0	0.77	0.1677	0.01449	0.00001449	0	0
0.104	0	0	0	0.77	0.183	0.01456	0.00002912	0	0
0.102	0	0	0	0.77	0.1726	0.01452	4.356E-05	0	0
0.099	0	0	0	0.77	0.179	0.01453	0.00004359	0	0
0.096	0	0	0	0.77	0.1841	0.01456	5.824E-05	0	0
0.092	0	0	0	0.77	0.1902	0.0146	5.84E-05	0	0
0.088	0	0	0	0.77	0.1941	0.01461	7.305E-05	0	0
0.083	0	0	0	0.77	0.1995	0.01464	8.784E-05	0	0
0.077	0	0	0	0.77	0.2029	0.01465	8.79E-05	0	0
0.071	0	0	0	0.77	0.2041	0.01466	0.00010262	0	0
0.064	0	0	0	0.77	0.2046	0.01466	0.00010262	0	0
0.057	0	0	0	0.77	0.2054	0.01469	0.00010283	0	0
0.05	0	0	0	0.77	0.2043	0.01466	0.00011728	0	0
0.042	0	0	0	0.77	0.2035	0.01465	0.0001172	0	0
0.034	0	0	0	0.77	0.2027	0.01465	0.0001172	0	0
0.026	0	0	0	0.77	0.2017	0.01464	0.00013176	0	0
0.017	0	0	0	0.77	0.1998	0.01464	0.00011712	0	0
0.009	0	0	0	0.77	0.1968	0.01464	0.00013176	0	0
0	0	0	0	0.77	0.1923	0.0146	0	0	0
						CDwing	0.00153658	Cmwing	0

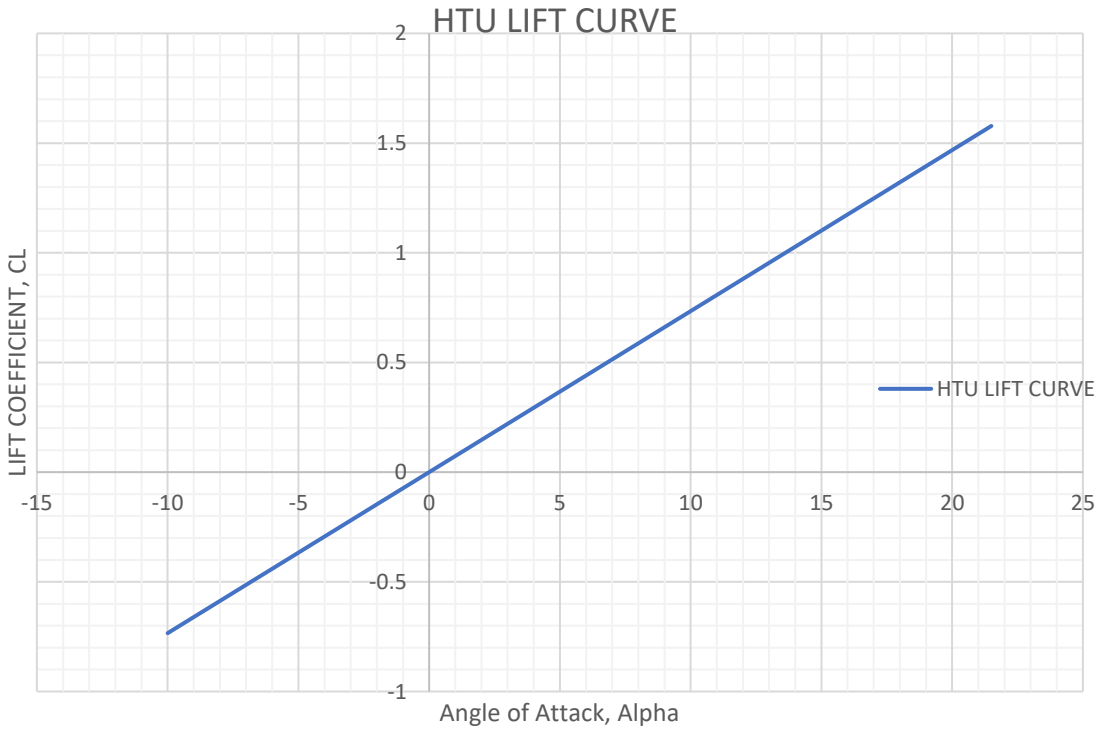

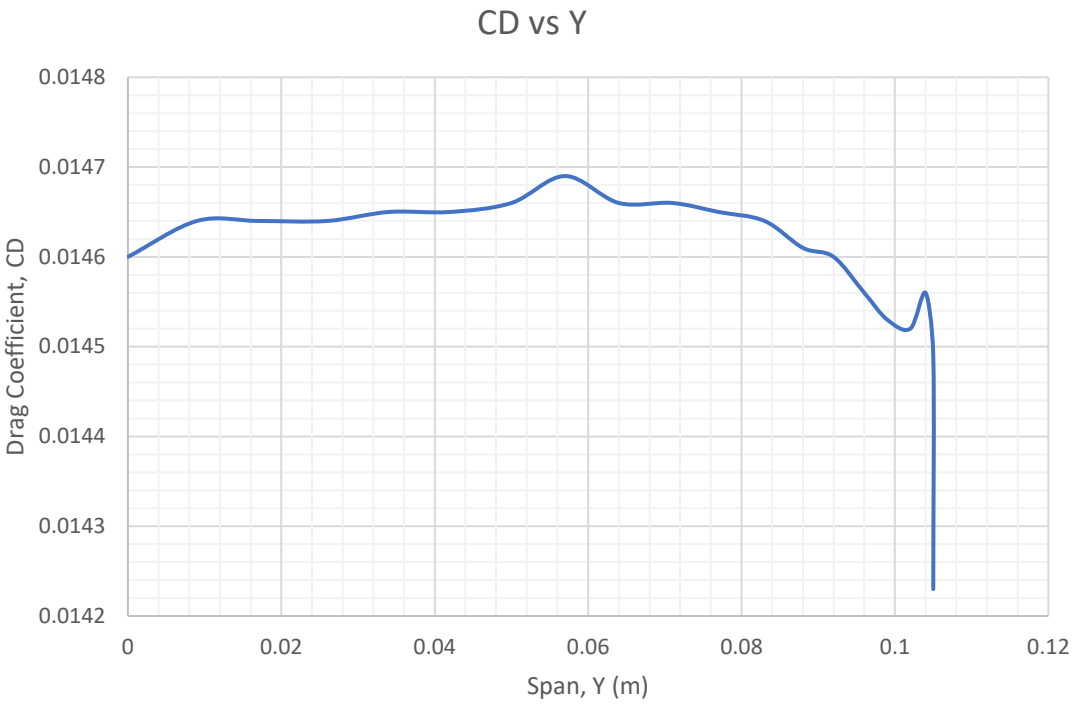
CD vs Y
Drag Coefficient, CD
0.0148
0.0147
0.0146
0.0145
0.0144
0.0143
0.0142
0
0.02
0.04
0.06
0.08
0.1
0.12
Span, Y (m)

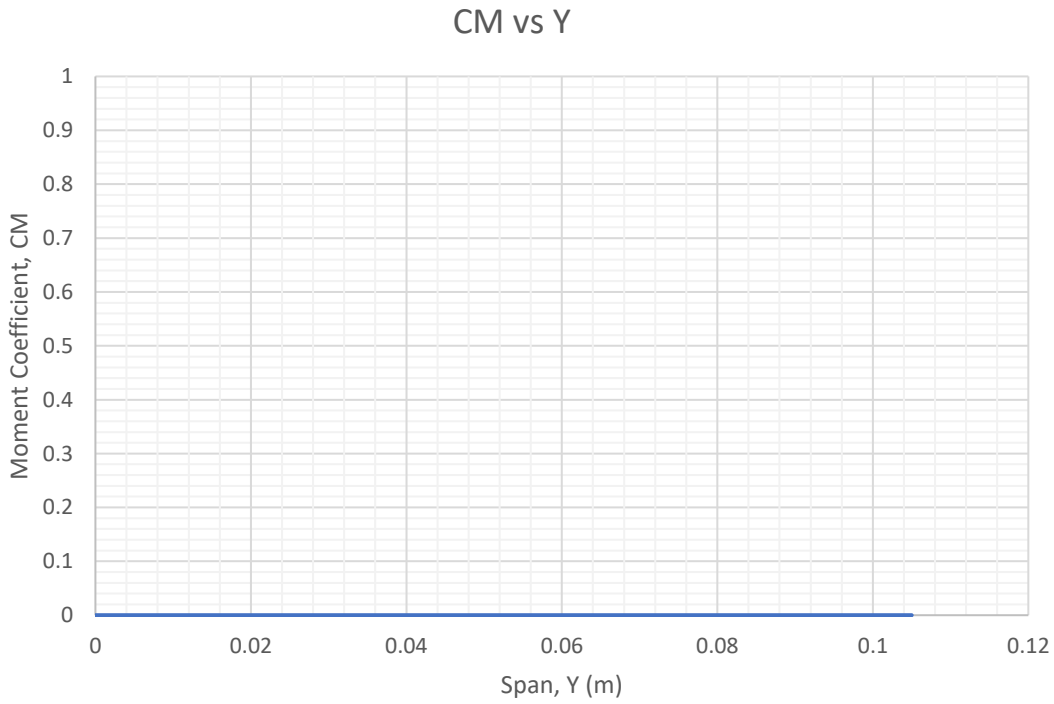
CM vs Y
Moment Coefficient, CM
1
0.9
0.8
0.7
0.6
0.5
0.4
0.3
0.2
0.1
0
0
0.02
0.04
0.06
0.08
0.1
0.12
Span, Y (m)

14.2.2 Elevator Deflection -15°

14.2.2.1 Maximum Lift Coefficient

Results overview:

Area of the wing S = 0.011 m2
Aspect ratio Lambda = 4.036
Max. lift coefficient of the wing is Clwingmax = 0.6345
Lift curve slope of the wing = 4.2054 rad-1
Angle of zero-lift coefficient (in the wing root) Alfa0wing = 0 ° (without the influence of flaps and ailerons)
Glauert coefficient delta = 0.0007 (for the calculation of induced drag - calculated from normal distribution)
Induced drag coefficient Cxi = 0.0318 (for the lift coefficient of the wing Clwing = 0.6345)
Symetric deflection of aileron dsym = -7.5° (negative value = deflected up)
Antisymetric deflection of aileron dasym = 7.5°
Pitch moment coefficient caused by deflected aileron cmx = 0.059 (from antisymetric distribution)

theta	z	c	cln	cl0	claisym	claiantis	clfl	cldam	clp	cltotal
0	0.105	0.005	0	0	0	0	0	0	0.61	0
4.737	0.105	0.007	0.8386	0	0	-0.2697	0	0	0.61	0.2623
9.474	0.104	0.013	0.9148	0	0	-0.2937	0	0	0.61	0.2866
14.211	0.102	0.02	0.8629	0	0	-0.2763	0	0	0.61	0.2712
18.947	0.099	0.025	0.8952	0	0	-0.2854	0	0	0.61	0.2825
23.684	0.096	0.03	0.9204	0	0	-0.2918	0	0	0.61	0.2921
28.421	0.092	0.034	0.9512	0	0	-0.2994	0	0	0.61	0.3041
33.158	0.088	0.038	0.9707	0	0	-0.3027	0	0	0.61	0.3131
37.895	0.083	0.041	0.9975	0	0	-0.3075	0	0	0.61	0.3254
42.632	0.077	0.044	1.0145	0	0	-0.3081	0	0	0.61	0.3355
47.368	0.071	0.047	1.0204	0	0	-0.3043	0	0	0.61	0.3431
52.105	0.064	0.051	1.0228	0	0	-0.2979	0	0	0.61	0.351
56.842	0.057	0.053	1.0272	0	0	-0.2903	0	0	0.61	0.3614
61.579	0.05	0.057	1.0213	0	0	-0.2775	0	0	0.61	0.3705
66.316	0.042	0.059	1.0173	0	0	-0.2621	0	0	0.61	0.3833
71.053	0.034	0.061	1.0134	0	0	-0.2424	0	0	0.61	0.4005
75.789	0.026	0.063	1.0083	0	0	-0.216	0	0	0.61	0.4237
80.526	0.017	0.065	0.9988	0	0	-0.1784	0	0	0.61	0.4553
85.263	0.009	0.067	0.984	0	0	-0.121	0	0	0.61	0.5033
90	0	0.069	0.9614	0	0	0	0	0	0.61	0.61

Results of Glauert III

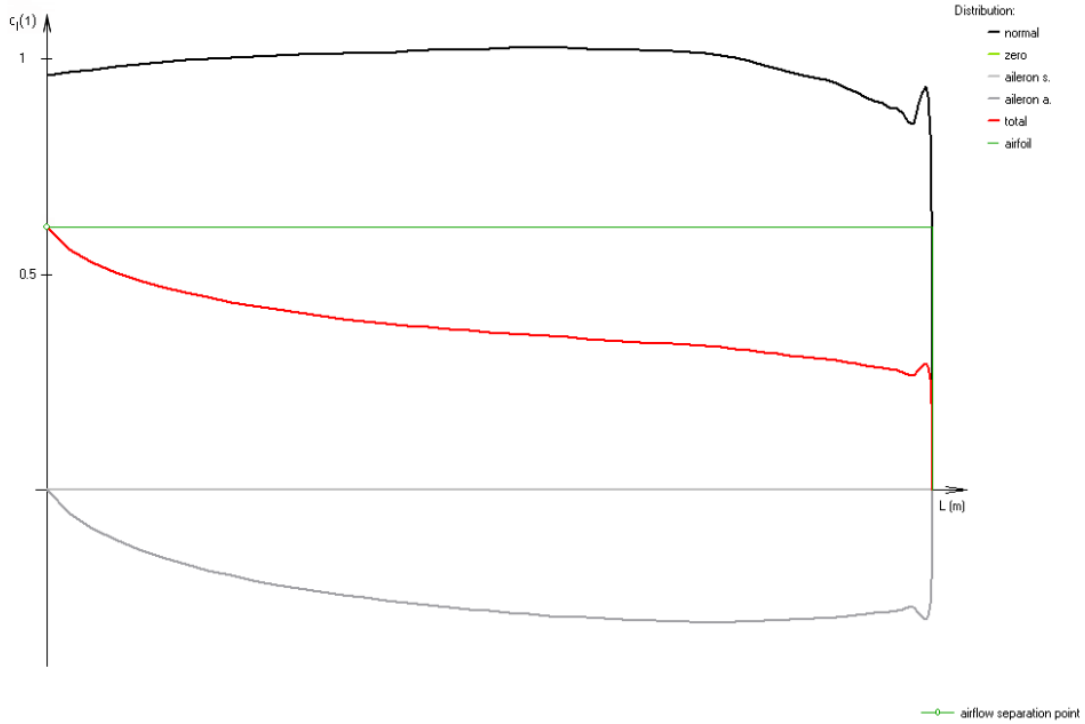

Z	CLAISYM	CLAIANTISYM	CLDAM	CLP	CLTOTAL	CD	CDWING(Z)	CM	CMWING(Z)
0.105	0	0	0	0.61	0	0.0362	0	0.125	0
0.105	0	-0.27	0	0.61	0.2623	0.058	5.8E-05	0.084	8.4E-05
0.104	0	-0.294	0	0.61	0.2866	0.06	0.00012	0.08	0.00016
0.102	0	-0.276	0	0.61	0.2712	0.0585	0.0001755	0.082	0.000246
0.099	0	-0.285	0	0.61	0.2825	0.06	0.00018	0.08	0.00024
0.096	0	-0.292	0	0.61	0.2921	0.061	0.000244	0.078	0.000312
0.092	0	-0.299	0	0.61	0.3041	0.062	0.000248	0.073	0.000292
0.088	0	-0.303	0	0.61	0.3131	0.064	0.00032	0.072	0.00036
0.083	0	-0.308	0	0.61	0.3254	0.0645	0.000387	0.0695	0.000417
0.077	0	-0.308	0	0.61	0.3355	0.066	0.000396	0.067	0.000402
0.071	0	-0.304	0	0.61	0.3431	0.067	0.000469	0.065	0.000455
0.064	0	-0.298	0	0.61	0.351	0.068	0.000476	0.062	0.000434
0.057	0	-0.29	0	0.61	0.3614	0.07	0.00049	0.06	0.00042
0.05	0	-0.278	0	0.61	0.3705	0.071	0.000568	0.058	0.000464
0.042	0	-0.262	0	0.61	0.3833	0.072	0.000576	0.055	0.00044
0.034	0	-0.242	0	0.61	0.4005	0.074	0.000592	0.05	0.0004
0.026	0	-0.216	0	0.61	0.4237	0.0765	0.0006885	0.044	0.000396
0.017	0	-0.178	0	0.61	0.4553	0.081	0.000648	0.036	0.000288
0.009	0	-0.121	0	0.61	0.5033	0.088	0.000792	0.026	0.000234
0	0	0	0	0.61	0.61	0.115	0	0.002	0
						Cdwing	0.007428	Cmwing	0.006044

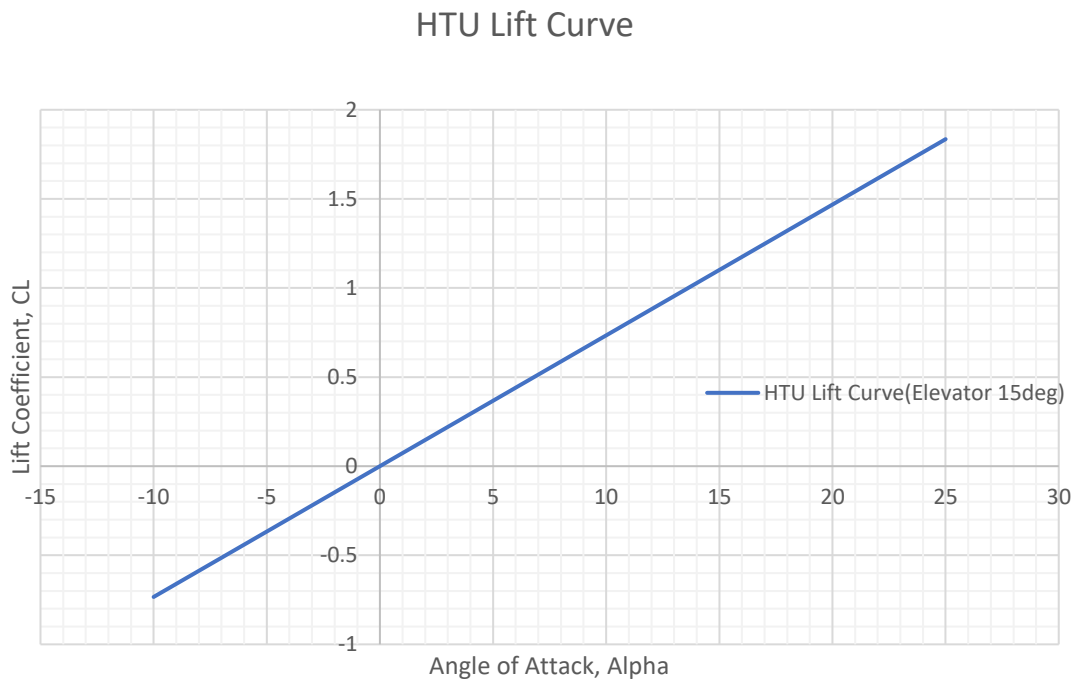

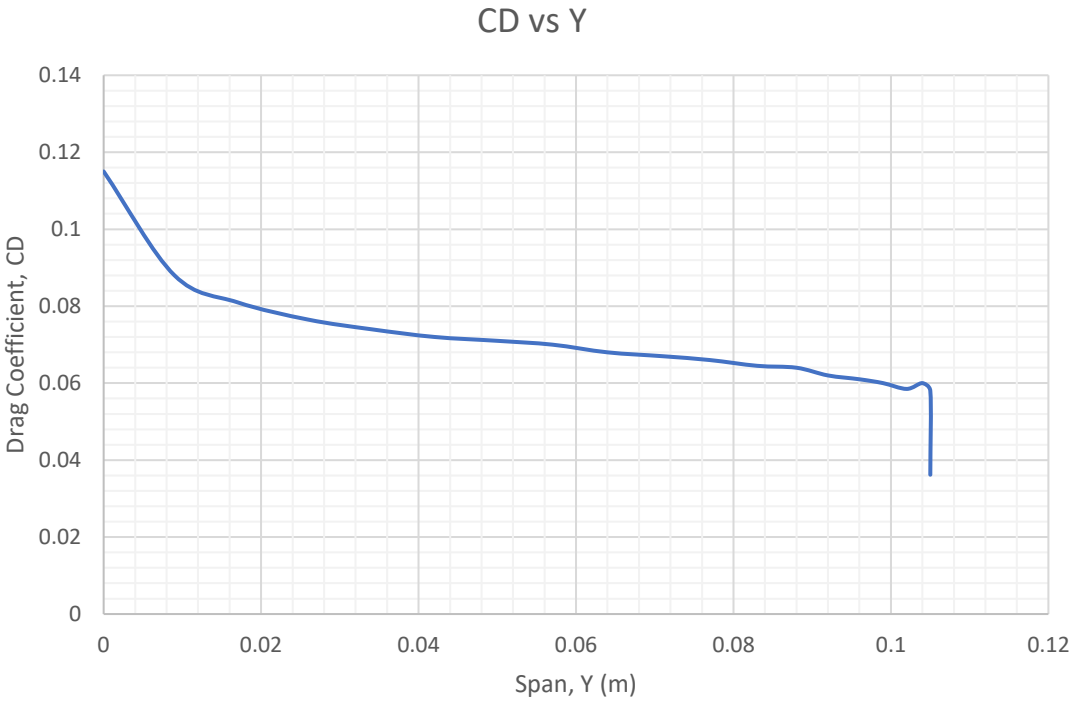
CD vs Y
Drag Coefficient, CD
0.14
0.12
0.1
0.08
0.06
0.04
0.02
0
0
0.02
0.04
0.06
0.08
0.1
0.12
Span, Y (m)

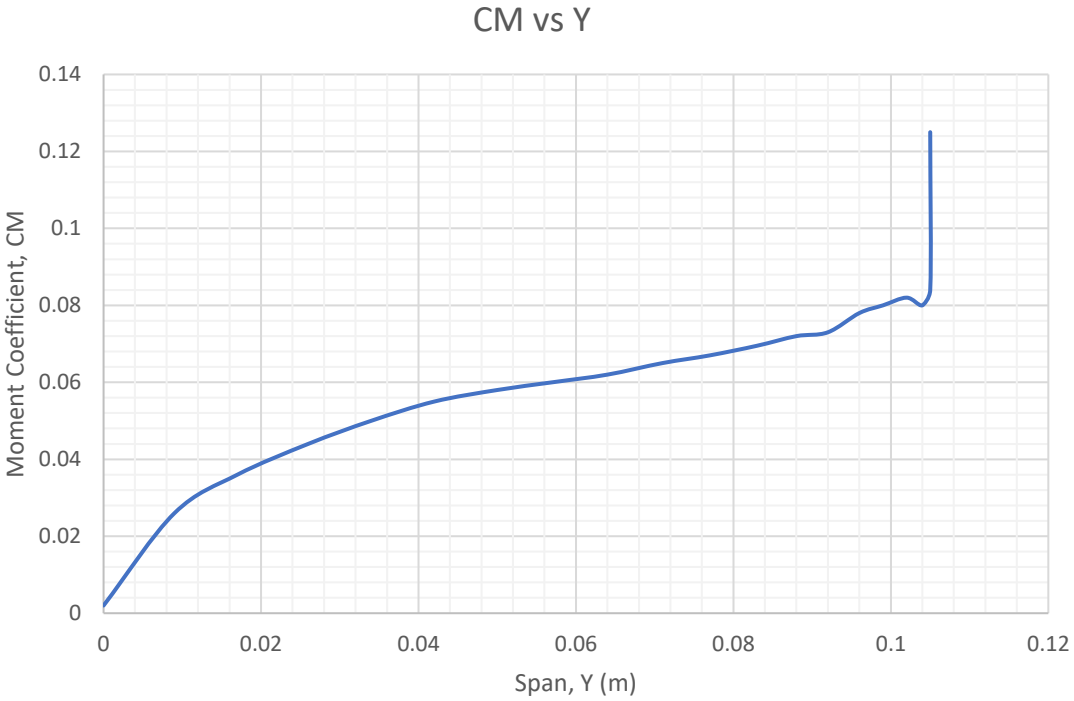
CM vs Y
Moment Coefficient, CM
0.14
0.12
0.1
0.08
0.06
0.04
0.02
0
0
0.02
0.04
0.06
0.08
0.1
0.12
Span, Y (m)

14.2.2.2 Cruise Lift Coefficient

Results overview:

Area of the wing S = 0.011 m2
Aspect ratio Lambda = 4.036
Requested lift coefficient of the wing is Clwing = 0.2
Max. lift coefficient of the wing is Clwingmax = 0.6345
Lift curve slope of the wing = 4.2054 rad-1
Angle of zero-lift coefficient (in the wing root) Alfa0wing = 0 ° (without the influence of flaps and ailerons)
Glauert coefficient delta = 0.0007 (for the calculation of induced drag - calculated from normal distribution)
Induced drag coefficient Cxi = 0.0032 (for the lift coefficient of the wing Clwing = 0.2)
Symetric deflection of aileron dsym = -7.5° (negative value = deflected up)
Antisymetric deflection of aileron dasym = 7.5°
Pitch moment coefficient caused by deflected aileron cmx = 0.059 (from antisymetric distribution)

theta	z	c	cln	cl0	claisym	claiantis	clfl	cldam	clp	cltotal
0	0.105	0.005	0	0	0	0	0	0	0.61	0
4.737	0.105	0.007	0.8386	0	0	-0.2697	0	0	0.61	-0.102
9.474	0.104	0.013	0.9148	0	0	-0.2937	0	0	0.61	-0.1108
14.211	0.102	0.02	0.8629	0	0	-0.2763	0	0	0.61	-0.1037
18.947	0.099	0.025	0.8952	0	0	-0.2854	0	0	0.61	-0.1064
23.684	0.096	0.03	0.9204	0	0	-0.2918	0	0	0.61	-0.1078
28.421	0.092	0.034	0.9512	0	0	-0.2994	0	0	0.61	-0.1092
33.158	0.088	0.038	0.9707	0	0	-0.3027	0	0	0.61	-0.1086
37.895	0.083	0.041	0.9975	0	0	-0.3075	0	0	0.61	-0.108
42.632	0.077	0.044	1.0145	0	0	-0.3081	0	0	0.61	-0.1053
47.368	0.071	0.047	1.0204	0	0	-0.3043	0	0	0.61	-0.1002
52.105	0.064	0.051	1.0228	0	0	-0.2979	0	0	0.61	-0.0933
56.842	0.057	0.053	1.0272	0	0	-0.2903	0	0	0.61	-0.0849
61.579	0.05	0.057	1.0213	0	0	-0.2775	0	0	0.61	-0.0732
66.316	0.042	0.059	1.0173	0	0	-0.2621	0	0	0.61	-0.0587
71.053	0.034	0.061	1.0134	0	0	-0.2424	0	0	0.61	-0.0398
75.789	0.026	0.063	1.0083	0	0	-0.216	0	0	0.61	-0.0144
80.526	0.017	0.065	0.9988	0	0	-0.1784	0	0	0.61	0.0213
85.263	0.009	0.067	0.984	0	0	-0.121	0	0	0.61	0.0758
90	0	0.069	0.9614	0	0	0	0	0	0.61	0.1923

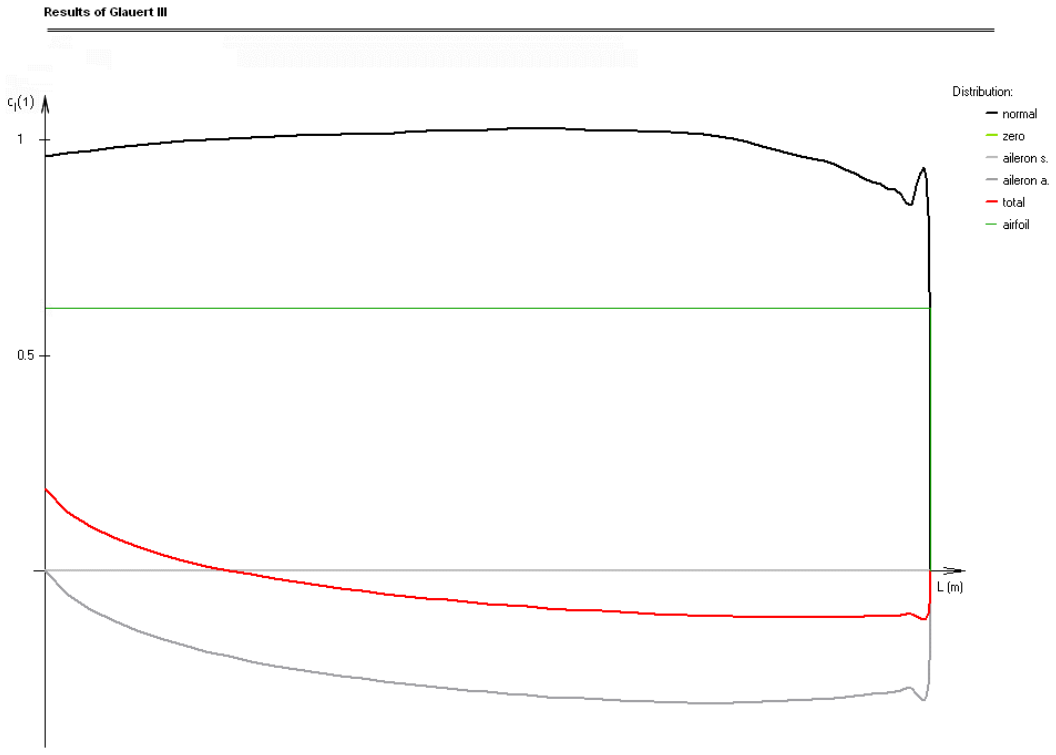

Z	CLAISYM	CLAIANTISYM	CLDAM	CLP	CLTOTAL	CD	CDWING(Z)	CM	CMWING(Z)
0.105	0	0	0	0.61	0	0.0367	0	0.125	0
0.105	0	-0.27	0	0.61	-0.102	0.0364	3.64E-05	0.113	0.000113
0.104	0	-0.294	0	0.61	-0.1108	0.0363	7.26E-05	0.1128	0.0002256
0.102	0	-0.276	0	0.61	-0.1037	0.03639	0.000109	0.113	0.000339
0.099	0	-0.285	0	0.61	-0.1064	0.03638	0.000109	0.1129	0.0003387
0.096	0	-0.292	0	0.61	-0.1078	0.03638	0.000146	0.1129	0.0004516
0.092	0	-0.299	0	0.61	-0.1092	0.0363	0.000145	0.1128	0.0004512
0.088	0	-0.303	0	0.61	-0.1086	0.0363	0.000182	0.1129	0.0005645
0.083	0	-0.308	0	0.61	-0.108	0.0363	0.000218	0.113	0.000678
0.077	0	-0.308	0	0.61	-0.1053	0.03639	0.000218	0.1128	0.0006768
0.071	0	-0.304	0	0.61	-0.1002	0.0364	0.000255	0.113	0.000791
0.064	0	-0.298	0	0.61	-0.0933	0.03643	0.000255	0.1135	0.0007945
0.057	0	-0.29	0	0.61	-0.0849	0.03645	0.000255	0.1136	0.0007952
0.05	0	-0.278	0	0.61	-0.0732	0.03648	0.000292	0.1142	0.0009136
0.042	0	-0.262	0	0.61	-0.0587	0.0365	0.000292	0.1158	0.0009264
0.034	0	-0.242	0	0.61	-0.0398	0.0367	0.000294	0.127	0.001016
0.026	0	-0.216	0	0.61	-0.0144	0.0367	0.00033	0.125	0.001125
0.017	0	-0.178	0	0.61	0.0213	0.0355	0.000284	0.13	0.00104
0.009	0	-0.121	0	0.61	0.0758	0.038	0.000342	0.118	0.001062
0	0	0	0	0.61	0.1923	0.05	0	0.11	0
						CDwing	0.003834	Cmwing	0.0123021

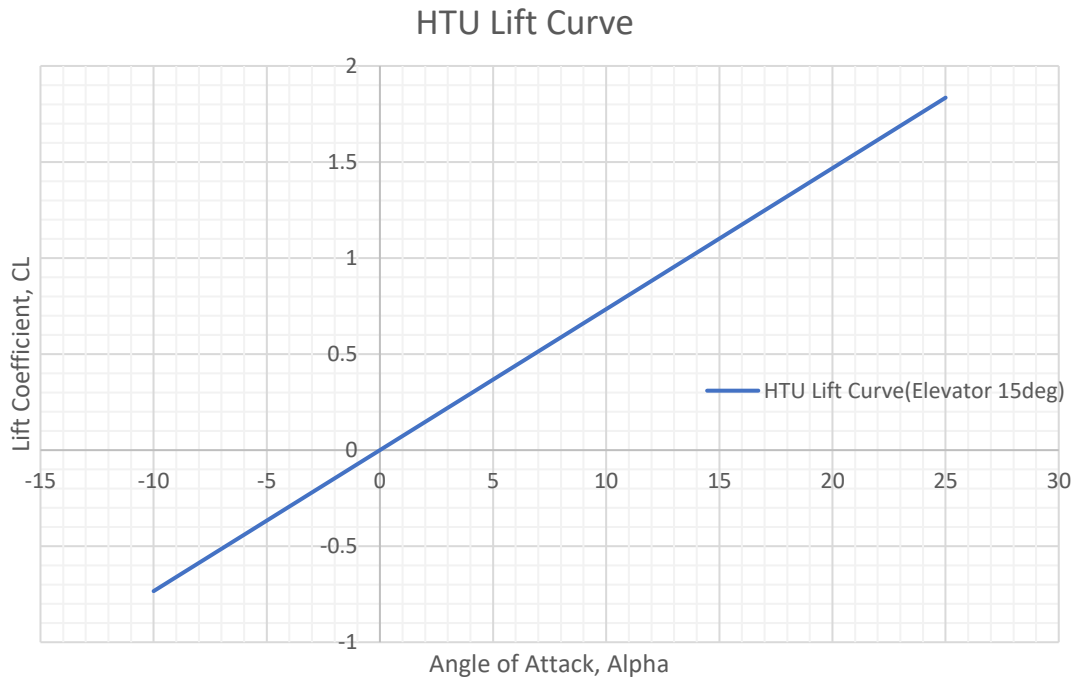

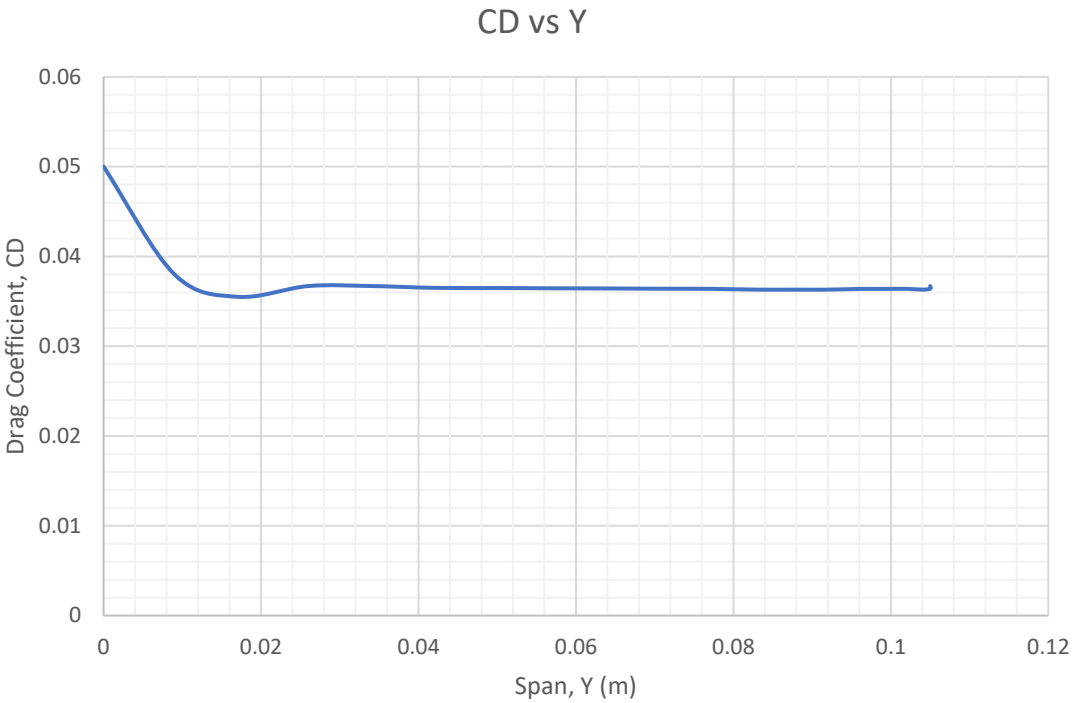
CD vs Y
Drag Coefficient, CD
0.06
0.05
0.04
0.03
0.02
0.01
0
0
0.02
0.04
0.06
0.08
0.1
0.12
Span, Y (m)

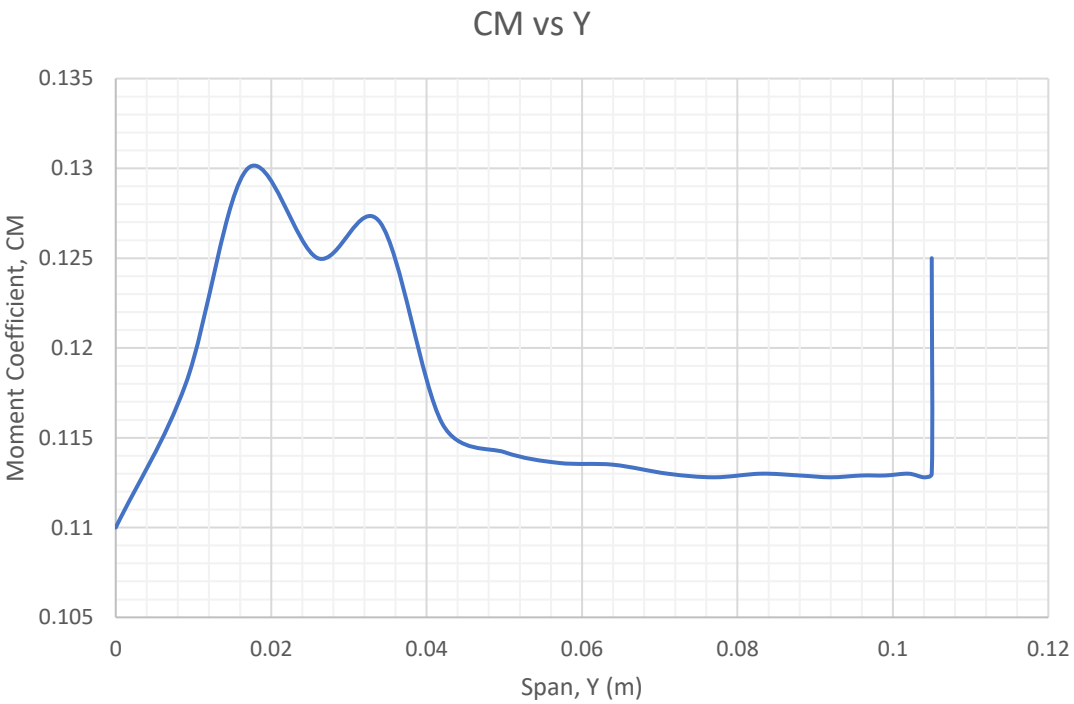
CM vs Y
Moment Coefficient, CM
0.135
0.13
0.125
0.12
0.115
0.11
0.105
0
0.02
0.04
0.06
0.08
0.1
0.12
Span, Y (m)